



**THEORETICAL STUDY OF THE  
EFFECTS OF DI-MUONIC MOLECULES  
ON MUON-CATALYZED FUSION**

DISSERTATION

Eugene V. Sheely, Lieutenant Colonel, USA

**DEPARTMENT OF THE AIR FORCE  
AIR UNIVERSITY**

**AIR FORCE INSTITUTE OF TECHNOLOGY**

---

**Wright-Patterson Air Force Base, Ohio**

DISTRIBUTION STATEMENT A; APPROVED FOR PUBLIC RELEASE; DISTRIBUTION  
UNLIMITED

The views expressed in this thesis are those of the author and do not reflect the official policy or position of the United States Air Force, the Department of Defense, or the United States Government. This material is declared a work of the US Government and is not subject to copyright protection in the United States.

THEORETICAL STUDY OF THE EFFECTS OF DI-MUONIC  
MOLECULES ON MUON-CATALYZED FUSION

DISSERTATION

Presented to the Faculty

Department of Engineering Physics

Graduate School of Engineering and Management

Air Force Institute of Technology

Air University

Air Education and Training Command

In Partial Fulfillment of the Requirements for the  
Degree of Doctor of Philosophy in Nuclear Engineering

Eugene V. Sheely, BS, MS, PhD

Lieutenant Colonel, USA

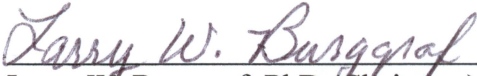
8 March 2012

DISTRIBUTION STATEMENT A; APPROVED FOR PUBLIC RELEASE;  
DISTRIBUTION UNLIMITED


THEORETICAL STUDY OF THE EFFECTS OF DI-MUONIC  
MOLECULES ON MUON-CATALYZED FUSION

Eugene V. Sheely, BS, MS, PhD  
Lieutenant Colonel, USA

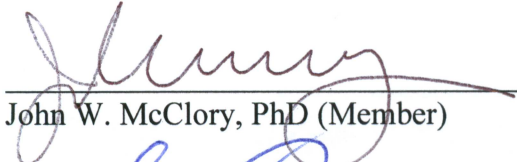
Approved:

  
Larry W. Burggraf, PhD (Chairman)

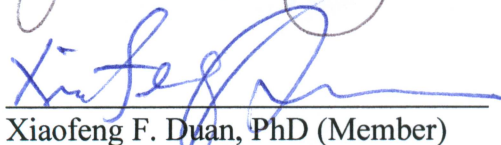
5 Mar 2012  
Date

  
David E. Weeks, PhD (Member)

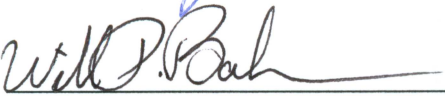
16 Feb 12  
Date

  
John W. McClory, PhD (Member)

15 Feb 12  
Date


  
Xiaofeng F. Duan, PhD (Member)

16 Feb 12  
Date

  
William P. Baker, PhD (Member)

15 Feb 12  
Date

Accepted:

  
M. U. Thomas, PhD  
Dean, Graduate School of Engineering  
and Management

8 Mar 2012  
Date

### ***Abstract***

This document presents a theoretical study di-muonic hydrogen and helium molecules that have the potential of enhancing the muon-catalyzed fusion reaction rate. In order to study these di-muonic molecules a method of non-adiabatic quantum mechanics referred to as a General Particle Orbital (GPO) method was developed. Three mechanisms that have the possibility of enhancing the muon-catalyzed fusion rate were discovered. Two involve the formation of di-muonic hydrogen molecules, and the other uses di-muonic molecules to liberate muons stuck to  ${}^3\text{He}$  nuclei. The effects of muon spin on di-muonic hydrogen molecules was studied. The nuclear separation in di-muonic hydrogen molecules with parallel muon spin is too great for the molecules to have a fusion rate which can enhance the fusion yield. The possibility of these molecules transitioning to single muon molecules or triatomic oblate symmetric top molecules which may fuse faster is examined. Using two muons to catalyze  ${}^3\text{He}$ - ${}^3\text{He}$  fusion is shown to be impractical; however, using two muons to catalyze  ${}^3\text{He}$ - $d$  fusion is possible. While studying the physical properties of di-muonic hydrogen and helium molecules some unique properties were discovered. Correlation interactions in these molecules result in an increase in the calculated nuclear bond length.

*To my wonderful family*

## *Table of Contents*

<i>Abstract</i> .....	v
<i>List of Figures</i> .....	x
<i>List of Tables</i> .....	xii
I. Introduction .....	1
II. Background .....	5
2.1 Muons .....	5
2.2 Muon-Catalyzed Fusion.....	8
2.2.1 History .....	8
2.2.2 Single-Muon Catalyzed Fusion Process.....	10
2.3 Muon-Catalyzed Fusion Yield.....	19
2.3.1 Muon Production.....	19
2.3.2 Increasing the number of fusions per muon .....	20
2.3.2.1 Muonic-molecular reaction rates .....	20
2.3.2.2 Muon Sticking to Fusion Products.....	21
2.3.2.3 Muon Scavenging.....	22
2.4 Applications of Muon-Catalyzed Fusion with Currently Obtainable Yields .....	23
2.5 Conclusions.....	24
III. Novel Muon-Catalyzed Fusion Reaction Paths .....	34
3.1 Addition of Positive Muons and Positrons .....	34
3.2 A Novel Approach to Decrease Muon Loss Due to Sticking .....	35
3.3 Two-Muon Catalyzed-Fusion .....	40
3.4 Enhance Fusion Yields with Electromagnetic Radiation.....	42
3.5 Conclusions.....	43
IV. General Multi-Configurational HF-SCF/CI Method to Model Molecules Made of Multiple Types of Quantum Particles .....	46
4.1 Introduction.....	46
4.2 Theory .....	50
4.2.1 GPO Hartree-Fock Method.....	50
4.2.2 Configuration Interaction.....	56
4.2.3 Basis Set Development .....	59
4.3 Applications .....	62
4.3.1 Contributions to the CI Energy .....	62
4.3.2 Bi-Muo Hydrogen Molecules .....	66

4.4	Conclusions.....	70
V.	Correlation Interactions in Di-Muonic Hydrogen Molecules .....	79
5.1	Introduction.....	79
5.2	Methods.....	80
5.3	Results.....	82
5.4	Conclusions.....	85
VI.	Di-Muonic Helium Molecules.....	89
6.1	Introduction.....	89
6.2	Methods.....	91
6.3	Results and Discussion .....	100
6.3.1	${}^3\text{He}+{}^3\text{He}$ .....	100
6.3.2	${}^3\text{He}+d$ .....	102
6.4	Conclusions.....	107
VII.	Reaction Paths of $p\mu\mu p^{(T)}$ and $p\mu p\mu p^{(T)}$ .....	111
7.1	Introduction.....	111
7.2	Methods.....	112
7.3	Results and Discussion .....	115
7.4	Conclusions.....	124
VIII.	Di-muonic Hydrogen Reaction Kinetics.....	128
8.1	Introduction.....	128
8.2	Methods.....	130
8.3	Results and Discussion .....	144
8.4	Conclusions.....	155
IX.	Conclusions.....	159
Appendix A.	Single Muon, Muon-Catalyzed Fusion Reactions and Rate Equations.....	167
Appendix B.	Equilibrium Concentration of Hydrogen Isotopes .....	216
Bibliography	.....	221



## *List of Figures*

Figure		Page
2-1	Major processes in the $p\mu d$ muon-catalyzed fusion reaction cycle.....	14
2-2	Major processes in the $p\mu t$ muon-catalyzed fusion reaction cycle .....	15
2-3	Major processes in the $d\mu d$ muon-catalyzed fusion reaction cycle.....	16
2-4	Major processes in the $d\mu t$ muon-catalyzed fusion reaction cycle .....	17
2-5	Major processes in the $t\mu t$ muon-catalyzed fusion reaction cycle .....	18
3-1	Reaction cycle for using $d\mu$ - $^3\text{He}\mu$ fusion to regenerate $\mu^-$ during $d\mu d$ muon-catalyzed fusion .....	38
3-2	Reaction cycle for using $^3\text{He}\mu$ - $^3\text{He}\mu$ fusion to regenerate $\mu^-$ during $d\mu d$ muon-catalyzed fusion .....	39
3-3	Reaction cycle for $d\mu d^+$ and $d\mu\mu d$ fusion.....	41
6-1	$(^3\text{He}\mu^3\text{He}\mu)^{2+}$ potential energy verses bond length with respect to free $(^3\text{He}\mu)^+$ ions .....	101
6-2	Eigenvalues $v=0$ and $v=1$ of $\hat{H}$ for $(^3\text{He}\mu^3\text{He}\mu)^{2+}$ .....	102
6-3	Comparison of $(^3\text{He}\mu\mu d)^+$ potential energy curves with and without nuclear volume being considered .....	103
6-4	$(^3\text{He}\mu\mu d)^+$ potential energy curve with nuclear volume and bound vibrational energy levels included in the calculations .....	104
6-5	Calculated ground state ( $v=0$ ) vibrational spectra of $(^3\text{He}\mu\mu d)^+$ nuclei.....	106
7-1	Binding energy with respect to $p\mu$ of the bound rotational states ( $J$ ) and ( $J, G$ ) of $p\mu\mu p$ , $p\mu p^+$ , and $p\mu p\mu p^+$ .....	123
7-2	The first few muonic energy levels of $p\mu$ .....	124

8-1	Maximum possible fusion yield increase resulting from di-muo hydrogen reactions formed by $d\bar{\mu}x + d\bar{\mu}x$ collisions .....	146
8-2	Maximum possible decrease in fusion yield, as a function of negative muon flux, resulting from di-muo hydrogen reactions formed by $d\bar{\mu}x + d\bar{\mu}x$ collisions .....	147
8-3	Maximum possible fusion yield increase resulting from di-muo hydrogen reactions formed by $dd\bar{\mu}d + d\bar{\mu}$ collisions .....	148-149
8-4	Maximum possible decrease in fusion yield, as a function of negative muon flux, resulting from di-muo hydrogen reactions formed by $dd\bar{\mu}d + d\bar{\mu}$ collisions.....	150-151
8-5	Maximum possible fusion yield increase resulting from di-muo hydrogen reactions formed by $d\bar{\mu}x + x\bar{\mu}$ collisions.....	152-153
8-6	Maximum possible decrease in fusion yield, as a function of negative muon flux, resulting from di-muo hydrogen reactions formed by $d\bar{\mu}x + x\bar{\mu}$ collisions .....	154

## *List of Tables*

Table	Page
3-1 Formation rate ( $\lambda$ ) of ground vibrational state $(dt\mu)d$ and $(dt\mu)t$ at 300 K.....	35
4-1 Effects of basis set size on HF and FCI energy of $p\mu\mu p$ .....	64
4-2 HF optimized verses HF-CI optimized CI calculations of $p\mu p^+$ .....	66
4-3 Equilibrium bond length and binding energy of $p\mu\mu p$ and $p\mu p^+$ .....	68
4-4 HF/FCI equilibrium bond length and binding energy of $p\mu\mu p$ .....	69
4-5 HF/CI equilibrium bond length and binding energy of $p\mu\mu p$ with limited active CI molecular orbitals.....	69
4-6 Equilibrium Geometry of $t\mu\mu t$ .....	70
5-1 Nuclear bond lengths of $p\mu\mu p$ and $p\mu p^+$ with respect to correlation energy.....	83
5-2 $p\mu\mu p$ correlation energy .....	84
5-3 The effect of particle spin states on the binding energy and equilibrium p-p bond length of $p\mu\mu p$ .....	85
6-1 Potential energy, as compared to free particles, of hydrogen and helium muonic-atoms .....	94
6-2 Binding energy of the $J=0$ and $J=1$ vibrational states of $(^3He\mu\mu d)^+$ .....	105
6-3 The magnitude of nuclear vibrations of $(^3He\mu\mu d)^+$ .....	105
7-1 FCI results for $p\mu\mu p$ using 2s1p basis sets.....	116
7-2 CI results for $p\mu p\mu p^+$ with singlet and triplet particle spin in ground vibrational and rotational states.....	121

7-3	Binding energy with respect to $p\mu$ for the bound rotational states ( $J$ ) of $p\mu p^+$ and ( $J,K$ ) of $p\mu\mu p$ and $p\mu p\mu p^+$ .....	122
8-1	Theoretical maximum reaction rate obtainable with a negative muon flux of $1.5 \times 10^{16}$ muons/s focused into a volume of $1\text{cm}^3$ .....	133
8-2	Upper bounds di-muo reaction rate constants at 300 K and liquid hydrogen density .....	135

# THEORETICAL STUDY OF THE EFFECTS OF DI-MUONIC MOLECULES ON MUON-CATALYZED FUSION

## **I. Introduction**

Since its discovery in 1947 researchers have hoped that muon-catalyzed fusion could provide a means of providing an almost endless supply of fusion energy. While great strides have been made in understanding the muon-catalyzed fusion process, so far the yields obtained fall short of what has been hoped for. Some proposed mechanisms for producing energy via hybrid fusion-fission reactors hold some promise, however, no practical path to useful quantities of pure fusion energy has yet been found.

This document outlines a unique method of using non-adiabatic quantum mechanics to study muonic molecules. The method is used to study two-muon catalytic processes that are predicted to have significant effects on the overall fusion yield when the thermal muon flux is large (see Chapter 8). Reactions which have the potential of increasing the muon-catalyzed fusion rate and reactions that could free muons stuck to helium nuclei are presented.

The second chapter in this document outlines many of the properties of muons which are important to muon-catalyzed fusion and gives a history of muon-catalyzed fusion research. Included in this chapter are sections which discuss how single muon

catalyzed fusion occurs and many of the factors that affect fusion yields. The chapter is concluded with a short discussion on uses of muon-catalyzed fusion with currently obtainable yields.

Chapter 3 gives an introduction to the two muon processes that are discussed in detail throughout the remainder of this document. Changes to the muon-catalyzed fusion cycle, that are expected to occur when the thermal muon flux is high, are presented.

Chapter 4 presents a general multi-configurational quantum mechanical method of modeling molecules that allows any number of any type (*i.e.*, mass and charge) of quantum particles in the presence of fixed (*i.e.*, classical) particles to be studied. The methods presented in Chapter 4 are particularly useful for studying exotic particles that cannot be accurately modeled using the Born-Oppenheimer approximation. Of particular importance to this chapter are the methods of calculating correlation interactions between particles. These interactions are shown to contribute significantly to the physical properties of the muonic molecules studied.

In Chapter 5 the effects of correlation interactions on the binding energy and bond length of di-muonic hydrogen molecules are presented. It is shown that the relative impact of these interactions is much greater in muonic molecules than it is with similar conventional molecules which contain only protons, neutrons, and electrons. These interactions are responsible for much of the binding energy di-muonic hydrogen molecules contain and they have a significant impact on the nuclear bond lengths. It is shown that these correlation interactions result in the nuclear bond lengths being larger than what would occur if these interactions did not exist. These results are surprising, in

that they are significantly different than what has been observed in conventional hydrogen molecules.

Of all of the factors which limit the maximum obtainable muon-catalyzed fusion yield, none is more important than the fact that muons sometimes *stick* to helium nuclei. Chapter 6 analyzes the possibility of using di-muonic fusion processes to free muons *stuck* to helium-3 nuclei. Quasi-classical molecular dynamics is used to calculate the vibrational energy levels and vibrational spectra of the di-muonic molecules presented in this section.

Many of the di-muonic hydrogen molecules which may form in a muon-catalyzed fusion reaction chamber, with a high thermal muon flux, have bond lengths that are too large for the molecules to have a significant fusion rate (see Chapter 5). If these molecules are to contribute to an increase in the muon-catalyzed fusion yield a mechanism for them to transfer energy and form molecules that do have high fusion rates must exist. Chapter 7 analyzes some reaction paths that could transform di-muonic hydrogen molecules with relatively large bond lengths to molecular species that have much more closely bound nuclei. Quantum rotational and vibrational energy levels are calculated as part of this analysis.

Chapter 8 of this document examines the kinetics of reaction paths that could lead to the formation of di-muonic hydrogen molecules. Upper bounds on the fusion yield that could result from different reaction paths are determined. Additionally, lower bounds of the muon flux that could result in these reaction mechanisms contributing significantly to the overall fusion yield are determined. From this information the scope

of reaction paths which have the possibility of enhancing muon-catalyzed fusion is narrowed and reaction paths which can be neglected are identified.



## II. Background

This chapter gives an overview of some of the properties of muons and the muon-catalyzed fusion process as it is currently understood. Some of the unique properties of muons and the manner in which they have been used are discussed. Emphasis is given to the history of muon-catalyzed fusion and the factors which affect obtainable yields. The chapter ends with a short discussion of possible uses of muon-catalyzed fusion with currently obtainable fusion rates.

The theoretical systems studied in this dissertation are limited to muonic molecules; however, the models developed can be applied directly to other types of exotic particle systems. Additionally, the methods presented in this document allow properties of conventional molecules that can't be calculated using most *ab-initio* code to be studied. Examples of this are K x-ray isotope shifts and differences in the binding energy of different isotopes of the same type of atom.[1:51]

### 2.1 Muons

There are two types of muons: one which has a -1 charge, the same as an electron, and its antiparticle which has a +1 charge, the same as a proton. The rest mass of a muon is 206.7682823 times that of an electron,  $\left( \sim 207m_e \text{ or } \sim \frac{1}{9}m_p \right)$ . [2; 3] As a result, a negative muon is often referred to as a heavy electron.

Muons are unstable particles with relatively short half-life's of about  $2.20 \times 10^{-6} s^{-1}$ . [2; 3] The actual half-life's of the particles varies, depending on if the

particle is negative or positive, bound, or free, etc. Muons can decay by several paths. By far the most common is for positive muons ( $\mu^+$ ) to decay into a positron ( $e^+$ ), electron neutrino ( $\nu_e$ ) and muon anti-neutrino ( $\bar{\nu}_\mu$ ), and for negative muons ( $\mu^-$ ) to decay into an electron ( $e^-$ ), an electron anti-neutrino ( $\bar{\nu}_e$ ), and a muon neutrino ( $\nu_\mu$ ).[4:2]

$$\mu^+ \longrightarrow e^+ + \bar{\nu}_\mu + \nu_e \quad (2.1)$$

$$\mu^- \longrightarrow e^- + \nu_\mu + \bar{\nu}_e \quad (2.2)$$

There are two primary sources of muons, decay products of accelerator produced particles ( $\geq 140$  MeV particles) [4:17; 5:367-385] and decay products from particles produced when primary cosmic rays interact with the atmosphere.[6:323] Accelerator produced muons can be produced and/or moderated to yield muons with energies between about an eV and 100 GeV. Cosmic ray muons have typical energies in the GeV to TeV range. The moderation of cosmic ray muons is problematic. Due to their energy, cosmic muons are extremely penetrating, and when moderated, the resulting flux is so low as to make them unusable for most applications requiring muons in the thermal and near thermal range. As a result, research which requires low energy muons, such as studies involving the absorption of muons by matter, are almost always performed using accelerator produced muons. Research which can use higher energy muons, such as studies involving the scattering of muons are often performed using cosmic ray muons.[4]

The ability of muons (both positive and negative) to probe the composition of material and the ability of negative muons to catalyze nuclear fusion is of particular interest.[7; 8; 9; 10; 11; 12] In order to use muons to study the composition of matter, muons scattered by matter can be analyzed, or molecular compounds containing muons can be studied by many of the same methods used to study conventional molecules.[1] The ability of muons to catalyze nuclear fusion will be discussed in great detail later in this document.

While muon scattering experiments using both negative and positive muons can be performed, those using positive muons are more common. Material density as a function of position can be studied by comparing the energy and angle of incoming and outgoing muons. Cosmic muons penetrate material so well that it is possible to use them to generate 3-D density diagrams of objects as large as the Mayan pyramids.[13; 14; 15; 16; 17; 18; 19] For obvious reasons, interest has been generated in using muons to search cargo ships and buildings for contraband.[20; 21; 22; 23]

In addition to analyzing material by scattering muons through it, slow (*i.e.*, low energy) muons can be absorbed by material, forming muonic molecules. These muonic molecules can be studied by many of the same methods used to study conventional molecules. By studying the properties of these muonic molecules, it is often possible to determine information about the parent molecule, which absorbed the muon. As an example, when forming muonic molecules, negative muons will most often initially form a compound in which the principle quantum number ( $n$ ) is very large (*i.e.*,  $\geq 14$ ). As the muon loses energy, transitioning from one muonic state to another, characteristic x-rays

are emitted which can be used to identify the atoms and/or molecules to which they are bound.

Perhaps the most studied method of using muons to characterize matter is muon spin rotation/relaxation/resonance ( $\mu SR$ ). A good review of this method can be found in *Introductory Muon Science*, by Kametada Nagamine.[4:100-166; 24]

## 2.2 Muon-Catalyzed Fusion

### 2.2.1 History

Muon-catalyzed fusion was first proposed by F. Charles Frank in 1947.[25] The concept was simple; if a heavy, negatively charged particle replaces an electron in a hydrogen molecule, the heavy negative particle will spend most of its time between the nuclei pulling them together and shielding them from each other. If one or both of the closely bound hydrogen nuclei are heavy isotopes of hydrogen (*i.e.*, deuterium and/or tritium), this process would allow the nuclei to get so close together that nuclear fusion could occur.

Unaware of Charles Frank's prediction that muon-catalyzed fusion could occur; in 1948 Andrei Sakharov made the same prediction and estimated the fusion rate for  $d\mu t$  fusion, where  $d$  and  $t$  represent deuterium and tritium nuclei respectively.[26] The symbol  $\mu$  is used to represent negative muons. Due to the short half-life of muons, (*i.e.*,  $\sim 2.2 \times 10^{-6}$  s) he estimated that the average number of fusions catalyzed per muon would be slightly greater than one.

About 10 years later Luis Alvarez from the University of California, Berkeley ran some experiments in which he observed muon-catalyzed fusion. At first Luis Alvarez

and his colleagues were very excited. They thought they had solved the world's energy problems. A few quick calculations, however, convinced them that the energy released by the process is much less than the energy necessary to produce muons.[27] For the next several years, muon-catalyzed fusion was looked at as an interesting phenomenon that was unlikely to result in practical applications.

In 1977 Semen Gershtein from the Institute of High Energy Physics in Serpukhov, USSR and Leonid Ponomarev from the Joint Institute for Nuclear Research, Dubna, USSR predicted that  $d\mu t$  fusion could form via a resonant process in which the energy released on binding could be divided between molecular vibrations and rotations. This process was predicted to enhance the  $d\mu t$  formation rate.[28]

Steve Jones, who worked at the Idaho National Engineering Laboratory (INEL) read the predictions of Gerstein and Ponomarev and was eager to test their hypothesis. In 1982 this desire was realized at the Los Alamos Meson Physics Facility (LAMPF). The results of Jones's and coworkers' experiments showed that the  $d\mu t$  formation rate and the  $d-t$  fusion rate were even higher than Gerstein and Ponomarev predicted.[29] This discovery generated great excitement amongst the researchers.[30]

Over the next several years the single-muon, catalyzed fusion process was studied in great detail. It was shown that muon-catalyzed fusion could occur at temperatures as low as 4 K.[31] Yields as high as 150 fusions per muon were observed in the laboratory.[32]

Despite all of the positive results, there was one overwhelming factor that continued to limit obtainable yields. Some of the muons would stick to helium nuclei formed during fusion and remain attached until they decayed.[33] Attempts have been

made to find ways to strip these muons from the helium nuclei, but so far no satisfactory solution to this problem has been found.[31; 34; 35; 36; 37]

As of the writing of this document, no attempt to optimize the reaction temperature, which is predicted to be somewhere between 1200 K and 4000 K, nor to study the process at reasonably achievable high gas pressure has been made.[7] The fusion yield under optimized conditions is calculated to be around 300 fusions per muon.[38; 39] This is short of the approximately 1000 fusions per muon that is necessary for this process to be a practical source of energy.[38; 40; 41; 42; 43; 44]

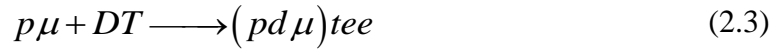
While there are ways to increase the muon-catalyzed fusion reaction rate (*e.g.*, increasing the pressure or optimizing the reaction temperature), and thereby the fusion yield; there are two additional factors that need to be addressed if single-muon catalyzed fusion is going to be useful as an energy source: (1) the energy required to produce muons, and (2) the number of muons stuck to helium nuclei. It is generally held that one or both of these factors must be addressed in order for single-muon catalyzed fusion to become a practical source of energy.

### 2.2.2 Single-Muon, Catalyzed Fusion Process

When a muon is inserted into a reaction chamber containing protium ( $^1H$  or  $P$ ), deuterium ( $^2H$  or  $D$ ), and/or tritium ( $^3H$  or  $T$ ), a muonic atom (*i.e.*,  $p\mu$ ,  $d\mu$  or  $t\mu$ ) is formed where  $p$ ,  $d$  and  $t$  represent the nuclei of protium, deuterium and tritium respectively. When the muonic atom is first formed it is in an excited state with a principle quantum number ( $n$ ) approximately equal to 14 (see Chapter 7 of this document or reference [45]). The excited muonic hydrogen atom loses energy via x-ray emission. While in an excited

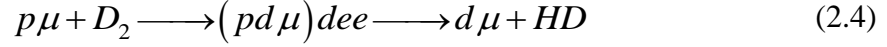
state the muon may transfer to other hydrogen nuclei via exchange reactions. When the muonic-atom reaches or approaches the ground state it can participate in additional reactions which form tri-nuclear molecules (see Appendix A).

When a muonic hydrogen atom in or near its ground muonic state (*i.e.*,  $n = 1$ ), collides with a diatomic hydrogen molecule a tri-atomic muonic molecule sometimes forms. For example,

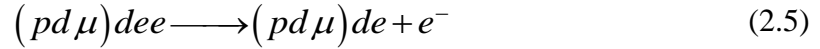


Two of the nuclei will be bound very close to each other (*i.e.*,  $\sim 0.005 \text{ \AA}$ ) by the muon. The third nucleus is bound to the first two with a bond length approximately equal to the nuclear bond length of a diatomic hydrogen ion  $H_2^+$ .

For some of the tri-atomic muonic molecules [*i.e.*,  $(dd\mu)xee$ ,  $(dt\mu)xee$ , and  $(tt\mu)xee$ , where  $x$  represents the nuclei of any hydrogen isotope] bound excited vibrational and rotational states between the two tightly bound atoms exists (*e.g.*  $v=1$ ,  $J=1$ ). The small amount of binding energy present in these excited exotic molecules is distributed between vibrational and rotational energy. This process, known as resonant formation, is the reason some muon-catalyzed fusion reactions occur much more rapidly than originally predicted. Most of the time this weakly bound tri-atomic muonic molecule will quickly dissociate, the muon staying with the heavier of the two nuclei to which it is closely associated. For example,



Some of the tri-atomic muonic molecules will de-excite by Auger de-excitation rather than dissociate, resulting in a more tightly bound, more stable compound. For example,



Once the tri-atomic muonic molecule is formed, the nuclei bound together by the muon can fuse; if the isotope pair is one for which fusion is possible. Although rotationally and vibrationally excited muonic hydrogen molecules sometimes fuse, it is more likely that this will happen when the molecule is in its ground state.

Once fusion has taken place, the catalytic muon can be freed, allowing it to catalyze another fusion event, or it can *stick* (*i.e.*, bind) to one of the particles formed during fusion. When negative muons stick to a fusion product they most commonly stick to the product of highest charge (*e.g.*,  ${}^4\text{He}$ ). When fusion results in multiple products of the same charge being formed, such as



if the muon sticks to one of the product nuclei, it will most often stick to the fusion product of greatest mass (*e.g.*,  $t$ ).



The probability of a muon sticking to a fusion product during the fusion process depends not only on the charge and mass of the fusion products, but also on the energy and isotopic makeup of the tri-atomic species that fuse. Sticking may be thought of as being due to the matching of the muon kinetic energy in the initial state with that of bound final states on the recoiling daughter nucleus. The closer these energies match, the higher the probability of sticking.[46] The effective probability of a muon sticking to a helium nucleus during  $d\mu t$  fusion (*i.e.*,  $\omega_s = 0.0043$ ) is much less than the probability of it sticking during  $p\mu d$  (*i.e.*,  $\omega_{pd} = 0.99$ ),  $p\mu t$  (*i.e.*,  $\omega_{pt} = 0.94$ ),  $d\mu d$  (*i.e.*,  $\omega_d = 0.122$ ), or  $t\mu t$  (*i.e.*,  $\omega_t = 0.14$ ) fusion.[7; 10; 12; 31:47; 48; 49; 50; 51; 52; 53; 54; 55; 56; 57; 58]  $d\mu t$  forms more rapidly and fuses quicker than  $d\mu d$  and  $t\mu t$ , therefore the reaction paths leading to  $d\mu t$  fusion have predominated in the study of muon-catalyzed fusion.[7; 8; 9; 10; 47]

$p\mu d$  and  $p\mu t$  do not have bound excited vibrational states;[4:76-77] therefore fusion paths which lead to the fusion of these isotope pairs are much slower than those in which exclusively heavy isotopes of hydrogen fuse.

Figures 2-1 to 2-5 depict the most common muon-catalyzed fusion reaction paths. The diagrams do not, however, show all of the reactions which occur. Appendix A gives a more complete list of single muon catalyzed fusion reaction steps and rate equations which facilitate the study of muon-catalyzed fusion kinetics.

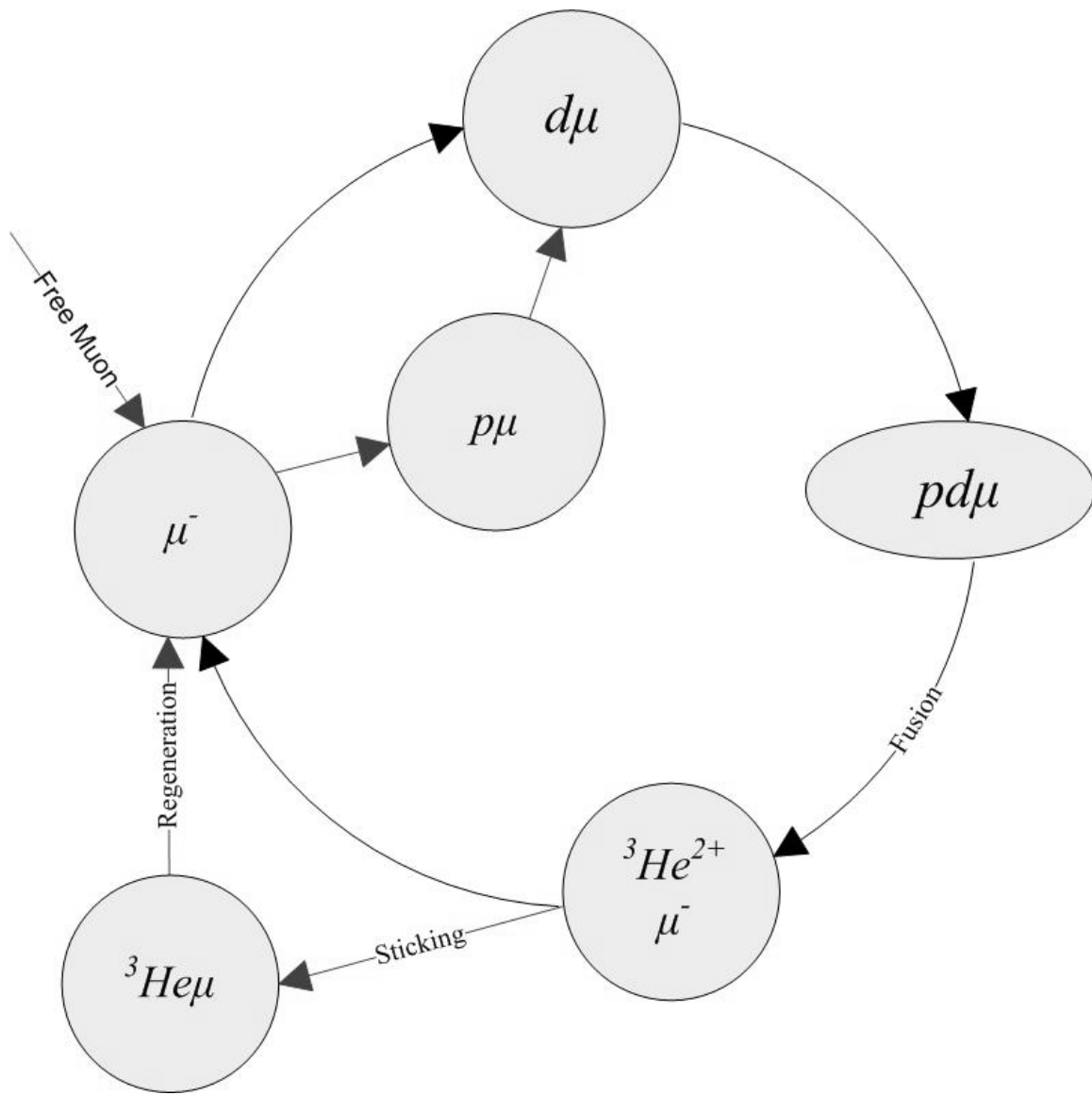
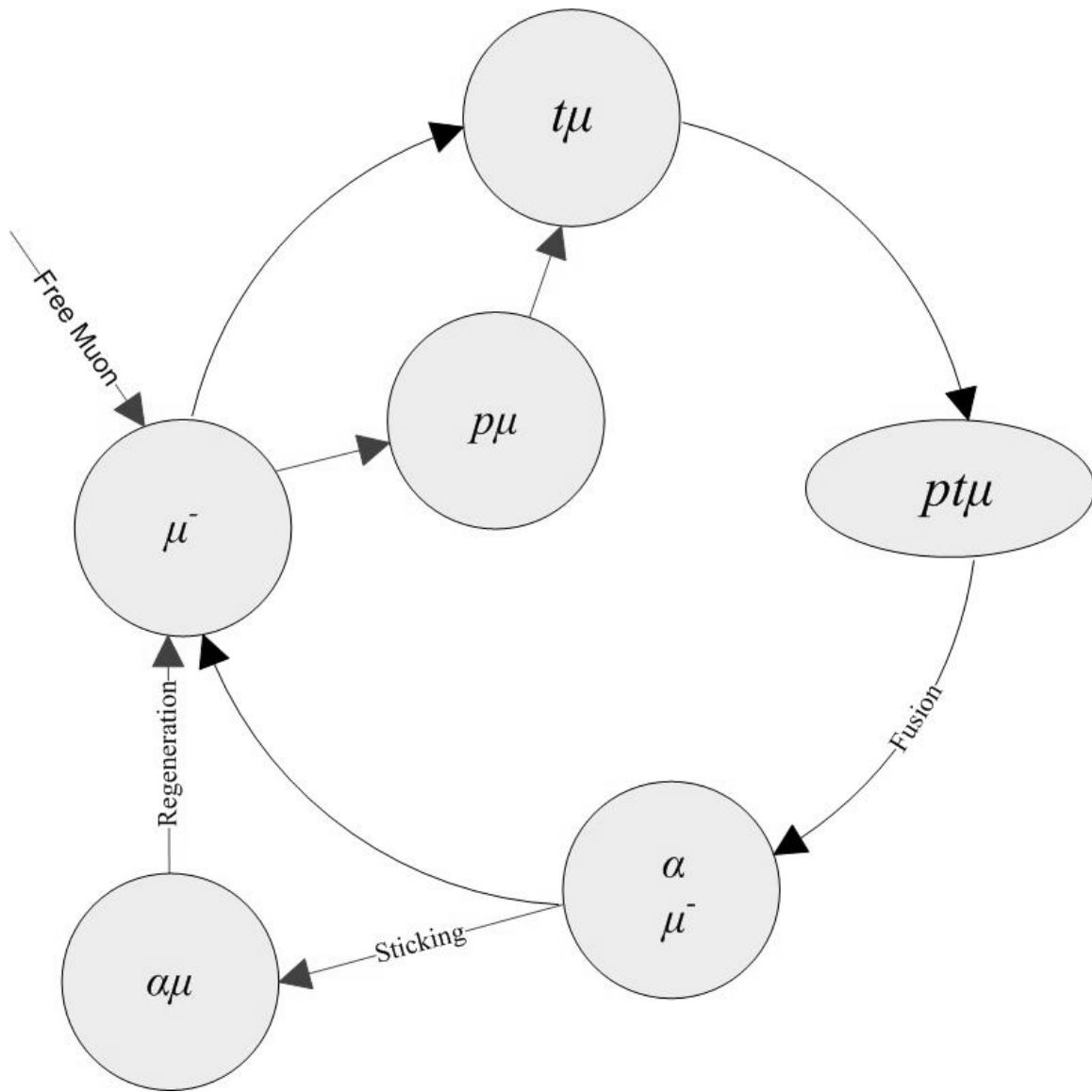


Figure 2-1. Major processes in the  $p\mu d$  muon-catalyzed fusion reaction cycle.



**Figure 2-2. Major processes in the  $p\mu t$  muon-catalyzed fusion reaction cycle.**

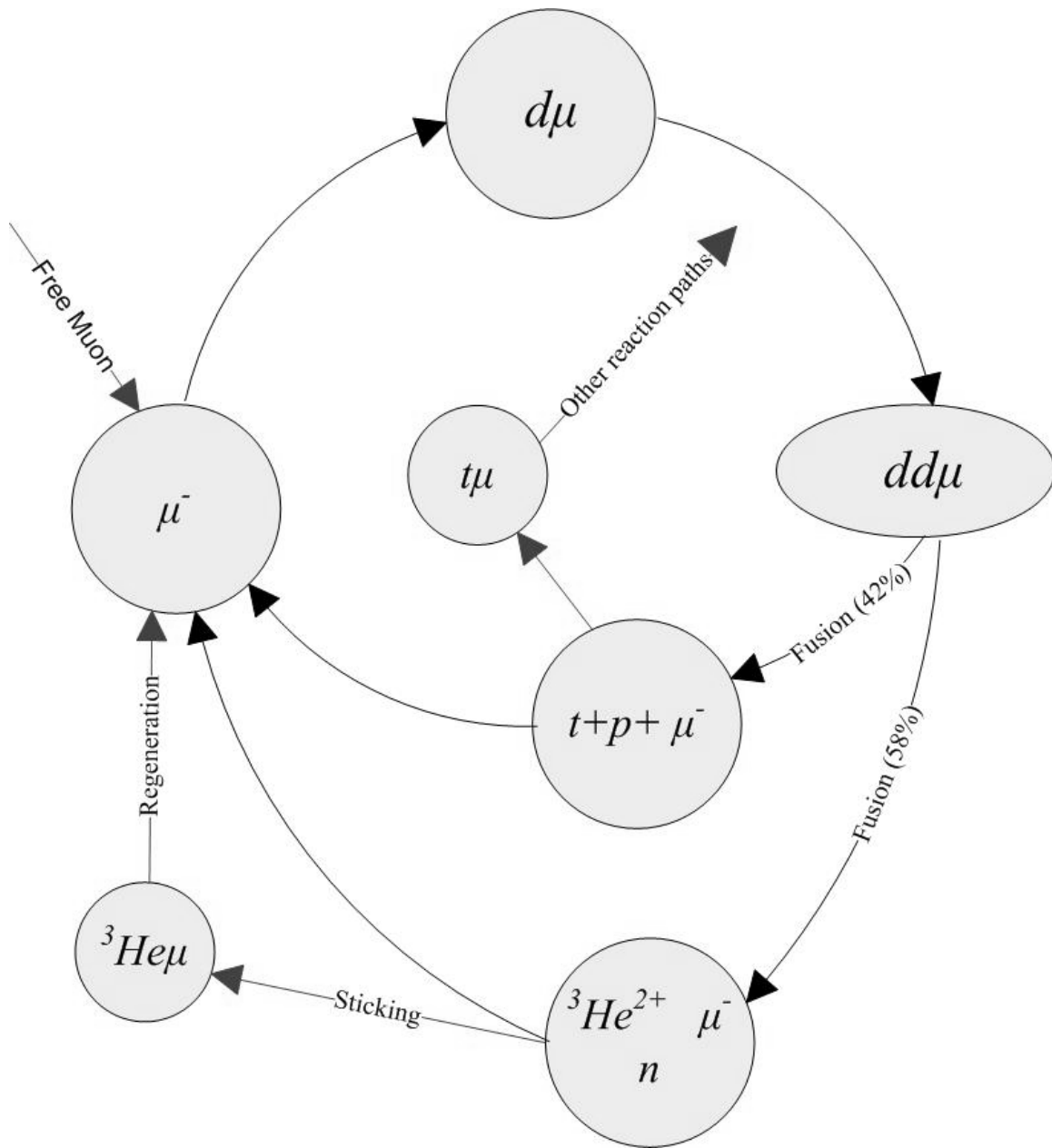


Figure 2-3. Major processes in the  $d\mu d$  muon-catalyzed fusion reaction cycle.

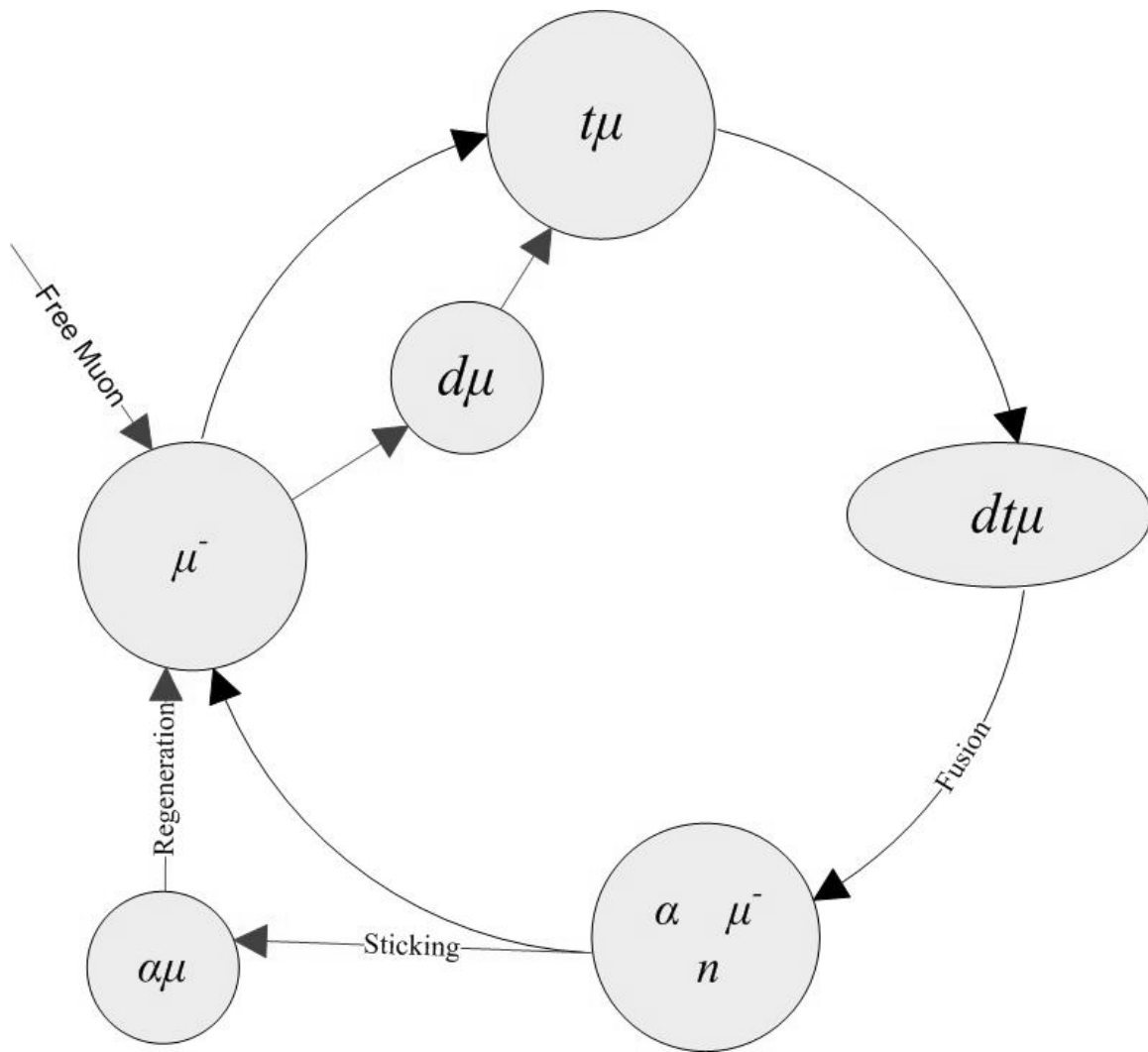
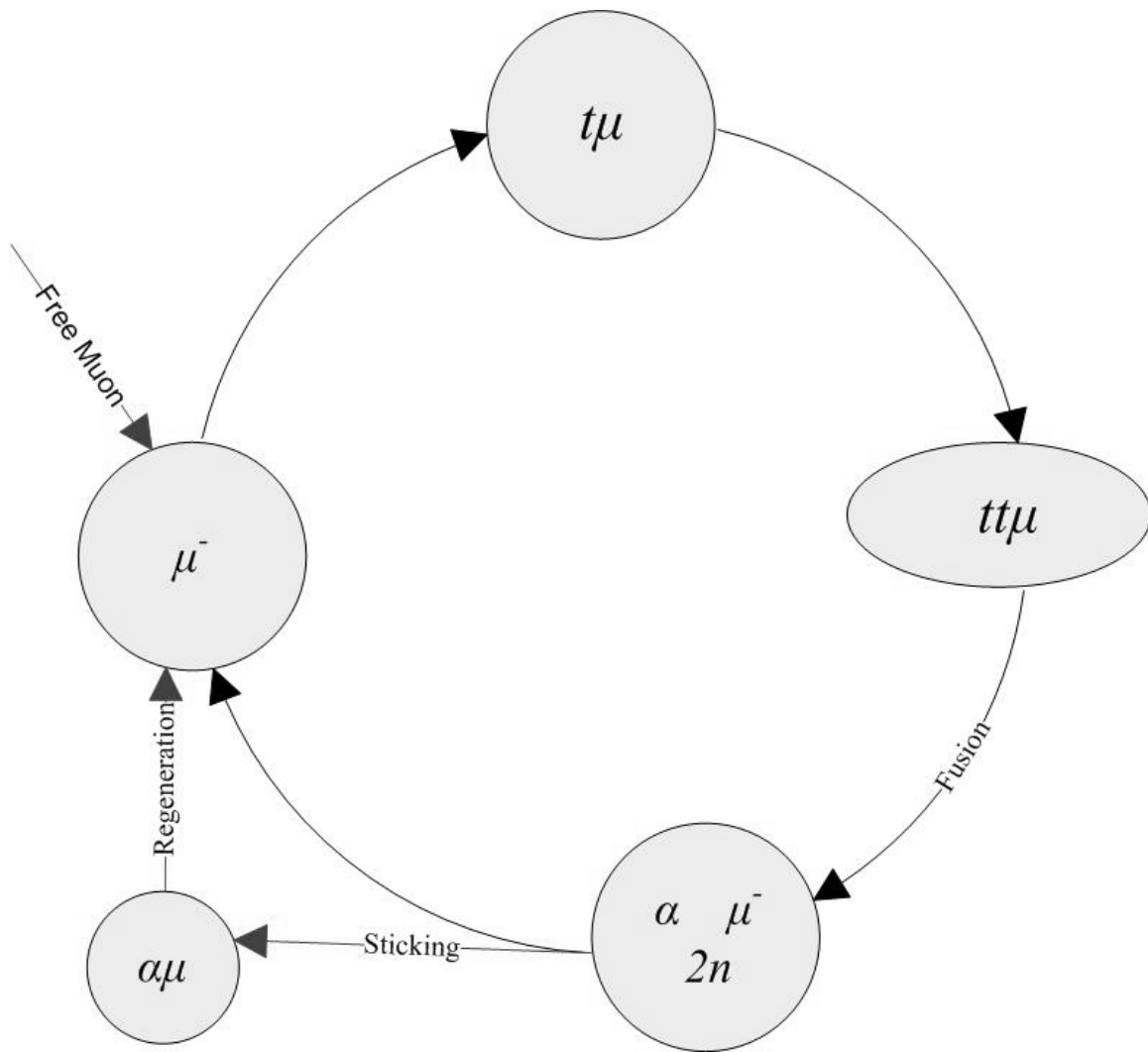


Figure 2-4. Major processes in the  $d\mu t$  muon-catalyzed fusion reaction cycle.



**Figure 2-5. Major processes in the  $t\mu t$  muon-catalyzed fusion reaction cycle.**

## 2.3 Muon-Catalyzed Fusion Yield

The initial impetus for most scientists pursuing muon-catalyzed fusion was a hope that it would provide a cheap, clean, and abundant source of energy. Due to  $\alpha$ -sticking (*i.e.*, muons sticking to  $^4\text{He}$  nuclei), the energy required to produce muons, and to a lesser degree the tri-atomic formation rates (*e.g.*,  $dd\mu d$ ), the goal of using muon-catalyzed fusion as a clean and efficient energy source has not been realized.

In order for single-muon catalyzed fusion to become an efficient source of energy, the energy required to produce muons must decrease, the number of fusions catalyzed per muon must increase, or a hybrid reactor must be used. Research in all three of these directions has proceeded, with some success. There has not, however, been sufficient success for a pure fusion reactor based on muon-catalyzed fusion to be feasible.

In 1978 Yu. Petrov presented the idea of a hybrid fusion-fission reactor based on muon-catalyzed fusion.[59; 60] It is generally believed that using existing technology, such a reactor could be built. In addition to energy production, muon-catalyzed fusion could be used to produce reactor or weapons grade plutonium-239 (see Section 2.5).

### 2.3.1 Muon Production

If the energy required to produce muons is decreased significantly, the feasibility of muon-catalyzed fusion as a pure fusion source of energy could change. A considerable amount of research aimed at reducing the energy required to produce muons continues, and some improvements have been attained; yet not enough for a pure fusion reactor to be designed.[1:17-39] While muon production is an important and interesting area of research, it is not dealt with in any detail in this document. This document

emphasizes the study of mechanisms that have the potential of increasing the number of fusions per muon obtainable.

### 2.3.2 Increasing the Number of Fusions per Muon

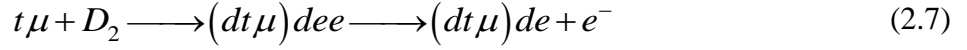
There are three factors that limit the average number of fusions muons can catalyze: 1) the muon half-life, 2) the muonic molecular reaction rates, and 3) the probability that muons are pulled out of a reaction cycle through  $\alpha$ -sticking or muon scavenging by non-reactive molecules (The terms  $\alpha$ -sticking and scavenging will be defined in sections 2.3.2.2 and 2.3.2.3 respectively). There is no proven way of significantly affecting the muon half-life, but there are things that can be done to affect the other two factors.

2.3.2.1 Muonic Molecular Reaction Rates. The slowest steps in the muon-catalyzed reaction cycles are the formation rates of  $p\mu d$ ,  $p\mu t$ ,  $d\mu d$ ,  $d\mu t$ , and  $t\mu t$  (see figures 5-1 through 5-5). As was mentioned in section 2.3.2, due to the existence of bound excited vibrational and rotational states, resonance stabilization occurs. This results in  $d\mu d$ ,  $d\mu t$ , and  $t\mu t$  forming more rapidly than  $p\mu d$ , and  $p\mu t$  which do not have bound excited vibrational states.[61] In order to significantly increase the muonic molecular reaction rates the rate these muonic-molecules form must increase, or a novel reaction path must be followed.

In actuality, the muonic hydrogen molecules  $p\mu d$ ,  $p\mu t$ ,  $d\mu d$ ,  $d\mu t$ , and  $t\mu t$  shown in Figures 2-1 through 2-5 are not normally formed in low-temperature muon-catalyzed fusion (see Appendix A). What is formed are tri-nuclear species in which two hydrogen nuclei are closely muonically bound (*e.g.*, 0.005 Å) and a third hydrogen atom is



electronically bound to the first two with a bond distance of approximately 1.06 Å. For example,



Although the electronically bound, nucleus does not have a significant impact on the rate at which the closely bound hydrogen nuclei fuse, it does have a significant impact on the formation rate of the tri-nuclear molecular species  $dd\mu p$ ,  $dd\mu d$ ,  $dd\mu t$ ,  $dt\mu p$ ,  $dt\mu d$ ,  $dt\mu t$ ,  $tt\mu p$ ,  $tt\mu d$ , and  $tt\mu t$  and can impact the rate which the ground rotational and vibrational states are reached. This impact is due to the existence of weakly bound rotational and vibrational states. The energy released on binding can be distributed between vibrations and rotations.[62]

2.3.2.2 Muon Sticking to Fusion Product. During muon-catalyzed fusion, muons will sometimes bind (*i.e.*, stick) to nuclei formed during fusion. When fusion results in products of different charge being formed, if the muon *sticks* to one of the products, it will almost always be to the product of greatest charge. When nuclei of different mass, but the same charge are formed, the muon will most often stick to the heavier product; if it sticks at all. It is currently believed that the probability a muon will stick to the lighter fusion product is so small that it can be neglected in describing muon-catalyzed fusion mechanisms.[47]

When fusion results in the formation of a muonic atom, or a muonic atomic ion, the muonic atom or ion will be in an excited muonic state. After formation of the muonic

atom or ion, collisions can cause the release, or transfer of the muon. This process is referred to as *stripping*. When a *stuck* muon is transferred to a molecule that allows it to continue catalyzing nuclear fusion, the process is known as *regeneration*. Stripping occurs readily when the muonic atom or ion is in a highly excited muonic state. It is less likely to occur when the atom or ion is in a low excited state, or in its ground state. The probability that a muon will stick to a fusion product ( $\omega$ ) minus the probability that it will be regenerated ( $R$ ) is referred to as an effective sticking constant ( $\omega^0$ ).

$$\omega^0 = \omega - R \quad (2.8)$$

Being that the probability of regeneration is dependent upon the probability of collisions occurring and on the energy of the collisions; there must be some density and temperature dependence on the effective sticking constant. As temperature and pressure increase the effective sticking probability decreases.[43; 50; 63; 64; 49]

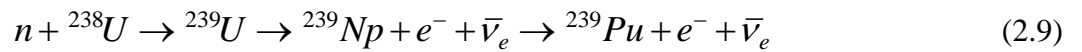
Many methods of enhancing regeneration have been considered, but as of the writing of this document, no effective method of preventing sticking or of regenerating muons stuck during fusion has been demonstrated.[63; 65; 64; 43; 66; 67; 68; 69] Regeneration in electric fields has been considered and may hold some promise.[70]

2.3.2.3 Muon Scavenging. In addition to muons sticking to fusion products, they can be removed from the catalytic fusion cycle by binding to non-reactive atoms within the reaction chamber or which make up the chamber walls. This process is referred to as *scavenging*. The probability of muon scavenging occurring is directly

proportional to the probability of muons, muonic atoms, and muonic ions colliding with atoms incapable of undergoing low temperature fusion. Therefore, the pressure, temperature, volume and inside surface area of the reaction chamber affects the scavenging rate and probability. Additionally, the concentration, nuclear charge, and mass of non-reactive atoms within the chamber affect the scavenging process and rate.

## 2.4 Applications of Muon-Catalyzed Fusion with Currently Obtainable Yields

While a pure fusion energy source is the goal most investigators studying muon-catalyzed fusion have pursued, it is not the only application of the process. Each  $d-t$  fusion produces a 14.1 MeV neutron and about 17.6 MeV of total energy. If a Uranium-238 (U-238) blanket is placed around the reaction chamber, each of these neutrons could initiate U-238 fission, releasing an additional 200 MeV of energy. This may well be high enough for muon-catalyzed fusion to be considered a practical energy source using current technology. During the fission process an average of about 4.1 neutrons per fission is produced. These neutrons are lower in energy than the  $dt$  fusion neutrons and rarely initiate further U-238 fission. These neutrons can, however, be absorbed by U-238, producing U-239 which decays to Pu-239



This method could be used to produce very high purity Pu-239 which could then be used in fission reactors or weapons. Assuming a maximum muon-catalyzed fusion yield of 300 fusions per muon, each muon could catalyze the production of 1230 atoms of

Pu-239. Assuming the maximum negative muon flux to be equal to that produced at the Gatchina synchrocyclotron ( $1.5 \times 10^{16} \mu^-/\text{s}$ ) [1:34] where the scientist who first proposed this method worked,[59; 60; 47] an upper limit for plutonium production is 231 kg/year. The total number of fissions resulting from one negative muon is about 1500 fissions (*i.e.*, considering both U-238 fusion and Pu-239). The total energy produced would be greater than 300 GeV per muon. These numbers represent an upper limit on the energy and number of fissions that could be produced, but even considering much lower efficiency, the usefulness of this process can be seen.

In addition to energy and Pu-239 production, there is another practical application of muon-catalyzed fusion. It can be used to produce slow, mono-energetic muons which are useful in many types of experiments.[4:32] Most sources of muons result in a wide spectrum of muons being produced. If moderated muons are shot into hydrogen, the muons released after fusion will be nearly mono-energetic. The energy of these mono-energetic muons will depend on which muon-catalyzed fusion reaction occurs, which depends on the isotopic mix of the reacting hydrogen.

## 2.5 Conclusions

In order for single-muon catalyzed fusion to be a useful source of energy, the energy required to produce muons must decrease, the number of fusions per muon must increase, or a hybrid reactor (*e.g.*, fusion-fission) must be used.

Advances in methods of muon production have been made, but the energy cost per muon is still too high for a pure fusion reactor based on currently tested muon-catalyzed fusion reactions.[4:17-39] While the design of a feasible pure fusion, muon-

catalyzed fusion reactor is likely a long way off, viable hybrid fusion-fission reactors could be built using existing technology.

## References

- [1] K. Nagamine, *Introductory Muon Science*, Cambridge: Cambridge University Press, 2003.
- [2] G. Kane, *Modern Elementary Particle Physics: The Fundamental Particles and Forces?*, Boulder: Westview Press, 1993.
- [3] A. Bettini, *Introduction to Elementary Particle Physics*, New York: Cambridge University Press, 2008.
- [4] National Research Council (U.S.), *Elementary-Particle Physics*, Elementary-Particle Physic, Washington DC: National Academy Press, 1990.
- [5] F. Halzen and A. D. Martin, *Quarks and Leptons: an Introductory Course in Modern Particle Physics*, New York: John Wiley and Sons, 1984.
- [6] K. M. Krane, *Introductory Nuclear Physics*, New York: John Wiley and Sons, Inc., 1988, p. 52.
- [7] P. J. Mohr, B. N. Taylor and D. B. Newell, "CODATA Recommended Values of the Fundamental Physical Constants: 2006," *Journal of Physical Chemistry Reference Data*, vol. 37, no. 3, pp. 1187-1284, 2008.
- [8] P. J. Mohr, B. N. Taylor and D. B. Newell, "CODATA Recommended Values of the Fundamental Physical Constants: 2006," *Reviews of Modern Physics*, vol. 80, no. 2, pp. 633-730, 2008.
- [9] J. J. Bevelacqua, *Basic Health Physics, Problems and Solutions*, New York: John Wiley & Sons, inc., 1999.
- [10] R. K. Adir and H. Kasha, "Cosmic Ray Muons," in *Muon Physics: Electromagnetic Interactions*, vol. 1, V. W. Hughes and C. S. Wu, Eds., New York, Academic Press, 1977, pp. 323-385.
- [11] S. E. Jones, "Muon-Catalysed Fusion Revisited," *Nature*, vol. 321, no. 6066, pp. 127-133, 1986.
- [12] L. I. Ponomarev, "Muon-Catalyzed Fusion and Fundamental Physics," *Hyperfine Interactions*, vol. 103, pp. 137-145, 1996.

- [13] J. Rafelski and S. E. Jones, "Cold Nuclear Fusion," *Scientific American*, pp. 84-90, 1987.
- [14] W. H. Breunlich, P. Kammel, J. S. Cohen and M. Leon, "Muon-Catalyzed Fusion," *Annual Review of Nuclear and Particle Science*, vol. 39, pp. 311-355, 1989.
- [15] K. Nagamine and M. Kamimura, "Muon Catalyzed Fusion: Interplay Between Nuclear and Atomic Physics," *Advances in Nuclear Physics*, vol. 24, pp. 151-205, 1998.
- [16] H. E. Refaelski, D. Harley, G. R. Shin and J. Rafelski, "Cold Fusion: Muon-Catalysed Fusion," *Journal of Physics B: Atomic, Molecular and Optical Physics*, vol. 24, pp. 1469-1516, 1991.
- [17] M. Hopkin, "Archaeology: Pyramid Power," *Nature*, vol. 430, no. 7002, p. 828, 2004.
- [18] R. Alfaro, E. Belmont-Moreno, A. Cervantes, V. Grabski, j. M. López-Robles, L. Manzanilla, A. Martínez-Dávalos, M. Moreno and A. Menchaca-Rocha, "A Muon Detector to be Installed at the Pyramid of the Sun," *Revista Mexicana de Física*, vol. 49, no. 4, pp. 54-59, 2003.
- [19] V. Grabski, A. Morales, R. Reche and O. Orozco, "Feasibility for p+/p- Flow-Ratio Evaluation in the 0.5-1.5 TeV Primary Energy Range, Based on Moon-Shadow Muon Measurements, to be Carried Out in the Pyramid of the Sun, Teotihuacan, Experiment," *Proceedings of the 30th International Cosmic Ray Conference*, vol. 5 (HE part 2), pp. 1543-1546, 2007.
- [20] R. Alfaro, E. Belmont, V. Grabski, L. Manzanilla, A. Martinez-Davalos, A. Menchaca-Rocha, M. Moreno and A. Sandoval, "Searching for Possible Hidden Chambers in the Pyramid of the Sun," in *Proceedings of the 30th International Cosmic Ray Conference*, Mérida, 2007.
- [21] R. Alfaro, "Radiographic Images Produced by Cosmic-Ray Muons," in *Particles and Fields, Part B: Commemorative Volume of the Division of Particles and Fields of the Mexican Physical Society*, Mexico City, 2006.
- [22] F. I. Bedewi, A. Goned and A. H. Girgis, "Energy Spectrum and Angular Distribution of Cosmic Ray Muons in the Range 50-70 GeV," *Journal of Physics A*, vol. 5, no. 2, pp. 292-302, 1972.

- [23] L. W. Alvarez, J. A. Anderson, F. E. Bedwei, J. Burkhard, A. Fakhry, A. Girgis, A. Goneid, H. Fikhry, D. Iverson, G. Lynch, Z. Miligy, A. Hilmy, M. Sharkawi and L. Yazolino, "Search for Hidden Chambers in the Pyramids," *Science*, vol. 167, no. 3919, pp. 832-839, 1970.
- [24] W. C. Priedhorsky, K. N. Borozdin, G. E. Hogan, C. Morris, A. Saunders, L. J. Schultz and M. E. Teasdale, "Detection of High-Z Objects Using Multiple Scattering of Cosmic Ray Muons," *Review of Scientific Instruments*, vol. 74, no. 10, pp. 4294-4297, 2003.
- [25] T. Konkel, "Container Security: Preventing a Nuclear Catastrophe," *The Journal of International Policy Solutions*, pp. 1-23, 2006.
- [26] C. L. Morris, C. C. Alexander, J. D. Bacon, K. N. Borozdin, D. J. Clark, R. Chartrand, C. J. Espinoza, A. M. Fraser, M. C. Galassi, J. A. Green, J. S. Gonzales, J. J. Gomez, N. W. Hengartner, A. V. imenko, M. c. Makela, J. J. Medina, F. E. Pazuchanics, W. C. Priedhorsky, J. C. Ramsey, A. Saunders, R. C. Schirato, L. J. Schultz, M. Sossong, J. and G. S. Blanpied, "Tomographic Imaging with Cosmic Ray Muons," *Science & Global Security*, vol. 16, no. 1 & 2, pp. 37-53, 2008.
- [27] R. C. Hoch, *Advances in Cosmic Ray Muon Tomography Reconstruction Algorithms*, Florida Institute of Technology, 2009.
- [28] Heming, E. Roduner, I. D. Reid, P. Louwrier, W. F., J. W. Schneider, H. Deller, W. Odermatt, B. D. Patterson, H. Simmler, B. Pumpin and I. M. Savic, "The Separation of Chemical Reactivity and Heisenberg Spin-Exchange Effects in a Radical-Radical reaction by Avoided Level Crossing  $\mu$ SR," *Chemical Physics*, vol. 129, no. 3, pp. 335-350, 1989.
- [29] F. C. Frank, "Hypothetical Alternative Energy Sources for the 'Second Meson' Events," *Nature*, pp. 525-527, 1947.
- [30] A. D. Sakharov, "Passivnye Mezony," Moscow, 1948.
- [31] A. Fisher, "Cold Fusion," *Popular Science*, pp. 54-55, 100, 1987.
- [32] S. S. Gerstein and L. I. Ponomarev, " $\mu^-$  Meson Catalysis of Nuclear Fusion in a Mixture of Deuterium and Tritium," *Physics Letters B*, vol. 72, no. 1, pp. 80-82, 1977.



- [33] S. E. Jones, A. N. Anderson, A. J. Caffrey, J. B. Walter, K. D. Watts, J. N. Bradbury, P. A. M. Gram, M. Leon, H. Maltrud and M. A. Paciotti, "Experimental Investigation of Muon-Catalyzed d-t Fusion," *Physical Review Letters*, vol. 51, pp. 1757-1760, 1983.
- [34] M. A. Paciotti, A. N. Anderson, A. J. Caffrey and S. E. Jones, [Interview]. 1988.
- [35] M. A. Paciotti, O. K. Baker, J. N. Bradbury, J. S. Cohen, M. Leon, H. R. Maltrud, L. L. Sturgess, S. E. Jones, P. Li, L. M. Rees, E. V. Sheely, J. K. Shurtleff, S. F. Taylor, A. N. Anderson, A. J. Caffrey, J. M. Zabriskie, F. D. Brooks, W. A. Cilliers, J. D. Davis, J. England, B. A., G. J. Pyle, G. T. A. Squier, A. Bertin, M. Bruschi, M. Piccinini, A. Vitale, A. Zoccoli, V. R. Bom, C. W. E. van Eijk, H. de Haan and G. H. Eaton, "First Direct Measurement of  $\alpha$ - $\mu$  Sticking in dt- $\mu$ CF," *American Institute of Physics Conference Proceedings*, vol. 181, pp. 38-51, 1988.
- [36] S. E. Jones, A. Anderson, A. J. Caffrey, C. d. Van Sicien, K. D. Watts, J. N. Bradbury, J. S. Cohen, p. A. M. Gram, M. Leon, H. R. Maltrud and M. A. Paciotti, "Observation of Unexpected Density Effects in Muon-Catalyzed d-t Fusion," *Physical Review Letters*, vol. 56, pp. 588-591, 1986.
- [37] J. D. Jackson, "Catalysis of Nuclear Reactions between Hydrogen Isotopes by  $\mu$ -Mesons," *Physical Review*, vol. 106, no. 2, pp. 330-339, 1957.
- [38] R. M. Kulsrud, "A Proposed Method for Reducing the Sticking Constant in M. C. F.," *American Institute of Physics Conference Proceedings*, vol. 181, pp. 367-380, 1988.
- [39] H. E. Rafelski and B. Müller, "Density Dependent Stopping Power and Muon Sticking in Muon-Catalyzed D-T Fusion," *American Institute of Physics Conference Proceedings*, vol. 181, pp. 355-366, 1988.
- [40] M. Kamimura, "Effect of Nuclear Interaction on Muon Sticking to Helium in Muon-Catalyzed d-t Fusion," *American Institute of Physics Conference Proceedings*, vol. 181, pp. 330-343, 1988.
- [41] M. Danos, L. C. Biedenharn and A. Stahlhofen, "Comprehensive Theory of Nuclear Effects on the Intrinsic Sticking Probability: I," *American Institute of Physics Conference Proceedings*, vol. 181, pp. 308-319, 1988.
- [42] P. Froelich and G. Larson, " $\alpha\mu$  Stripping by Ionization in Dense Deuterium/Tritium Mixture, and its Implication for Muon Catalyzed Fusion," *Journal of Molecular Structure: Theochem*, vol. 199, pp. 189-200, 1989.

- [43] S. Eliezer, "Muon Catalyzed Nuclear Fusion," *Laser and Particle Beams*, vol. 6, pp. 63-81, 1988.
- [44] J. Rafelski, "The Challenges of Muon Catalyzed Fusion," *American Institute of Physics Conference Proceedings*, vol. 181, pp. 451-464, 1988.
- [45] R. Gajewski, "The Political Economy of Muon-Catalyzed Fusion Research," *American Institute of Physics Conference Proceedings*, vol. 181, pp. xi-xii, 1988.
- [46] D. Harley, B. Muller and J. Rafelski, "Muon Catalysed Fusion of Nuclei with  $Z > 1$ ," *Journal of Physics G: Nuclear and Particle Physics*, vol. 16, no. 2, pp. 281-294, 1990.
- [47] M. Jändel, P. Froelich, G. Larson and C. D. Stodden, "Reactivation of  $\alpha\mu$  in Muon-Catalyzed Fusion Under Plasma Conditions," *Physical Review A*, vol. 40, pp. 2799-2802, 1989.
- [48] G. Cripps, A. A. Harms and B. Goel, "Muon Catalyzed Fusion of Deuterium-Tritium at Elevated Densities," *Hyperfine Interactions*, vol. 77, no. 1, pp. 181-199, 1993.
- [49] J. S. Cohen, "Slowing down and capture of negative muons by hydrogen: Classical-trajectory Monte Carlo calculation," *Physical Review A: Atomic, Molecular, and Optical Physics*, vol. 27, no. 1, pp. 167-179.
- [50] W. H. Breunlich, P. Kammel, J. S. Cohen and M. Leon, "Muon-Catalyzed Fusion," *Annual Review of Nuclear and Particle Science*, vol. 39, pp. 311-355, 1989.
- [51] L. I. Ponomarev, "Muon Catalysed Fusion," *Contemporary Physics*, vol. 31, no. 4, pp. 219-245, 1990.
- [52] C. Petitjean, D. V. Balin, V. N. Baturin, P. Baumann, W. H. Breunlich, T. Case, K. M. Crowe, H. Daniel, Y. Grigoriev, F. J. Hartmann, A. I. Ilyin, M. Jeitler, P. Kammel, B. Lauss, K. Lou, E. M. Maev, J. Marton, M. Muhlbauer, G. E. Petrov, W. Prymas, W. Schott, G. G. Semenchuk, Y. Smirenin, A. A. Vorobyov, N. I. Voropaev, P. Wojciechowski and J. Zmeskal, "Experimental Survey of the Sticking Problem in Muon Catalyzed de Fusion," *Hyperfine Interactions*, vol. 82, no. 1-4, pp. 273-293, 1993.

- [53] J. D. Davies, J. B. A. Dngland, G. J. Pyle, G. T. A. Squier, F. D. Brooks, W. A. Cilliers, A. Bertin, M. Bruschi, M. Piccinini, A. Vitale, A. Zoccoli, S. E. Jones, V. R. Bom, C. W. E. van Eijk, H. de Hann, A. H. Anderson, M. A. Paciotti, G. H. Eaton and B. Alper, "A Direct Measurement of the Alpha-Muon Sticking Coefficient in Muon-Catalysed d-t Fusion," *Journal of Physics G: Nuclear and Particle Physics*, vol. 16, no. 10, pp. 1529-1538, 1990.
- [54] C. D. Stodden, H. J. Monkhorst, K. Szalewicz and T. G. Winter, "Muon Reactivation in Muon-Catalyzed d-t Fusion from Accurate p-He<sup>+</sup> Stripping and Excitation Cross Sections," *Physical Review A*, vol. 41, no. 3, pp. 1281-1292, 1990.
- [55] S. E. Jones, "Survey of Experimental Results in Muon-Catalyzed Fusion," *American Institute of Physics Conference Proceedings*, vol. 181, pp. 2-15, 1988.
- [56] K. Magamine, T. Matsuzaki, K. Ishida, S. N. Nakamura, N. Kawamura and Y. Matsuda, "Contribution of Muon Catalyzed Fusion to Fusion Energy Development," in *18th International Conference on Fusion Energy 2000*, 2000.
- [57] D. V. Balin, V. I. Maev, G. G. Medvedev, G. G. Semenchuk, Y. V. Smirenin, A. A. Vorobyov, A. A. Vorobyov and Y. K. lite, "Experimental Investigation of the Muon Catalyzed dd-Fusion," *Physics Letters B*, vol. 141, no. 3-4, pp. 173-176, 1984.
- [58] H. Bossy, H. Daniel, F. J. Hartmann, H. S. Plendi, G. Schmidt and T. von Egidy, "Determination of Muonic Helium X-Ray Yields after Muon-Catalyzed pd, dd, and dt Fusion," *Physical Review Letters*, vol. 59, pp. 2864-2867, 1987.
- [59] K. Nagamine, T. Matsuzaki, K. Ishida, Y. Hirata, Y. Watanabe, R. Kadono, Y. Miyake, K. Nishiyama, S. E. Jones and H. R. Maltrud, "Muonic x-ray measurement on the mu- sticking probability for muon catalyzed fusion in liquid d-t mixture," *Muon Catalyzed Fusion*, vol. 1, pp. 137-138, 1987.
- [60] K. Nagamine, K. Ishida, S. Sakamoto, Y. Watanabe and T. Matsuzaki, "X-Ray Measurement on Muon to Alpha Sticking in Muon Catalyzed d-t Fusion; Present and Future," *Hyperfine Interactions*, vol. 82, no. 1-4, pp. 343-353, 1993.
- [61] T. Matsuzaki, K. Nagamine, K. Ishida, S. N. Nakamura, N. Kawamura, M. Tanase, M. Kato, K. Kurosawa, M. Hashimoto, H. Sugai, K. Kudo, N. Takeda and G. Eaton, "Muon Catalyzed Fusion and Muon to <sup>3</sup>He Transfer in Solid T2 Studied by X-ray and Neutron Detection," *RIKEN Review*, vol. 20, pp. 18-20, 1999.

- [62] T. Matsuzaki, K. Nagamine, K. Ishida, S. N. Nakamura, N. Kawamura, M. Tanase, M. Kato, K. Kurosawa, M. Hashimoto, H. Sugai, K. Kudo, N. Takeda and G. Eaton, "Muon-Catalyzed Fusion and Muon to  $^3\text{He}$  Transfer in Solid T<sub>2</sub> Studied by X-ray and Neutron Detection," *Hyperfine Interactions*, vol. 118, no. 1-4, pp. 229-234, 1999.
- [63] Y. V. Petrov, "Muon Catalysis for Energy Production by Nuclear Fusion," *Nature*, vol. 285, pp. 466-468, 1980.
- [64] Y. V. Petrov, "Conceptual scheme of a hybrid mesocatalytic fusion reactor," *Atomnaya Énergiya*, vol. 63, no. 5, p. 333-341, 1987.
- [65] M. Leon, "Theory of Muonic Molecule Formation: Survey of Progress and Open Questions," *Hyperfine Interactions*, vol. 82, pp. 151-160, 1993.
- [66] M. Leon, "Theory of muonic molecule formation: Survey of progress and open questions," *Hyperfine Interactions*, vol. 82, no. 1-4, pp. 151-160, 1993.
- [67] M. R. Pahlavani and S. M. Motevalli, "The Probability of Muon Sticking and X-Ray Yields in the Muon Catalyzed Fusion Cycle in a Deuterium and Tritium Mixture," *ACTA Physica Polonica B*, vol. 39, no. 3, pp. 683-694, 2008.
- [68] B. Jeziorski, K. Szalewicz, A. Scrinzi, X. Zhao and R. Moszynski, "Muon Sticking Fractions for S States of the  $\text{td}\mu$  Ion Including the Effects of Nuclear Interactions," *Physical Review A*, vol. 43, no. 3, pp. 1281-1292, 1991.
- [69] M. R. Pahlavani and S. M. Motevalli, "Study of Muon Catalyzed Fusion in Deuterium-Tritium Fuel under Compressive Conditions," *ACTA Physica Polonica B*, vol. 40, no. 2, pp. 319-329, 2009.
- [70] S. Saini and K. C. Kulander, "Muon Catalyzed Fusion: Muon Capture by Proton From K- and L-Shells of  $\alpha\mu^*$ ," *Chines Journal of Physics*, vol. 29, no. 2, pp. 115-129, 1991.
- [71] C. D. Stodden, H. J. Monkhorst, K. Szalewicz and T. G. Winter, "Muon Reactivation in Muon-Catalyzed d-t Fusion from Accurate p-He<sup>+</sup> Stripping and Excitation Cross Sections," *Physical Review A*, vol. 41, no. 3, pp. 1281-1292, 1990.
- [72] L. Burggraf, Interviewee, *Muon Regeneration in Electric Fields*. [Interview]. Aug 2010.

- [73] E. V. Sheely, S. E. Jones, L. M. Rees, S. F. Shurtleff, S. F. Taylor and J. M. Thorne, "Predicted Methods of Changing the Muon Catalized Fusion Cycling Rate," *American Institute of Physics Conference Proceedings*, vol. 181, pp. 79-91, 1988.
- [74] Z. Henis, S. Eliezer and V. B. Mandelzweig, "Can the  $\mu\alpha$  Stripping Probability be Enhanced by Strong Electromagnetic Fields?," *Physics Letters A*, vol. 146, no. 4, pp. 222-225, 1990.

### III. Novel Muon-Catalyzed Fusion Reaction Paths

In this chapter three novel muon-catalyzed fusion reaction paths which have the potential to increase the number of fusions per muon that can be catalyzed will be presented: 1) replacing the weakly bound hydrogen nuclei in tri-nuclear muonic molecules with a positive muon or a positron, 2) using di-muonic reactions to free stuck muons, and 3) using di muonic-reactions to increase the formation rate of tri-nuclear muonic hydrogen. The second and third of these novel reaction paths will be addressed in detail in Chapters 6 through 8 of this document.

#### 3.1 Addition of Positive Muons and Positrons

During muon-catalysis of hydrogen fusion, molecules of the form  $(x\mu y)zee$  are formed where  $x$ ,  $y$  and  $z$  represent hydrogen isotopes.  $\mu$  and  $e$  represent negative muons and electrons respectively.  $x$ ,  $y$  and  $z$  may or may not be equivalent. The equilibrium bond length between  $x$  and  $y$  is about 0.005 Å. The  $x$ - $z$  and  $y$ - $z$  bond length is around 0.74 Å (see Chapters 4 and 7).

The rate at which the isotopes  $x$  and  $y$  fuse is affected very little by the mass of  $z$ ; however, the rate of  $(xy\mu)zee$  formation is strongly influenced by the mass of  $z$  (see Table 3-1).[1; 2; 3; 4; 5]. When  $z$  represent the three hydrogen isotopes  $p$ ,  $d$ , and  $t$  (*i.e.*,  $^1H$ ,  $^2H$ , and  $^3H$  respectively) the lighter the mass of  $z$ , the faster the formation rate. From this, the question arises, what happens if the mass of  $z$  is decreased even further by substitution with a positive muon or a positron? The binding energy will decrease as a result of the smaller mass. In the case of a positive muon being added to the system, the

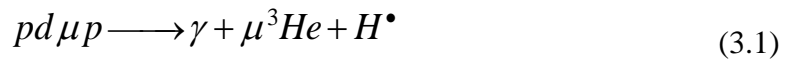
binding energy will increase as a result of correlation energy between the oppositely charged particles (the closer the mass of the particles is to each other, the greater the correlation energy). In the case of a positron, the correlation energy would further decrease due to the relative difference in mass between a negative muon and a positron. Which of these factors predominates and how they affect the excited state binding energy and molecular formation rate is an open question. The author is unaware of any calculations or experiments having been performed to address these questions.

**Table 3.1. Formation rate ( $\lambda$ ) of ground vibrational state  $(dt\mu)d$  and  $(dt\mu)t$  at 300 K. Values are experimental, taken from reference.[6; 7]**

Molecule	$\lambda(\text{s}^{-1})$
$(dt\mu)p$	$2 \times 10^{10}$
$(dt\mu)d$	$4 \times 10^8$
$(dt\mu)t$	$2 \times 10^7$

### 3.2 A Novel Approach to Decrease Muon Loss Due to Sticking

One of the products of  $p$ - $d$  and  $d$ - $d$  fusion is  ${}^3\text{He}$ ; some of the muons which catalyze fusion reactions will bind to a  ${}^3\text{He}$  nucleus:



$$pd\mu d \longrightarrow \gamma + \mu^3He + D^\bullet \quad (3.2)$$

$$dd\mu p \longrightarrow \mu^3He + H^\bullet + n_1 \quad (3.3)$$

$$dd\mu d \longrightarrow \mu^3He + D^\bullet + n_1 \quad (3.4)$$

This process is referred to as muon sticking. In the case of  $d$ — $d$  fusion the probability of the muon sticking to  $^3He$  is about 12%. An effective method of stripping the muons from the  $^3He$  nucleus so that the muons can continue to catalyze fusion events has so far not been demonstrated.

An alternative to stripping the muon from the  $^3He$  nucleus is to fuse the  $^3He$  via the reactions:

$$D + ^3He \longrightarrow ^4He + p \quad (3.5)$$

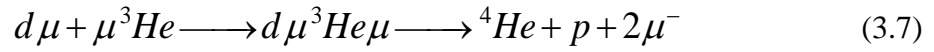
or

$$^3He + ^3He \longrightarrow ^4He + 2p \quad (3.6)$$

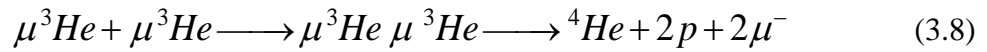
The problem with this approach is that the Coulombic repulsion between these nuclei is greater than the repulsion between two hydrogen nuclei. As a result, a single muon



doesn't bring the nuclei close enough together for them to fuse. What had not been studied, prior to the results presented in this document, is what happens when there are two negative muons participating in the reactions. For example:



and



(see Figures 3-1 and 3-2). These reactions will be studied in detail and presented in Chapter 6.

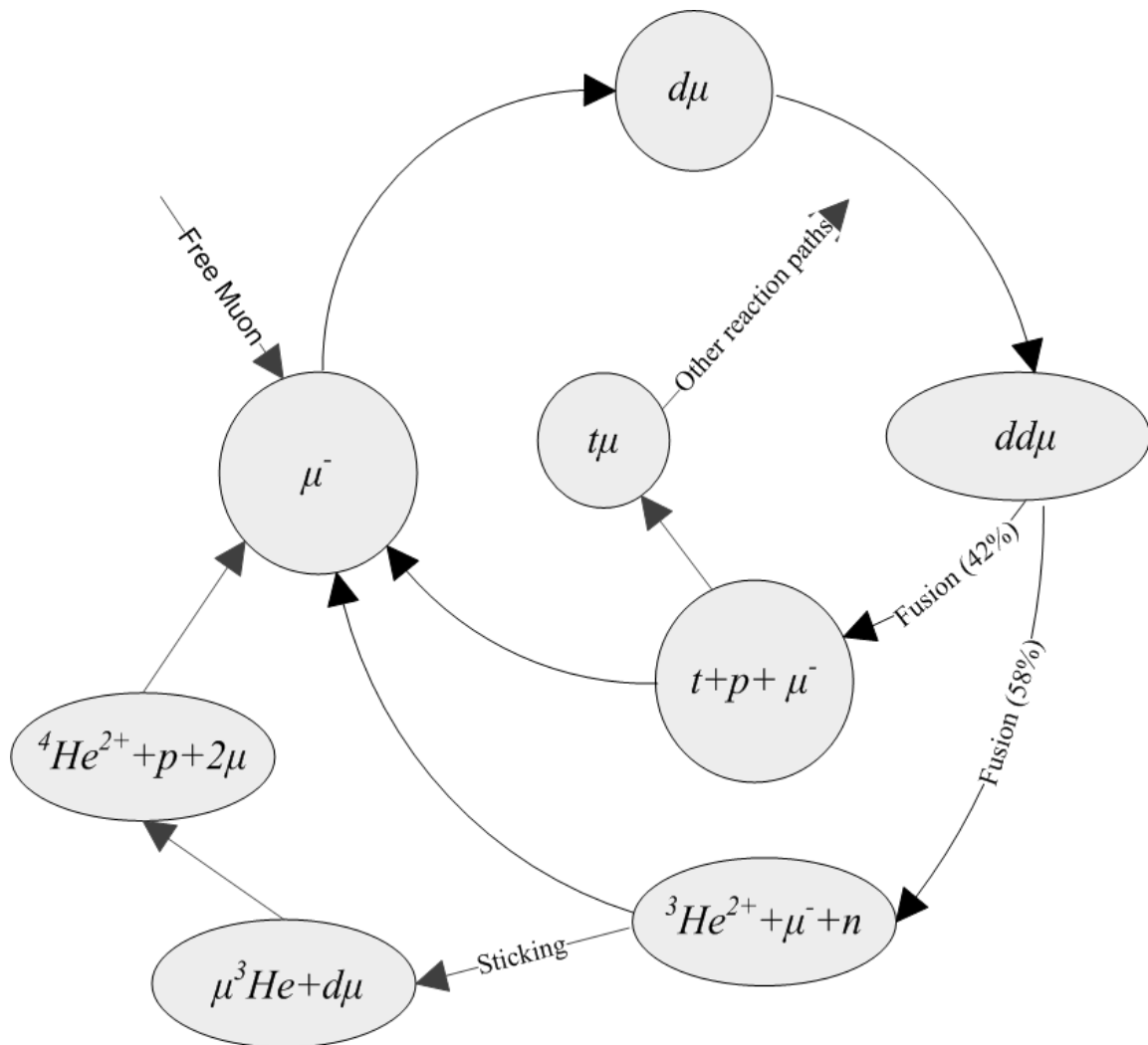


**Figure 3-1** Reaction cycle for using  $d\mu$ - ${}^3\text{He}\mu$  fusion to regenerate  $\mu^-$  during  $d\mu d$  muon-catalyzed fusion.

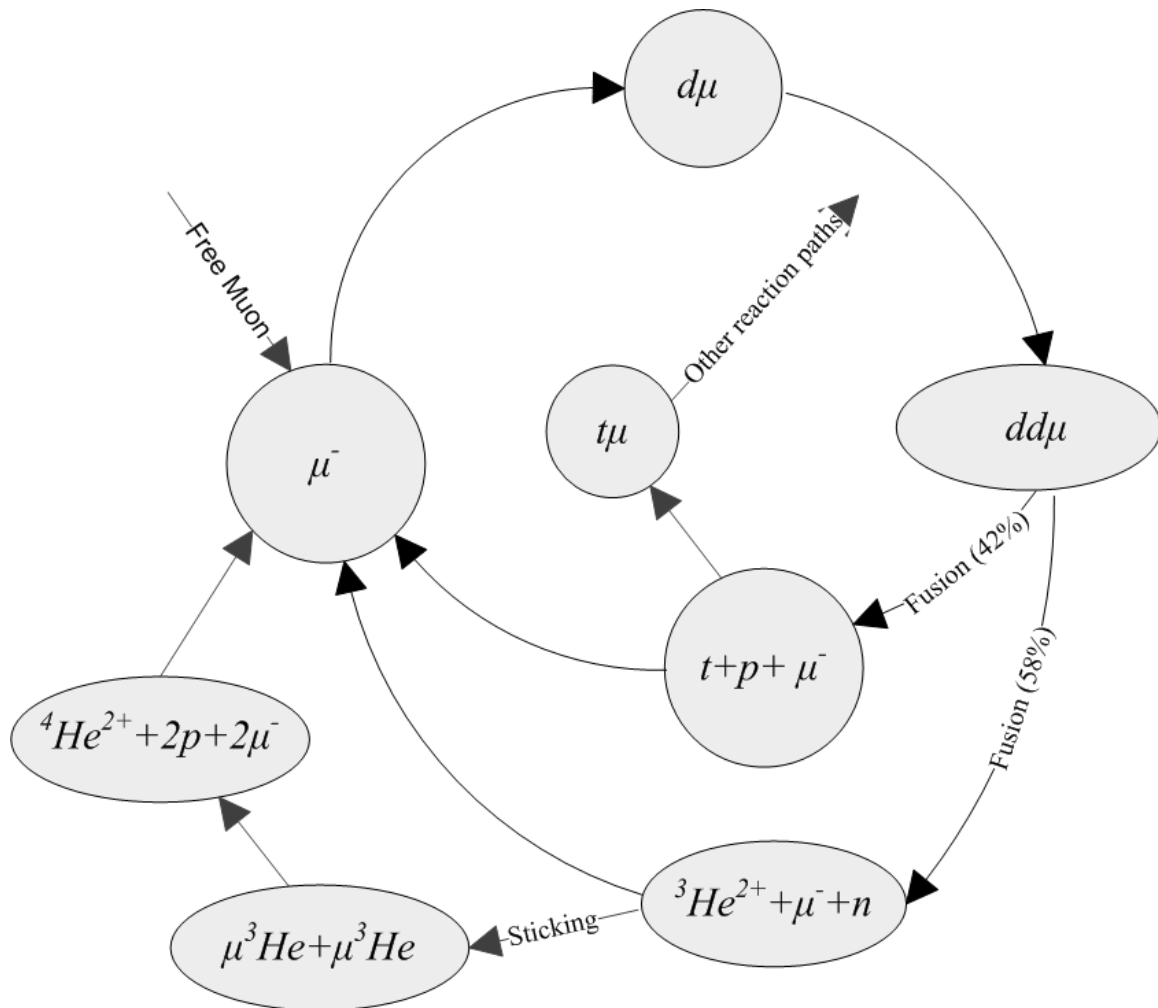


**Figure 3-2** Reaction cycle for using  ${}^3\text{He}\mu$ - ${}^3\text{He}\mu$  fusion to regenerate  $\mu^-$  during  $d\mu d$  muon-catalyzed fusion.

### 3.3 Two-Muon Catalyzed-Fusion

The slowest step in a homogeneous single-muon catalyzed fusion reaction chain is often considered to be the formation of tri-nuclear molecules that result in fusion (see Figures 2-1 to 2-5 and Appendix A). In actuality, this muonic molecular system forms readily; however, it most often forms in a rotationally and vibrationally excited state that is only slightly bound. In excited states, the molecules are much more likely to dissociate than to fuse, or fall to a more stable vibrational and rotational state which later fuses. The formation rate most often reported in the literature is not the average rate of formation; rather it is an effective rate. It represents the average rate of formation of a tri-nuclear molecule which later fuses (*i.e.*, those which dissociate are neglected).[6; 8]

Prior to this work, it was not certain what would happen if exotic hydrogen molecules containing two negative muons were formed (see Chapters 4, 5 and 7). It was predicted that the bond distance between the hydrogen molecules would be shorter, resulting in a system which fuses more rapidly, possibly from an excited state.[9] Some di-muonic hydrogen molecules are bound more strongly than single muon molecules and have richer rotational manifolds. Figures 3-3 and 3-4 gives examples of how the presence of di-muonic hydrogen molecules could change a muon-catalyzed fusion reaction cycle.

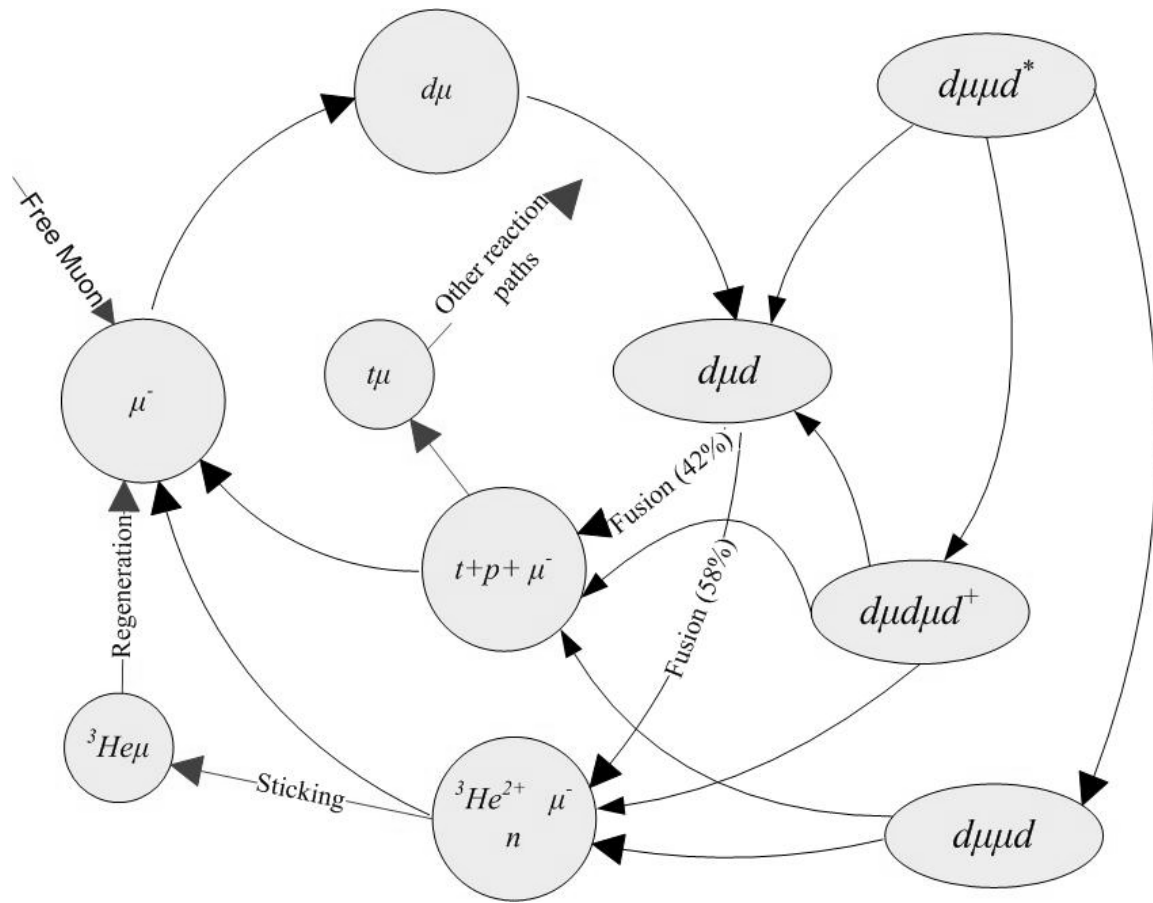


**Figure 3-3** Reaction cycle for  $d\mu d^+$  and  $d\mu\mu d$  fusion.

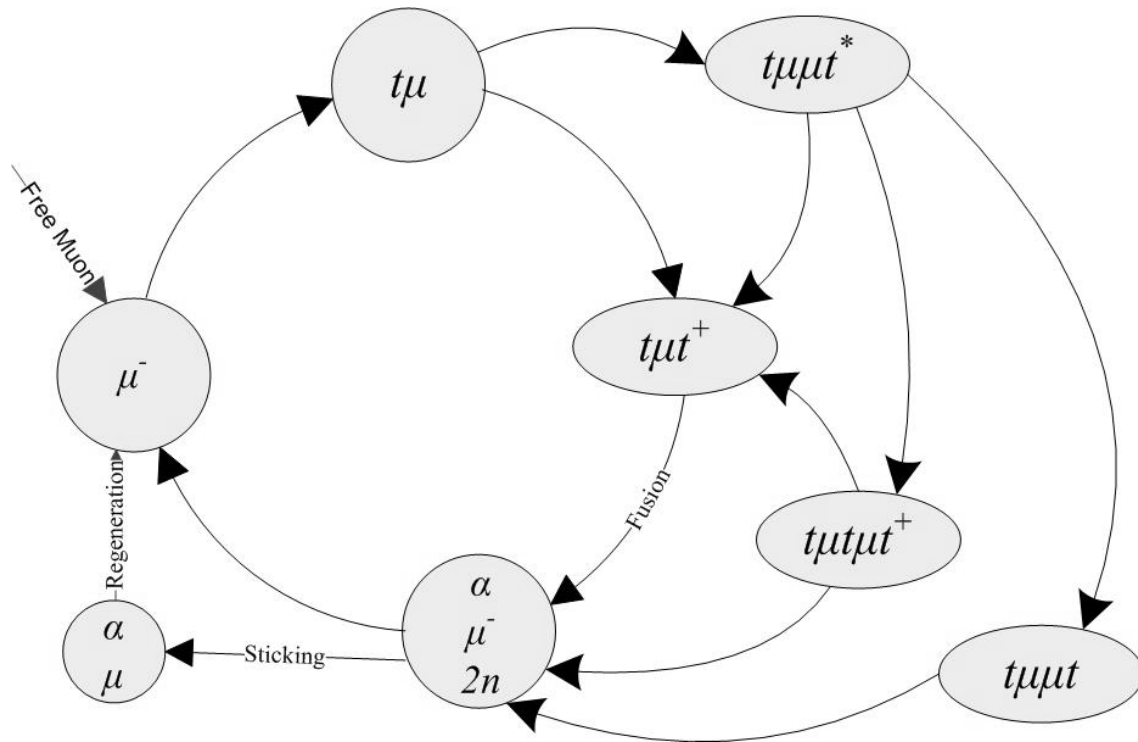


Figure 3-4 Reaction cycle for  $t\mu t^+$  and  $t\mu\mu t$  fusion.

### 3.4 Enhance Fusion Yields with Electromagnetic Radiation

Spatially coherent electromagnetic radiation could be used to selectively break apart undesirable molecules within a fusion reaction chamber. [10; 11] An obvious place where this could be applied is in freeing muons bound to nonreactive nuclei. Not having a method of efficiently regenerating muons bound to helium nuclei is one of the major factors preventing muon-catalyzed fusion from being an efficient stand alone source of energy. In addition to freeing bound muons, electromagnetic radiation could be used to dissociate undesirable hydrogen molecules. An example of when this would be desirable is when deuterium and tritium are both present in a reaction chamber. At optimum

muon-catalyzed fusion reaction temperatures the reaction rate of DT with muonic hydrogen atoms is slower than the reaction rates of  $D_2$  and  $T_2$ . Due to the presence of tritium betas, at optimum reaction temperatures, mixtures of  $D_2$  and  $T_2$  quickly reach equilibrium with DT. The use of photons to selectively dissociate DT molecules could have benefits. The benefits of using electromagnetic radiation in this manner need to be weighed against the energy cost of its production.

While the use of lasers to enhance muon-catalyzed fusion yields is worthy of study; it is not the only method of decreasing the concentration of undesirable molecules in reaction chambers, or of freeing bound muons. For example, synthetic zeolites could be used to separate molecular isotopes of hydrogen [12; 10] as could thermal diffusion and gas chromatography.[10]

### **3.5 Conclusions**

There are several novel reaction paths that have the possibility of increasing the number of fusions catalyzed per muon. This includes adding positive muons or positrons to the fusing muonic molecules and using multiple negative muons to increase the reaction rate. Two methods of using multiple negative muons to increase the number of fusions per muon that can be obtained were discussed in this chapter. The majority of this dissertation is devoted to the study of these methods.

## References

- [1] M. P. Faifman and L. I. Ponomarev, "Resonant Formation of  $dt\mu$  mesic molecules in the triple  $H_2+D_2+T_2$  Mixture," *Physics Letters B*, vol. 265, pp. 201-206, 1991.
- [2] M. P. Faifman, L. I. Men'shikov and T. A. Strizh, "Studies on muonic dynamics of liquid D–T–H in  $dt\mu$ ," *Muon Catalyzed Fusion*, vol. 4, p. 1, 1989.
- [3] W. H. Breunlich, P. Kammel, J. S. Cohen and M. Leon, "Muon-Catalyzed Fusion," *Annual Review of Nuclear and Particle Science*, vol. 39, pp. 311-355, 1989.
- [4] M. Leon, "Theory of Muonic Molecule Formation: Survey of Progress and Open Questions," *Hyperfine Interactions*, vol. 82, pp. 151-160, 1993.
- [5] I. A. Alekseev, I. A. Baranov, V. A. Novozhilov, G. A. Sukhorukova and V. D. Trenin, "Separation of Hydrogen Isotopes  $H_2$ -HT and  $D_2$ -DT by Adsorption on NaA Synthetic Zeolites," *Atomnaya Energiya*, vol. 54, no. 6, pp. 409-411, 1982.
- [6] Y. Hamahata, E. Hiyama and M. Kamimura, "Non-Adiabatic Four-Body Calculation of Double-Muonic Hydrogen Molecules," *Hyperfine Interactions*, vol. 138, no. 187-190, 2001.
- [7] L. I. Ponomarev, "Muon Catalysed Fusion," *Contemporary Physics*, vol. 31, no. 4, pp. 219-245, 1990.
- [8] L. I. Ponomarev, "Muon-Catalyzed Fusion and Fundamental Physics," *Hyperfine Interactions*, vol. 103, pp. 137-145, 1996.
- [9] W. H. Breunlich, P. Kammel, J. S. Cohen and M. Leon, "Muon-Catalyzed Fusion," *Annual Review of Nuclear and Particle Science*, vol. 39, pp. 311-355, 1989.
- [10] H. E. Rafelski, D. Harley, G. R. Shin and J. Rafelski, "Cold Fusion: Muon-Catalysed Fusion," *Journal of Physics B: Atomic, Molecular and Optical Physics*, vol. 24, pp. 1469-1516, 1991.
- [11] Z. Henis, S. Eliezer and V. B. Mandelzweig, "Can the Mu-alpha Stripping Probability be Enhanced by Strong Electromagnetic Fields?," *Physics Letters A*, vol. 146, no. 4, pp. 222-225, 1990.



- [12] E. V. Sheely, S. E. Jones, L. M. Rees, S. F. Shurtleff, S. F. Taylor and J. M. Thorne,  
"Predicted Methods of Changing the Muon Catalized Fusion Cycling Rate,"  
*American Institute of Physics Conference Proceedings*, vol. 181, pp. 79-91, 1988.

## **IV. General Particle Orbital Method of Modeling**

### **Molecules Made of Multiple Types of Quantum Particles**

#### **4.1 Introduction**

In order to model physical properties of muonic hydrogen and helium molecules a General Particle Orbital (GPO) method of non-adiabatic quantum mechanics was developed. The GPO method is based on non-adiabatic Hartree-Fock—configuration interaction (HF /CI) methods. It facilitates the modeling of particles with multiple types (*i.e.*, mass and charge) of quantum particles. Although the method was developed to study muonic-molecules, its usefulness is not limited to molecules containing muons. Other types of exotic molecules and conventional molecules with some or all of the nuclei being modeled as quantum particles can be studied.

Non-adiabatic methods of quantum mechanics can be used to study the properties of molecular systems in which nuclei are not accurately modeled as fixed points under the Born-Oppenheimer approximation (*e.g.*, see References [1] through [11]). Methods capable of modeling non-adiabatic systems are particularly useful when studying molecular systems containing exotic particles in which more than one type of particle must be modeled quantum mechanically.[12; 13; 14; 15; 16] Due to the computational complexity of non-adiabatic methods, their use has traditionally been limited to comparatively small molecular systems.

Nuclear Electronic Orbital (NEO) methods were developed in order to facilitate the study of quantum chemical effects between protons and electrons in larger molecular

systems.[2; 17; 18; 7; 8; 9; 10; 11] These NEO methods treat electrons and selected protons as quantum particles, while treating other nuclei classically. In 2007 these methods were expanded to describe systems containing electrons and positrons in the presence of classical nuclei.[19; 20] While it is valuable for describing positron chemistry, this modified NEO method was limited to the study of systems containing two types of quantum particles, one positive, and one negative. In this work, the NEO method is extended to model systems made up of several different types (*i.e.*, mass and charge) of quantum particles. Since the method described in this paper is not limited to the chemistry of ordinary molecules having electron and nuclear orbitals, but can be applied to Coulombic orbitals for particles of any mass and charge, this extension is referred to as a “General Particle Orbital” (GPO) method.

While the GPO method does not, in principle, limit the number of different types of quantum particles that can be described in a molecule, computational resources available can limit its applications. Code for its current manifestation is not an efficient code for multi-processor computers nor does it take full advantage of the molecular symmetry that exists in many molecular systems. Calculations involving more than three types of quantum particles are currently very demanding due to the large computational resources needed to accurately model these systems. This is particularly true when correlation energy is calculated by configuration interaction (CI). Correlation interactions make significant contribution to the molecular stability of the systems described in this paper. Future modifications of the code will likely address its deficiencies and increase the size of molecular systems which can be accurately modeled. A computational strength of NEO and GPO methods, that can enhance efficiency, is that

some particles in modeled molecular systems can be treated quantum-mechanically while other particles are treated classically.

The ability to accurately calculate physical properties of a molecular system in which some of the particles are considered quantum-mechanically, and others are considered classically may not be limited to systems having negative and positive particles with large mass differences. Often particles do not interact strongly due to their locations within a molecule. As a result, their quantum interactions with each other can be ignored. For example, in some muonic molecules, due to the highly localized muon density, it may be possible to accurately consider weakly interacting nuclei classically, even when their mass is comparatively close to that of a muon.

Hartree-Fock and CI molecular orbital theories are the basis for the GPO extension of NEO presented in this chapter. For HF and post-HF methods, the choice of basis sets and basis set locations is of great importance to the accuracy of calculations; this GPO method is no exception. Approaches and challenges of optimizing basis sets and basis set center locations while using a minimum of computational resources are discussed in this chapter.

There are several factors which are often addressed in post-HF methods, which significantly influence Coulombic interactions in many exotic molecular systems. Among these are correlation energy (*i.e.*, especially correlation between different types of particles), relativistic effects, nuclear volume effects, vacuum polarization, and charge density effects (*i.e.*, effects of nuclear electromagnetic structure and nuclear polarization).[21; 22; 23; 24; 25; 26] The relative importance of each of these factors depends on the particular system being studied. In this work only correlation energy,

which is arguably the most important of these factors in low-Z muonic molecules, is considered.

While there are many methods of calculating the correlation energy between quantum particles, [8; 27:193-228,226,383,430,448-449,455; 28:61,231-269,238] only configuration interactions (CI) will be addressed in this paper. A CI application of the NEO method to model non-adiabatic quantum mechanics for quantum protons and electrons was published previously.[2] In this paper the method is expanded to model any number of different types of quantum particles.

Accurately calculating the correlation energy between quantum particles using CI methods can be computationally demanding and require significant resources. This is particularly true when calculating the interactions between different types of particles. Calculations in this chapter illustrate the GPO method using CI to account for correlation interactions between particles. For molecular systems containing negligible static correlation, it is not necessary to account for dynamic correlation, between all particles, using a single method. For example, in a system containing quantum protons and electrons, the electron-electron correlation energy and the proton-proton correlation energy could be calculated by one method (*e.g.*, CI) and the electron-proton correlation energy could be calculated by an entirely different method (*e.g.*, explicit correlation).[10; 29; 30]

## 4.2 Theory

In this section, Hartree-Fock (HF) and configuration interaction (CI) methods are developed in a formalism useful to study systems that involve any number and type of quantum Fermions in the presence of classical particles. These methods are particularly useful in the study of exotic particle molecular systems that contain multiple types (*i.e.*, various mass and charge combinations) of quantum particles. The methods presented were developed to study Fermions; however, they can be used, without modification, to study systems containing Bosons, as long as all quantum Bosons in the system are distinguishable (*i.e.*, have different mass and/or charge).

### 4.2.1 GPO Hartree-Fock method

In the derivations which follow an open-shell unrestricted Hartree-Fock method is combined with a closed-shell restricted method to allow multiple types of quantum particles to be modeled simultaneously in a system using whichever method is most appropriate for each type of particle (*e.g.*, electrons, muons, positrons, etc.).

The Hamiltonian operator can be written in the form

$$\hat{H} = -\frac{\hbar^2}{2} \sum_{\alpha}^N \frac{1}{m_{\alpha}} \nabla_{\alpha}^2 + \sum_{\alpha}^N \sum_{\beta > \alpha}^N V_{\alpha\beta} \quad (4.1)$$

where  $N$  is the total number of particles in the system.  $V_{\alpha\beta}$  can be any function describing a Coulombic potential with the distance between particles  $r_{\alpha\beta}$  and particles charge  $Z_{\alpha}$  and  $Z_{\beta}$ . For conventional molecules it is common practice to use the Born–

Oppenheimer approximation and to break the Hamiltonian operator into one and two quantum particle terms (*i.e.*, one-electron and two-electron terms). When one of the interacting particles is at a fixed location, a one-quantum particle term  $h_{\alpha\beta}$  results. When neither interacting particle can be assumed to be fixed, the expectation value of the particle's contribution to the Hamiltonian is a two-quantum particle multi-center integral

$$\langle \chi_i \chi_j \nmid \chi_k \chi_l \rangle = \int_{-\infty}^{\infty} \int_{-\infty}^{\infty} \chi_i^*(x_\alpha) \chi_j^*(x_\beta) V_{\alpha\beta} \chi_k(x_\alpha) \chi_l(x_\beta) dx_\alpha dx_\beta \quad (4.2)$$

where  $\chi_i$  represents spin orbitals.

If  $h$  represents core-Hamiltonian operators for quantum particles in the field of classical (*i.e.*, fixed-location) particles, the total energy of the system [2; 19:27; 28:126] is

$$\begin{aligned} E = & \sum_{i=1}^N \langle \chi_i | h | \chi_i \rangle + \frac{1}{2} \sum_{\mu=1}^n \sum_{i=1}^{N_\mu} \sum_{j=1}^{N_\mu} \left[ \langle \chi_i^\mu \chi_j^\mu \nmid \chi_i^\mu \chi_j^\mu \rangle - \langle \chi_i^\mu \chi_i^\mu \nmid \chi_j^\mu \chi_j^\mu \rangle \right] \\ & + \sum_{\mu=1}^n \sum_{\nu > \mu}^n \sum_{i=1}^{N_\mu} \sum_{j=1}^{N_\nu} \langle \chi_i^\mu \chi_j^\nu \nmid \chi_i^\mu \chi_j^\nu \rangle \end{aligned} \quad (4.3)$$

where  $N$  is the total number of quantum particles;  $N_i$  is the number of particles of type  $i$ ; and  $n$  is the number of types of particles being considered quantum mechanically.

Therefore,

$$N = \sum_{i=1}^n N_i \quad (4.4)$$

It should be noted that  $\langle \chi_i \chi_j \mp \chi_k \chi_l \rangle$  is not equivalent to the common notation  $\langle \chi_i \chi_j | \chi_k \chi_l \rangle$ .  $\langle \chi_i \chi_j \mp \chi_k \chi_l \rangle$  allows for any charge (*i.e.*, attraction or repulsion) and  $V_{\alpha\beta}$  does not have to be proportional to  $\frac{1}{r_{\alpha\beta}}$ .  $V_{\alpha\beta}$  can be any appropriate functions of  $r_{\alpha\beta}$ ,  $Z_\alpha$  and  $Z_\beta$ . Potentials which are not proportional to  $\frac{1}{r_{\alpha\beta}}$  are needed when nuclear volume is included in quantum mechanical calculations.

[note: All of the *ab initio* calculations presented in this dissertation use a potential proportional to  $\frac{1}{r_{\alpha\beta}}$ . A correction to this potential is included in some of the calculations using a post-Hartree-Fock perturbation method which is presented in Chapter 6. The methods of including nuclear volume presented in Chapter 6 can only be considered accurate for muonic molecules that have light nuclei (*i.e.*, nuclei from the first few rows of the periodic table). In order to accurately model interactions of muons with larger nuclei it is necessary to include an appropriate potential in the *ab initio* calculations.]

It is possible to solve for the Hartree-Fock energy in terms of closed or open shell configurations. A closed shell configuration is one in which all of the occupied valence shells are full (*i.e.*, contain indistinguishable paired particles). An open shell



configuration is one in which some or all of the occupied valence shells contain only one particle. In the discussion which follows, closed shell particles are modeled using restricted Hartree-Fock methods and open shell particles are modeled using unrestricted Hartree-Fock methods.[28; 27] If the number of restricted closed shell particles of type  $cl$  is defined as  $N_{cl}$  and the number of unrestricted open shell particles of type  $op$  is defined as  $N_{op}$ , where  $cl = \{1, 2, \dots, n_{closed}\}$  and  $op = \{n_{closed} + 1, n_{closed} + 2, \dots, n\}$ , then the Hartree-Fock energy of a system containing any number of any type of restricted low-spin and/or unrestricted high-spin quantum particles is

$$\begin{aligned}
E = & \sum_{i=1}^N \langle \psi_i | h | \psi_i \rangle + \frac{1}{2} \sum_{op=(n_{closed}+1)}^n \sum_{i=1}^{N_{op}} \sum_{j=1}^{N_{op}} \left[ \langle \psi_i^{op} \psi_j^{op} \mp \psi_i^{op} \psi_j^{op} \rangle - \langle \psi_i^{op} \psi_i^{op} \mp \psi_j^{op} \psi_j^{op} \rangle \right] \\
& + \sum_{cl=1}^{n_{closed}} \sum_{i=1}^{\frac{N_{cl}}{2}} \sum_{j=1}^{\frac{N_{cl}}{2}} \left[ 2 \langle \psi_i^{cl} \psi_j^{cl} \mp \psi_i^{cl} \psi_j^{cl} \rangle - \langle \psi_i^{cl} \psi_i^{cl} \mp \psi_j^{cl} \psi_j^{cl} \rangle \right] \\
& + \sum_{\mu=1}^n \sum_{\nu>\mu}^n \sum_{i=1}^{N_{op}} \sum_{j=1}^{N_{cl}} \langle \psi_i^{\mu} \psi_j^{\nu} \mp \psi_i^{\mu} \psi_j^{\nu} \rangle
\end{aligned} \tag{4.5}$$

where  $\psi$  represents spatial orbitals,  $n$  is the number of particle types, and  $n_{closed}$  is the number of particle types in which all of the particles of that type reside in closed shells.[2; 19:27; 28:134]

Using the variational method to minimize energy, Fock operators can be expressed as:

$$f^{cl}(1) = h(1) + \sum_j^{\frac{N_{cl}}{2}} [2J_j^{cl}(1) - K_j^{cl}(1)] - \sum_{l \neq cl}^{n_{closed}} \sum_{i=1}^{N_{cl}} J_i^l(1) \quad (4.6)$$

and

$$f^{op}(1) = h(1) + \sum_j^{N_{op}} [J_j^{op}(1) - K_j^{op}(1)] - \sum_{\substack{l > n_{closed} \\ l \neq op}}^n \sum_i^{N_{op}} J_i^l(1) \quad (4.7)$$

where Coulomb and exchange operators are defined as

$$J_j(1) = \int \psi_j^*(2) V_{1,2} \psi_j(2) d\mathbf{r}_2 \quad (4.8)$$

and

$$K_j(1) \psi_i(1) = \left[ \int \psi_j^*(2) V_{1,2} \psi_i(2) d\mathbf{r}_2 \right] \psi_j(1) \quad (4.9)$$

The Hartree-Fock-Roothan equations, coefficient matrix elements and charge-density bond-order matrix elements ( $P_{\lambda\sigma}$ ) are the same as ordinarily defined.[2; 28:137; 27] The one-quantum particle terms in the Fock matrix ( $h_{\alpha\beta}$ ) are defined the same for restricted closed and unrestricted open shell particle types.[2; 28:71] The two-quantum particle terms in the Fock matrix are not the same for the unrestricted open shell case and

the restricted closed shell case. If  $N_{bf}^{cl}$  and  $N_{bf}^{op}$  are the number of basis functions combined to approximate the wave functions for particles of type  $cl$  and  $op$  respectively, then the two quantum particle terms  $G_{\mu\nu}^{cl}$  and  $G_{\mu\nu}^{op}$  are defined as:

$$G_{\mu\nu}^{cl} = \sum_{\lambda=1}^{N_{bf}^{cl,i}} \sum_{\sigma=1}^{N_{bf}^{cl,i}} P_{\lambda\sigma}^{cl} \left[ \langle \phi_{\mu}^{cl} \phi_{\sigma}^{cl} \ddagger \phi_{\nu}^{cl} \phi_{\lambda}^{cl} \rangle - \frac{1}{2} \langle \phi_{\mu}^{cl} \phi_{\nu}^{cl} \ddagger \phi_{\sigma}^{cl} \phi_{\lambda}^{cl} \rangle \right] \quad (4.10)$$

and

$$G_{\mu\nu}^{op} = \sum_{\lambda=1}^{N_{bf}^{op,i}} \sum_{\sigma=1}^{N_{bf}^{op,i}} P_{\lambda\sigma}^{un} \left[ \langle \phi_{\mu}^{op} \phi_{\sigma}^{op} \ddagger \phi_{\nu}^{op} \phi_{\lambda}^{op} \rangle - \langle \phi_{\mu}^{op} \phi_{\nu}^{op} \ddagger \phi_{\sigma}^{op} \phi_{\lambda}^{op} \rangle \right] \quad (4.11)$$

From these equations the Fock matrix elements  $(F_{\mu\nu}^k)$  can be derived

$$F_{\mu\nu}^k = h_{\mu\nu}^k + G_{\mu\nu}^k + \sum_{l \neq k}^n \sum_{\lambda=1}^{N_{bf}^l} \sum_{\sigma=1}^{N_{bf}^l} P_{\lambda\sigma}^l \langle \phi_{\mu}^k \phi_{\sigma}^l \ddagger \phi_{\nu}^k \phi_{\lambda}^l \rangle \quad (4.12)$$

where  $k$  represents all types of particles, open or closed shell.

These Hartree-Fock-Roothaan equations were solved iteratively using convergence accelerators developed previously for electronic structure theory.[31] The Fock equations for each particle were fully converged sequentially after each step in the iterative procedure.

#### 4.2.2 Configuration Interaction

A configuration interaction (CI) wave function  $\psi_{total}$  can be expressed as a linear combination of configuration functions,  $\Phi$ . For a system of  $n$  types of quantum particles this is

$$\psi_{total} = \sum_{k_1=1}^{N_{CI}^1} \sum_{k_2=1}^{N_{CI}^2} \cdots \sum_{k_n=1}^{N_{CI}^n} C_{(k_1, k_2, \dots, k_n)} \prod_{i=1}^n \Phi_{k_i}^i \quad (4.13)$$

where  $N_{CI}^i$  is the number of quantum determinants of particles of type  $i$ . If  $N_{so}^i$  is the total number of spin orbitals of a given type  $i$ ,

$$N_{CI}^i = \frac{N_{so}^i!}{N_i! (N_{so}^i - N_i)!} \quad (4.14)$$

for  $N_i$  particles of type  $i$ . The total number of quantum determinants is

$$N_{CI}^{total} = \prod_{i=1}^n N_{CI}^i \quad (4.15)$$

The total CI energy  $E_{total} = \langle \Psi_{total} | \hat{H}_{total} | \Psi_{total} \rangle$  is

$$E_{total} = \sum_{k_1=1}^{N_{CI}^1} \sum_{k_2=1}^{N_{CI}^2} \cdots \sum_{k_n=1}^{N_{CI}^n} \left[ \sum_{l_1=1}^{N_{CI}^1} \sum_{l_2=1}^{N_{CI}^2} \cdots \sum_{l_n=1}^{N_{CI}^n} C_{(k_1, k_2, \dots, k_n)} C_{(l_1, l_2, \dots, l_n)} H_{CI} \right] \quad (4.16)$$

where  $H_{CI} \equiv \left\langle \prod_{i=1}^n \Phi_{k_i}^i \left| \hat{H}_{total} \right| \prod_{i=1}^n \Phi_{l_i}^i \right\rangle$  can be expressed as

$$\begin{aligned}
H_{CI} = & \sum_i^n \left\langle \Phi_{k_i}^i \left| \sum_{\alpha}^{N_i} h^i(\alpha) \right| \Phi_{l_i}^i \right\rangle \prod_{j \neq i}^n \delta_{k_j l_j} + \sum_i^n \left\langle \Phi_{k_i}^i \left| \sum_{\alpha}^{N_i} \sum_{\beta > 1}^{N_i} V_{\alpha\beta}^{ii} \right| \Phi_{l_i}^i \right\rangle \prod_{j \neq i}^n \delta_{k_j l_j} \\
& + \sum_i^n \sum_{j > i}^n \left\langle \Phi_{k_i}^i \Phi_{k_j}^j \left| \sum_{\alpha}^{N_i} \sum_{\beta \neq \alpha}^{N_j} V_{\alpha\beta}^{ij} \right| \Phi_{l_i}^i \Phi_{l_j}^j \right\rangle
\end{aligned} \tag{4.17}$$

$N_i$  is the number of particles of type  $i$  and  $n$  is the number of quantum particles the system contains.

If we define spatial shift operators  $\hat{E}_{\alpha_m \beta_m}$  between particles  $\alpha$  and  $\beta$  of type  $m$ , in terms of spin-creation ( $\uparrow$ ) and annihilation ( $\downarrow$ ) operators ( $a$ ),

$$\hat{E}_{\alpha_m \beta_m} = \hat{E}_{\alpha_m \beta_m}^{\uparrow} + \hat{E}_{\alpha_m \beta_m}^{\downarrow} = a_{\alpha_m \uparrow}^{\dagger} a_{\beta_m \uparrow} + a_{\alpha_m \downarrow}^{\dagger} a_{\beta_m \downarrow} \tag{4.18}$$

then  $H_{CI}$  can be expressed in terms of spatial orbitals ( $\psi$ )

$$\begin{aligned}
H_{CI} = & \sum_i^n \left\{ \sum_{\alpha_i}^{N_{MO}^i} \sum_{\beta_i}^{N_{MO}^i} \left\langle \Phi_{k_i}^i \left| \hat{E}_{\alpha_i \beta_i} \right| \Phi_{l_i}^i \right\rangle h_{\alpha_i \beta_i}^i \right. \\
& + \frac{1}{2} \sum_{\alpha_i}^{N_{MO}^i} \sum_{\beta_i}^{N_{MO}^i} \sum_{\mu_i}^{N_{MO}^i} \sum_{\nu_i}^{N_{MO}^i} \left\langle \Phi_{k_i}^i \left| \hat{E}_{\alpha_i \beta_i} \hat{E}_{\mu_i \nu_i} - \delta_{\beta_i \mu_i} \hat{E}_{\alpha_i \nu_i} \right| \Phi_{l_i}^i \right\rangle \left\langle \psi_{\alpha_i} \psi_{\beta_i} \mp \psi_{\alpha_j} \psi_{\beta_j} \right\rangle \left. \right\} \prod_{j \neq i}^n \delta_{k_j l_j} \quad (4.19) \\
& + \sum_i^n \sum_{j > i}^n \left\{ \sum_{\alpha_i}^{N_{MO}^i} \sum_{\beta_i}^{N_{MO}^i} \sum_{\alpha_j}^{N_{MO}^j} \sum_{\beta_j}^{N_{MO}^j} \left\langle \Phi_{k_i}^i \left| \hat{E}_{\alpha_i \beta_i} \right| \Phi_{l_i}^i \right\rangle \left\langle \Phi_{k_j}^j \left| \hat{E}_{\alpha_j \beta_j} \right| \Phi_{l_j}^j \right\rangle \left\langle \psi_{\alpha_i} \psi_{\beta_i} \mp \psi_{\alpha_j} \psi_{\beta_j} \right\rangle \right\}
\end{aligned}$$

where  $N_{MO}^i$  is the number of molecular orbitals of particle  $i$  in the configuration space.

From this it follows that the total energy of the system is

$$\begin{aligned}
E_{total} = & \sum_i^n \left\{ \sum_{\alpha_i}^{N_{MO}^i} \sum_{\beta_i}^{N_{MO}^i} \gamma_{\alpha_i \beta_i}^i h_{\alpha_i \beta_i}^i + \frac{1}{2} \sum_{\alpha_i}^{N_{MO}^i} \sum_{\beta_i}^{N_{MO}^i} \sum_{\mu_i}^{N_{MO}^i} \sum_{\nu_i}^{N_{MO}^i} \Gamma_{\alpha_i \beta_i \mu_i \nu_i}^i \left\langle \psi_{\alpha_i} \psi_{\beta_i} \mp \psi_{\alpha_j} \psi_{\beta_j} \right\rangle \right\} \\
& + \sum_i^n \sum_{j > i}^n \left\{ \sum_{\alpha_i}^{N_{MO}^i} \sum_{\beta_i}^{N_{MO}^i} \sum_{\alpha_j}^{N_{MO}^j} \sum_{\beta_j}^{N_{MO}^j} \Gamma_{\alpha_i \beta_i \alpha_j \beta_j}^{ij} \left\langle \psi_{\alpha_i} \psi_{\beta_i} \mp \psi_{\alpha_j} \psi_{\beta_j} \right\rangle \right\} \quad (4.20)
\end{aligned}$$

where the density matrix elements are defined as

$$\gamma_{\alpha_m \beta_m}^m = \sum_{k_1=1}^{N_{CI}^1} \sum_{k_2=1}^{N_{CI}^2} \cdots \sum_{k_n=1}^{N_{CI}^n} \left[ \sum_{l_1=1}^{N_{CI}^1} \sum_{l_2=1}^{N_{CI}^2} \cdots \sum_{l_n=1}^{N_{CI}^n} C_{(k_1, k_2, \dots, k_n)} C_{(l_1, l_2, \dots, l_n)} \left\langle \Phi_{k_m}^m \left| \hat{E}_{\alpha_m \beta_m} \right| \Phi_{l_m}^m \right\rangle \prod_{i \neq m}^n \delta_{k_i l_i} \right] \quad (4.21)$$

$$\begin{aligned}
\Gamma_{\alpha_m \beta_m \mu_m \nu_m}^m = & \sum_{k_1=1}^{N_{CI}^1} \sum_{k_2=1}^{N_{CI}^2} \cdots \sum_{k_n=1}^{N_{CI}^n} \left\{ \sum_{l_1=1}^{N_{CI}^1} \sum_{l_2=1}^{N_{CI}^2} \cdots \sum_{l_n=1}^{N_{CI}^n} \left[ C_{(k_1, k_2, \dots, k_n)} C_{(l_1, l_2, \dots, l_n)} \right. \right. \\
& \left. \left. \left\langle \Phi_{k_m}^m \left| \hat{E}_{\alpha_m \beta_m} \hat{E}_{\mu_m \nu_m} - \delta_{\beta_m \mu_m} \hat{E}_{\alpha_m \nu_m} \right| \Phi_{l_m}^m \right\rangle \prod_{i \neq m}^n \delta_{k_i l_i} \right] \right\} \quad (4.22)
\end{aligned}$$

and

$$\Gamma_{\alpha_m \beta_m}^{mp} = \sum_{k_1=1}^{N_{CI}^1} \sum_{k_2=1}^{N_{CI}^2} \cdots \sum_{k_n=1}^{N_{CI}^n} \left[ \sum_{l_1=1}^{N_{CI}^1} \sum_{l_2=1}^{N_{CI}^2} \cdots \sum_{l_n=1}^{N_{CI}^n} C_{(k_1, k_2, \dots, k_n)} C_{(l_1, l_2, \dots, l_n)} \right. \\ \left. \left\langle \Phi_{k_m}^m \left| \hat{E}_{\alpha_m \beta_m} \right| \Phi_{l_m}^m \right\rangle \left\langle \Phi_{k_p}^p \left| \hat{E}_{\alpha_p \beta_p} \right| \Phi_{l_p}^p \right\rangle \right] \quad (4.23)$$

If the variation method is used to minimize the total energy with respect to the CI coefficients  $C_{(k_1, k_2, \dots, k_n)}$ , then the CI coefficients and corresponding vibrational-Coulombic ground and excited state energies may be determined by diagonalizing the CI Hamiltonian matrix. This method allows any choice of multiplicity for all of the Fermionic nuclei, thereby facilitating the study of systems of particles having different spin states.[2]

#### 4.2.3 Basis Set Development

As originally developed, NEO implemented post-Hartree-Fock methods for molecules having two types of quantum particles, one positive and one negative.[2; 11; 18; 29; 30; 32; 33; 34; 35; 36; 37; 38] Using these procedures, the total number of self-consistent-field (SCF) iterations that must be performed in order to obtain density convergence is the product of the number of iterations ( $U$ ) needed for each type of quantum particle ( $i$ ). Expanding the procedure to  $n$  types of quantum particles; the total number of SCF iterations needed to obtain density convergence is

$$\text{Total \# of SCF iterations} = \prod_{i=1}^n U_i \quad (4.24)$$

As a result, minimizing the time required to perform individual SCF iterations becomes more important as the number of types of quantum particles in modeled systems increases. The importance of having the most efficient basis functions possible increases exponentially with the number of quantum particles, and the relative importance of the time required to perform the integration decreases. Choosing small, efficient sets of basis functions to represent a molecular orbital necessitates fewer HF-SCF iterations to obtain converged density for each type of particle. As the number of basis set functions decreases not only does the time required for each SCF iteration decrease, but most often, the number of iterations required usually decreases as well. The advantage of using Gaussian basis sets diminishes as the number of types of quantum particles in a system increases.

When representing molecular orbitals as linear combinations of Gaussian type atomic basis functions, optimization of the orbital exponents becomes ever more complex as the number of atomic basis functions increases. The computational resources needed to perform these optimizations increases and the difficulty of obtaining SCF convergence increases with increasing basis set size. Many methods of optimization result in exponents ( $a_i$ ) converging to the same value when atomic basis functions have the same azimuthal quantum number ( $l$ ). This is a particularly significant problem with the muonic molecules presented in this paper, due to the small separation distance between interacting particles. Several methods of circumventing this problem have been



developed. The best know of these methods are even-tempered [39; 40; 41; 42; 43; 44] and well-tempered [45; 46; 47; 48; 49; 50] basis set methods.

Considerable improvement over even-tempered and well-tempered basis sets can be obtained through the use of the Legendre polynomial optimization method.[51] With this method, the Gaussian exponents are represented as

$$\alpha_i = \exp \left[ \sum_{k=0}^{C-1} A_k P_k \left( \frac{2i-2}{N-1} - 1 \right) \right] \quad (4.25)$$

where  $A_k$  are variational parameters,  $C$  is the number of Gaussian functions combined and  $P_k$  are orthonormal Legendre polynomials.[51] This is the method employed to optimize electron, muon, and nuclear basis sets for the results presented in this document.

The problem of coefficients converging to the same values, resulting in linear dependant basis sets, is more common when uncontracted Gaussian basis sets are used than when Slater and contracted Gaussian basis sets are used. This is primarily a result of smaller values of  $C$  commonly being used with these types of basis sets.

In order to improve the basis sets used to represent quantum orbitals, additional basis functions can be added to basis sets, or auxiliary basis sets can be formed and centered at different geometric locations. When applying limited computational resources there is no hard-and-fast improvement rule whether it is better to increase the number of auxiliary basis set centers or to increase the size of the basis sets. The answer to this dilemma depends on the system being studied and the basis sets being compared.

### 4.3 Applications

The effects of correlation energy, basis set center coordinates, and basis set sizes, for  $p\mu\mu p$  and  $t\mu\mu t$  are addressed in this section. Here,  $p$  and  $t$  represent  $^1H$  and  $^3H$  nuclei, respectively, and  $\mu$  represents a negative-muon. In this chapter, dynamic correlation energy is calculated using configuration interactions (CI) methods.

One of the difficulties encountered treating molecular systems having different types of quantum particles that have similar masses, using GPO methods, is that basis sets in general are not transferable between molecular systems or even different molecular geometries. In general basis sets and system geometries are strongly coupled except when all oppositely charged quantum particle types have significantly different masses. As a result, the basis set coefficients and molecular geometry must be optimized simultaneously to attain accurate results. In order to perform a full optimization of the molecules presented in this document, a basis set for each type of particle was optimized in turn, then the geometry was optimized. This process was repeated iteratively, until a minimum energy configuration was found.

#### 4.3.1 Contributions to the CI Energy

In the discussion which follows, the results of applying the GPO/CI method to muonic hydrogen molecules is discussed. Calculations of separate particle-particle correlation energy for different types of particle interactions is presented. The effects of basis set size on the CI energy of these systems are addressed and the limitations of optimizing basis sets and geometries at the HF level, then using these optimized

parameters to perform CI calculations, rather than optimizing the parameters at the CI level is evaluated.

Full-CI (FCI) can be an accurate method of calculating non-relativistic correlation energy, but its usefulness is limited by computational requirement that can be overwhelming when calculating configuration interactions between different types of particles. The calculation of CI energy requires the solution of a Slater determinant (*i.e.*, CI determinant). The majority of the computational resources needed to calculate CI energy results from the storage of the elements of CI matrices and the solution of these determinants. If the calculation of the CI energy for one type of quantum particle (*e.g.*, muons) requires finding the roots of an  $(m \times m)$  Hamiltonian, and the calculation of the CI energy of a second type of quantum particle (*e.g.*, electrons) requires finding the roots of a  $(p \times p)$  Hamiltonian, then the calculation of the CI energy between the different types of particles (*e.g.*, electrons and muons) requires finding the roots of a Hamiltonian that is  $(m \bullet p) \times (m \bullet p)$  in size. As a result, the calculation of FCI energy for systems containing multiple types of quantum particles requires significantly greater computational resources than are required for molecular systems containing only one type of quantum particle.

**Table 4-1. Effects of basis set size on HF and FCI energy of  $p\mu\mu p$ . The FCI energy is calculated separately for different types of interactions. Basis sets and  $p$ - $p$  bond distances were optimized at the HF level. For columns 2 thru 4, the CI energy was calculated using FCI methods and the basis sets indicated. In column 5 the HF energy was calculated using 4s3p muon basis sets and a 2s6p proton basis sets.  $\mu\mu$  CI energy and  $\mu p$  CI energy was calculated at the FCI level also using 4s3p and 2s6p basis sets for muons and protons respectively. The  $\mu p$  CI energy was calculated using FCI with 4s3p muon and 2s2p proton basis sets. All of the particles were treated quantum mechanically.**

Muon basis sets	2s	4s3p	4s3p	Combined
Proton Basis Sets	2s2p	2s2p	2s6p	Results
HF energy <sup>a</sup>	-2.955674	-2.962424	-2.962480	-2.962480
$\mu$ — $\mu$ CI energy <sup>a</sup>	-0.112286	-0.193636	-0.193667	-0.193667
$p$ — $p$ CI energy <sup>a</sup>	-0.076096	-0.082950	-0.083391	-0.083391
$\mu$ — $p$ CI energy <sup>a</sup>	-0.227296	-0.845830		-0.845830
Total CI energy <sup>a</sup>	-0.415678	-1.122416		-1.122888
HF/CI energy <sup>a</sup>	-3.371352	-4.084839		-4.085368

<sup>a</sup>Energy is reported in keV

Fortunately, there is no requirement that the same method of calculating dynamic correlation energy be used to calculate the interactions between all types of particles in a molecular system. Different methods of calculating correlation energy (*e.g.*, perturbation theory, explicit correlation, etc.) can be used for different interactions in the same molecular system. In Table 4-1, the correlation energy as a function of basis set size and particle type for  $p\mu\mu p$  is presented. Several significant factors can be noted from an analysis of these calculations. 1) The  $pp$ ,  $\mu\mu$ , and  $\mu p$  correlation energy all contribute significantly to the overall energy of the systems. 2) When comparing the correlation energy between particles of the same type (*e.g.*,  $\mu\mu$  or  $pp$ ) the smaller the mass of the particles (*i.e.*, greater the quantum character) the greater the correlation energy. 3) The correlation energy between particles of different types (*e.g.*,  $\mu p$ ) is greater than the correlation energy between particles of the same type. 4) For the systems studied, the

calculation of correlation energy using GPO/CI methods is affected significantly by basis set size, but not as significantly as is the Hartree-Fock energy. As a result, it is possible to improve computational efficiency by calculating the HF energy with larger basis sets than are used for the more expensive CI calculations and then add the HF and CI energies together. An example of where this has been done is given in Column 5 of Table 4-1.

Studies were performed which optimized geometry and basis sets at the HF level, then used these optimized parameters to calculate the CI energy.[2] The CI results presented thus far in this paper are the result of this type of analysis. While it can be argued that this type of analysis can be used to efficiently optimize geometries and basis sets, particularly when only one type of quantum particle is present or when there is a large mass difference between the types of quantum particles studied (*e.g.*, nuclei and electrons), for the muonic molecular systems presented in this paper sizable errors resulted from this approach (see Table 4-2). While more accurate results are produced, optimizing the geometry and basis sets at the FCI level can present challenges for systems of the type presented in this chapter. In order to obtain accurate results, the basis sets and geometries must be optimized simultaneously. Often hundreds, or even thousands of individual GPO calculations must be carried out in order to perform these optimizations. As a result, there are significant computational limitations on how large and how many basis sets can be used when FCI optimization is performed. Table 4-2 shows the results of two FCI level calculations performed using the same size basis sets, one with HF optimized basis sets and geometry, and one with CI optimized parameters. As can be seen from the table, the difference in the calculated HF/CI energy is noteworthy, but the difference in the calculated bond length is of even greater

significance. For muonic molecular systems of the type presented in this paper, using limited computational resources, it is better to use a relatively small basis set and perform a FCI optimization than to use a larger basis set and optimize at the HF level.

**Table 4-2. HF optimized verses HF/CI optimized CI calculations of  $p\mu p^+$ . The results in column 2 were obtained by optimizing the basis sets and bond length at the HF level, then calculating the FCI energy of the muonic molecular system. The results in column 3 were obtained by optimizing the basis sets and bond length at the FCI level. The muon and proton basis sets were centered at the same locations, the positions of greatest proton density. 4s3p muon basis sets and a 2s2p proton basis sets were used for the calculations. All of the particles were treated quantum mechanically.**

	HF optimized	FCI optimized
Bond length <sup>a</sup>	0.006088	0.003655
HF energy <sup>b</sup>	-1.4061	-1.3959
p—p correlation energy <sup>b</sup>	-0.06006	-0.06712
$\mu$ —p correlation energy <sup>b</sup>	-0.47942	-0.50431
HF/CI energy <sup>b</sup>	-1.9404	-1.9674

<sup>a</sup>The equilibrium proton separation distance is reported in angstroms (Å)

<sup>b</sup>Energy is reported in keV

#### 4.3.2 Di-muonic Hydrogen Molecules

In this section two studies which used the GPO method are presented: 1) the geometry and binding energy of  $p\mu p$  is optimized using various basis sets, and 2) the bond length of  $t\mu t$  was calculated and compared using fixed and quantum tritons. Molecular geometries (*i.e.*, equilibrium nuclei positions) were determined from the expectation values of particle density. The term *bond length* refers to the distance between the expectation values of nuclei density. For the symmetric muonic molecules presented in this paper, the coordinates of highest nuclear density are the same as the coordinates of the optimized basis set positions to at least 4 significant figures (Å) $\mu$ . This is not, however, expected to be the case for non-symmetric molecular systems.

In order to accurately calculate the geometry and binding energy of the muonic molecules presented in this section the basis sets and the basis set center locations were simultaneously optimized. Use of basis sets optimized at other center locations, or the use of basis set center locations optimized with other basis sets often resulted in differences of several electron volts (eV) in the calculated binding energy. Likewise, changing the basis set size of one particle necessitated the optimization of the basis sets of the other particles, if accurate results were to be obtained. Due to the symmetry of the molecular systems presented in this paper, basis sets for equivalent particles were constrained to have equivalent basis sets.

Due to the computational resources needed to accurately include correlation energy and other post Hartree-Fock corrections to the calculations; it is necessary to limit the size of basis sets. Results obtained using different size basis sets are compared in Tables 4-3 through 4-5. Table 4-3 compares the binding energy for various size basis sets. Basis sets and bond distances were optimized at the HF level, then HF/FCI calculations were performed under the optimized conditions. For comparison purposes, the bond distance and binding energy of  $p\mu p^+$ , calculated at a comparable level of theory, is also shown. Table 4-4 compares three FCI calculations which have similar time and memory requirements, but for which the number of Gaussian equations used are divided up differently between muons and protons. Table 4-5 compares results in which different numbers of molecular orbitals are included in the CI calculations [*i.e.*, complete active space method (CAS)]. The molecular orbitals which result in the largest contributions to the HF energy are those which were included in the CI calculations.

The calculated  $p\mu\mu p$  binding energy of 410.5 eV can be compared to previously published values of 374.5 eV [15] (see Tables 4-4 and 4-5). It should be noted that the previously published results neglected  $p\mu$  correlation interactions. The significance of  $p\mu$  correlation interactions will be discussed in detail in Chapter 5.

The calculated binding energy of  $p\mu p^+$  presented in Table 4-3 is 260.6 eV. This can be compared to published values of 253.2 eV.[52] The previously published  $p\mu p^+$  calculations used larger basis sets than those used in the calculations presented in this chapter. The  $p\mu\mu p$  and  $p\mu p^+$  results presented in Table 4-3 demonstrate weaknesses of using small basis sets and optimizing at the HF level.

**Table 4-3. Equilibrium bond length and binding energy of  $p\mu\mu p$  and  $p\mu p^+$ . The muon basis sets, proton basis sets and equilibrium geometry were optimized simultaneously for each calculation at the HF level. The binding energy was calculated at the FCI level using HF optimized basis sets and bond distance. All of the particles were treated quantum mechanically.**

	$p\mu\mu p$	$p\mu\mu p$	$p\mu\mu p$	$p\mu p^+$
Muon Basis Sets	4s3p	4s3p	2s	4s3p
Proton Basis Sets	2s6p	2s2p	2s2p	2s2p
HF Bond Length <sup>a</sup>	0.003639	0.003609	0.005377	0.006088
Binding Energy <sup>b</sup>		402.4567	441.8192	260.6276

<sup>a</sup>The bond length is reported in angstroms (Å)

<sup>b</sup>The binding energy is reported in eV



**Table 4-4. Equilibrium bond length and binding energy of  $p\mu\mu p$ .** The muon basis sets, proton basis sets and equilibrium bond distance were optimized simultaneously for each calculation at the FCI level using the variational principle. The binding energy was calculated at the FCI level using FCI optimized basis sets and bond distance. All of the particles were treated quantum mechanically.

Muon Basis Sets	2s1p	2s	2s2p
Proton Basis Sets	2s1p	2s2p	2s
Bond Length <sup>a</sup>	0.005012	0.004376	0.005988
Binding Energy <sup>b</sup>	410.525	406.968	362.173

<sup>a</sup>The bond length is reported in angstroms (Å)

<sup>b</sup>The binding energy is reported in eV

**Table 4-5. Equilibrium bond length and binding energy of  $p\mu\mu p$ .** 2s2p muon basis sets and 2s2p proton basis sets were used. The muon basis sets, proton basis sets and equilibrium bond distance were optimized simultaneously at the CI level using CAS methods and varying numbers of active molecular orbitals (MOs). All of the particles were treated quantum mechanically.

Active $\mu^-$ MOs	10	8	6	4
Active Nuc. MOs	10	8	6	4
Bond Length <sup>a</sup>	.005013	.004420	.004298	.004046
Total Energy <sup>b</sup>	-3,927.0	-3,751.2	-3,541.2	-3,235.6
Binding Energy <sup>b</sup>	410.5103			

<sup>a</sup>The bond length is reported in angstroms (Å)

<sup>b</sup>The energy is reported in eV

From Tables 4-3, 4-4, and 4-5 it can be seen that correlation interactions result in an increase in the calculated  $p$ - $p$  bond distance in  $p\mu\mu p$  molecules.

The Born-Oppenheimer approximation is not, of course, an accurate assumption when used to model interactions between oppositely charged quantum particles of similar size. While understanding this, the author was uncertain about how much the calculated bond-length would vary if one or both of the nuclei were fixed. Notwithstanding the error resulting from application of the Born-Oppenheimer approximation, fixing the

nuclei could eliminate other errors in the calculations. It has been shown that fixing one nuclei eliminates translational “contamination,” and fixing two nuclei eliminates translational and rotational “contamination” in the calculated results.[29; 30; 53; 54] Table 4-6 shows results for  $t\mu\mu t$  where all four particles are considered quantum mechanically, where one of the nuclei is fixed and where both nuclei are fixed.

**Table 4-6. Equilibrium Geometry of  $t\mu\mu t$ . 4s3p muon and 2s2p triton basis sets were used. Correlation energy corrections were included by CAS/CI methods with five active molecular orbitals (MOs) per quantum particle (10 muon MO's and 5 MO's for each quantum triton). The muon basis sets, triton basis sets and separation distance were optimized simultaneously for each calculation at the CI level. Both muons were treated quantum mechanically. Tritons were treated classically and quantum mechanically, as shown.**

Number of Quantum Protons	0	1	2
Bond Length <sup>a</sup>	0.003002	0.003754	0.004032

<sup>a</sup>The bond length is reported in angstroms (Å)

#### 4.4 Conclusions

The non-adiabatic ab-initio methods outlined in this paper allow the study of molecular systems containing any number of any type (*i.e.*, mass and charge) of quantum particles in systems that may also contain classical (*i.e.*, fixed) particles. The size of the systems studied, the number of quantum particles, and the types of quantum particles are limited only by the computational facilities available.

The ab-initio HF/CI methods described in this paper have been applied to some muonic molecular systems. It was found that basis sets optimized for these systems could not in general be accurately transferred to similar systems. In order to obtain accurate results, the basis sets for each type of particle and the molecular geometry

needed to be optimized simultaneously. Failure to do this resulted in errors that were sometimes several tens of electron volts. It was additionally shown that for muonic hydrogen molecules, of the type studied in this paper, the optimization must include correlation energy if accurate results are to be obtained. Optimizing at the HF level, then adding CI to the final results is not sufficient. The basis sets used in the studies presented in this paper were optimized using Legendre polynomial optimization, because this method of optimization yields better results (*i.e.*, lower variational energy) than does the more common even-tempered and well-tempered basis set methods.[51]

For di-muonic hydrogen molecules the  $pp$ ,  $\mu\mu$ , and  $p\mu$  correlation interactions all contribute significantly to the overall energy of the systems. When comparing the correlation energy between particles of the same type (*e.g.*,  $\mu\mu$  or  $pp$ ) the greater the quantum character (*i.e.*, smaller the mass) of the particles, the greater the correlation energy. The correlation energy between particles of different types (*e.g.*,  $p\mu$ ) is greater than the correlation energy between particles of the same type. The calculation of correlation energy using GPO/CI methods is affected significantly by basis set size, but not affected as much as is the Hartree-Fock energy (at least for the systems studied) (see Tables 4-1 and 4-2).

The feasibility of using different methods (*e.g.*, different CI levels) to calculate different contributions to the dynamic correlation energy was demonstrated. When static correlation is negligible, as it is for all of the calculations presented in this chapter, there is no requirement that the same basis sets, or even the same methods of calculating dynamic correlation energy be used for interactions between all particles, or all types of particles. The use of different basis sets to calculate the HF energy and different

contributions to the correlation energy was demonstrated. Situations where this can improve HF/CI energy calculations were discussed.

## References

- [1] M. Born and J. R. Oppenheimer, "Zur Quantentheorie der Moleküln," *Annalen der Physik*, vol. 84, pp. 457-484, 1927.
- [2] S. P. Webb, T. Iordanov and S. Hammes-Schiffer, "Multiconfigurational Nuclear-Electronic Orbital Approach: Incorporation of Nuclear Quantum Effects in Electronic Structure Calculations," *Journal of Chemical Physics*, vol. 117, pp. 4160-4118, 2002.
- [3] H. Nakai, K. Sodeyama and M. Hoshino, "Non-Born-Oppenheimer Theory for Simultaneous Determination of Vibrational and Electronic Excited States: ab initio NO+MO/CIS theory," *Chemical Physics Letters*, vol. 345, pp. 118-124, 2001.
- [4] M. Cafiero, S. Bubin and L. Adamowicz, "Non-Born-Oppenheimer Calculations of Atoms and Molecules," *Physical Chemistry Chemical Physics*, no. 5, pp. 1491-1501, 2003.
- [5] Y. Itou, K. Mori, T. Udagawa, M. Tachikawa, T. Ishimoto and U. Nagashima, "Quantum Treatment of Hydrogen Nuclei in Primary Kinetic Isotope Effects in a Thermal [1,5]-Sigmatropic Hydrogen (or Deuterium) Shift from (Z)-1,3-Pentadiene," *International Journal Quantum Chememistry*, vol. 111, no. 2, pp. 261-267, 2007.
- [6] M. Tachikawa, "Simultaneous Optimization of Gaussian Type Function Exponents for Electron and Positron with Full-CI Wavefunction – Application to Ground and Excited States of Positronic Compounds with Multi-Component Molecular Orbital Approach," *Chemical Physics Letters*, vol. 350, pp. 269-276, 2001.
- [7] J. H. Skone, M. V. Pak and S. Hammes-Schiffer, "Nuclear-Electronic Orbital Nonorthogonal Configuration Interaction Approach," *J. Chem. Phys.*, no. 123, 134108, 2005.
- [8] C. Swalina, M. V. Pak and S. Hammes-Schiffer, "Alternative Formulation of Many-Body Perturbation Theory for Electron-Proton Correlation," *Chemical Physics Letters*, vol. 404, pp. 394-399, 2005.
- [9] C. Swalina, M. V. Pak and S. Hammes-Schiffer, "Analysis of the Nuclear-Electronic Orbital Method for Model Hydrogen Transfer Systems," *J. Chem. Phys.*, no. 123, 014303, 2005.

- [10] C. Swalina, M. V. Pak, A. Chakraborty and S. Hammes-Schiffer, "Explicit Dynamical Electron--Proton Correlation in the Nuclear--Electronic Orbital Framework," *Journal of Physical Chemistry A*, vol. 110, no. 33, pp. 9983-9987, 2006.
- [11] M. V. Pak, A. Chakraborty and S. Hammes-Schiffer, "Analysis of Nuclear Quantum Effects on Hydrogen Bonding," *Journal of Physical Chemistry, A*, vol. 111, no. 11, pp. 2206-2212, 2007.
- [12] S. Krzysztol and J. Bogumil, "Nonadiabatic Calculations for  $td\mu$  Relevant for Muon Catalyzed Fusion," *International Journal of Quantum Chemistry*, vol. 40, no. S25, pp. 671-686, 1991.
- [13] K. Szalewicz, B. Jeziorski, A. Scrinzi, X. Zhao, R. Moszynski, W. Kolos, P. Froelich, H. Monkhorst and A. Velenik, "Effects of Nuclear Forces in Muon-Catalyzed Fusion: Nonadiabatic Treatment of Energy Shifts and Fusion Rates for S States of  $td\mu$ ," *Physical Review A, atomic, molecular, and optical physics*, vol. 42, no. 7, pp. 3768-3778, 1990.
- [14] A. Boukour, R. Hewitt and C. Leclercq-Willain, "The Coulomb Capture of Negative Muons by Hydrogen Atoms in the Non-Adiabatic Close-Coupling Approximation," *Hyperfine Interactions*, Vols. 101-102, no. 1, pp. 263-269, 1996.
- [15] Y. Hamahata, E. Hiyama and M. Kamimura, "Non-Adiabatic Four-Body Calculation of Double-Muonic Hydrogen Molecules," in *Hyperfine Interactions*, 2001.
- [16] E. V. Sheely, L. W. Burggraf, P. E. Adamson, F. D. Xiaofeng and M. W. Schmidt, "Application of GAMESS/NEO to Quantum Calculations of Muonic Molecules," in *Advanced Science Research Symposium 2009 Positron, Muon and other exotic particle beams for materials and atomic/molecular sciences (ASR2009)*, vol. 225 no. 1, Tokai, 2010.
- [17] M. V. Pak, S. P. Swalina, S. P. Webb and S. Hammes-Schiffer, "Application of the Nuclear-Electronic Orbital Method to Hydrogen Transfer Systems: Multiple Centers and Multiconfigurational Wavefunctions," *Chem. Phys.*, no. 304, 227-236, 2004.
- [18] M. V. Pak and S. Hammes-Schiffer, "Electron-Proton Correlation for Hydrogen Tunneling Systems," *Physical Review Letters*, vol. 92, no. 10, pp. 103002:1-4, 2004.
- [19] P. E. Adamson, A General Quantum Mechanical Method to Predict Positron Spectroscopy, PhD dissertation, AFIT/DS/ENP/07-04. Graduate School of Management and Engineering, Air Force Institute of Technology (AU), Wright-Patterson AFB OH, June 2007 (0704-0188).

- [20] P. E. Adamson, X. F. Duan, L. W. Burggraf, M. V. Pak, C. Swalina and S. Hammes-Schiffer, "Modeling Positrons in Molecular Electronic Structure Calculations with the Nuclear-Electronic Orbital Method," *Journal of Physical Chemistry A*, vol. 112, no. 6, pp. 1346-1351, 2008.
- [21] E. V. Sheely, L. W. Burggraf, P. E. Adamson, D. F. Xiaofeng and M. W. Schmidt, "Application of GAMESS/NEO to quantum calculations of muonic molecules," vol. 225, pp. 1-8, 2009.
- [22] L. I. Ponomarev, "Muon Catalysed Fusion," *Contemporary Physics*, vol. 31, no. 4, pp. 219-245, 1990.
- [23] G. Aissing and H. J. Monkhorst, "Relativistic Corrections to Binding Energies of Muonic Molecules," *Physical Review A: Atomic, Molecular, and Optical Physics*, vol. 42, no. 7, pp. 3789-3794, 1990.
- [24] D. D. Bakalov and V. I. Korobov, "Relativistic Corrections to Energy Levels of Weakly Bound States of Mesic Molecules  $dd\mu$  and  $dt\mu$ ," *JINR Rapid Communications*, vol. 35, no. 2, pp. 15-20, 1989.
- [25] J. Aguilar, E. Rafael and D. Greynat, "Muon Anomaly From Lepton Vacuum Polarization and the Mellin-Barnes Representation," *Physical Review D, particles, fields, gravitation and cosmology*, vol. 77, pp. 093010:1-27, 2008.
- [26] E. Pallante, "The Hadronic Vacuum Polarization Contribution to the Muon  $g-2$  in the Quark-Resonance Model," *Physics Letters B*, vol. 341, pp. 221-227, 1994.
- [27] I. N. Levine, Quantum Chemistry, Boston: Allyn and Bacon, Inc., 1983.
- [28] A. Szabo and N. S. Ostlund, Modern Quantum Chemistry, Introduction to Advanced Electronic Structure Theory, Mineola: Dover Publications, inc., 1989.
- [29] A. Chakraborty, M. V. Pak and S. Hammes-Schiffer, "Inclusion of Explicit Electron-Proton Correlation in the Nuclear-Electronic Orbital Approach Using Gaussian-Type Geminal Functions," *Journal of Chemical Physics*, no. 122, pp. 014101:1-13, 2008.
- [30] A. Chakraborty and S. Hammes-Schiffer, "Density Matrix Formulation of the Nuclear-Electronic Orbital Approach with Explicit Electron-Proton Correlation," *Journal of Chemical Physics*, vol. 129, pp. 204101:1-16, 2008.
- [31] P. Pulay, "Improved SCF Convergence Acceleration," *Journal of Computational Chemistry*, vol. 3, no. 4, pp. 556-560, 1982.

- [32] B. Auer, M. V. Pak and S. Hammes-Schiffer, "Nuclear-Electronic Orbital Method within the Fragment Molecular Orbital Approach," *Journal of Physical Chemistry C*, vol. 114, no. 12, pp. 5582-5588, 2010.
- [33] T. Jordanov and S. Hammes-Schiffer, "Vibrational Analysis for the Nuclear-Electronic Orbital Method," *Journal of Chemical Physics*, pp. 9489-9496, 2003.
- [34] M. V. Pak, A. Chakraborty and S. Hammes-Schiffer, "Calculation of the Positron Annihilation Rate in PsH with the Positronic Extension of the Explicitly Correlated Nuclear-Electronic Orbital Method," *Journal of Physical Chemistry A*, vol. 113, no. 16, pp. 4004-4008, 2009.
- [35] A. Reyes, M. V. Pak and S. Hammes-Schiffer, "Investigation of isotope Effects with the Nuclear-Electronic Orbital Approach," *Journal of Chemical Physics*, vol. 123, pp. 064104:1-8, 2005.
- [36] A. Reyes, M. V. Pak and S. Hammes-Schiffer, "Investigation of isotope effects with the nuclear-electronic orbital approach," *Journal of Chemical Physics*, pp. 064104, Pages 1-8, 2005.
- [37] C. Swalina and S. Hammes-Schiffer, "Impact of Nuclear Quantum Effects on the Molecular Structure of Bihalides and the Hydrogen Fluoride Dimer," *Journal of Physical Chemistry A*, vol. 109, no. 45, pp. 10410-10417, 2005.
- [38] C. Swalina, M. V. Pak and S. Hammes-Schiffer, "Analysis of the Nuclear-Electronic Orbital Method for Model Hydrogen Transfer Systems," *Journal of Chemical Physics*, vol. 123, no. 1, pp. 014303:1-6, 2005.
- [39] R. D. Bardo and K. Ruedenberg, "Even-Tempered Atomic Orbitals. III. Economic Deployment of Gaussian Primitives in Expanding Atomic SCF Orbitals," *Journal of Chemical Physics*, vol. 59, no. 11, pp. 5956-5965, 1973.
- [40] R. D. Bardo and K. Ruedenberg, "Even-Tempered Atomic Orbitals. IV. Atomic Orbital Bases with Pseudoscaling Capability for Molecular Calculations," *Journal of Chemical Physics*, vol. 59, no. 11, pp. 5966-77, 1973.
- [41] R. D. Bardo and K. Ruedenberg, "Even-Tempered Atomic Orbitals. VI. Optimal Orbital Exponents and Optimal Contractions of Gaussian Primitives for Hydrogen, Carbon, and Oxygen in Molecules," *Journal of Chemical Physics*, vol. 60, no. 3, pp. 918-931, 1974.



- [42] R. D. Bardo and K. Ruedenberg, "Even-Tempered Atomic Orbitals. VII. Theoretical Equilibrium Geometries and Reaction Energies for Carbon Suboxide and Other Molecules Containing Carbon, Oxygen, and Hydrogen," *Journal of Chemical Physics*, vol. 60, no. 3, pp. 932-936, 1974.
- [43] R. C. Raffenetti, "Even-Tempered Atomic Orbitals II. Atomic Self-Consistent-Field Wave Functions in Terms of Even-Tempered Exponential Bases," *Journal of Chemical Physics*, vol. 59, pp. 5936-5950, 1973.
- [44] R. C. Raffenetti and K. Ruedenberg, "Even-Tempered Atomic Orbitals V. SCF Calculations of Trialkali Ions with Pseudo-scaled Non-Orthogonal Bases," *Journal of Chemical Physics*, vol. 59, pp. 5978-5991, 1973.
- [45] O. Matsuoka and S. Huzinaga, "Relativistic Well-Tempered Gaussian Basis Sets," *Chemical Physics Letters*, vol. 140, no. 6, pp. 567-571, 1987.
- [46] O. Matsuoka and S. Huzinaga, "Well-Tempered Gaussian Basis Set Expansions of Roothaan-Hartree-Fock Atomic Wavefunctions for Lithium through Mercury," *Journal of Molecular Structure: THEOCHEM*, vol. 167, no. 1-2, pp. 1-209, 1988.
- [47] S. Huzinaga and M. Klobukowski, "The Well-Tempered GTF Basis Set and the ab initio Molecular Calculation," *Journal of Molecular Structure: THEOCHEM*, vol. 135, pp. 403-408, 1986.
- [48] S. Huzinaga, M. Klobukowski and H. Tatewaki, "The Well-Tempered GTF Basis Sets and their Applications in the SCF Calculations," *Canadian Journal of Chemistry*, vol. 63, pp. 1812-1828, 1985.
- [49] S. Huzinaga and M. Klobukowski, "Well-Tempered Gaussian Basis Sets for the Calculation of Matrix Hartree—Fock Wavefunctions," *Chemical Physics Letters*, vol. 212, no. 3-4, pp. 260-264, 1993.
- [50] S. Huzinaga and M. Miguel, "A Comparison of the Geometrical Sequence Formula and the Well-Tempered Formulas for Generating GTO Basis Orbital Exponents," *Chemical Physics Letters*, vol. 175, no. 4, pp. 289-291, 1990.
- [51] G. A. Petersson and S. Zhong, "On the Optimization of Gaussian Basis Sets," *Journal of Chemical Physics*, vol. 118, no. 3, pp. 1101-1109, 2003.
- [52] S. A. Alexander, H. J. Monkhorst and K. Szalewicz, "A Comparison of Muonic Molecular Calculations," vol. 181, pp. 246-258, 1988.

- [53] C. Swalina, M. V. Pak, A. Chakraborty and S. Hammes-Schiffer, "Explicit Dynamical Electron-Proton Correlation in the Nuclear-Electronic Orbital Framework," *J. Phys. Chem. A*, no. 110, 9983-9987, 2006.
- [54] H. Nakai, H. Minoru, K. Miyamoto and S. Hyodo, "Elimination of Translational and Rotational Motions in Nuclear Orbital plus Molecular Orbital Theory," *Journal of Chemical Physics*, vol. 122, pp. 164101:1-10, 2005.

## V. Di-Muonic Hydrogen Molecules

### 5.1 Introduction

This chapter uses the General Particle Orbital (GPO) HF-SCF/CI method presented in Chapter 4 to calculate equilibrium bond lengths and binding energies of di-muonic hydrogen molecules and to study the effects of correlation interactions on these systems. Both parallel and anti-parallel particle spin states are addressed. Only ground muonic state molecules will be presented in this chapter. The di-muonic hydrogen molecules studied in this chapter do not have bound excited muonic states. Excited rotational and vibrational states of di-muonic hydrogen molecules are addressed in Chapter 7.

Dynamic correlation is shown to have large effects on the physical properties of di-muonic hydrogen molecules. As a result, correlation effects of these molecules were studied in detail and are presented in this chapter. Dynamic correlation between quantum particles results in the total energy of molecular systems being lower than that which is calculated using Hartree-Fock (HF) methods. In most electronic molecules the electron correlation results in bond distances being shorter than those calculated using HF methods, without dynamic correlation. In this chapter the exotic molecule  $p\mu\mu p$ , where  $p$  and  $\mu$  represent protons and negative muons respectively, is compared with the  $p\mu p^+$  molecular ion. Qualitative differences in correlation interactions between muonic molecules and corresponding electronic molecules is illustrated. In di-muonic molecules such as  $p\mu\mu p$ , muon-proton and muon-muon correlation interactions result in an increase

in the equilibrium bond distance compared with that calculated using HF methods alone. This comparison highlights the dominant influence of  $p\mu$  correlation energy in  $p\mu\mu p$  molecules and analyzes the major effects of particle spin multiplicity on the binding energy and equilibrium nuclear separation.

## 5.2 Methods

In order to model equilibrium bond distances and binding energies using GPO methods it is first necessary to optimize basis functions for particle wavefunctions and the coordinates of basis set centers. For most electronic molecular systems these optimizations are not strongly dependent on each other. It is possible to employ optimized basis sets between different molecular geometries and similar molecular systems.[1] Such is not possible with  $p\mu\mu p$ . The optimum coefficients for both proton and muon wavefunctions depend strongly upon each other and upon the coordinates of the basis set centers. For the GPO calculations presented in this chapter, basis sets and basis set coordinates were optimized simultaneously by an iterative scheme employing the variational principal (see Chapter 4). The proton basis sets were optimized first; the optimized proton basis sets were then used to optimize muon basis sets. These optimized basis sets were then used to optimize the locations of the basis set centers. This process was repeated iteratively dozens to hundreds of times until the lowest energy configuration was found. For all of the results presented in this chapter the muon and proton basis sets were collocated, therefore, only the separation distance between the basis set centers was optimized. The basis set coefficients were optimized using the Legendre polynomial optimization method [2] using a code written by Gary Kedzoria. This method, which has

been shown to have advantages over the more common even-tempered [3; 4; 5; 6; 7; 8] and well-tempered [9; 10; 11; 12; 13] methods is described elsewhere (see Chapter 4).[2]

After the basis sets and basis set centers were optimized, it was possible to calculate equilibrium bond distances and molecular binding energies. The average proton separation distances for  $p\mu\mu p$  and  $p\mu p^+$  were determined from the expectation values of proton density. For these symmetrical molecules, the distance between the optimized basis set centers and the expectation values of the protons densities were shown to be equal to at least 4 significant figures (*i.e.*,  $1\ \mu\text{\AA}$ ) (see Chapter 4).

In order to study different contributions to predictions of the dynamic correlation energy, the bond distance, the basis sets and basis set centers were optimized at different levels of theory: 1) at the HF level with no correlation correction, 2) at the HF /CI level, including only  $pp$  correlation, 3) at the HF /CI level including only  $\mu\mu$  correlation, and 4) at the HF/CI level, including all three types of particle correlation interactions,  $\mu\mu$ ,  $pp$ , and  $p\mu$ . The equilibrium proton bond distance was then calculated for each of these cases. The calculations were performed using 2s1p proton and muon basis sets with full-CI (FCI) and with 2s2p proton and muon basis sets using complete active space (CAS) methods, where the CI calculations used 10 active molecular orbitals for each of the types of particles. The molecular orbitals chosen were those which contributed most strongly to the HF energy. The calculations presented in this chapter treat all of the muons and nuclei quantum mechanically.

In addition to studying how different types of particle correlation contribute to nuclear separation, their individual contributions to the total correlation energy were also studied. For these studies the variational principal was used to minimize the CI energy

by optimizing the basis set coefficients and center coordinates with  $\mu\mu$ ,  $pp$ , and  $\mu p$  correlation all three being considered. These optimized basis sets and center locations were then used to calculate the individual contributions of  $\mu\mu$ ,  $pp$ , and  $\mu p$  to the total correlation energy.

The differences between the binding energy and bond distances for singlet and triplet muonic and protonic states of the  $p\mu\mu p$  molecular system was also studied.

### 5.3 Results

Table 5-1 summarizes a comparison of  $p\mu\mu p$  and  $p\mu p^+$  bond distances calculated by optimizing the coordinates of basis set centers while including different contribution of proton and muon correlation in the calculations. At the HF level, the  $p\mu\mu p$  bond distance is shorter than that of  $p\mu p^+$ ; however, when particle correlation is considered, the  $p\mu\mu p$  bond length is shown to be significantly longer (*i.e.* 37%) than that of  $p\mu p^+$ . For the  $p\mu p^+$  molecular ion, both  $pp$  and  $\mu p$  correlation contribute to reduce the  $pp$  bond distance. For the  $p\mu\mu p$  molecule  $pp$  correlation affects the bond distance more strongly than does  $\mu\mu$  correlation, shortening the equilibrium bond distance, whereas  $\mu\mu$  and  $\mu p$  correlation both contribute to an increased  $pp$  separation. For the analogous  $H_2$  molecule,  $ee$  and  $pp$  correlation interactions shorten the equilibrium  $pp$  bond distance.

**Table 5-1. Nuclear bond lengths of  $p\mu\mu p$  and  $p\mu p^+$  with respect to correlation energy. The bond distances were optimized assuming 1) no correlation (HF), 2)  $\mu\mu$  correlation only, 3)  $pp$  correlation only, and 4) all three included:  $\mu\mu$ ,  $pp$ , and  $\mu p$  correlation. Row 1 was calculated using 2s1p muon and 2s1p proton basis sets and FCI. Row 2 was calculated using 2s2p muon and 2s2p proton basis sets. Ten active muon molecular orbitals and 10 active proton molecular orbitals were used for the CAS/CI calculations. Row 3 was calculated using 4s3p muon basis sets and 2s2p proton basis sets and FCI.**

		Bond Distance (Å)			
		HF	$\mu\mu$ correlation	$pp$ correlation	$\mu\mu$ , $pp$ , $\mu p$ correlation
1	$p\mu\mu p$ (2s1p)	0.004573	0.004700	0.003176	0.005012
2	$p\mu\mu p$ (2s2p)	0.004112	0.004700	0.003167	0.005013
3	$p\mu p^+$	0.006975	NA	0.004349	0.003655

For the  $p\mu\mu p$  system, individual contributions to the total correlation energy were calculated separately (see Table 5-2).  $\mu\mu$  correlation energy is about 2½ times larger than  $pp$  correlation energy. This is interesting given the fact that  $pp$  correlation was shown to affect the equilibrium bond distance more than does  $\mu\mu$  correlation. The  $\mu p$  correlation energy is about four times larger than the  $\mu\mu$  correlation energy. These ratios are compared to those for  $H_2$  in which the author's calculations show that  $ee$  correlation energy and  $ep$  correlation energy are about equal (*i.e.*,  $\sim 0.9$  eV) while  $pp$  correlation energy in  $H_2$  is about 20 times less than  $ee$  or  $ep$  correlation energy.

**Table 5-2.  $p\mu\mu p$  correlation energy. Row 1 was calculated using 2s1p muon basis sets and 2s1p proton basis sets with FCI. Row 2 was calculated using 2s2p muon and 2s2p proton basis sets with 10 active muon molecular orbitals and 10 active proton molecular orbitals used for the CAS/CI calculations.**

		Correlation Energy (eV)			
		$\mu\mu$ correlation	$pp$ correlation	$\mu p$ correlation	$\mu\mu, pp, \mu p$ correlation
1	2s1p FCI	-183.2721	-77.9020	-724.1032	-985.2773
2	2s2p CAS/CI	-183.3006	-77.9064	-724.0254	-985.2324

The difference in calculated binding energy and proton equilibrium bond distances for  $p\mu\mu p$  when particles of the same type have paired spin (*i.e.*, singlet) and when they have parallel spin (*i.e.*, triplet) can be seen in Table 5-3. Note that for the system studied, there are comparatively small proton-proton spin-orbit influences. There is no significant difference in the binding energy or equilibrium bond distance for singlet or triplet proton states. This can be attributed to the larger mass and separation distance of the protons. The multiplicity of the muons does, however, have a significant impact on both the binding energy and the equilibrium bond distance. When the  $p\mu\mu p$  molecule is in the single muonic state,  $p\mu\mu p$  is strongly bound, with a binding energy of approximately 410 eV. When the molecule is in a triplet muonic state  $p\mu\mu p$  is very weakly bound (*i.e.*,  $\sim 0.074$  eV). The  $pp$  bond distance increases by a factor of almost five when going from a singlet to a triplet muonic state.

For conventional molecules (*i.e.*, molecules containing only nuclei and electrons), using the Born-Oppenheimer approximation, the dynamic correlation energy is limited to about 1% of the corresponding HF energy.[14:265] For  $p\mu\mu p$  dynamic correlation energy is calculated to be as much as 60% of the total energy (see Table 5-3).



**Table 5-3. The effect of particle spin states on the binding energy and equilibrium  $pp$  bond length of  $p\mu\mu p$ . FCI calculations were performed using 2s1p basis sets. The calculations utilizing 2s2p basis sets used 10 active muon molecular orbitals and 10 active proton molecular orbitals for the CI calculations.**

$\mu^-$	$p$	eV			Å
2s1p	2s1p	$E_{\text{HF}}$	$E_{\text{CI}}$	Binding Energy	Bond Distance
singlet	triplet	-2941.7077	-3926.9850	410.5254	0.005012
triplet	singlet	-1389.2584	-3543.7386	0.074040	0.023955
triplet	triplet	-2783.2935	-3543.7386	0.074040	0.023955

$\mu^-$	$p$	eV			Å
2s2p	2s2p	$E_{\text{HF}}$	$E_{\text{CI}}$	Binding Energy	Bond Distance
singlet	triplet	-2941.7289	-3926.9613	410.5103	0.005013
triplet	singlet	-1389.2719	-3543.7387	0.074094	0.023953
triplet	triplet	-2783.2778	-3543.7387	0.074091	0.023953

## 5.4 Conclusions

The important roles that  $\mu\mu$ ,  $pp$  and  $\mu p$  correlation interactions play in the binding of  $p\mu\mu p$  molecules was demonstrated. These interactions account for as much as 60% of the total energy of the muonic system. Of the three correlation contributions,  $\mu p$  correlation is by far the most important. This indicates that the results of previously published calculations, which neglect  $\mu p$  correlation interactions, cannot be expected to yield accurate binding energies.[15] As with other types of molecules, correlation effects can strengthen molecular bonding. Unlike most electronic molecules, however, correlation effects in the di-muonic hydrogen molecule  $p\mu\mu p$  result in an increase in the nuclear bond distance compared with  $p\mu p^+$ .

Whether nuclear spin is paired or unpaired does not have a significant impact on the binding energy or nuclear bond distance of  $p\mu\mu p$ . Muon spin does, however significantly affect both the binding energy and  $pp$  bond distance.  $p\mu\mu p$  molecules in a

singlet muon state have a binding energy of approximately 410 eV. When the muons are in a triplet spin state the binding energy is much weaker (i.e.,  $\sim .074$  eV).

## References

- [1] S. P. Webb, T. Iordanov and S. Hammes-Schiffer, "Multiconfigurational Nuclear-Electronic Orbital Approach: Incorporation of Nuclear Quantum Effects in Electronic Structure Calculations," *Journal of Chemical Physics*, vol. 117, pp. 4160-4118, 2002.
- [2] G. A. Petersson and S. Zhong, "On the Optimization of Gaussian Basis Sets," *Journal of Chemical Physics*, vol. 118, no. 3, pp. 1101-1109, 2003.
- [3] R. D. Bardo and K. Ruedenberg, "Even-Tempered Atomic Orbitals. III. Economic Deployment of Gaussian Primitives in Expanding Atomic SCF Orbitals," *Journal of Chemical Physics*, vol. 59, no. 11, pp. 5956-5965, 1973.
- [4] R. D. Bardo and K. Ruedenberg, "Even-Tempered Atomic Orbitals. IV. Atomic Orbital Bases with Pseudoscaling Capability for Molecular Calculations," *Journal of Chemical Physics*, vol. 59, no. 11, pp. 5966-77, 1973.
- [5] R. D. Bardo and K. Ruedenberg, "Even-Tempered Atomic Orbitals. VI. Optimal Orbital Exponents and Optimal Contractions of Gaussian Primitives for Hydrogen, Carbon, and Oxygen in Molecules," *Journal of Chemical Physics*, vol. 60, no. 3, pp. 918-931, 1974.
- [6] R. D. Bardo and K. Ruedenberg, "Even-Tempered Atomic Orbitals. VII. Theoretical Equilibrium Geometries and Reaction Energies for Carbon Suboxide and Other Molecules Containing Carbon, Oxygen, and Hydrogen," *Journal of Chemical Physics*, vol. 60, no. 3, pp. 932-936, 1974.
- [7] R. C. Raffenetti, "Even-Tempered Atomic Orbitals II. Atomic Self-Consistent-Field Wave Functions in Terms of Even-Tempered Exponential Bases," *Journal of Chemical Physics*, vol. 59, pp. 5936-5950, 1973.
- [8] R. C. Raffenetti and K. Ruedenberg, "Even-Tempered Atomic Orbitals V. SCF Calculations of Trialkali Ions with Pseudo-scaled Non-Orthogonal Bases," *Journal of Chemical Physics*, vol. 59, pp. 5978-5991, 1973.
- [9] O. Matsuoka and S. Huzinaga, "Relativistic Well-Tempered Gaussian Basis Sets," *Chemical Physics Letters*, vol. 140, no. 6, pp. 567-571, 1987.

- [10] O. Matsuoka and S. Huzinaga, "Well-Tempered Gaussian Basis Set Expansions of Roothaan-Hartree-Fock Atomic Wavefunctions for Lithium through Mercury," *Journal of Molecular Structure: THEOCHEM*, vol. 167, no. 1-2, pp. 1-209, 1988.
- [11] S. Huzinaga, M. Klobukowski and H. Tatewaki, "The Well-Tempered GTF Basis Sets and their Applications in the SCF Calculations," *Canadian Journal of Chemistry*, vol. 63, pp. 1812-1828, 1985.
- [12] S. Huzinaga and M. Klobukowski, "Well-Tempered Gaussian Basis Sets for the Calculation of Matrix Hartree—Fock Wavefunctions," *Chemical Physics Letters*, vol. 212, no. 3-4, pp. 260-264, 1993.
- [13] S. Huzinaga and M. Miguel, "A Comparison of the Geometrical Sequence Formula and the Well-Tempered Formulas for Generating GTO Basis Orbital Exponents," *Chemical Physics Letters*, vol. 175, no. 4, pp. 289-291, 1990.
- [14] I. N. Levine, *Quantum Chemistry*, Boston: Allyn and Bacon, Inc., 1983.
- [15] Y. Hamahata, E. Hiyama and M. Kamimura, "Non-Adiabatic Four-Body Calculation of Double-Muonic Hydrogen Molecules," *Hyperfine Interactions*, vol. 138, pp. 187-190, 2001.

## VI. Di-Muonic Helium Molecules

### 6.1 Introduction

Several factors limit the maximum obtainable muon-catalyzed fusion yield. Preeminent amongst these factors in the mono-muonic mechanisms is the sticking of muons to helium nuclei formed during the fusion processes outlined in Chapter 2 and Appendix A. This chapter examines the possibility of fusing di-muonic  ${}^3\text{He}$  molecules, formed during  $p$ - $d$  and  $d$ - $d$  fusion, liberating muons which are stuck to these nuclei.

Regardless of what modifications to the muon-catalyzed fusion reaction cycle are made, mono-muon catalyzed fusion cannot be a practical source of energy production unless muons can be prevented from sticking to helium, or can be stripped from helium after sticking occurs. Many attempts have been made to find a method of manipulating the sticking probability and of freeing stuck muons. As of the writing of this document, no effective methods have been developed. It has been shown that muon sticking and stripping are affected by temperature and pressure. Research indicates, however, that adjustment of these factors cannot, by themselves, solve the muon-catalyzed fusion sticking problem.[1]

In addition to sticking to helium during the fusion process, muons can be “scavenged” by helium in a reaction chamber. This can occur either as a result of collisions between helium and free muons or as the result of muon exchange reactions between helium and muonic hydrogen molecules. While it is possible to address this problem by removing helium to maintain a low concentration of helium in the reaction

chamber; being that helium is one of the products formed during muon-catalyzed fusion, its concentration and scavenging need to be addressed.

Two possible mechanisms for releasing some of the muons stuck to  ${}^3\text{He}$  during fusion are the fusion of two  ${}^3\text{He}$  nuclei and the fusion of a  ${}^3\text{He}$  nuclei and a deuteron. These reactions are represented in Equations 6.1 and 6.2. Helium-3, which is a product of  $p$ - $d$  and  $d$ - $d$  fusion can go on to fuse via the following nuclear reactions:



and



where  $p$ , and  $d$  represent protons and deuterons respectively. Some of the muons that participate in these reactions will be freed, enabling them to catalyze further fusion events. It is possible that helium nuclei, which are stuck to muons, can fuse and free the muons to catalyze additional fusion reactions. Due to the magnitude of the Coulombic repulsion of helium nuclei with other nuclei, single muons cannot be expected to catalyze helium fusion reactions. While most of the muons which participate in reactions 6.1 and 6.2 are expected to be liberated by the reaction, some of the muons will stick to the  ${}^4\text{He}$  nuclei formed during the reaction.[2; 3:72; 4]

If formed,  ${}^3\text{He}\mu{}^3\text{He}\mu$  and/or  ${}^3\text{He}\mu\mu d$  molecules have the possibility of fusing and liberating previously bound muons in the process. This chapter examines the bond lengths and vibrational properties of di-muonic  ${}^3\text{He}-{}^3\text{He}$  and  ${}^3\text{He}-d$  molecules to determine whether bound forms of these molecules exist, and if so, their equilibrium bond lengths and vibrational properties. The fusion rate of these molecules will depend, in part, on the separation distance between the nuclei.

## 6.2 Methods

In order to determine the equilibrium bond lengths of di-muonic  ${}^3\text{He}-{}^3\text{He}$  and  ${}^3\text{He}-d$  molecules the General Particle Orbital (GPO) method of non-adiabatic quantum mechanics described in Chapter 4 was used. Dynamic correlation was included in the calculations through the use of configuration interaction (CI) methods.[5; 6] The equilibrium bond length was calculated from the expectation value of nuclei density. For the  ${}^3\text{He}-{}^3\text{He}$  calculations the Born-Oppenheimer approximation was used and the nuclei positions were fixed for individual HF/CI calculations. The bond length for  ${}^3\text{He}-d$  was determined by fixing the  ${}^3\text{He}$  nuclei and modeling the deuteron and muons as quantum particles. The results of these calculations were compared to results in which both of the nuclei were fixed. The basis set parameters and basis set center locations were optimized simultaneously, at the CI level, using five active molecular orbitals per quantum particle.

When solving the Schrödinger equation for ordinary molecules it is most often assumed that the volume of nuclei is negligible. In the case of an electron and a proton the error generated by this approximation is about  $6\times 10^{-9}$  eV. Because a muonic

molecular hydrogen radius is about 200 times smaller than that of an electronic molecular hydrogen radius, significant errors can result from assuming the nuclear volume of muonic molecules to be zero. A first order approximation to the energy correction can be calculated using perturbation theory. This method of correcting for nuclear volume effects is considered accurate as long as the perturbation is limited to a small fraction of the total energy, as it is for nuclei from the first few rows of the periodic table. The potential energy  $V(r)$  is assumed to result from a point charge [5; 7:49-50; 8:1141-1147]

$$V(r) = -\frac{Ze^2}{4\pi \epsilon_0 r} \quad (6.3)$$

when the negative particle radius ( $r$ ) is greater than the mean nuclear radius ( $R$ ). When  $r \leq R$  the nuclei can be considered to be a uniformly charged sphere which results in a potential energy

$$V(r) = -\frac{Ze^2}{4\pi \epsilon_0 R} \left[ \frac{3}{2} - \frac{1}{2} \left( \frac{r}{R} \right)^2 \right] \quad (6.4)$$

where  $Z$  is the charge of the nucleus of interest.[7:49-51; 8:1141-1147] If  $\langle V \rangle$  is the expectation value of the potential energy, assuming a point mass, and  $\langle V' \rangle$  the expectation value calculated using equations (6.3) and (6.4) as described, then the potential energy correction ( $\Delta V$ ) for nuclear volume is



$$\Delta V = \langle V' \rangle - \langle V \rangle \quad (6.5)$$

The radial wave function used to calculate the expectation values can be approximated by Coulomb hydrogenic radial wave functions:

$$R_{nl}(r) = -\sqrt{\left(\frac{2Z}{na_0}\right)^3 \frac{(n-l-1)!}{2n[(n+l)!]}} \exp\left(-\frac{Zr}{na_0}\right) \left(\frac{2Zr}{na_0}\right)^l L_{n+l}^{2l+1}\left(\frac{2Zr}{na_0}\right) \quad (6.6)$$

where

$$a_0 \equiv \frac{4\pi \epsilon_0 \hbar^2}{\mu e^2} \quad (6.7)$$

and  $L_{n+l}^{2l+1}$  represents associated Laguerre Polynomials.  $n$  and  $l$  represent principle and azimuthal quantum numbers respectively. For the ground state (1s) this yields:

$$R_{1,1}(r) = 2\left(\frac{Z}{a}\right)^{\frac{3}{2}} \exp\left(-\frac{Zr}{a_0}\right) \quad (6.8)$$

and

$$\Delta V_{n=1} = \frac{e^2 Z^4}{\pi \epsilon_0 a_0^3} \int_0^R \left( r - \frac{3r^2}{2R} + \frac{r^4}{2R^3} \right) \exp\left(-\frac{2Zr}{a_0}\right) dr \quad (6.9)$$

which reduces to

$$\Delta V_{n=1} = \frac{e^2}{8\pi \epsilon_0 a_0 R^3 Z} \left[ 3a_0^3 - 3a_0 R^2 Z^2 + 2R^3 Z^3 - 3a_0 (a_0 + RZ)^2 \exp\left(-\frac{2RZ}{a_0}\right) \right] \quad (6.10)$$

Table 6-1 uses the methods described in this chapter to compare the potential energy of muonic hydrogen and helium atoms with and without nuclear volume included in the calculations.

**Table 6-1. Potential energy, as compared to free particles, of hydrogen and helium muonic-atoms.**

Atom	V with no nuclear volume <sup>a</sup>	V with nuclear volume <sup>a</sup>
$p\mu$	-2528.58	-2528.54
$d\mu$	-2663.29	-2663.22
$t\mu$	-2711.34	-2711.24
${}^3\text{He}\mu$	-10845.42	-10843.84
${}^4\text{He}\mu$	-10943.18	-10941.22

<sup>a</sup>Energy is reported in eV

A potential energy correction can be calculated for molecules containing more than one nucleus by first calculating the atomic correction terms  $\Delta V_i$  for each nucleus in the molecule. The total molecular correction ( $\Delta V_m$ ) is

$$\Delta V_m = \sum_{i=1}^N \frac{C_i}{D_i} \Delta V_i \quad (6.11)$$

where  $C_i$  represents the average muon charge density in each nuclei  $i$ , and  $D_i$  is the muon charge density in the nuclei  $i$  when the nuclei and muon are isolated from all other nuclei. Throughout this document, the nuclear radii ( $R$ ) have been approximated as  $R = 1.25A^{1/3}$  femtometers.[7:48,122]

The vibrational energy levels, vibrational frequency and magnitude of the nuclear vibrations were determined using quasi-classical methods. The quantum vibrational energy levels between nuclei were calculated using a quantum mechanical energy grid. The quantum vibrational energy levels between two particles were calculated, starting with [9]:

$$\hat{H} = \hat{T} + \hat{V} \quad (6.12)$$

where  $\hat{H}$  is the Hamiltonian operator of the system,  $\hat{T}$  is a kinetic energy operator and  $\hat{V}$  is a potential energy operator. Being that the kinetic energy operator for a harmonic approximation to the system is the same as the true kinetic energy operator, the Hamiltonian operator for a harmonic approximation ( $\hat{H}_{HO}$ ) to the system can be written as:

$$\hat{H}_{HO} = \hat{T} + \hat{V}_{harm} \quad (6.13)$$

where  $\hat{V}_{harm}$  is a harmonic approximation to the potential energy of the system. Adding both sides of the above equation to  $\hat{H}$  yields

$$\hat{H} = \hat{H}_{HO} + \hat{V} - \hat{V}_{harm} \quad (6.14)$$

Since it is possible to determine analytical expressions for the expectation values of  $\hat{H}_{HO}$  and  $\hat{V}_{harm}$ , and the expectation value of  $\hat{V}$  can be determined numerically by integrating a fit of a quantum mechanically determined energy grid, the expectation value of  $\hat{H}$  can be determined.

Through the use of ladder operators it is possible to determine an  $n \times n$  matrix which approximates  $\hat{H}$

$$\hat{H} = \begin{vmatrix} \langle 1 | \hat{H} | 1 \rangle & \langle 1 | \hat{H} | 2 \rangle & . & . & . & \langle 1 | \hat{H} | n \rangle \\ \langle 2 | \hat{H} | 1 \rangle & \langle 2 | \hat{H} | 2 \rangle & . & . & . & \langle 2 | \hat{H} | n \rangle \\ . & . & & & & . \\ . & . & & & & . \\ . & . & & & & . \\ \langle n | \hat{H} | 1 \rangle & \langle n | \hat{H} | 2 \rangle & . & . & . & \langle n | \hat{H} | n \rangle \end{vmatrix} \quad (6.15)$$

The matrix elements of  $\hat{H}$  are defined as:

$$\begin{aligned}
\langle i | \hat{H} | j \rangle = & \left\{ \hbar \omega \left( j + \frac{1}{2} \right) - \frac{\hbar^2 \alpha^2 D_e}{2\mu\omega} (1 + 2j) \right\} \delta_{i,j} \\
& - \frac{\hbar^2 \alpha^2 D_e}{2\mu\omega} \left\{ (j+1)^{\frac{1}{2}} (j+2)^{\frac{1}{2}} \delta_{i,j+2} + j^{\frac{1}{2}} (j-1)^{\frac{1}{2}} \delta_{i,j-2} \right\} \\
& + \int_{-\infty}^{\infty} \psi_j^*(x) \hat{V}(x) \psi_i(x) dx
\end{aligned} \tag{6.16}$$

where

$$\alpha = \sqrt{\frac{\mu_{red} \omega}{\hbar}} \tag{6.17}$$

and

$$\omega = \sqrt{\frac{\hat{V}''(R_{eq})}{\mu_{red}}} \tag{6.18}$$

$V''(R_{eq})$  is the second derivative of the potential energy with respect to bond length, evaluated at the equilibrium geometry  $R_{eq}$ .  $D_e$  is the equilibrium dissociation energy;  $\hbar$  is the reduced Planck's constant; and  $\mu_{red}$  is the reduced mass between the particles that were fixed for each quantum mechanical calculation.

If  $\psi_i(z)$  is defined as the harmonic-oscillator wave function  $\langle z | i \rangle$

$$\psi_i(z) = \langle z | i \rangle = N_i H_i(\alpha z) e^{-\frac{\alpha^2 z^2}{2}} \quad (6.19)$$

where  $H_i(\alpha z)$  represents Hermite polynomials:

$$\begin{aligned} H_0(\alpha z) &= 1 \\ H_1(\alpha z) &= 2\alpha z \\ H_2(\alpha z) &= 4\alpha^2 z^2 - 2 \\ &\vdots \\ H_i(\alpha z) &= 2\alpha z H_{i-1} - 2n H_{i-2}(\alpha z) \end{aligned} \quad (6.20)$$

and  $N_i$  refers to normalization constants:

$$N_i = \left( \frac{\alpha}{\pi^{\frac{1}{2}} 2^i i!} \right) \quad (6.21)$$

$z$  is the nuclei separation distance ( $x$ ) minus the equilibrium bond length ( $R_{eq}$ )

$$z = x - R_{eq} \quad (6.22)$$

If eigenvalues of  $\hat{H}$  are less than the molecules binding energy, then they represent quantum vibrational energy levels of the molecule. The larger  $n$  in Equation 6.15, the greater the accuracy of a given eigenvalue  $i$ .

By taking a numerical first derivative of the potential energy with respect to bond length and setting the derivative equal to zero, the potential energy minimum (*i.e.*, equilibrium geometry) can be found. The harmonic vibrational frequency of the nuclei is

$$\nu = \frac{1}{2\pi} \sqrt{\frac{\hat{V}''(R_{eq})}{\mu_{red}}} \quad (6.23)$$

In order to observe the anharmonic effects of internal kinetic energy on the vibrational frequency, Hamilton's equation of motion

$$\frac{\partial \hat{H}}{\partial q} = -\dot{p} \quad (6.24)$$

was solved for position ( $q$ ) and momentum ( $p$ ) (*i.e.*, in this case  $q$  is equal to the internuclear separation ( $x$ )).[10:992-1023] The symbol  $\hat{H}$  represents a classical Hamiltonian and is equal to the sum of the potential and kinetic energy operators. The vibrational spectra (*i.e.*, power spectral density) of the system was generated by taking the Fourier transform of the position, momentum, kinetic energy and potential energy as functions of time.[11:600-717; 12; 13]

## 6.3 Results and Discussion

### 6.3.1 $\mu$ $^3\text{He} + \mu$ $^3\text{He}$

Due to its small size,  $(^3\text{He}\mu)^+$  interacts with charged particles in a manner similar to how hydrogen nuclei interact, except when molecular separation distances are small ( $\lesssim 0.01$  Å). Due to the larger muon mass relative to an electron, muonic helium orbitals are approximately  $1/200^{\text{th}}$  the size of a helium electronic orbital. A significant portion of the muon density is calculated to be located within the helium nucleus (*i.e.*,  $\sim 3\%$ ). As a result of its small size, two  $(^3\text{He}\mu)^+$  ions interact with each other similarly to two +1 point charges, except when the nuclei are very close to each other ( $\lesssim 0.01$  Å). When the molecular separation is small, both muons interact with both nuclei resulting in a localized potential energy minimum. These results can be seen in Figures 6-1a, 6-1b and 6-1c.



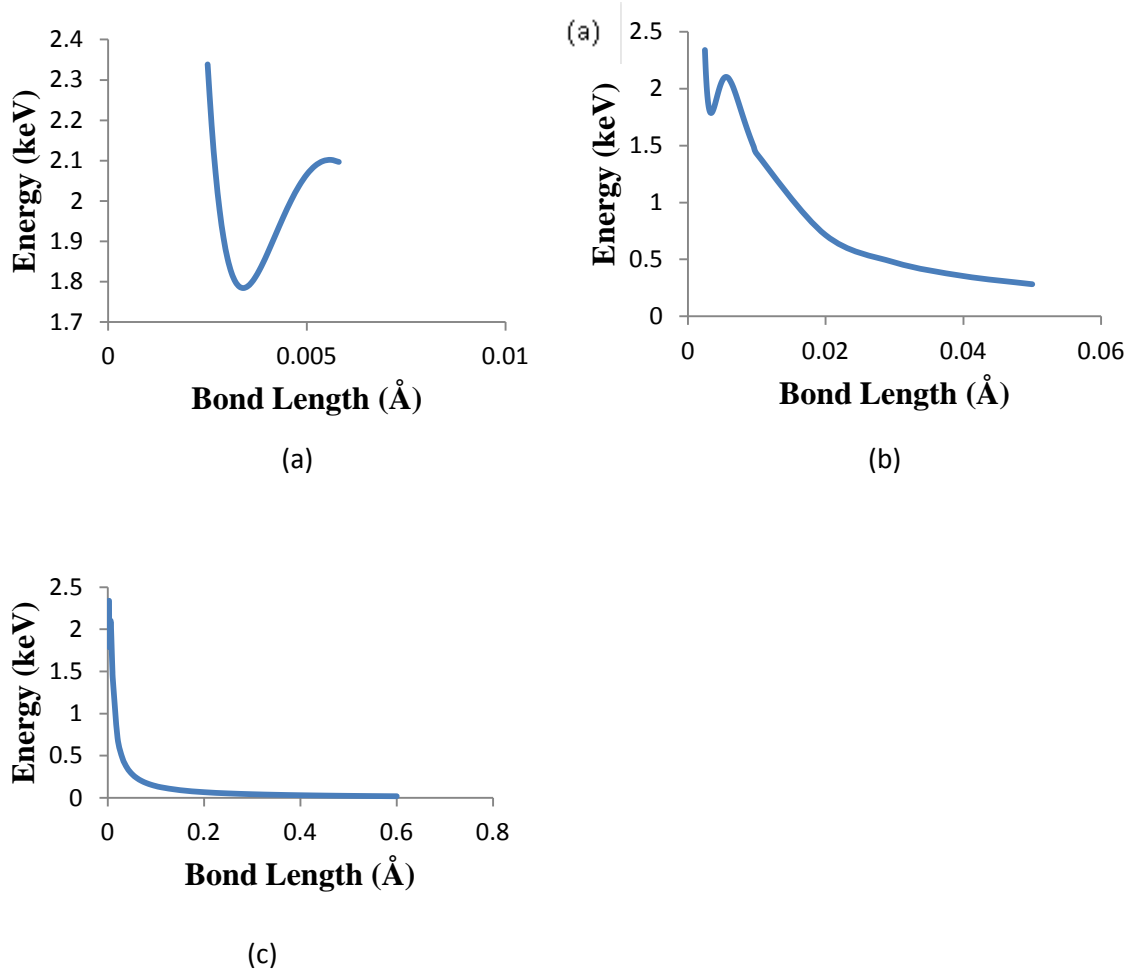
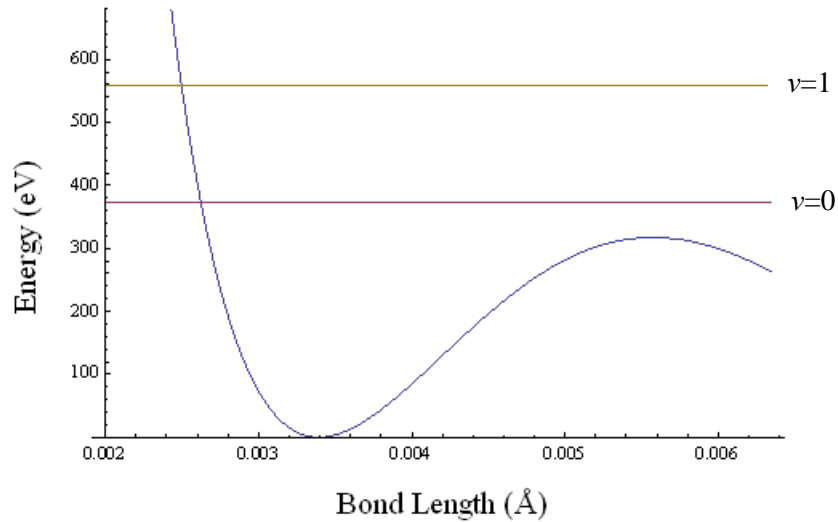


Figure 6-1a, 6-1b and 6-1c.  $(^3\text{He}\mu^3\text{He}\mu)^{2+}$  potential energy versus bond length with respect to free  $(^3\text{He}\mu)^+$  ions. 4s3p muon basis sets were centered on classical (*i.e.*, fixed)  $^3\text{He}$  nuclei. The localized energy minimum occurs at 0.003393 Å.

The eigenvalues of  $\hat{H}$  were calculated for the localized energy minimum. There are no bound vibrational states (see Figure 6-2). From these results it can be concluded that the di-muonic helium ion  $(^3\text{He}\mu^3\text{He}\mu)^{2+}$  is unstable and cannot be a pathway for producing significant quantities of fusion energy. It is likely that  $[(^3\text{He}\mu^3\text{He}\mu)e]^+$  and

$(^3\text{He}\mu^3\text{He}\mu)2e$  form bound molecules, however, the He-He bond lengths for these molecules are expected to be approximately equal to the bond lengths of  $^3\text{H}_2^+$  and  $^3\text{H}_2$  respectively. Therefore these molecules are expected to have negligible fusion rates. Including nuclear volume effects in the calculations does not change these results. Rather it results in a calculated eigenvalues of  $\hat{H}$ ,  $v=0$  and  $v=1$ , which are slightly more negative than when nuclear volume is neglected in the calculations.



**Figure 6-2. Eigenvalues  $v=0$  and  $v=1$  of  $\hat{H}$  for  $(^3\text{He}\mu^3\text{He}\mu)^{2+}$ . This shows there are no bound vibrational energy levels of the localized minimum.**

### 6.3.2 $^3\text{He} + d$

$(^3\text{He}\mu\mu d)^+$  was modeled two ways: 1) using classical nuclei and quantum muons and 2) using fixed  $^3\text{He}$  coordinates (*i.e.*, classical  $^3\text{He}$ ), a quantum deuteron and quantum muons. Both methods yielded similar results. All of the calculations were performed at

the FCI level with 4s3p muon basis sets. A 2s2p deuteron basis set was used. The muon basis sets were centered on the classical nuclei and collocated with the quantum deuteron basis set center coordinates. The basis sets and basis set center coordinates were optimized simultaneously.

A potential energy curve was calculated using the Born-Oppenheimer approximation. The energy was corrected to account for the muon density which is located within the nuclei. The results of this correction can be seen in Figure 6-3. The  ${}^3\text{He-d}$  equilibrium bond length was calculated to be 0.003732 Å. There are two bound vibrational states, the ground state ( $\nu=0$ ) and the first excited vibrational state ( $\nu=1$ ) (see Figure 6-4).

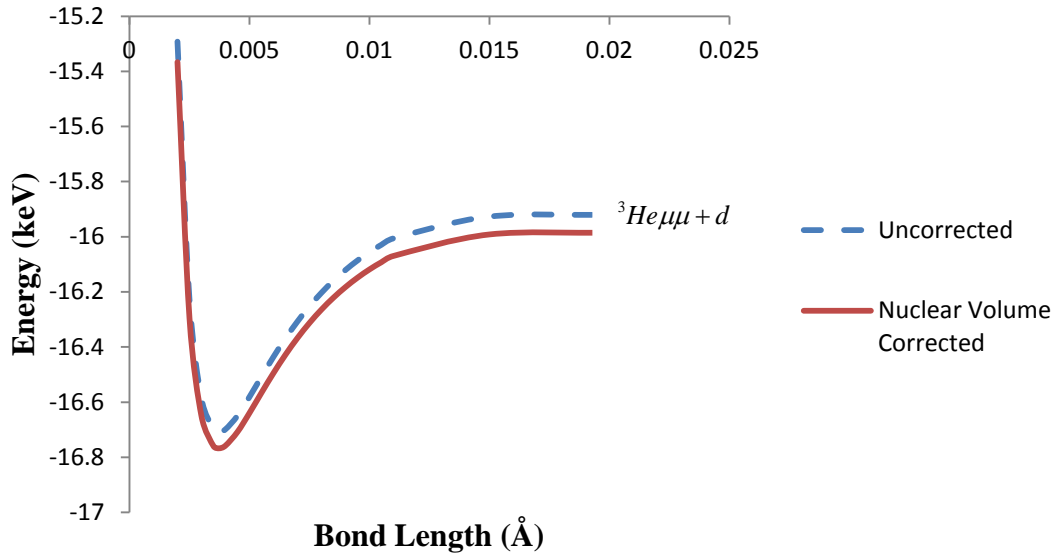


**Figure 6-3. Comparison of  $({}^3\text{He}\mu\mu d)^+$  potential energy curves with and without nuclear volume being considered. The energy represents the total energy of the muonic ion with respect to free particles. The nuclei were considered classically in the calculations shown.**

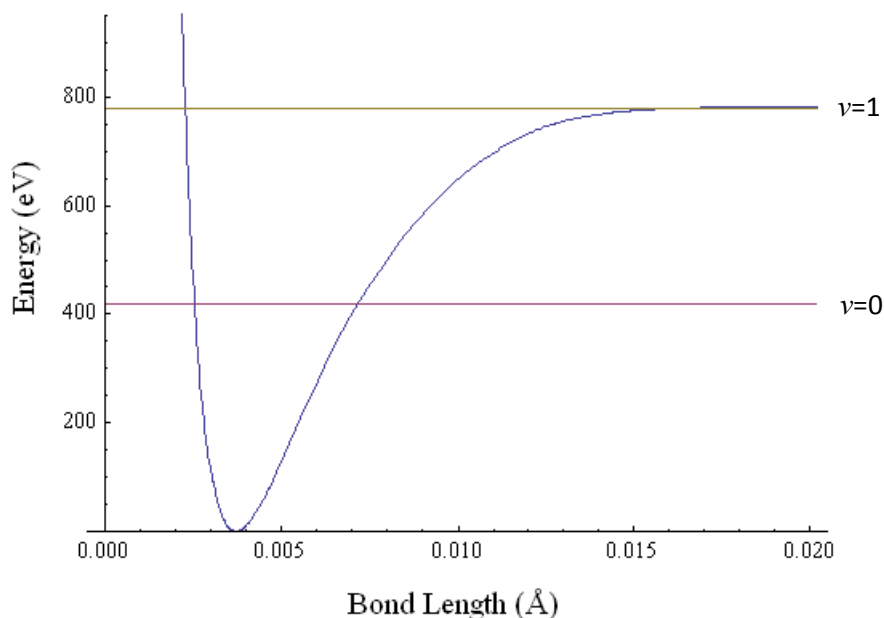


**Figure 6-4.  $(^3\text{He}\mu d)^+$  potential energy curve with nuclear volume and bound vibrational energy levels included in the calculations. The ground ( $v=0$ ) and first ( $v=1$ ) quantum vibrational energy states are shown. The potential energy minimum occurs at 0.003732 Å. The quantum mechanical points were interpolated between using cubic spline interpolation with fixed endpoints. The nuclei were considered classically in the calculations shown. A plot of the potential energy surface and vibrational energy levels calculated without including nuclear volume effects looks almost identical on this scale.**

Inclusion of nuclear volume effects in the calculations results in a decrease in the calculated binding energy (see Table 6-1 and 6-3). This is particularly the case for the  $v=1$  state, in which inclusion of nuclear volume effects results in a calculated binding energy that is almost an order of magnitude less than when nuclear volume effects are neglected.

**Table 6-2. Binding energy of the  $v=0$  and  $v=1$  vibrational states of  $(^3\text{He}\mu\mu d)^+$ .**

	Binding Energy (eV)	
	Nuclear Volume Corrected	No Volume Correction
$v=0$	364.9872	370.6573
$v=1$	0.1633	1.4430

Table 6-2 shows the minimum and maximum bond lengths which occur during nuclear vibrations. As can be seen, inclusion of nuclear volume in the calculations has very little effect on the calculated minimum separation distance between molecules. The maximum bond length of the  $v=1$  state is not reported since very small errors in the calculated binding energy result in large errors in the maximum bond length (see Figure 6-4).

**Table 6-3. The magnitude of nuclear vibrations of  $(^3\text{He}\mu\mu d)^+$  calculated with classical nuclei, with and without nuclear volume corrections.**

	Nuclear Volume Corrected		No Volume Correction	
	Minimum Bond Length	Maximum Bond Length	Minimum Bond Length	Maximum Bond Length
$v=0$	0.00255026	0.00715116	0.00255702	0.00714663
$v=1$	0.00228465		0.00228737	

The vibrational spectra and fundamental vibrational frequency of  $(^3\text{He}\mu\mu d)^+$  nuclei in the ground vibrational state ( $v=0$ ) was calculated by propagating a classical trajectory on the quasi-classical potential energy curve described previously (see Figure 6-4). The fundamental vibrational frequency was calculated to be  $1.515 \times 10^{17}$  Hz. This is considerably smaller than the harmonic vibrational frequency of  $2.408 \times 10^{17}$  Hz

calculated from the Hessian at the potential energy minimum. The large amount of anharmonicity which occurs in the bound vibrational states of this ion is the result of large changes in energy which occur with small shifts in nuclei position of closely bound muonic molecules. The excited state vibrational frequency contains a great degree of anharmonicity and is highly dependent on the energy of the  $v=1$  state. Small errors in the calculation of the potential energy result in large errors in the calculated frequency. As a result, the methods presented in this paper cannot be used to determine the vibrational frequency of the  $v=1$  state.

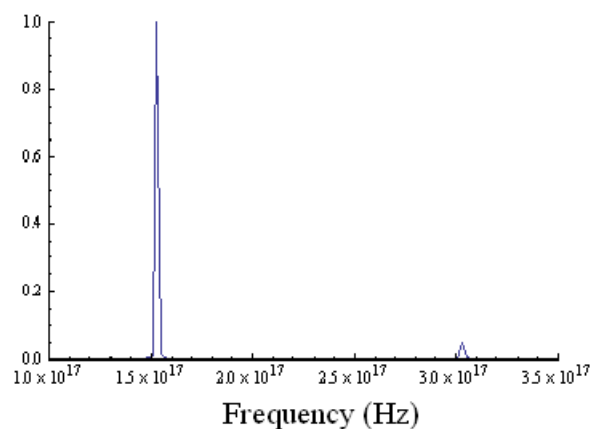


**Figure 6-5. Calculated ground state ( $v=0$ ) vibrational spectra of  $(^3\text{He}\mu\mu d)^+$  nuclei.**

Using a fixed  $^3\text{He}$  nucleus and a quantum deuteron, the bond length ( $r$ ) was calculated as the distance between the  $^3\text{He}$  coordinate and the expectation value of the deuteron density. The deuteron basis set was transferred from an optimized  $d\mu\mu d$  molecule. The muon basis sets were centered on the  $^3\text{He}$  and on the coordinates of the expectation value of the deuteron density. The muon basis sets were optimized

simultaneously for the  $({}^3\text{He}\mu\mu d)^+$  molecular ion. The results yielded an equilibrium bond length  $r = .002375 \text{ \AA}$  which is shorter than that calculated with two fixed nuclei  $r = 0.003732 \text{ \AA}$ . These bond lengths are shorter than the bond lengths of muonic hydrogen molecules which have been shown to have large fusion rate constants ( $> 10^7 \text{ s}^{-1}$ ).[14]

#### 6.4. Conclusions

$({}^3\text{He}\mu{}^3\text{He}\mu)^{2+}$  does not form a bound molecule. A quasi-classical potential energy surface indicates that a localized potential energy minimum exists when the nuclei are separated by about  $3.4 \text{ m\AA}$ ; however, no bound vibrational states occur in this region. These results indicate that  ${}^3\text{He}\mu{}^3\text{He}\mu$  will not participate in a feasible muon-catalyzed fusion reaction path, nor will it result in a viable muon stripping mechanism.

$({}^3\text{He}\mu\mu d)^+$  forms a bound system with two bound vibrational states ( $v=0$  and  $v=1$ ). The binding energy of these states is  $E(v=0) = 365 \text{ eV}$  and  $E(v=1) = 0.16 \text{ eV}$ . The calculation of the excited state binding energy is strongly influenced by nuclei volume. Neglecting nuclei volume results in almost an order of magnitude greater binding energy being calculated. The bond length between the nuclei was calculated using the Born-Oppenheimer approximation to be  $3.7 \text{ m\AA}$  and was calculated to be  $2.4 \text{ m\AA}$  when the deuteron was considered non-adiabatically. The ground state vibrational frequency is  $152 \text{ PHz}$ .

In conclusion, the formation of  $({}^3\text{He}\mu\mu d)^+$  has the potential of enhancing the muon-catalyzed reaction rate (*i.e.*, number of fusions catalyzed per muon).  $({}^3\text{He}\mu{}^3\text{He}\mu)^{2+}$  cannot significantly change the overall fusion rate.



## References

- [1] W. H. Breunlich, P. Kammel, J. S. Cohen and M. Leon, "Muon-Catalyzed Fusion," *Annual Review of Nuclear and Particle Science*, vol. 39, pp. 311-355, 1989.
- [2] K. Nagamine, K. Ishida, S. Sakamoto, Y. Watanabe and T. Matsuzaki, "X-Ray Measurement on Muon to Alpha Sticking in Muon Catalyzed d-t Fusion; Present and Future," *Hyperfine Interactions*, vol. 82, no. 1-4, pp. 343-353, 1993.
- [3] K. Nagamine, *Introductory Muon Science*, Cambridge: Cambridge University Press, 2003.
- [4] L. I. Ponomarev, "Muon Catalysed Fusion," *Contemporary Physics*, vol. 31, no. 4, pp. 219-245, 1990.
- [5] E. V. Sheely, L. W. Burggraf, P. E. Adamson, F. D. Xiaofeng and M. W. Schmidt, "Application of GAMESS/NEO to Quantum Calculations of Muonic Molecules," in *Advanced Science Research Symposium 2009 Positron, Muon and other exotic particle beams for materials and atomic/molecular sciences (ASR2009)*, vol. 225 no. 1, Tokai, 2010.
- [6] S. P. Webb, T. Jordanov and S. Hammes-Schiffer, "Multiconfigurational Nuclear-Electronic Orbital Approach: Incorporation of Nuclear Quantum Effects in Electronic Structure Calculations," *Journal of Chemical Physics*, vol. 117, pp. 4160-4118, 2002.
- [7] K. M. Krane, *Introductory Nuclear Physics*, New York: John Wiley and Sons, Inc., 1988, p. 52.
- [8] C. Cohen-Tannoudji, B. Diu and F. Laloë, *Quantum Mechanics*, ed. 2 ed., vol. 1, New York: John Wiley and Sons, 1977.
- [9] D. E. Weeks, *Molecular Orbital Theory*, Air Force Institute of Technology, 2009.
- [10] W. F. van Gunsteren and H. J. C. Berendsen, "Computer Simulation of Molecular Dynamics: Methodology, Applications and Perspectives in Chemistry," *Angewandte Chemie, International Edition in English*, vol. 29, pp. 992-1023, 1990.
- [11] W. H. Press, B. P. Teukolsky, W. T. Vetterling and B. P. Flannery, *Numerical Recipes, the Art of Scientific Computing*, 5th ed., Cambridge: Cambridge University Press, 2007.

- [12] S. L. Marple, Digital Spectral Analysis with Applications, Upper Saddle River: Prentice-Hall, 1987.
- [13] E. V. Sheely, Quasi-Classical Molecular Dynamics of Weakly Bound Donor-Acceptor Complexes, Ann Arbor: UMI, Bell & Howell, 1997.
- [14] L. I. Ponomarev, "Muon-Catalyzed Fusion and Fundamental Physics," *Hyperfine Interactions*, vol. 103, pp. 137-145, 1996.

## VII. Reactions paths of $p\mu\mu p^{(T)}$ and $p\mu p\mu p^{(T)}$

### 7.1 Introduction

If formed in a muon-catalyzed fusion chamber, di-muonic hydrogen molecules are expected to affect the muon-catalyzed fusion rate. Whether the effect will be positive or negative depends on the rate the di-muonic molecules fuse or transform into molecules which fuse. If this process is fast, compared to single fusion reaction paths, the fusion yield will be enhanced. If the process is slow, di-muonic reactions will have a quenching effect on the muon-catalyzed fusion process.

Di-muonic hydrogen molecules can form in a triplet muon spin state. Due to the large bond length of these molecules, they cannot be expected to have a significant fusion rate (see Chapter 5). As a result, if these molecules are to enhance the muon-catalyzed fusion rate, reaction paths that transform these molecules into species which do fuse rapidly must exist. The probability of these reactions occurring depends on the energy of the excited vibrational and rotational states and upon the methods available to transfer this energy. In this chapter a calculation of the energy of these modes will be presented and methods of transferring this energy will be examined.

While there are many possible isotopic combinations of muonic hydrogen molecules which can be formed, molecules containing only protons, muons, and electrons will be used as proxies in this chapter for molecules containing other isotopic hydrogen combinations. Deuterons and tritons are expected to undergo similar muonic reactions to those experienced by protons, with the exception that some of the muonic molecules

formed with the heavier nuclei may have appreciable fusion rates. Due to the lower mass and increased quantum character of protons, as compared to deuterons and tritons, the binding energy will be lower, and the bond distances greater than for molecules composed exclusively of the larger nuclei.

## 7.2 Methods

In order for a reaction to occur it must be energetically favorable and a viable reaction path must exist which results in an overall positive change in entropy. The energy of a reaction ( $\Delta E$ ) can be defined as the difference in the total energy between reactants and products. Activation energy ( $E_{act}$ ) is the energy of any barrier between reactants and products that must be surmounted or tunneled through in order to get a reaction to proceed. If  $\Delta E$  is negative the reaction is exothermic and will proceed, with its rate being determined, in part, by  $E_{act}$ . When  $\Delta E$  is positive the reaction is endothermic and will not proceed unless energy is added to the system.

Basis set size, methods of including correlation energy, and many other factors contribute to the accuracy to which the energy of a system can be determined. Since the same types of computational errors typically occur amongst reactants and products, if the same computational methods and levels of theory are used to calculate reactants, intermediates (*e.g.*, transition states) and products, many of the same errors will occur on both sides of the equation and will therefore cancel. It is therefore important when calculating  $\Delta E$  and  $E_{act}$  to use the same basis sets, methods, and levels of including correlation energy for all of the species participating in the reactions.

The choice of basis sets significantly affects the calculated values of  $\Delta E$ . As was mentioned in previous chapters, transferring basis sets optimized for one muonic molecule to another molecular system, instead of re-optimizing the basis sets can result in significantly higher energies being calculated. The choice of basis sets optimized can be used to determine error limits on the calculated values of  $\Delta E$ . If basis sets optimized for reactants are used, the calculated values of  $\Delta E$  and  $E_{act}$  are upper bounds to the most accurate values obtainable at a given level of theory. If basis sets are optimized using products, the values of  $\Delta E$  and/or  $E_{act}$  calculated will be lower bounds. Therefore, while the optimum basis set for a given reaction may not be achieved, basis set optimization error can be bounded. Basis sets for reactants and products were optimized using the procedures presented in Chapter 4. In order to establish error limits,  $\Delta E$  was calculated using both reactant and product optimized basis sets. Bond lengths were optimized individually for each molecule being studied.

The calculations presented in this chapter were performed using 2s1p muon and proton basis sets. Correlation interactions were included in most of the di-nuclear calculations using full CI (FCI) methods. Using available software and computational facilities, it was not possible to fully optimize the  $p\mu p\mu p^+$  basis sets at the FCI level. For this reason,  $p\mu p\mu p^+$  calculations were performed using basis sets optimized for  $p\mu p^+$ .  $p\mu p\mu p^+$  bond length calculations were performed using 8 active muon molecular orbitals and 8 active proton molecular orbitals. It is likely that future software modifications will parallelize and take advantage of symmetry in the CI code, thereby allowing larger basis sets to be used and larger molecules to be studied.

The quantum vibrational energy levels of the molecules presented in this chapter were calculated using the methods presented in Chapter 6. The rotational energy ( $\varepsilon$ ) was determined by scaling results obtained for similar molecules. The scaling factors were determined by assuming the molecules to be rigid rotors. The calculated rotational energy of  $p\mu p^+$  was scaled to determine the rotational energy levels of the  $p\mu\mu p$  molecules, using the relationship,

$$\varepsilon_2(J_2) = \frac{\varepsilon_1(J_1)}{r_2^2} r_1^2 \left( \frac{m_1}{m_2} \right) \left[ \frac{J_2(J_2+1)}{J_1(J_1+1)} \right] \quad (7.1)$$

which was derived from the rotational energy eigenvalue equation for a rigid rotor. Molecule (1) in equation 7.1 is  $p\mu p^+$  and molecule (2) is  $p\mu\mu p$ .  $J$  represents the rotational quantum numbers (*i.e.*,  $J = 0, 1, 2, \dots$ ),  $m_i$  is the mass of the molecules, and  $r_i$  is the distance between the expectation values of the nuclei ( $i = 1, 2$ ). For the muonic molecules, the mass was accounted for in the scaling factor by collapsing the proton mass onto the expectation coordinates of proton density and superimposing the muon mass distribution to get the total mass distribution. The rotational energy of the oblate symmetric top  $p\mu p\mu p^+$  was similarly determined by scaling  $^1H_3^+$ . Being that all of the rotational energy levels of interest are known for  $^1H_3^+$ , a different scaling factor was determined for each rotational energy level, using the same rotational quantum levels.[1; 2; 3; 4; 5]

$$\varepsilon_2(J, K) = \varepsilon_1(J, K) d^2 \left( \frac{m_1}{m_2} \right) \quad (7.2)$$

Where  $d$  is the ratio of the bond distances  $\frac{r_1}{r_2}$ .  $J$  and  $K$  represent the two rotational quantum numbers associated with symmetric top molecules.  $J$  corresponds to the principal axis of angular momentum and  $K$  corresponds to the angular momentum along the top axis (*i.e.*, the axes which has a unique moment of inertia).

### 7.3 Results and Discussion

Pairs of indistinguishable Fermions can exist in both singlet (*i.e.*, anti-parallel spin) and triplet (*i.e.*, parallel spin) states. Due to the mass of protons and their separation distance in the molecules studied in this section, the binding energy and bond length for singlet and triplet protons are approximately equal (see Chapter 5). Due to the lighter mass of muons, compared to protons, their spin has a significant impact on the physical properties of the di-muonic hydrogen molecules which were studied (see Table 7-1).

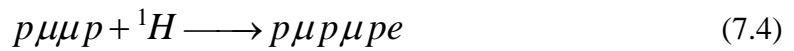
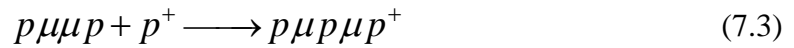
$p\mu\mu p$  is bound in both singlet and triplet muonic spin states hereafter designated as  $p\mu\mu p^{(S)}$  and  $p\mu\mu p^{(T)}$ , respectively. Bound excited vibrational states of  $p\mu\mu p$  do not exist. As can be seen in Table 7-1, the bond length of  $p\mu\mu p^{(T)}$  is more than four times greater than that of  $p\mu\mu p^{(S)}$ . In its ground state,  $p\mu\mu p^{(S)}$  has a relatively high binding energy and is very stable relative to dissociation into muonic atoms (*i.e.*,  $p\mu$ ). In comparison  $p\mu\mu p^{(T)}$  is more weakly bound. Setting the binding energy equal to  $k_B T_e$ ,

where  $k_B$  is the Boltzmann constant and  $T_e$  is temperature, the limiting  $T_e$  for  $p\mu\mu p^{(S)}$  and  $p\mu\mu p^{(T)}$  is  $4.76 \times 10^6$  K and 859 K respectively.

**Table 7-1. FCI results for  $p\mu\mu p$  using 2s1p basis sets. Binding energy (relative to  $p\mu$ ) and equilibrium  $p$ - $p$  bond length for different particle spin states for  $p\mu\mu p$  are shown. The binding energy of the ground rotational states ( $J=0$ ) of the ground ( $v=0$ ) and first excited ( $v=1$ ) vibrational quantum states are shown. Only the ground vibrational states are bound.**

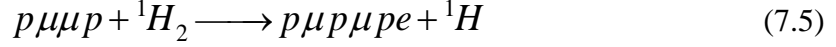
$\mu^-$	$p$	Binding Energy (eV)		Å
2s1p	2s1p	$v=0$	$v=1$	Bond Length
singlet	triplet	410.525	-56.938	0.005012
triplet	singlet	0.07404	-737.782	0.023955
triplet	triplet	0.07404	-737.722	0.023955

Upon collision with a proton, hydrogen atom ( $^1H$ ) or hydrogen molecule ( $^1H_2$ ),  $p\mu\mu p^{(S)}$  and  $p\mu\mu p^{(T)}$  can react to form the oblate symmetric top molecules  $p\mu p\mu p^+$  or  $p\mu p\mu p e$  if energy is efficiently transferred:



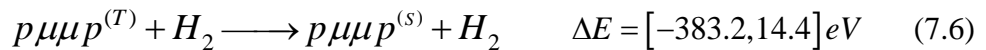
or

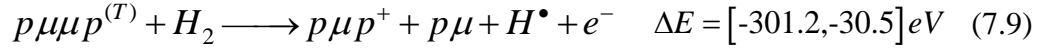
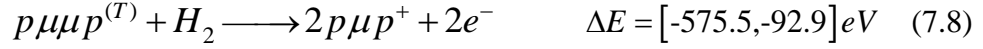




The fusion rate constants as a function of distance are approximately proportional to  $e^{-cx}$ , where  $c$  is a constant and  $x$  represents nuclear bond length. As a result, relatively small changes in nuclear separation can have a large impact on the rate of fusion. The  $p\mu\mu p^{(T)}$  bond length is more than six times the length of  $p\mu p^+$  (see Tables 5-1 and 7-1). The  $p$ - $p$  bond length in  $p\mu p\mu p^{(T)}$  is about three and a half times the length of the  $p$ - $p$  bond length in  $p\mu p^+$  (see Tables 5-1 and 7-2). As a result of the relatively long bond lengths in  $p\mu\mu p^{(T)}$  and  $p\mu p\mu p^{(T)}$ , fusion cannot be efficient, even if deuterons or tritons replace protons in the molecule. The bond length of the triplet molecules would need to decrease several fold for there to be sufficient overlap of the nuclear wave functions that fusion would be expected to occur at a rate comparable to the single muon catalyzed fusion rate.

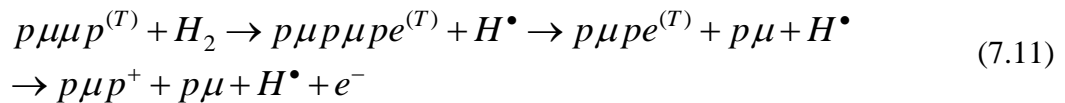
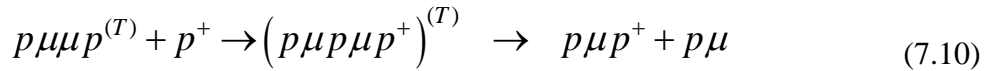
In order for di-muonic molecules with triplet muon spin to enhance the muon-catalyzed fusion reaction rate, their reactions must result in muons being freed, or in species which rapidly lead to fusion being formed. Otherwise the muon-catalyzed fusion cycle will be made inefficient by removal of muons from the reaction cycle. If  $p\mu\mu p^{(T)}$  collides with a proton, or hydrogen molecule, several reactions are possible. Most of these result in products and/or intermediates that are more closely bound being formed. Some examples of possible reactions are:



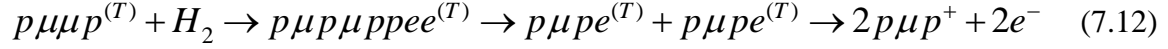


Mechanisms by which these reactions may occur are presented in the discussion which follows.

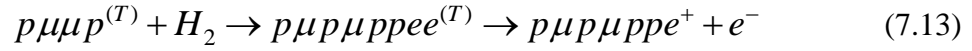
The first value of  $\Delta E$  listed was calculated using basis sets optimized with the products and can therefore be considered a lower bound of the level of theory being used (*i.e.*, HF/FCI with 2s1p muon and proton basis sets). The second value of  $\Delta E$  listed was calculated using basis sets optimized with the reactants, and can be considered an upper bound. These reactions are exothermic. The rate they occur depends on the reaction path and on the rate of competing reactions. Some possible reaction paths are:



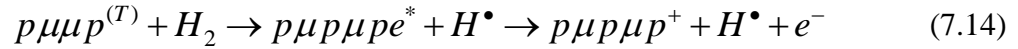
and



Some possible competing reactions are:



and



In order for a reaction to proceed rapidly, an efficient mechanism for the transfer of energy must operate. Energy may be transferred or released through collisions, Auger transitions, or high-energy x-ray emission. There are limits to the amount of energy that can be transferred by collisions, Auger transitions or x-ray emission. Collisional relaxation is only effective if the reaction coordinate couples energy into particle motion; reactions that rely on efficient collisional energy elimination usually proceed more rapidly when the difference in energy between reactants and products is comparable to relevant vibrational modes accessed in the reaction.[6; 7] For larger energy differences Auger electron transitions are more efficient. For example,  $t\mu t^+$  can go from an excited rotational-vibrational state  $(J,\nu) = (1,1)$  to the rotationally excited, ground vibrational state  $(1,0)$  via the release of an Auger electron ( $t$  represents a triton). This transition yields an energy release of approximately 244 eV.[8] The somewhat similar reaction,

(7.12) where the triplet, ground state vibrational and rotational molecule  $p\mu p\mu p\mu e$  transitions to the singlet ground rotational and vibrational state of  $p\mu p\mu p^+$  via an Auger transition is unlikely to proceed at a significant rate.  $\Delta E$  for the reaction is about -1.00 keV, and the energy of an Auger electron would need to be about 718.5 eV (see Figure 7-1 and Table 7-2). To a first order approximation, an electron can be expected to interact with  $(p\mu p\mu p^+)^{(S)}$  and  $(p\mu p\mu p^+)^{(T)}$  in a manner similar to how it would interact with a triton.  $p\mu p\mu p^+$  ions are small with a concentrated +1 charge and a mass similar to that of tritium. Being that Auger transitions with energies greater than 700 eV normally do not occur with nuclei that have an atomic number smaller than about 9, the energy of this transition is larger than could be expected to occur.[9; 10] The reaction path shown in reaction Equation 1.11 is unlikely to proceed at an appreciable rate for ground rotational states, for the same reason. (note:  $\Delta E$  and the energy of the Auger transition was calculated using basis sets optimized for  $p\mu p^+$ ). The only way these reactions could be expected to proceed at appreciable rates is if rapid transitions to excited rotational states occur. Figure 7-1, and Tables 7-2 and 7-3 compare the total energy (*i.e.*, energy compared to free unbound particles) of several muonic hydrogen molecules and molecular combinations. For the calculations presented in Figure 7-1, and Tables 7-1 and 7-3, basis sets and bond lengths were optimized simultaneously for  $p\mu$ ,  $p\mu p^+$ ,  $p\mu p\mu p^{(S)}$ , and  $p\mu p\mu p^{(T)}$  using 2s1p basis sets and FCI methods. The  $(p\mu p\mu p^+)^{(S)}$  and  $(p\mu p\mu p^+)^{(T)}$  bond lengths were optimized using the basis sets indicated and CI methods with 8 active muon and 8 active proton molecular orbitals. As can be seen from Figure 7-1 and Table 7-3,  $(p\mu p\mu p^+)^{(S)}$  has bound rotational states that are relatively close in energy to those of

$(p\mu p\mu p^+)^{(T)}$ , therefore, rapid transitions to the (2,1) and (3,3) rotational states of  $(p\mu p\mu p^+)^{(S)}$  are possible.

**Table 7-2. CI results for  $p\mu p\mu p^+$  with singlet and triplet particle spin in ground vibrational and rotational states. Binding energy (relative to  $p\mu$ ) and equilibrium  $p$ - $p$  bond length for different particle spin states are shown. Only the ground vibrational states are bound.**

$\mu^-$	$p$	Binding Energy (eV)	Bond Length (Å)
singlet	triplet	961.773	.005792
triplet	singlet	243.208	.01212
triplet	triplet	243.208	.01212

Some possible avenues to enhance fusion indicated by these calculations are processes that connect, with small energy differences, to cation species that can relax by Auger relaxation, for example:

$$p\mu\mu p^{(T)}(0,0) + p^+ \longrightarrow (p\mu p\mu p^+)^{(T)}(3,3) \quad (7.15)$$

$$(p\mu p\mu p^+)^{(T)}(3,3) \rightarrow \rightarrow (p\mu p\mu p^+)^{(T)}(2,1) \rightarrow p\mu p^+(1) + p\mu \quad (7.16)$$

and

$$(p\mu p\mu p^+)^{(T)}(3,3) \rightarrow \rightarrow (p\mu p\mu p^+)^{(T)}(0,0) \rightarrow p\mu p^+(0) + p\mu \quad (7.17)$$

**Table 7-3. Binding energy with respect to  $p\mu$  for the bound rotational states ( $J$ ) of  $p\mu p^+$  and ( $J,K$ ) of  $p\mu\mu p$  and  $p\mu p\mu p^+$  (see Figure 7-1). The rotational states shown all correspond to ground vibrational states. There are no excited vibrational states of the muonic-molecules shown. The binding energy of  $p\mu p^+$  was taken from reference.[8] ( $S$ ) represents singlet muonic spin states (*i.e.*, anti-parallel muon spin) and ( $T$ ) represents triplet muonic spin states (*i.e.*, parallel muon spin).**

(J)	Binding Energy (eV)			(J,K)	Binding Energy (eV)	
	$p\mu\mu p^{(S)}$	$p\mu\mu p^{(T)}$	$p\mu p^+$		$(p\mu p\mu p^+)^{(S)}$	$(p\mu p\mu p^+)^{(T)}$
(0)	410.525	0.07404	253.152	(0,0)	961.773	243.208
(1)	336.868		107.266	(1,0)	745.275	193.765
(2)	189.554			(1,1)	802.128	206.749
				(2,1)	370.865	108.258
				(2,2)	540.266	146.945
				(3,3)	176.716	63.919

Reactions which produce  $p\mu$  as a product can transfer a significant amount of energy to the bound muon. The quantum energy levels of the bound muon in  $p\mu$  can be calculated from

$$E(n) = \frac{Z^2 \mu}{2\hbar^2 n^2} \quad (7.18)$$

Where  $Z$  is the charge on the proton (+1),  $\mu$  is the reduced mass between the proton and the muon,  $\hbar$  is the reduced Planck's constant and  $n$  is the principle quantum number (see Figure 7-2). When forming muonic hydrogen atoms, negative muons will most often initially form a muonic atom in which the principle quantum number ( $n$ ) is very large (*i.e.*,  $\geq 14$ ). As the muon loses energy, transitioning from one state to another, characteristic x-rays are emitted.

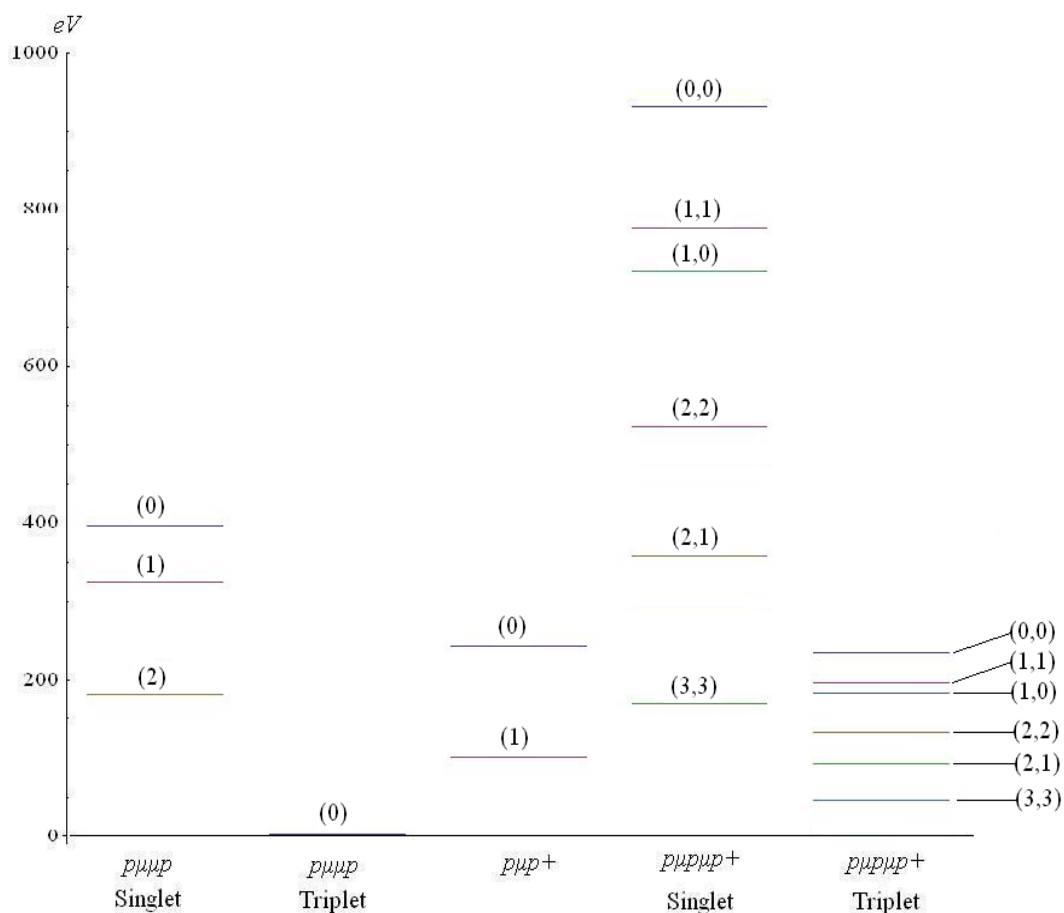


**Figure 7-1.** Binding energy with respect to  $p\mu$  of the bound rotational states ( $J$ ) of  $p\mu p^+$  and the bound rotational states ( $J, K$ ) of  $p\mu\mu p$  and  $p\mu p\mu p^+$  (see Table 7-3). Both singlet and triplet muonic spin states are shown. The rotational states shown all correspond to ground vibrational states. There are no excited vibrational states of the muonic-molecules shown. The binding energy of  $p\mu p^+$  was taken from reference.[8] The basis sets and bond lengths of  $p\mu\mu p$  and  $p\mu\mu p^{(T)}$  were optimized using 2s1p basis sets and FCI methods. The  $p\mu p\mu p^+$  and  $(p\mu p\mu p^+)^{(T)}$  bond lengths were optimized using optimized  $p\mu p^+$  basis sets and CI methods with 8 active muon and 8 active proton molecular orbitals. The ground state rotational and vibrational energy of  $p\mu p\mu p^+$  and  $(p\mu p\mu p^+)^{(T)}$  was calculated using the indicated bases sets and bond lengths at the FCI level. The ground rotational state (0,0) does not exist in the ground vibrational state of triatomic oblate symmetric top molecules [i.e.,  $(p\mu p\mu p^+)^{(S)}$  and  $(p\mu p\mu p^+)^{(T)}$ ].[5; 11; 12; 13] (1,1) is the lowest obtainable energy level for these molecules.

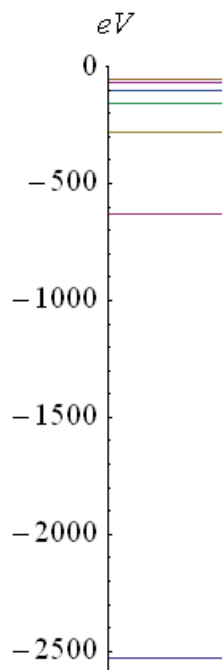


**Figure 7-2.** The first few muonic energy levels of  $p\mu$ . The ground state energy  $[E(1)]$  is - 2.52849 keV.

## 7.4 Conclusions

Di-muonic, di-hydrogen molecules can exist in singlet and triplet muon spin states. The triplet molecules are very weakly bound, and due to their bond length, cannot be expected to fuse at an appreciable rate.

Reaction paths by which triplet  $p\mu\mu p$  (i.e.,  $p\mu\mu p^{(T)}$ ) can be transformed into singlet  $p\mu\mu p$  (i.e.,  $p\mu\mu p^{(S)}$ ) or single muon hydrogen molecules were studied. All of the viable reaction paths involve collisions with other molecules and/or the formation of rotationally excited molecules. Singlet  $p\mu\mu p$  has three bound rotational states ( $J = 0, 1, 2$ ).  $p\mu\mu p^{(T)}$  is only bound in the ground rotational state. The equilibrium bond lengths of  $p\mu\mu p^{(T)}$  and  $p\mu\mu p^{(S)}$  are 5.012 and 23.955 mÅ respectively (see Table 7.1).



Both singlet and triplet (muon spin) forms of  $p\mu p\mu p^+$  exist. Both of these forms of the molecule have five bound rotationally excited states: (1,1), (1,0), (2,2), (2,1), and (3,3). The equilibrium positions of  $(p\mu p\mu p^+)^{(S)}$  and  $(p\mu p\mu p^+)^{(T)}$  nuclei form equilateral triangles with bond lengths of 5.792 and 12.12 mÅ respectively (see Table 7.2).

No vibrationally excited forms of  $p\mu\mu p$  or  $p\mu p\mu p^+$  exist. If heavy isotopes of hydrogen are substituted for the protons in these molecules, bound excited vibrational states may exist.

## References

- [1] C. M. Lindsay and B. J. McCall, "Comprehensive Evaluation and Compilation of H<sub>3</sub><sup>+</sup> Spectroscopy," *Journal of Molecular Spectroscopy*, vol. 210, no. 1, pp. 60-83, 2001.
- [2] B. M. Dinelli, L. Neale, O. L. Polyansky and J. Tennyson, "New Assignments for the Infrared Spectrum of H<sub>3</sub><sup>+</sup>," *Journal of molecular spectroscopy*, vol. 181, pp. 142-150, 1997.
- [3] O. L. Polyansky and J. Tennyson, "Ab initio Calculation of the Rotation-Vibration Energy Levels of H<sub>3</sub><sup>+</sup> and its Isotopomers to Spectroscopic Accuracy," *The Journal of Chemical Physics*, vol. 110, no. 11, pp. 5056-5064, 1999.
- [4] J. K. G. Watson, "The Vibration-Rotation Spectrum and Anharmonic Potential of H<sub>3</sub><sup>+</sup>," *Chemical Physics*, vol. 190, pp. 291-300, 1995.
- [5] G. D. Carney and R. N. Porter, "The Lowest Rotation States of H<sub>3</sub><sup>+</sup> and Symmetry Considerations in Dissociative e Capture," *The Journal of Chemical Physics*, vol. 66, no. 6, pp. 2756-2758, 1977.
- [6] L. I. Ponomarev, "Muon Catalysed Fusion," *Contemporary Physics*, vol. 31, no. 4, pp. 219-245, 1990.
- [7] L. I. Ponomarev, "Muon-Catalyzed Fusion and Fundamental Physics," *Hyperfine Interactions*, vol. 103, pp. 137-145, 1996.
- [8] S. A. Alexander, H. J. Monkhorst and K. Szalewicz, "A Comparison of Muonic Molecular Calculations," vol. 181, pp. 246-258, 1988.
- [9] K. D. Childs, B. A. Carlson, L. A. Vanier, J. F. Moulder, D. F. Paul, W. F. Stickle and D. G. Watson, "Handbook of Auger Electron Spectroscopy," in *Physical Electronics*, Eden Prairie, MN, 1995.
- [10] E. A. G. Armour, D. M. Lewis and S. Hara, "Calculations of the Auger deexcitation rate of  $dt\mu$  within the muonic quasimolecule  $(dt\mu)dee$ ," *Physical Review A*, vol. 46, no. 11, pp. 6888-6893, 1992.
- [11] K. N. Crabtree, B. A. Tom and B. J. McCall, "Nuclear Spin Dependence of the Reaction of H<sub>3</sub><sup>+</sup> with H<sub>2</sub>. I. Kinetics and Modeling," *The Journal of Chemical Physics*, vol. 134, no. 19, pp. 194311:1-13, 2011.

- [12] T. Oka and E. Epp, "The Nonthermal Rotational Distribution of  $\text{H}_3^+$ ," *The Astrophysical Journal*, vol. 613, no. 1, pp. 349-354, 2004.
- [13] T. Oka, "Spectroscopy and astronomy:  $\text{H}_3^+$  from the laboratory to the Galactic center," *Faraday Discussions*, vol. 150, no. 0, pp. 9-22, 2011.

## VIII. Di-Muonic Hydrogen Reaction Kinetics

### 8.1 Introduction

Determining a mechanism by which muon-catalyzed fusion can be used as a pure fusion source of energy has so far been elusive. A study of current experimental and theoretical literature leaves little hope that mono-muonic reaction mechanisms can result in sufficiently high fusion yields for this process to be used as a pure fusion source of energy (see Chapter 2 for a review of this literature). If a mechanism is to be found, which results in significantly higher yields than has thus far been observed, novel reaction paths must be investigated. As of the writing of this document, most studies of muon-catalyzed fusion have dealt with single muon hydrogen molecules.[1; 2; 3; 4; 5; 6; 7; 8; 9] In this dissertation a novel approach to muon-catalyzed fusion is investigated. The possibility that di-muonic molecular reactions can enhance the overall fusion yield is considered.

Di-muonic molecules have not contributed significantly to the observed reaction rate of muon-catalyzed fusion in any of the experimental studies performed to date. Few theoretical studies of these molecules exist in the literature, and no studies have been published which analyze the effects of di-muonic molecules on the muon-catalyzed fusion reaction rate.[10] This can be attributed to the low concentration of near-thermal muons (*i.e.*, low muon flux) that generate hydrogenic muonic molecules used in most muon-catalyzed fusion experiments performed to date.[10] For a given reaction chamber, as the concentration of thermal muons increases the contribution of di-muonic

molecular reactions will increase. To the author's knowledge, the concentration of thermal muons required to significantly influence muon-catalyzed fusion reaction rates, via di-muonic reactions, has not been published. A better understanding of potential mechanistic pathways that may contribute to muon-catalyzed fusion is needed to estimate whether di-muonic molecular reactions can significantly contribute to enhance muon-catalyzed fusion kinetics. Increasing the formation rate of di-muonic hydrogen molecules will not increase the fusion rate unless these species efficiently form and fuse, or provide a rapid pathway to enhance the formation of  $d\mu d^+$ ,  $d\mu t^+$ , or  $t\mu t^+$ , promoting ordinary muon catalysis. As was shown in Chapter's 4 and 5, the average distance between nuclei in di-muonic, di-nuclear hydrogen molecules is greater than in the corresponding mono-muonic molecules. Di-muonic hydrogen molecules can exist in singlet ( $S$ ) and triplet ( $T$ ) muonic spin states. The triplet molecules, which are more likely to form, cannot have a significant fusion rate, due to the long bond lengths of these molecules (see Chapter 7). Mechanisms by which these triplet molecules may be transformed into states or molecules which may have appreciable fusion cross-sections were discussed in Chapter 7.

In previous chapters physical properties of di-muonic hydrogen molecules and reactions they could undergo have been studied. In this chapter the reaction kinetics of paths that could lead to the formation of these molecules and lower bounds on the muon flux needed to form them in significant quantities will be presented. Although it is currently unknown if the reaction of di-muonic molecules will enhance or decrease the overall reaction yield, by studying potential reaction paths a lower bound on the muon flux required to yield significant di-muonic molecular effects can be established.

Additionally, it is possible to determine an upper bound on possible yield enhancement resulting from di-muonic muon-catalyzed fusion pathways.

## 8.2 Methods

In order for di-muonic hydrogen molecules to have a significant impact (negative or positive) on the rate of muon-catalyzed fusion, a substantial quantity of di-muonic molecules must be present in the reaction chamber. Additionally, the rates these molecules fuse, or go through a series of reactions leading to fusion, must be significantly different than the rates of competing single muon reactions and/or the sticking fractions of these reactions must be significantly different than competing single muon reactions.

The di-muonic hydrogen formation rate ( $r_{bi}$ ) can be estimated using the hard sphere collision frequency ( $z_{AB}$ )

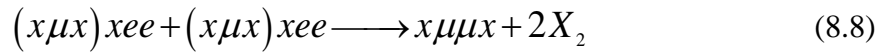
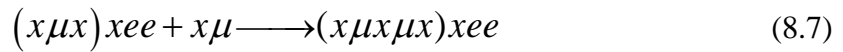
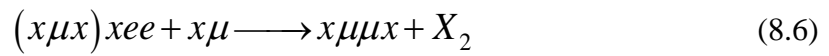
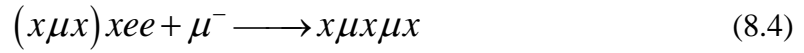
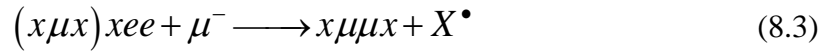
$$z_{AB} = n_A n_B \pi \sigma_{AB}^2 \left( \frac{8k_B T}{\pi \mu_{AB}} \right)^{\frac{1}{2}} \quad (8.1)$$

$$r_{bi} = n_A n_B \left[ \pi \sigma_{AB}^2 \left( \frac{8k_B T}{\pi \mu_{AB}} \right)^{\frac{1}{2}} e^{-\frac{E_{act}}{k_B T}} \right] \quad (8.2)$$

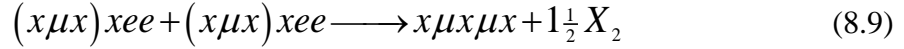
$n_A$ and $n_B$	Concentration of molecules A and B respectively
$\sigma_{AB}$	Collision cross-section
$\mu_{AB}$	Reduced mass of particles A and B
$T$	Temperature (K)
$k_B$	Boltzmann's constant
$E_{act}$	Activation energy

An upper bound of the reaction rate occurs when all collisions result in a reaction. In this case,  $E_{act} = 0$  and  $z_{AB} = r_{bi}$ .

In order to calculate the di-muonic hydrogen formation rates there are three species that can collide which need to be considered:  $\mu^-$ ,  $x\mu$ , and  $(x\mu x)xee$ , where  $x$  represents  $^1H$ ,  $^2H$ , and  $^3H$  nuclei.  $X$  represents  $^1H$ ,  $^2H$ , and  $^3H$  atoms. Following are some reactions which can result in the formation of di-muonic hydrogen molecules that will be considered in this chapter.



and



These reactions cannot form products efficiently, even though they are exothermic, unless energy is rapidly dissipated from the collision complex. In the cases of reactions 8.3, 8.6, 8.8 and 8.9 the non-muonic product could carry off this excess energy. In the case of reactions 8.4 and 8.7, the energy may be dissipated by Auger processes. Reaction 8.5 could occur if an excited rotational and/or vibrational state of  $x\mu\mu x$  exists in which the energy of reaction ( $\Delta E$ ) is dissipated between rotational and/or vibrational modes. Such a reaction mechanism can only exist if  $\Delta E$  is small.[4; 5] If excited vibrational and/or rotational states do exist, which make this reaction possible, the reverse reaction rate is expected to be close to that of the reaction rate. Therefore the only potential mechanisms for reaction 8.5 to occur involve collisions with a third body.[11]

As can be seen from Equations 8.1 and 8.2, the reaction rate depends on the number of collisions and upon the effectiveness of those collisions. The effectiveness of the collisions depends on the orientation and energy of the colliding species. It is common for muons to be input into a reaction chamber with energy greater than will react to form  $x\mu$ . When this is the case muons must be moderated through collisions before they can react. If the energy of effective collisions between  $\mu^-$  and  $X_2$  is significantly lower than that required to form products when muons collide with  $x\mu x$  the formation rate of the di-muonic molecules could be enhanced. If the energy of effective collisions between  $\mu^-$  and  $X_2$  is significantly higher than that required to form products when muons collide with  $x\mu x$  the formation rate of the di-muonic molecules via these



reaction paths would be slowed. The size of the difference in the effective collision energy of these molecules is unknown.

The maximum reaction rate will occur when the total number of muons are equally divided between the colliding species. Dividing all of the muons in a reaction chamber equally between reactants can be difficult or impossible. Being that the results of such calculations result in upper bounds to the reaction rate, there is, however, value in performing the calculations, even if these reaction conditions cannot be obtained. Any reaction which has an upper bound of its reaction rate which is too low to significantly affect the overall fusion rate can be neglected, and further analysis of this reaction path can be ignored. Taking this into account, upper bounds of reaction rates were calculated in this way (see Table 8-1).

Table 8-1 lists the maximum reaction rate (*i.e.*, collision frequency) for the reactants in Equations 8.3 through 8.7. The collision frequency is calculated for a muon flux of  $1.5 \times 10^{16}$  negative muons per second. This negative muon flux was chosen for the calculations because it is the highest continuous flux known to be available at a currently operating accelerator.[12:34]

**Table 8-1. Theoretical maximum reaction rate obtainable with a negative muon flux of  $1.5 \times 10^{16}$  muons/s focused into a volume of  $1\text{cm}^3$ .  $A + B \longrightarrow \text{Products}$ . An excess of  $H_2$  in the reaction chamber is assumed.**

<b>A</b>	<b>B</b>	Max reaction rate at 300 K (s <sup>-1</sup> )	Max reaction rate at 1000 K (s <sup>-1</sup> )	Max reaction rate at 4000 K (s <sup>-1</sup> )
$p\mu pp$	$p\mu$	$9.24 \times 10^{21}$	$1.69 \times 10^{22}$	$3.37 \times 10^{22}$
$p\mu$	$p\mu$	$7.72 \times 10^{17}$	$1.41 \times 10^{18}$	$2.82 \times 10^{18}$
$p\mu pp$	$\mu$	$2.53 \times 10^{22}$	$4.61 \times 10^{22}$	$9.23 \times 10^{22}$

Due to the low collision frequency of  $p\mu + p\mu$  and the energy dissipation problems discussed previously,  $p\mu + p\mu$  reactions will not be considered further.

Upper bounds for reaction rate constants ( $\lambda$ ) for reactions 8.3 through 8.9 can be calculated (*i.e.*,  $E_{act} = 0$ ) using a hard sphere model,

$$\lambda = \pi \sigma_{AB}^2 \left( \frac{8k_B T}{\pi \mu_{AB}} \right)^{\frac{1}{2}} e^{-\frac{E_{act}}{k_B T}} \quad (8.10)$$

These values vary slightly, depending on the hydrogen isotopes being considered (see Table 8-2). The reaction cross section ( $\sigma$ ) was taken as the sum of the hard-sphere radii of the reactants. The hard-sphere radii for  $x\mu$  was taken as hard-sphere radii of  $xe$ , divided by the reduced mass ratio  $\left( \frac{\mu_{x\mu}}{\mu_{xe}} \right)$ . The hard-sphere radii for  $(x\mu x)x$  was assumed to be equal to the radii of similar size molecules  $X_2$ .

**Table 8-2. Upper bounds of the reaction rate constants for reactions 8.3 through 8.6 at 300 K and liquid hydrogen density. All hydrogen isotope combinations are shown.  $A + B \longrightarrow Products$**

A	B	$\lambda(10^{12}s^{-1})$	A	B	$\lambda(10^{12}s^{-1})$
$p_3\mu$	$\mu^-$	69.7	$pd_2\mu$	$\mu^-$	69.2
$p_3\mu$	$p\mu$	25.5	$pd_2\mu$	$p\mu$	24.1
$p_3\mu$	$d\mu$	20.6	$pd_2\mu$	$d\mu$	18.9
$p_3\mu$	$t\mu$	18.5	$pd_2\mu$	$t\mu$	16.6
$d_3\mu$	$\mu^-$	69.1	$pt_2\mu$	$\mu^-$	69.0
$d_3\mu$	$p\mu$	23.8	$pt_2\mu$	$p\mu$	23.5
$d_3\mu$	$d\mu$	18.4	$pt_2\mu$	$d\mu$	18.1
$d_3\mu$	$t\mu$	16.1	$pt_2\mu$	$t\mu$	15.7
$t_3\mu$	$\mu^-$	68.9	$d_2t\mu$	$\mu^-$	69.0
$t_3\mu$	$p\mu$	23.2	$d_2t\mu$	$p\mu$	23.5
$t_3\mu$	$d\mu$	17.6	$d_2t\mu$	$d\mu$	18.1
$t_3\mu$	$t\mu$	15.2	$d_2t\mu$	$t\mu$	15.7
$p_2d\mu$	$\mu^-$	69.4	$dt_2\mu$	$\mu^-$	68.9
$p_2d\mu$	$p\mu$	24.7	$dt_2\mu$	$p\mu$	23.3
$p_2d\mu$	$d\mu$	19.5	$dt_2\mu$	$d\mu$	17.8
$p_2d\mu$	$t\mu$	17.3	$dt_2\mu$	$t\mu$	15.4
$p_2t\mu$	$\mu^-$	69.2	$d_2t\mu$	$d_2t\mu$	45.7
$p_2t\mu$	$p\mu$	24.1	$d_2t\mu$	$dt_2\mu$	47.2
$p_2t\mu$	$d\mu$	18.9	$dt_2\mu$	$dt_2\mu$	48.8
$p_2t\mu$	$t\mu$	16.6			

$x\mu\mu x$  can form in singlet or triplet muonic spin states depending on the amount of excess energy carried off by  $X^*$  or  $X_2$  (see Equations 8.3, 8.6, 8.8 and 8.9, and Figure 7-1). The singlet spin state of this molecule may have a rapid fusion rate when heavy hydrogen isotopes are involved (*e.g.*,  $\lambda \geq 10^7 s^{-1}$ ). Triplet state molecules cannot have rapid fusion rates due to the large nuclear bond distances involved in these molecules. (see Section 7.3 of this document).

In order for  $(x\mu x\mu x)xee$  to form, via Equation 8.7, the binding energy may be divided between excited vibrational and/or rotational quantum states. This can only

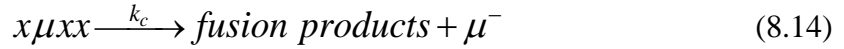
occur for reactions with very small values of  $\Delta E$ . [13] As a result,  $p\mu p\mu p^+$  cannot form with anti-parallel muon spin via reaction 8.6 (see Figure 7-1) (note: The binding energy is calculated to be too large for an Auger transition to carry off all of the binding energy). When heavier isotopes of hydrogen are involved, singlet molecules similar to  $p\mu p\mu p^+$  may form due to the existence of weakly bound excited vibrational states. The singlet states of this molecule may have rapid fusion rates, but triplet muon spin states of this molecule cannot have rapid fusion rates due to the magnitude of the nuclear bond lengths (see Chapters 4 and 5)

Although  $x\mu\mu x^{(T)}$  and  $x\mu x\mu x^{(T)}$  cannot have rapid fusion rates (*e.g.*,  $\lambda \geq 10^7 s^{-1}$ ) due to the relatively large nuclear bond length of these molecules; these molecules may react and form molecules with significantly shorter bond lengths. These reactions are discussed in detail in Chapter 7.

In Appendix A kinetic rate equations for single muon, muon-catalyzed fusion are developed. These equations can be simplified considerably, when  $x$  is allowed to represent all hydrogen isotopes for which a given reaction is possible. In the discussion which follows, it is assumed that the reaction conditions are such that the free radicals  $H^\bullet$ ,  $D^\bullet$ , and  $T^\bullet$  do not exist in significant quantities (*e.g.*, temperature  $< 2000$  K).  $\lambda_0$  represents the decay rate constant of negative muons ( $\lambda_0 = 4.55 \times 10^5 s^{-1}$ ). [3] In the equations which follow, electrons and products whose formulation doesn't have a significant impact on the overall muon-catalyzed fusion rate have not been shown. The simplified reaction equations are:



and



$x\mu xx$  can form via reversible resonant pathways (*i.e.*, Equation 8.12) and non-resonant, non-reversible pathways (*i.e.*, Equation 8.13). Which of these reactions predominates or significantly contribute to the overall fusion yield depends on which hydrogen isotopes are involved in the reactions.

It is common practice to combine the rate constants that affect the concentration of  $x\mu xx$  to form an *effective* rate constant ( $k_b$ ) that more closely represents what is observed experimentally. For the resonance pathways this is done by taking the rate equation

$$\frac{\partial [x\mu xx]}{\partial t} = \lambda_{x\mu}^{res} [x\mu][X_2] - (\Gamma + k_c)[x\mu xx] \quad (8.15)$$

and setting it equal to

$$\frac{\partial [x\mu xx]}{\partial t} = k_b [x\mu] [X_2] - k_c [x\mu xx] \quad (8.16)$$

which corresponds to the *effective* reaction equation



where  $\lambda_{x\mu}^{res}$ ,  $\lambda_{x\mu}^{nr}$ ,  $\Gamma$ ,  $k_a$ ,  $k_b$ , and  $k_c$  are rate constants defined in Equations 8.12 thru 8.14.

Using the *steady state* approximation  $\frac{\partial [x\mu xx]}{\partial t} = 0$  and

$$k_b = \lambda_{x\mu}^{res} \left( \frac{k_c}{\Gamma + k_c} \right) \quad (8.18)$$

When non-resonant paths and different spin states of  $x\mu$  ( $F$ ) and  $x\mu xx$  ( $S$ ) are added to the equation,

$$k_b = \lambda_{x\mu}^{nr} + \sum_S \lambda_{x\mu,FS}^{res} \left( \frac{k_c}{\sum_F \Gamma_{FS} + k_c} \right) \quad (8.19)$$

Then it follows that the reaction rate equations for these effective reaction paths are:

$$\frac{\partial [x\mu]}{\partial t} = k_a [X_2] [\mu^-] - [x\mu] \{k_b [X_2] + \lambda_0\} \quad (8.20)$$

$$\frac{\partial [x\mu_{xx}]}{\partial t} = k_b [X_2] [x\mu] - (k_c + \lambda_0) [xx\mu x] \quad (8.21)$$

$$\frac{\partial [\mu^-]}{\partial t} = k_c (1 - B\omega) [x\mu_{xx}] - [\mu^-] \{k_a [X_2] + \lambda_0\} \quad (8.22)$$

and

$$\frac{\partial [products]}{\partial t} = k_c [x\mu_{xx}] \quad (8.23)$$

where

$$[\mu^-] = [\mu_{total}^-] - [x\mu] - [x\mu_{xx}] - B\omega [products] \quad (8.24)$$

and

$$\left[ \mu_{total}^- \right] = \left[ \mu_0^- \right] e^{-\lambda_0 t} \quad (8.25)$$

The *He* path branching ratio  $B$  equals 1, except for *d-d* fusion. The *He* sticking fraction is  $\omega$  and  $\mu_0^-$  represents the initial muon concentration in a pulsed system.

If a continuous muon flux ( $\Phi$ ) is added to the reaction chamber, then

$$\frac{\partial \left[ \mu_{total}^- \right]}{\partial t} = \Phi - \lambda_0 \left[ \mu_{total}^- \right] \quad (8.26)$$

A steady state (SS) of  $\mu_{total}^-$  can be determined by considering  $\lim_{t \rightarrow \infty} \frac{\partial \left[ \mu_{total}^- \right]}{\partial t} = 0$  and consequently,

$$\left[ \mu_{total}^- \right]_{ss} = \frac{\Phi}{\lambda_0} \quad (8.27)$$

In the case of *d-t* fusion the above simplified equations assume near equal concentrations of deuterium and tritium and neglect many of the less significant reaction paths. A more complete analysis could be performed using the equations presented in Appendix A and the isotope concentration calculation methods presented in Appendix B. Using the simplified equations a maximum muon-catalyzed fusion yield of 160 fusions/muon is calculated if only single-muon catalysis occurs in significant amounts. This compares to an observed experimental value of 150 fusions/muon.[2; 3]



The following di-muonic reactions can be added to Equations 8.11, 8.14 and 8.17:

$$x\mu xx + \mu^- \xrightarrow{k_d} x\mu\mu x \quad (8.28)$$

$$x\mu xx + \mu^- \xrightarrow{k_e} x\mu x\mu x \quad (8.29)$$

$$x\mu xx + x\mu \xrightarrow{k_f} x\mu\mu x + x_2 \quad (8.30)$$

$$x\mu xx + x\mu \xrightarrow{k_g} x\mu x\mu x + x \quad (8.31)$$

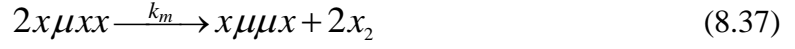
$$x\mu\mu x + X_2 \xrightarrow{k_h} x\mu x\mu x \quad (8.32)$$

$$x\mu\mu x \xrightarrow{k_i} \text{fusion products} + 2\mu^- \quad (8.33)$$

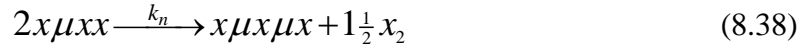
$$x\mu x\mu x + X_2 \xrightarrow{k_j} 2x\mu x \quad (8.34)$$

$$x\mu x \xrightarrow{k_k} \text{fusion products} + \mu^- \quad (8.35)$$

$$x\mu x\mu x \xrightarrow{k_l} \text{fusion products} + 2\mu^- \quad (8.36)$$



and



The rate equations, with the di-muonic reaction paths included become:

$$\frac{\partial [x\mu]}{\partial t} = k_a [X_2] [\mu^-] - [x\mu] \{k_b [X_2] + \lambda_0\} - (k_f + k_g) [x\mu xx] [x\mu] \quad (8.39)$$

$$\begin{aligned} \frac{\partial [x\mu xx]}{\partial t} = & k_b [X_2] [x\mu] - (k_c + \lambda_0) [xx\mu x] - (k_f + k_g) [x\mu xx] [x\mu] \\ & - (k_m + k_n) [x\mu xx]^2 \end{aligned} \quad (8.40)$$

$$\frac{\partial [x\mu x]}{\partial t} = -(\lambda_0 + k_k) [x\mu x] + 2k_j [x\mu x\mu x] [X_2] \quad (8.41)$$

$$\begin{aligned} \frac{\partial [x\mu\mu x]}{\partial t} = & -(\lambda_0 + k_i) [x\mu\mu x] - k_h [x\mu\mu x] [x_2] + k_f [x\mu] [x\mu xx] \\ & + k_m [x\mu xx]^2 \end{aligned} \quad (8.42)$$

$$\begin{aligned} \frac{\partial [x\mu x\mu x]}{\partial t} = & -(\lambda_0 + k_l + k_j [X_2])[x\mu x\mu x] + k_g [x\mu][x\mu x] \\ & + k_h [x\mu\mu x][X_2] + k_n [x\mu x]^2 \end{aligned} \quad (8.43)$$

$$\begin{aligned} \frac{\partial [\mu^-]}{\partial t} = & -\{k_a [X_2] + \lambda_0\}[\mu^-] + k_c (1 - B\omega)[x\mu x] + 2k_l [x\mu x\mu x] \\ & + 2k_i [x\mu\mu x] + k_k [x\mu x] \end{aligned} \quad (8.44)$$

$$\frac{\partial [products]}{\partial t} = k_c [x\mu x] + k_i [x\mu\mu x] + k_k [x\mu x] + k_l [x\mu x\mu x] \quad (8.45)$$

and

$$\begin{aligned} [\mu^-] = & [\mu_{total}^-] - [x\mu] - [x\mu x] - [x\mu x] - [x\mu\mu x] \\ & - [x\mu x\mu x] - B\omega [products] \end{aligned} \quad (8.46)$$

It may be noted that the terms  $k_d [x\mu x][\mu^-]$  and  $k_e [x\mu x][\mu^-]$  have not been included in the above equations. This is because these terms are negligible when compared to the terms  $k_f [x\mu x][x\mu]$  and  $k_g [x\mu x][x\mu]$ . If rate constants significantly different from those used in this study are used, then the appropriateness of neglecting these terms should be reassessed.[1; 5]

The probability of  $x\mu x + x\mu x$  collisions resulting in the formation of di-muonic molecules depends, in part, on the binding energy of the  $x\mu x$  portion of the molecule.

The possibility of these collisions resulting in the formation of di-muonic molecules only exists when the  $x\mu x$  binding energy is very small (*e.g.*,  $\sim 0.5$  eV) as it is in the case of the excited vibrational and rotational state (1,1) of  $d\mu t$ . [14]  $d\mu d$  and  $t\mu t$  are bound too tightly to expect these collisions to result in the formation of significant quantities of di-muonic molecules via this reaction path. In the case of  $d\mu t$  collisions it is unknown if  $E_{act}$  for this reaction is low enough for these collisions to contribute significantly to the overall fusion yield. For this reason, these reactions have been considered in the discussion which follows.

The reaction rate constants used for the calculations presented in this chapter have been taken from references [1] and [5], or are presented in Table 8-2 of this document. The rate constants calculated in this section, as well as those taken from other references have all been normalized to liquid hydrogen density and 300 K (*i.e.*,  $4.25 \times 10^{22}$  molecules/cm<sup>3</sup>). The rate equations presented in this chapter (*i.e.*,  $k$  and  $\lambda$ ) can be adjusted to account for pressure [*i.e.*,  $k(P)$  and  $\lambda(P)$ ] by multiplying the rate constants which depend on pressure (*i.e.*, those which are multiplied by the concentration of  $X_2$  in the rate equations) by  $5.75374 \times 10^{-4}$  times the pressure in atmospheres. This includes the effective rate constant  $k_b$ , since  $k_c$  and  $\Gamma_{FS}$  are independent of pressure and

$$\begin{aligned}
 k_b(P) &= \lambda_{x\mu}^{nr}(P) + \sum_S \lambda_{x\mu,FS}^{res}(P) \left( \frac{k_c}{\sum_F \Gamma_{FS} + k_c} \right) \\
 &= 5.75374 \times 10^{-4} \text{ Pressure} \left[ \lambda_{x\mu}^{nr} + \sum_S \lambda_{x\mu,FS}^{res} \left( \frac{k_c}{\sum_F \Gamma_{FS} + k_c} \right) \right] \\
 &= 5.75374 \times 10^{-4} \text{ Pressure } k_b
 \end{aligned} \tag{8.47}$$

### 8.3 Results and Discussion

This chapter examines reaction paths that may lead to the formation of di-muonic hydrogen molecules and the muon flux needed to form these molecules in significant quantities. The reaction paths studied are limited to systems containing only deuterium and/or tritium. The reactions conditions assume protium concentrations to be negligible. The muon flux required to significantly affect the muon-catalyzed fusion yield depends on which reaction paths predominate and which isotopes are present.

The muonic hydrogen molecules in greatest concentration in a muon-catalyzed fusion chamber are  $x\mu xx$ . As a result, if  $x\mu xx + x\mu xx$  collisions are efficient at forming di-muonic hydrogen molecules these reactions will predominate relative to other di-muonic hydrogen formation paths. As was discussed in the previous section, due to the binding energy and Coulombic repulsion of the  $x\mu x$  portion of these molecules,  $d\mu dd$  and  $t\mu tt$  molecules are not likely to have large reaction rates for this reaction path [*i.e.*, the activation energy ( $E_{act}$ ) is too large]. As a result, these reaction paths can be neglected for all molecules, except  $d\mu tx$ . By assuming  $E_{act} = 0$  (*i.e.*, all  $d\mu tx + d\mu tx$  collisions result in di-muonic molecules being formed), a lower bound on the muon flux required to significantly affect the overall fusion rate can be determined. If this effect will be positive or negative depends on the fusion rate of the molecules formed (see Chapter 7).

If  $E_{act} = 0$  for the reactions discussed above, and the di-muonic molecules formed quickly go to fusion products, then a continuous negative muon flux as low as  $10^5$  could

result in di-muonic reactions increasing the overall fusion yield by as much as 10% , and a flux as low as  $3 \times 10^5$  could double the total yield (see Figure 8-1).

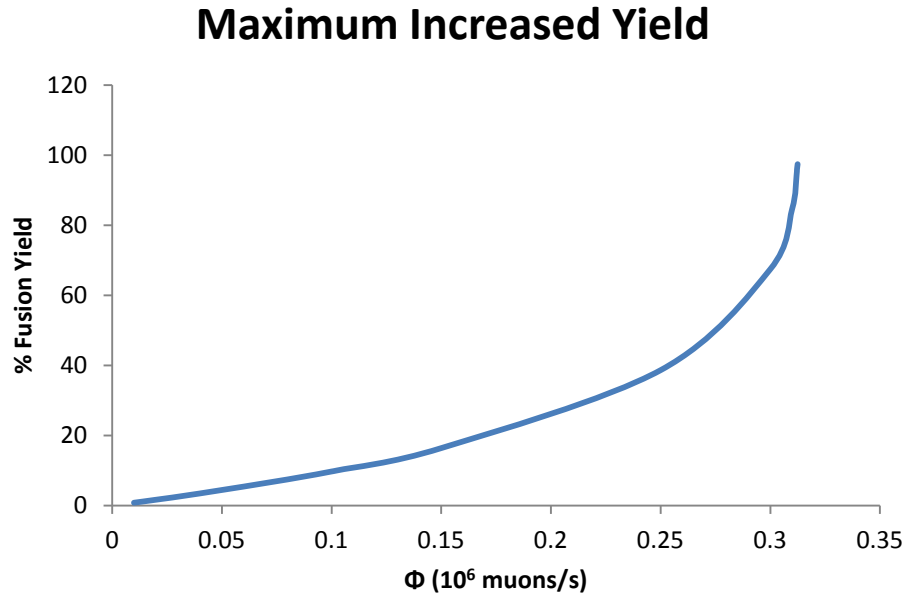
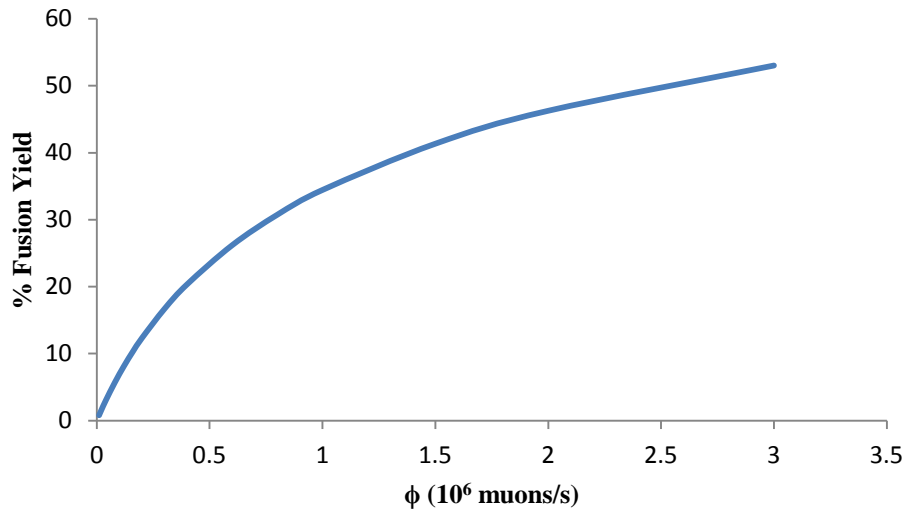


**Figure 8-1. Maximum possible fusion yield increase resulting from di-muonic hydrogen reactions formed by  $d\mu x + d\mu x$  collisions.**

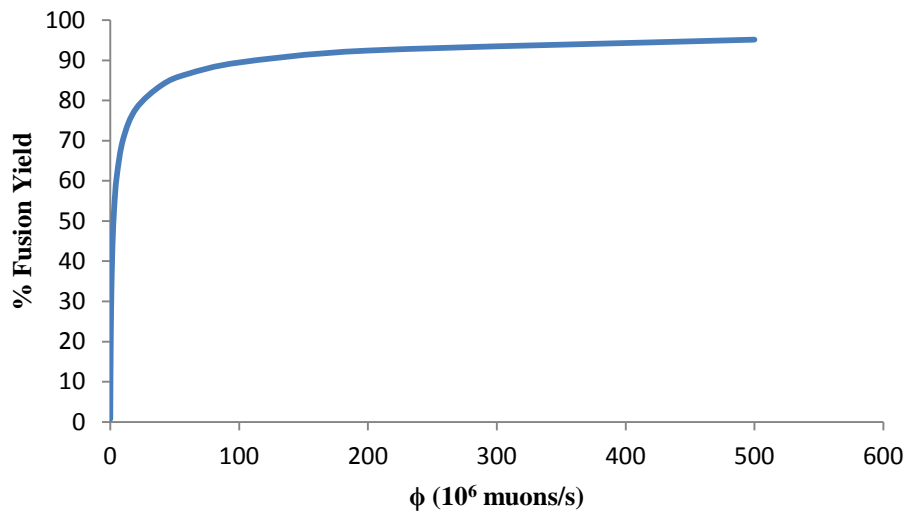
On the other hand, if  $E_{act} = 0$  and the di-muonic molecules formed do not result in significant fusion reactions, but rather, bind up the muons so they are no longer available to participate in catalysis, a negative muon flux of  $1.5 \times 10^5$  could decrease the fusion yield by as much as 10%, and a flux of  $5 \times 10^8$  could quench the fusion rate by as much as 95% (see Figure 8-2).

## Maximum Di-Muo Quenching



(a)

## Maximum Di-Muo Quenching

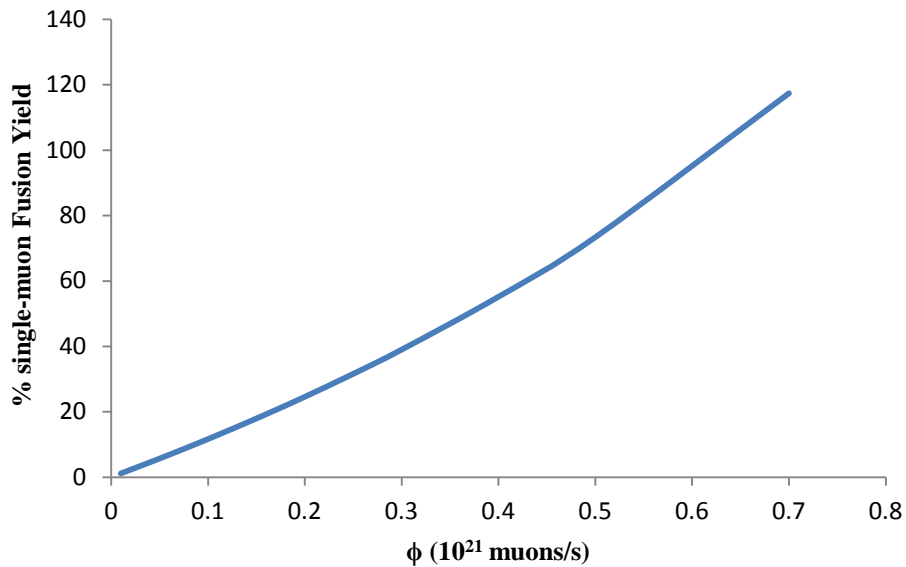


(b)

**Figures 8-2a and 8-2b. Maximum possible decrease in fusion yield, as a function of negative muon flux, resulting from di-muonic hydrogen reactions formed by  $d\bar{\mu}x + d\bar{\mu}x$  collisions.**

If the reaction rate for  $d\mu tx + d\mu tx$  is much lower than the collision rate (*i.e.*,  $E_{act}$  is large) and doesn't result in the formation of significant quantities of di-muonic hydrogen molecules, then the di-muonic reactions which could have the greatest effect on the fusion rate are those involving  $x\mu + x\mu xx$  collisions. Assuming  $E_{act}$  for these reactions to be zero (*i.e.*, all collisions result in the formation of di-muonic molecules), the lowest muon flux which can result in a significant increase in the fusion yield can be calculated. The lowest flux for which these reactions could be observed will occur in an all deuterium system. For these reactions to increase the fusion yield by 10%, a continuous negative muon flux of at least  $1.5 \times 10^{20}$  is needed (see Figure 8-3a).

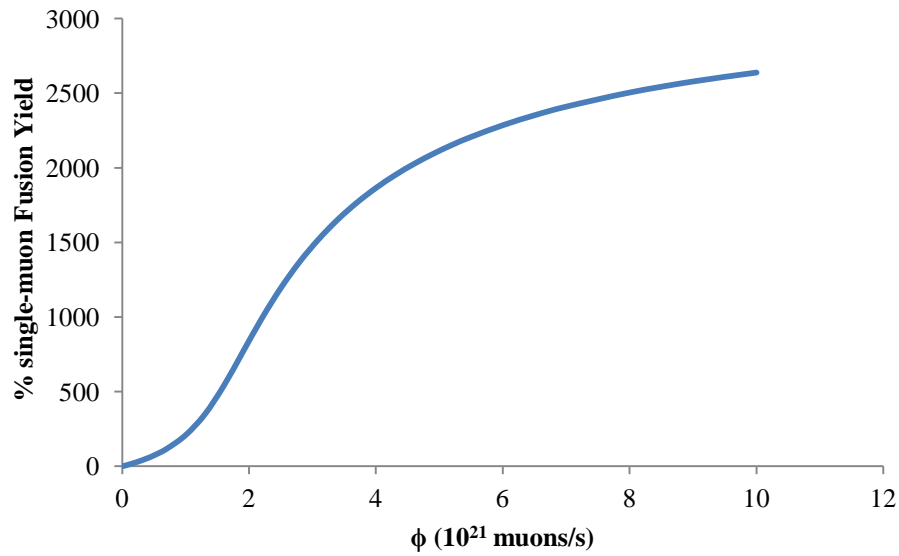
### Maximum Increased Yield



(a)

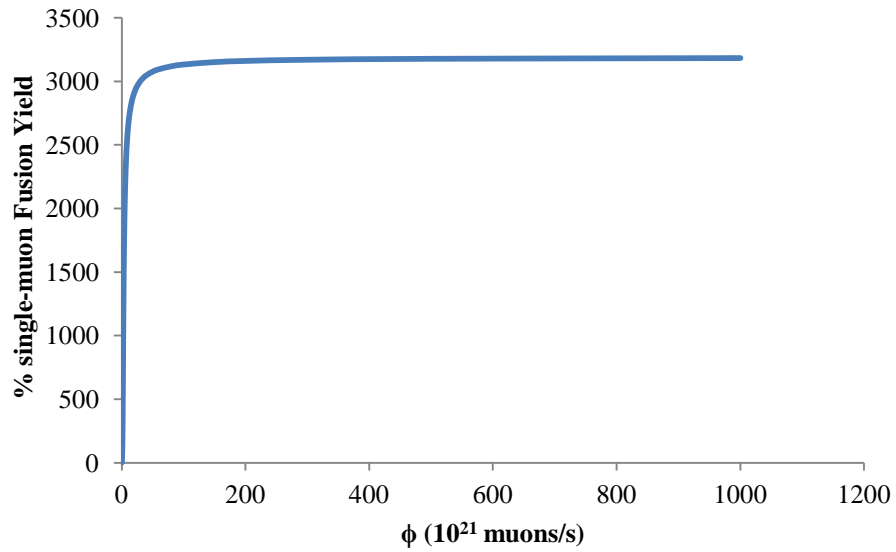


## Maximum Increased Yield



(b)

## Maximum Increased Yield

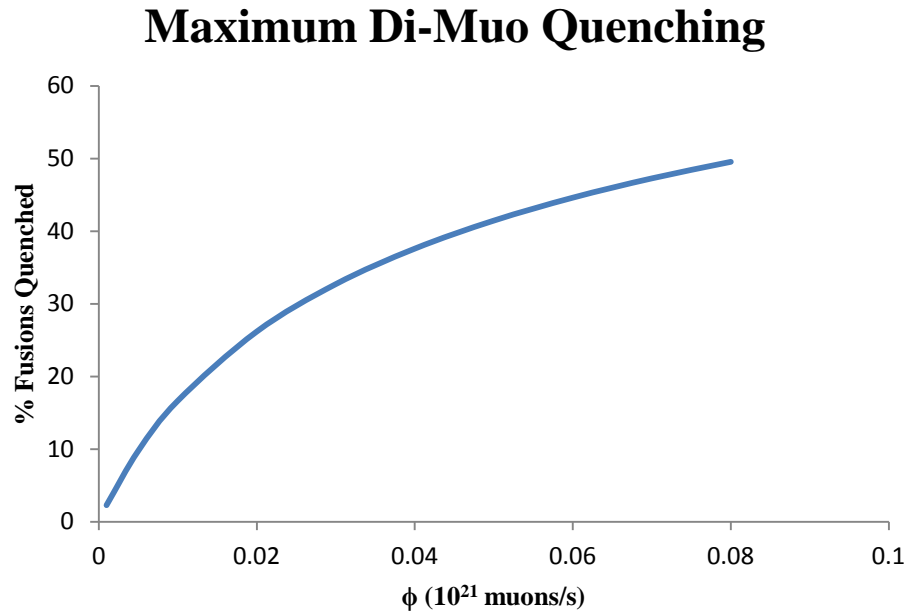


(c)

Figures 8-3a, 8-3b and 8-3c. Maximum possible fusion yield increase resulting from di-muonic hydrogen reactions formed by  $dd\mu d + d\mu$  collisions.

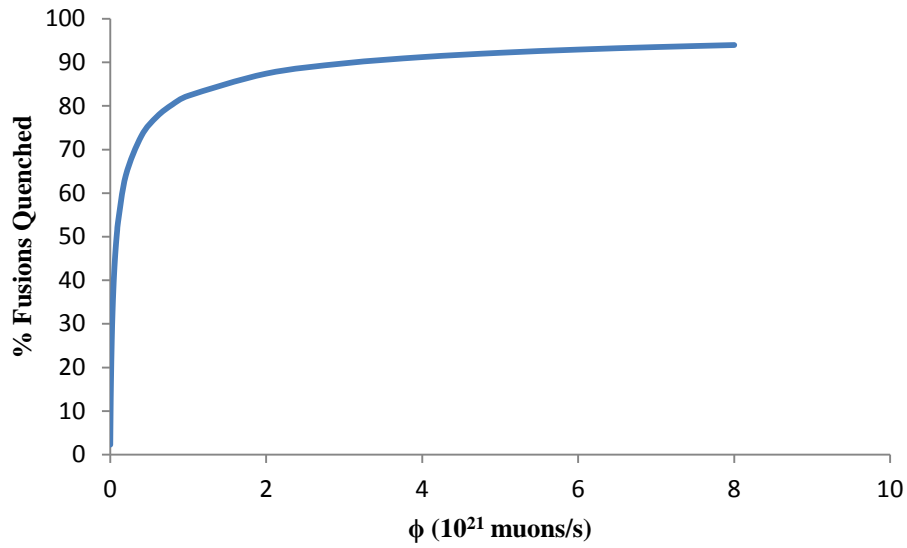
At higher flux an upper-bound on the fusion increase that could be obtained via these di-muonic reactions can be determined. Up to a 30 fold increase in the  $d$ - $d$  fusion rate is possible (see Figure 8-3).

If the di-muonic molecules  $d\mu\mu d$  or  $d\mu d\mu d$  form readily, but don't lead to fusion products, a quenching effect occurs (see Figure 8-4).



(a)

## Maximum Di-Muo Quenching

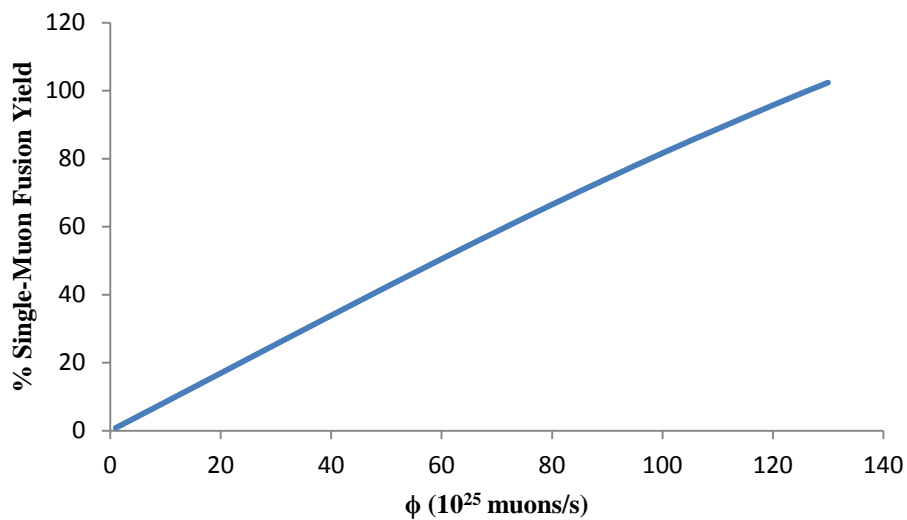


(b)

**Figures 8-4a and 8-4b. Maximum possible decrease in fusion yield, as a function of negative muon flux, resulting from di-muonic hydrogen reactions formed by  $dd\mu d + d\mu$  collisions.**

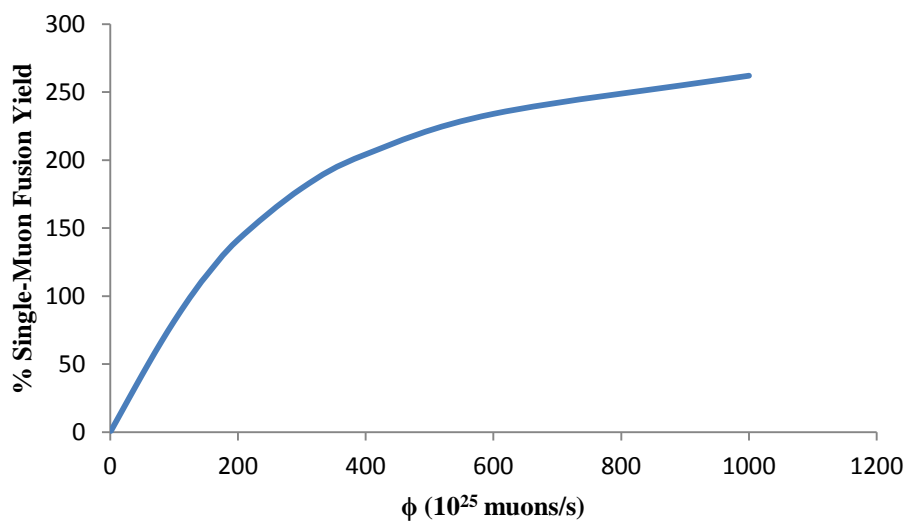
For  $d$ - $t$  fusion the same effects are predicted, but they will occur at a much higher muon flux (see Figures 8-5 and 8-6).

## Maximum Increased Yield



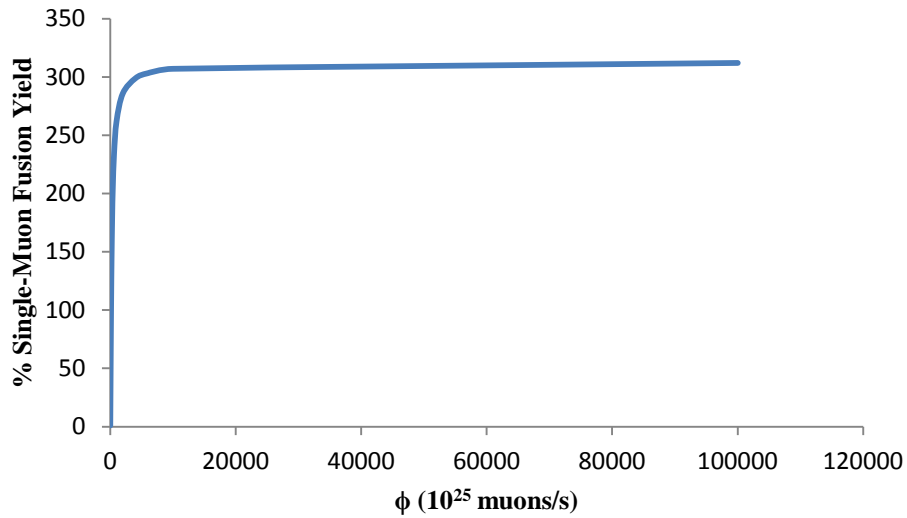
(a)

## Maximum Increased Yield



(b)

## Maximum Increased Yield



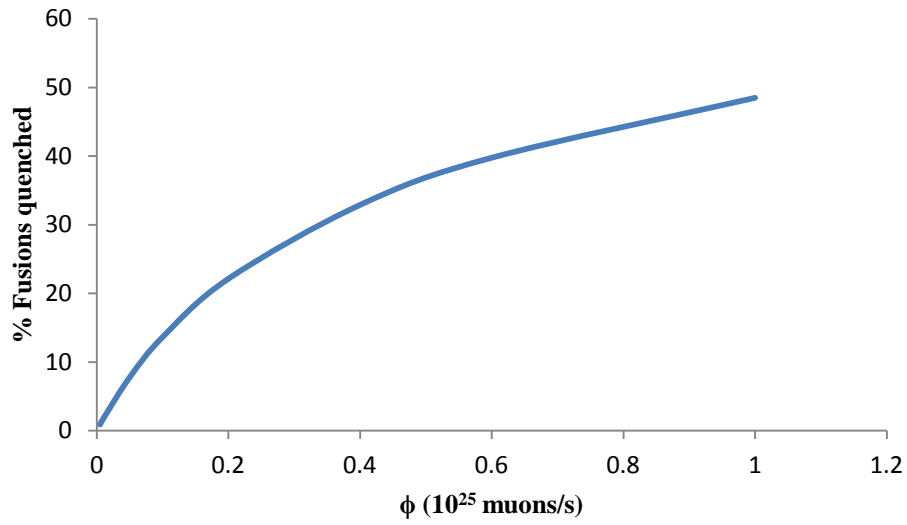
(c)

**Figures 8-5a, 8-5b and 8-5c. Maximum possible fusion yield increase resulting from di-muonic hydrogen reactions formed by  $d\mu x + x\mu$  collisions.**

As can be seen from Figure 8-5c, a three-fold increase in the fusion yield is an upper bound on what can be obtained via this reaction pathway, and this, only with an extremely high muon flux, which is currently unobtainable.

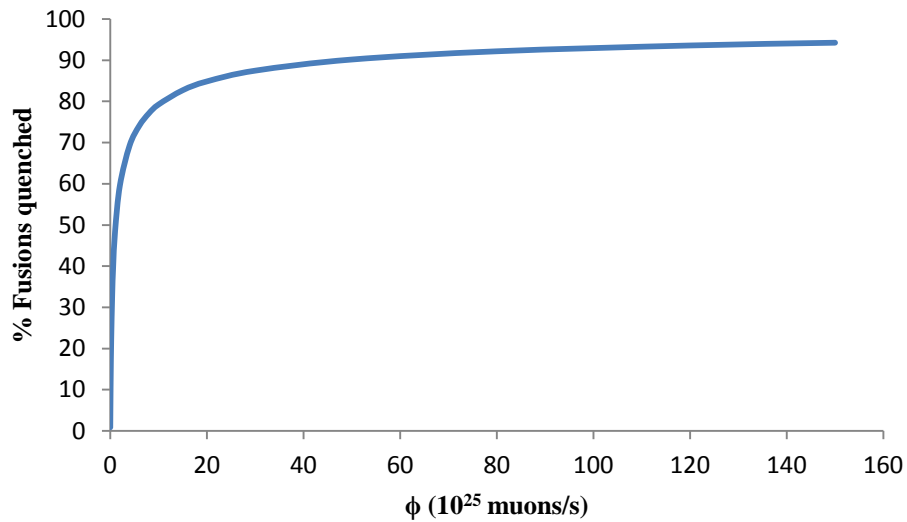
If quenching occurs, the effects will not be noticed at a muon flux lower than about  $10^{24}$ . A 50% decrease in yield could not occur with a flux lower than about  $10^{25}$  (see Figure 8-6).

## Maximum Di-Muo Quenching



(a)

## Maximum Di-Muo Quenching



(b)

Figures 8-6a and 8-6b. Maximum possible decrease in fusion yield, as a function of negative muon flux, resulting from di-muonic hydrogen reactions formed by  $d\mu x + x\mu$  collisions.

## 8.4 Conclusions

Di-muonic hydrogen molecules have the potential of affecting the overall fusion rate positively or negatively (see Chapter 7). No di-muonic effects will be observed, however, unless a significant quantity of these molecules are formed. In this chapter lower bounds on the muon flux needed to observe these effects were presented.

In order for di-muonic hydrogen reactions to contribute significantly to the overall muon-catalyzed fusion yield the muon flux must be greater than has traditionally been used for muon-catalyzed fusion experiments. The lowest continuous muon flux for which di-muonic reactions could be important to the overall fusion yield is about  $10^5$  muons/s.

Di-muonic reactions can be important at this relatively low flux, only if  $x\mu xx + x\mu xx$  collisions are highly likely to result in the formation of di-muonic molecules. Due to the binding energy and Coulombic repulsion between the  $x\mu x$  portions of the molecules,  $d\mu dd$  and  $t\mu tt$  molecules cannot be expected to form di-muonic molecules at a significant rate via this mechanism. The only apparent possibility for this reaction mechanism to be important is if  $d\mu tx + d\mu tx$  collisions readily form di-muonic molecules.

If  $d\mu tx + d\mu tx$  reactions do not have a significant probability of occurring (*i.e.*, the activation energy is large), then  $x\mu xx + x\mu$  reactions could be significant. For d-d fusion these reactions cannot be observed at significant rates if the muon flux is below about  $1.5 \times 10^{20}$  fusions/muon. A maximum increased fusion yield of up to 3,000% is possible. For  $d-t$  fusion, this reaction path could result in 10% quenching at a flux of  $10^{24}$  muons/fusion. If di-muonic hydrogen results in an increase in the  $d-t$  fusion yield, the

lowest flux which could result in a 10% increase is  $10^{26}$  muons/s, with a maximum possible yield increase of 300%.



## References

- [1] W. H. Breunlich, P. Kammel, J. S. Cohen and M. Leon, "Muon-Catalyzed Fusion," *Annual Review of Nuclear and Particle Science* , vol. 39, pp. 311-355, 1989.
- [2] S. E. Jones, "Muon-Catalysed Fusion Revisited," *Nature*, vol. 321, no. 6066, pp. 127-133, 1986.
- [3] S. E. Jones, "Survey of Experimental Results in Muon-Catalyzed Fusion," in *American Institute of Physics Conference Proceedings*, vol. 181, Sanibel Island, FL, 1988.
- [4] L. I. Ponomarev, "Muon Catalysed Fusion," *Contemporary Physics*, vol. 31, no. 4, pp. 219-245, 1990.
- [5] L. I. Ponomarev, "Muon-Catalyzed Fusion and Fundamental Physics," *Hyperfine Interactions*, vol. 103, pp. 137-145, 1996.
- [6] J. Rafelski, "The Challenges of Muon Catalyzed Fusion," in *American Institute of Physics Conference Proceedings*, vol. 181, Sanibel Island, FL, 1988.
- [7] J. Rafelski and S. E. Jones, "Cold Nuclear Fusion," *Scientific American*, vol. 255, no. 7, pp. 84-89, 1987.
- [8] H. E. Rafelski, D. Harley, G. R. Shin and J. Rafelski, "Cold Fusion: Muon-Catalysed Fusion," *Journal of Physics B: Atomic, Molecular and Optical Physics*, vol. 24, pp. 1469-1516, 1991.
- [9] M. Leon, "Theory of muonic molecule formation: Survey of progress and open questions," *Hyperfine Interactions* , vol. 82, no. 1-4, pp. 151-160, 1993.
- [10] Y. Hamahata, E. Hiyama and M. Kamimura, "Non-Adiabatic Four-Body Calculation of Double-Muonic Hydrogen Molecules," *Hyperfine Interactions*, vol. 138, pp. 187-190, 2001.
- [11] M. Leon, "Theory of Muonic Molecule Formation: Survey of Progress and Open Questions," *Hyperfine Interactions*, vol. 82, pp. 151-160, 1993.
- [12] K. Nagamine, *Introductory Muon Science*, Cambridge: Cambridge University Press, 2003.

- [13] M. P. Faifman and L. I. Ponomarev, "Resonant Formation of  $dt\mu$  Mesic Molecules in the Triple  $H_2+D_2+T_2$  Mixture," *Physics Letters B*, vol. 265, pp. 201-206, 1991.
- [14] S. A. Alexander, H. J. Monkhorst and K. Szalewicz, "A Comparison of Muonic Molecular Calculations," vol. 181, pp. 246-258, 1988.

## IX. Conclusions

In order for muon-catalyzed fusion to become an efficient source of pure fusion energy novel reaction mechanisms must be considered. Since the discovery of muon-catalyzed fusion in 1947 considerable research has been conducted on single-muon catalytic processes (see Chapter 2 and Appendix A). Although great strides have been made towards understanding muon catalysis, the yields obtained have been about an order of magnitude lower than what is required to produce a pure fusion reactor. Two factors have significantly limited the maximum obtainable yield: 1) the formation rate of molecules which efficiently fuse and 2) the sticking of muons to helium nuclei. It has been calculated that under optimum conditions (*e.g.*, temperature and pressure) single muon catalysis could yield up to 300 fusions/muon.[1:97; 2; 3] This continues to fall short of the at least 1000 fusions/muon required to produce a pure fusion reactor.[3; 4; 5; 6; 7; 8] The greatest hope of using muon catalysis as a source of pure fusion energy lies in the discovery of novel reaction mechanisms.

When the thermal muon flux in a reaction chamber is low, the concentration of di-muonic hydrogen molecules is insignificant; however, as the flux increases, di-muonic species are expected to play an increasing role in affecting the fusion yield. This document examines di-muonic hydrogen and helium molecules and the possibility that these exotic compounds can enhance the number of fusions per muon obtainable. In order for di-muonic molecules to enhance the fusion yield the formation rate of molecules which efficiently fuse must increase, and/or these molecules must facilitate the liberation of muons stuck to helium nuclei. The work presented in this dissertation examines both of these possibilities.

In order to facilitate the study of muonic molecules, and in general, any exotic molecule with a sufficiently long half-life for its chemical properties to be of interest, a General Particle Orbital (GPO) method of non-adiabatic quantum mechanics was developed. This non-adiabatic multi-configurational ab-initio method, which is outlined in Chapter 4, facilitates the study of molecular systems containing any number of any type (*i.e.*, mass and charge) of quantum particles in systems that may also contain classical (*i.e.*, fixed) particles. The size of the systems studied, the number of quantum particles, and the types of quantum particles is limited only by the computational facilities available. The results of using this GPO method to study di-muonic molecular properties are presented in Chapters 4 through 7.

Dynamic correlation interactions between particles have a large impact on the binding energy and bond length of the muonic molecules presented in this document (see Chapter 5). Configuration interaction (CI) methods of accounting for these interactions have been developed and presented (see Chapter 4). For di-muonic protium molecules the  $pp$ ,  $\mu\mu$ , and  $p\mu$  correlation interactions all contribute significantly to the overall energy of the systems. These interactions account for as much as 60% of the total energy of muonic protium systems. Of the three correlation contributions,  $p\mu$  correlation is by far the most important. This indicates that the results of previously published calculations, which neglect  $p\mu$  correlation interactions, cannot be expected to have accurate binding energies.[9] The calculation of dynamic correlation energy using GPO/CI methods is affected significantly by basis set size, but not affected as significantly as is the Hartree-Fock Energy (at least for the systems studied).

The work presented in this document shows that di-muonic hydrogen molecules have some unusual properties. Diatomic di-muonic hydrogen molecules (*e.g.*,  $p\mu\mu p$ ) have a larger equilibrium  $p$ - $p$  bond length than does corresponding single-muon molecules (*e.g.*,  $p\mu p^+$ ). This

effect is the result of strong dynamic correlation interactions between particles (see Chapters 4 and 5). Additionally, in di-nuclear hydrogen molecules, the vibrational excitation energy of the nuclei is higher than the transition energy between singlet and triplet muons (*i.e.*, anti-parallel and parallel muon spin). Using  $p\mu\mu p$  as an example, it was shown that bound singlet and triplet muon spin states and multiple excited rotational states of this molecule exist (see Chapter 7). The equilibrium bond length of the triplet molecules was calculated to be almost five times larger than that of the singlet molecules (see Table 6-3). It was shown that bound excited vibrational levels of  $p\mu\mu p$  do not exist. Although significant differences between molecules with parallel and anti-parallel muon spin were identified, the same cannot be said about nuclear spin. The calculated physical properties of the molecule were indistinguishable for parallel and anti-parallel nuclear spin states. This does not mean that nuclear spin is not important to the muon-catalyzed fusion process. The possibility that nuclear spin affects physical properties that were not calculated as part of this work (*e.g.*, fusion rates) exists.

The formation rate of muonic hydrogen molecules which have little energy transfer between reactants and products is predicted to be much higher than for those reactions which involve the transfer of large amounts of energy.[10; 11] Given this fact, it is more likely that  $p\mu\mu p$  will form in the triplet muonic spin state than in the singlet state (see Figure 7-1). The nuclear bond length of the parallel muon spin molecules is too large for them to have a significant fusion rate.[4] As a result, if the existence of di-muonic hydrogen molecules is to enhance the muon-catalyzed fusion yield, an efficient mechanism for transitioning triplet di-muonic molecules to molecules which do have a high fusion rate must exist. No efficient means by which the triplet molecules being discussed could transition into more tightly bound anti-parallel spin states were found.

Methods by which the triplet state diatomic molecules can transition to single muon molecules (*e.g.*,  $p\mu p^+$ ) or singlet state triatomic oblate symmetric top molecules (*e.g.*,  $p\mu p\mu p$  and  $p\mu p\mu p e$ ) which have much shorter nuclear bond lengths (*e.g.*,  $\sim 0.003 \text{ \AA}$ ) have been identified (see Chapter 7). All of the possible reaction paths for these reactions involve collisions with other molecules and/or the formation of rotationally excited molecules. Singlet  $p\mu p\mu p$  has three bound rotational states ( $J = 0, 1, 2$ ).  $p\mu p\mu p^{(T)}$  is only bound in the ground rotational state. Both singlet and triplet (muon spin) forms of  $p\mu p\mu p^+$  exist. Both of these forms of the molecule have five bound rotationally excited states: (1,1), (1,0), (2,2), (2,1), (3,3) (see Chapter 7). No bound vibrationally excited forms of  $p\mu p\mu p$  or  $p\mu p\mu p^+$  exist. Vibrationally excited forms of comparable molecules containing heavy hydrogen isotopes may exist, but this has so far not been calculated.

There are two di-muonic reaction paths which have the possibility of increasing the muon-catalyzed reaction yield sufficiently that muon-catalyzed fusion could become a standalone source of energy. The first possibility is for  $d\mu t x + d\mu t x$  collisions to result in the formation of di-muonic hydrogen molecules which quickly react to form fusion products. The second possibility is for  $d\mu d d + d\mu$  collisions to result in di-muonic hydrogen molecules which quickly go to fusion products, while at the same time  $\mu^3\text{He} + d\mu$  collisions result in fusions which release muons, thereby decreasing the effective sticking constant (*i.e.*, fraction of muons bound to  $^3\text{He}$  nuclei).

In order for  $d\mu t x + d\mu t x$  collisions to significantly increase the fusion yield, the activation energy ( $E_{act}$ ) leading to di-muonic hydrogen formation must be low. If  $E_{act}$  for this reaction is near zero, then muon fluxes as low as  $10^5$  may result in significant increases in the overall fusion yield (see Figure 8-1).

If  $E_{act}$  for this reaction is large, then a muon flux of greater than  $10^{24}$  will be needed to observe changes in the  $d-t$  fusion rate due to di-muonic molecular effects and an increase in yield of 300% is an upper bound on what is possible.

For di-muonic reactions to significantly impact  $d-d$  fusion a negative muon flux greater than  $10^{20}$  is needed. An upper bound on possible yield enhancement due to di-muonic deuterium molecules was calculated to be 3,000%. Although this reaction alone is not likely to increase the fusion yield sufficiently for it to be used as a standalone source of energy, if coupled with a decrease in the effective  ${}^3\text{He}$  sticking constant, then there is a chance that  $d-d$  muon-catalyzed fusion could become viable.

A method of using di-muonic molecules to liberate muons *stuck* to helium nuclei was considered. One of the products of  $d-d$  and  $d-p$  fusion is  ${}^3\text{He}$ . The possibility of using two muons to catalyze  ${}^3\text{He}-{}^3\text{He}$  and  $d-{}^3\text{He}$  fusion was studied. Although a localized energy minimum for  $({}^3\text{He}\mu{}^3\text{He}\mu)^{2+}$  exists when the nuclei separation is around 0.0034 Å, no bound vibrational state of this ion exists (see Figures 6-1 and 6-2). Therefore, using two muons to catalyze  ${}^3\text{He}-{}^3\text{He}$  fusion is not a viable option. The results of using two muons to catalyze  $d-{}^3\text{He}$  fusion were a bit better. Two bound vibrational states were identified with an equilibrium nuclear bond length of about 0.0037 Å (see Figure 6-4 and Table 6-1). In order to accurately calculate the vibrational energy levels it was necessary to include nuclear volume in the calculations. Assuming the nuclei to be point charges results in a calculated binding energy of the  $J=1$  vibrational state almost an order of magnitude larger than when nuclear volume is considered (see Figure 6-3 and Table 6-1). Due to the existence of a very weakly bound vibrational state of this molecule (*i.e.*, Binding Energy  $\approx$  0.16 eV) there is a strong possibility that a resonant formation mechanism

exists which could enhance the formation rate of this molecule (see References [1:82-83], [4], [10], [11], [12], [13], and [14] for an example of a similar resonance formation mechanism).



## References

- [1] K. Nagamine, *Introductory Muon Science*, Cambridge: Cambridge University Press, 2003.
- [2] S. Eliezer, "Muon Catalyzed Nuclear Fusion," *Laser and Particle Beams*, vol. 6, pp. 63-81, 1988.
- [3] P. Froelich and G. Larson, " $\alpha\mu$  Stripping by Ionization in Dense Deuterium/Tritium Mixture, and its Implication for Muon Catalyzed Fusion," *Journal of Molecular Structure: Theochem*, vol. 199, pp. 189-200, 1989.
- [4] J. Rafelski, "The Challenges of Muon Catalyzed Fusion," in *American Institute of Physics Conference Proceedings*, vol. 181, Sanibel Island, FL, 1988.
- [5] R. Gajewski, "The Political Economy of Muon-Catalyzed Fusion Research," in *American Institute of Physics Conference Proceedings*, Vol. 181, Sanibel Island, FL, 1988.
- [6] D. Harley, B. Muller and J. Rafelski, "Muon Catalysed Fusion of Nuclei with  $Z > 1$ ," *Journal of Physics G: Nuclear and Particle Physics*, vol. 16, no. 2, pp. 281-294, 1990.
- [7] M. Jändel, P. Froelich, G. Larson and C. D. Stodden, "Reactivation of  $\alpha\mu$  in Muon-Catalyzed Fusion under Plasma Conditions," *Physical Review A*, vol. 40, no. 5, pp. 2799-2802, 1989.
- [8] G. Cripps, A. A. Harms and B. Goel, "Muon Catalyzed Fusion of Deuterium-Tritium at Elevated Densities," *Hyperfine Interactions*, vol. 77, no. 1, pp. 181-199, 1993.
- [9] Y. Hamahata, E. Hiyama and M. Kamimura, "Non-Adiabatic Four-Body Calculation of Double-Muonic Hydrogen Molecules," *Hyperfine Interactions*, vol. 138, pp. 187-190, 2001.
- [10] L. I. Ponomarev, "Muon-Catalyzed Fusion and Fundamental Physics," *Hyperfine Interactions*, vol. 103, pp. 137-145, 1996.
- [11] L. I. Ponomarev, "Muon Catalysed Fusion," *Contemporary Physics*, vol. 31, no. 4, pp. 219-245, 1990.
- [12] W. H. Breunlich, P. Kammel, J. S. Cohen and M. Leon, "Muon-Catalyzed Fusion," *Annual Review of Nuclear and Particle Science*, vol. 39, pp. 311-355, 1989.
- [13] S. E. Jones, "Muon-Catalysed Fusion Revisited," *Nature*, vol. 321, no. 6066, pp. 127-133, 1986.

- [14] J. Rafelski and S. E. Jones, "Cold Nuclear Fusion," *Scientific American*, vol. 255, no. 7, pp. 84-89, 1987.

## Appendix A. Single Muon, Muon-Catalyzed Fusion Reactions and Rate Equations

While the basic idea of a negative muon replacing an electron in a hydrogen atom bringing the nuclei closer together and thereby catalyzing fusion may sound like a simple concept, the number of reaction steps involved and the complexity of the rate equations is significant. This appendix outlines the reaction steps involved in muon-catalyzed fusion and presents kinetic rate equations which correspond to these equations. It may be possible to consider systems that do not contain appreciable concentrations of tritium, thereby simplifying these equations considerably. It is, however, unlikely that any system could contain sufficiently low concentrations of protium or deuterium so as to make complete neglect of these isotopes possible. Due to the difference in magnitude of certain reaction rates and relative concentrations of isotopes, much can be done to simplify the kinetic equations of specific systems as the limit for some of the terms approach zero. No attempt to simplify the equations in this manner has been made in this appendix; all of the terms are presented, regardless of the size of the reaction rate constants.

In a hydrogen only system, there are 13 reactions that form the monatomic muonic molecules  $p\mu$ ,  $d\mu$ , and  $t\mu$ . The probability of a specific muonic molecule forming via a specific path is dependent upon the collision rate, molecular orientation, energy of the reacting particles (*i.e.*, temperature of the system) and the height of the energy barrier that must be overcome in order for a reaction to occur. Following is a list of the reactions

between hydrogen and muons that form monatomic muonic molecules: [note: in the following equations  $H$  refers to protium (*i.e.*,  $^1H$ ), and  $p$  refers to a proton (*i.e.*,  $^1H$  nucleus)]. It should be noted that many of the equations in this section are not balanced. In most cases the only products shown are the muonic-molecules. Most papers on muon-catalyzed fusion ignore the contribution of atomic hydrogen isotopes. While this approximation is appropriate for cryogenic systems, it is not at temperatures which are likely to produce optimum muon-catalyzed fusion yields. In the equations which follow, atomic hydrogen has been included:



$$D_2 + \mu^- \xrightarrow{\lambda_7} d\mu \quad (\text{A.7})$$

$$DT + \mu^- \xrightarrow{\lambda_8} d\mu \quad (\text{A.8})$$

$$T^\bullet + \mu^- \xrightarrow{\lambda_9} t\mu \quad (\text{A.9})$$

$$HT + \mu^- \xrightarrow{\lambda_{10}} t\mu \quad (\text{A.10})$$

$$DT + \mu^- \xrightarrow{\lambda_{11}} t\mu \quad (\text{A.11})$$

and

$$T_2 + \mu^- \xrightarrow{\lambda_{12}} t\mu \quad (\text{A.12})$$

Once formed, there are several reaction paths the monatomic hydrogen muonic molecules can follow: 1) The muon can decay, most often into an electron, an electron-antineutrino, and a muon-neutrino.[1:2] 2) The muon can be transferred, forming another monatomic muonic molecule via the reactions:

$$p\mu + D^\bullet \xrightarrow{\lambda_{13}} d\mu \quad (\text{A.13})$$

$$p\mu + T^\bullet \xrightarrow{\lambda_{14}} t\mu \quad (\text{A.14})$$

$$p\mu + HD \xrightarrow{\lambda_{15}} d\mu \quad (\text{A.15})$$

$$p\mu + HT \xrightarrow{\lambda_{16}} t\mu \quad (\text{A.16})$$

$$p\mu + D_2 \xrightarrow{\lambda_{17}} d\mu \quad (\text{A.17})$$

$$p\mu + DT \xrightarrow{\lambda_{18}} d\mu \quad (\text{A.18})$$

$$p\mu + DT \xrightarrow{\lambda_{19}} t\mu \quad (\text{A.19})$$

$$p\mu + T_2 \xrightarrow{\lambda_{20}} t\mu \quad (\text{A.20})$$

$$d\mu + H^\bullet \xrightarrow{\lambda_{21}} p\mu \quad (\text{A.21})$$

$$d\mu + T^\bullet \xrightarrow{\lambda_{22}} t\mu \quad (\text{A.22})$$

$$d\mu + H_2 \xrightarrow{\lambda_{23}} p\mu \quad (\text{A.23})$$

$$d\mu + HD \xrightarrow{\lambda_{24}} p\mu \quad (\text{A.24})$$

$$d\mu + HT \xrightarrow{\lambda_{25}} p\mu \quad (\text{A.25})$$

$$d\mu + HT \xrightarrow{\lambda_{26}} t\mu \quad (\text{A.26})$$

$$d\mu + DT \xrightarrow{\lambda_{27}} t\mu \quad (\text{A.27})$$

$$d\mu + T_2 \xrightarrow{\lambda_{28}} t\mu \quad (\text{A.28})$$

$$t\mu + H^\bullet \xrightarrow{\lambda_{29}} p\mu \quad (\text{A.29})$$

$$t\mu + D^\bullet \xrightarrow{\lambda_{30}} d\mu \quad (\text{A.30})$$

$$t\mu + H_2 \xrightarrow{\lambda_{31}} p\mu \quad (\text{A.31})$$

$$t\mu + HD \xrightarrow{\lambda_{32}} p\mu \quad (\text{A.32})$$

$$t\mu + HD \xrightarrow{\lambda_{33}} d\mu \quad (\text{A.33})$$

$$t\mu + D_2 \xrightarrow{\lambda_{34}} d\mu \quad (\text{A.34})$$

$$t\mu + HT \xrightarrow{\lambda_{35}} p\mu \quad (\text{A.35})$$

and

$$t\mu + DT \xrightarrow{\lambda_{36}} d\mu \quad (\text{A.36})$$

The probability of an exchange reaction in which the muon is transferred from a heavier isotope to a lighter isotope of hydrogen is so small that it can be neglected. This is primarily due to the difference in the binding energy. 3) The tri-atomic muonic molecules (pp $\mu$ )pee, (pp $\mu$ )dee, (pd $\mu$ )pee, (pd $\mu$ )dee, (pp $\mu$ )tee, (pt $\mu$ )pee, (pd $\mu$ )tee, (pt $\mu$ )dee, (pt $\mu$ )tee, (dp $\mu$ )pee, (dp $\mu$ )dee, (dd $\mu$ )pee, (dd $\mu$ )dee, (dp $\mu$ )tee, (dt $\mu$ )pee, (dd $\mu$ )tee, (dt $\mu$ )dee, (dt $\mu$ )tee, (tp $\mu$ )pee, (tp $\mu$ )dee, (td $\mu$ )pee, (td $\mu$ )dee, (tp $\mu$ )tee, (tt $\mu$ )pee, (td $\mu$ )tee, (tt $\mu$ )dee and (tt $\mu$ )tee can form via the following reactions:

$$p\mu + H_2 \left( \uparrow \uparrow \right) \xrightarrow{\lambda_{37}} (pp\mu) p \quad (\text{A.37})$$

$$p\mu + H_2 \left( \uparrow \downarrow \right) \xrightarrow{\lambda_{38}} (pp\mu) p \quad (\text{A.38})$$

$$p\mu + HD \xrightarrow{\lambda_{39}} (pp\mu) d \quad (\text{A.39})$$



$$p\mu + HD \xrightarrow{\lambda_{40}} (pd\mu)p \quad (\text{A.40})$$

$$p\mu + D_2(\uparrow\uparrow) \xrightarrow{\lambda_{41}} (pd\mu)d \quad (\text{A.41})$$

$$p\mu + D_2(\uparrow\downarrow) \xrightarrow{\lambda_{42}} (pd\mu)d \quad (\text{A.42})$$

$$p\mu + HT \xrightarrow{\lambda_{43}} (pp\mu)t \quad (\text{A.43})$$

$$p\mu + HT \xrightarrow{\lambda_{44}} (pt\mu)p \quad (\text{A.44})$$

$$p\mu + DT \xrightarrow{\lambda_{45}} (pd\mu)t \quad (\text{A.45})$$

$$p\mu + DT \xrightarrow{\lambda_{46}} (pt\mu)d \quad (\text{A.46})$$

$$p\mu + T_2(\uparrow\uparrow) \xrightarrow{\lambda_{47}} (pt\mu)t \quad (\text{A.47})$$

$$p\mu + T_2(\uparrow\downarrow) \xrightarrow{\lambda_{48}} (pt\mu)t \quad (\text{A.48})$$

$$d\mu + H_2(\uparrow\uparrow) \xrightarrow{\lambda_{49}} (pd\mu)p \quad (\text{A.49})$$

$$d\mu + H_2(\uparrow\downarrow) \xrightarrow{\lambda_{50}} (pd\mu)p \quad (\text{A.50})$$

$$d\mu + HD \xrightarrow{\lambda_{51}} (pd\mu)d \quad (\text{A.51})$$

$$d\mu + HD \xrightarrow{\lambda_{52}} (dd\mu)p \quad (\text{A.52})$$

$$d\mu + D_2(\uparrow\uparrow) \xrightarrow{\lambda_{53}} (dd\mu)d \quad (\text{A.53})$$

$$d\mu + D_2(\uparrow\downarrow) \xrightarrow{\lambda_{54}} (dd\mu)d \quad (\text{A.54})$$

$$d\mu + HT \xrightarrow{\lambda_{55}} (pd\mu)t \quad (\text{A.55})$$

$$d\mu + HT \xrightarrow{\lambda_{56}} (dt\mu)p \quad (\text{A.56})$$

$$d\mu + DT \xrightarrow{\lambda_{57}} (dd\mu)t \quad (\text{A.57})$$

$$d\mu + DT \xrightarrow{\lambda_{58}} (dt\mu)d \quad (\text{A.58})$$

$$d\mu + T_2(\uparrow\uparrow) \xrightarrow{\lambda_{59}} (dt\mu)t \quad (\text{A.59})$$

$$d\mu + T_2(\uparrow\downarrow) \xrightarrow{\lambda_{60}} (dt\mu)t \quad (\text{A.60})$$

$$t\mu + H_2(\uparrow\uparrow) \xrightarrow{\lambda_{61}} (pt\mu)p \quad (\text{A.61})$$

$$t\mu + H_2(\uparrow\downarrow) \xrightarrow{\lambda_{62}} (pt\mu)p \quad (\text{A.62})$$

$$t\mu + HD \xrightarrow{\lambda_{63}} (pt\mu)d \quad (\text{A.63})$$

$$t\mu + HD \xrightarrow{\lambda_{64}} (dt\mu)p \quad (\text{A.64})$$

$$t\mu + D_2(\uparrow\uparrow) \xrightarrow{\lambda_{65}} (dt\mu)d \quad (\text{A.65})$$

$$t\mu + D_2(\uparrow\downarrow) \xrightarrow{\lambda_{66}} (dt\mu)d \quad (\text{A.66})$$

$$t\mu + HT \xrightarrow{\lambda_{67}} (pt\mu)t \quad (\text{A.67})$$

$$t\mu + HT \xrightarrow{\lambda_{68}} (tt\mu) p \quad (\text{A.68})$$

$$t\mu + DT \xrightarrow{\lambda_{69}} (dt\mu) t \quad (\text{A.69})$$

$$t\mu + DT \xrightarrow{\lambda_{70}} (tt\mu) d \quad (\text{A.70})$$

$$t\mu + T_2(\uparrow\uparrow) \xrightarrow{\lambda_{71}} (tt\mu) t \quad (\text{A.71})$$

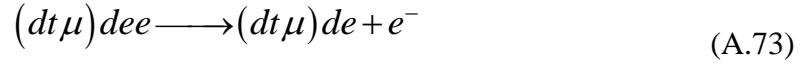
and

$$t\mu + T_2(\uparrow\downarrow) \xrightarrow{\lambda_{72}} (tt\mu) t \quad (\text{A.72})$$

where  $(\uparrow\uparrow)$  represents parallel nuclear spin and  $(\uparrow\downarrow)$  represents anti-parallel nuclear spin. When a monatomic muonic hydrogen atom collides with a heavier hydrogen atom the probability that an exchange reaction will occur is greater than the probability of a tri-atomic muonic molecule forming.

There are several reaction paths these tri-atomic muonic molecules can follow: The muon can decay away, causing the molecule to break apart and the muon-catalyzed cycling chain to cease. An exchange reaction can occur, forming a different tri-atomic muonic molecule. The tri-atomic exotic molecules can dissociate, most often with the

muon being bound to the more massive of the two nuclei it was closest to. It can lose energy through an Auger transition such as



or, nuclear fusion can occur, giving off energy and a variety of particles. After Auger stabilization the molecule can decay, fuse or collide with another molecule and dissociate.

Before presenting the reaction paths the tri-atomic muonic molecules can follow there is another term which needs to be defined, the sticking constant ( $\omega_i$ ). This is the probability that when muon-catalyzed-fusion occurs the muon will stick to a fusion product.

In most cases muon sticking is a non-desirable effect since it precludes the muon from catalyzing further fusion reactions. A notable exception to this is when  $dd\mu p$ ,  $dd\mu d$  or  $dd\mu t$  fuse forming tritium and a proton. In these cases if the muon sticks to the products they can immediately enter back into the reaction sequences listed in this section. Although  ${}^3\text{He}$  can fuse via muon-catalyzed fusion, the probability is small due to a relatively large separation distance between the fusing particles. As a result,  ${}^3\text{He}$  fusion has been neglected in the reactions presented in this section.

Following are exchange reactions tri-atomic muonic molecules can participate in, in a hydrogen only system

$$(pp\mu)p + D^\bullet \xrightarrow{\lambda_{73}} (pp\mu)d + H^\bullet \quad (\text{A.74})$$

$$(pp\mu)p + T^\bullet \xrightarrow{\lambda_{74}} (pp\mu)t + H^\bullet \quad (\text{A.75})$$

$$(pp\mu)p + HD \xrightarrow{\lambda_{75}} (pp\mu)d + H_2 \quad (\text{A.76})$$

$$(pp\mu)p + HT \xrightarrow{\lambda_{76}} (pp\mu)t + H_2 \quad (\text{A.77})$$

$$(pp\mu)p + D_2(\uparrow\uparrow) \xrightarrow{\lambda_{77}} (pp\mu)d + HD \quad (\text{A.78})$$

$$(pp\mu)p + D_2(\uparrow\downarrow) \xrightarrow{\lambda_{78}} (pp\mu)d + HD \quad (\text{A.79})$$

$$(pp\mu)p + DT \xrightarrow{\lambda_{79}} (pp\mu)d + HT \quad (\text{A.80})$$

$$(pp\mu)p + DT \xrightarrow{\lambda_{80}} (pp\mu)t + HD \quad (\text{A.81})$$

$$(pp\mu)p + T_2(\uparrow\uparrow) \xrightarrow{\lambda_{81}} (pp\mu)t + HT \quad (\text{A.82})$$

$$(pp\mu)p + T_2(\uparrow\downarrow) \xrightarrow{\lambda_{82}} (pp\mu)t + HT \quad (\text{A.83})$$

$$(pp\mu)d + H^\bullet \xrightarrow{\lambda_{83}} (pp\mu)p + D^\bullet \quad (\text{A.84})$$

$$(pp\mu)d + T^\bullet \xrightarrow{\lambda_{84}} (pp\mu)t + D^\bullet \quad (\text{A.85})$$

$$(pp\mu)d + H_2(\uparrow\uparrow) \xrightarrow{\lambda_{85}} (pp\mu)p + HD \quad (\text{A.86})$$

$$(pp\mu)d + H_2(\uparrow\downarrow) \xrightarrow{\lambda_{86}} (pp\mu)p + HD \quad (\text{A.87})$$

$$(pp\mu)d + HD \xrightarrow{\lambda_{87}} (pp\mu)p + D_2 \quad (\text{A.88})$$

$$(pp\mu)d + HT \xrightarrow{\lambda_{88}} (pp\mu)p + DT \quad (\text{A.89})$$

$$(pp\mu)d + HT \xrightarrow{\lambda_{89}} (pp\mu)t + HD \quad (\text{A.90})$$

$$(pp\mu)d + DT \xrightarrow{\lambda_{90}} (pp\mu)t + D_2 \quad (\text{A.91})$$

$$(pp\mu)d + T_2(\uparrow\uparrow) \xrightarrow{\lambda_{91}} (pp\mu)t + DT \quad (\text{A.92})$$

$$(pp\mu)d + T_2(\uparrow\downarrow) \xrightarrow{\lambda_{92}} (pp\mu)t + DT \quad (\text{A.93})$$

$$(pp\mu)t + H^\bullet \xrightarrow{\lambda_{93}} (pp\mu)p + T^\bullet \quad (\text{A.94})$$

$$(pp\mu)t + D^\bullet \xrightarrow{\lambda_{94}} (pp\mu)d + T^\bullet \quad (\text{A.95})$$

$$(pp\mu)t + H_2(\uparrow\uparrow) \xrightarrow{\lambda_{95}} (pp\mu)p + HT \quad (\text{A.96})$$

$$(pp\mu)t + H_2(\uparrow\downarrow) \xrightarrow{\lambda_{96}} (pp\mu)p + HT \quad (\text{A.97})$$

$$(pp\mu)t + HD \xrightarrow{\lambda_{97}} (pp\mu)p + DT \quad (\text{A.98})$$

$$(pp\mu)t + HD \xrightarrow{\lambda_{98}} (pp\mu)d + HT \quad (\text{A.99})$$

$$(pp\mu)t + D_2(\uparrow\uparrow) \xrightarrow{\lambda_{99}} (pp\mu)d + DT \quad (\text{A.100})$$

$$(pp\mu)t + D_2(\uparrow\downarrow) \xrightarrow{\lambda_{100}} (pp\mu)d + DT \quad (\text{A.101})$$

$$(pp\mu)t + HT \xrightarrow{\lambda_{101}} (pp\mu)p + T_2 \quad (\text{A.102})$$



$$(pp\mu)t + DT \xrightarrow{\lambda_{402}} (pp\mu)d + T_2 \quad (\text{A.103})$$

$$(pd\mu)p + D^\bullet \xrightarrow{\lambda_{403}} (pd\mu)d + H^\bullet \quad (\text{A.104})$$

$$(pd\mu)p + T^\bullet \xrightarrow{\lambda_{404}} (pd\mu)t + H^\bullet \quad (\text{A.105})$$

$$(pd\mu)p + HD \xrightarrow{\lambda_{405}} (pd\mu)d + H_2 \quad (\text{A.106})$$

$$(pd\mu)p + HT \xrightarrow{\lambda_{406}} (pd\mu)t + H_2 \quad (\text{A.107})$$

$$(pd\mu)p + D_2(\uparrow\uparrow) \xrightarrow{\lambda_{407}} (pd\mu)d + HD \quad (\text{A.108})$$

$$(pd\mu)p + D_2(\uparrow\downarrow) \xrightarrow{\lambda_{408}} (pd\mu)d + HD \quad (\text{A.109})$$

$$(pd\mu)p + DT \xrightarrow{\lambda_{409}} (pd\mu)d + HT \quad (\text{A.110})$$

$$(pd\mu)p + DT \xrightarrow{\lambda_{410}} (pd\mu)t + HD \quad (\text{A.111})$$

$$(pd\mu)p + T_2(\uparrow\uparrow) \xrightarrow{\lambda_{111}} (pd\mu)t + HT \quad (\text{A.112})$$

$$(pd\mu)p + T_2(\uparrow\downarrow) \xrightarrow{\lambda_{112}} (pd\mu)t + HT \quad (\text{A.113})$$

$$(pd\mu)d + H^\bullet \xrightarrow{\lambda_{113}} (pd\mu)p + D^\bullet \quad (\text{A.114})$$

$$(pd\mu)d + T^\bullet \xrightarrow{\lambda_{114}} (pd\mu)t + D^\bullet \quad (\text{A.115})$$

$$(pd\mu)d + H_2(\uparrow\uparrow) \xrightarrow{\lambda_{115}} (pd\mu)p + HD \quad (\text{A.116})$$

$$(pd\mu)d + H_2(\uparrow\downarrow) \xrightarrow{\lambda_{116}} (pd\mu)p + HD \quad (\text{A.117})$$

$$(pd\mu)d + HD \xrightarrow{\lambda_{117}} (pd\mu)p + D_2 \quad (\text{A.118})$$

$$(pd\mu)d + HT \xrightarrow{\lambda_{118}} (pd\mu)p + DT \quad (\text{A.119})$$

$$(pd\mu)d + HT \xrightarrow{\lambda_{119}} (pd\mu)t + HD \quad (\text{A.120})$$

$$(pd\mu)d + DT \xrightarrow{\lambda_{120}} (pd\mu)t + D_2 \quad (\text{A.121})$$

$$(pd\mu)d + T_2(\uparrow\uparrow) \xrightarrow{\lambda_{121}} (pd\mu)t + DT \quad (\text{A.122})$$

$$(pd\mu)d + T_2(\uparrow\downarrow) \xrightarrow{\lambda_{122}} (pd\mu)t + DT \quad (\text{A.123})$$

$$(pd\mu)t + H^\bullet \xrightarrow{\lambda_{123}} (pd\mu)p + T^\bullet \quad (\text{A.124})$$

$$(pd\mu)t + D^\bullet \xrightarrow{\lambda_{124}} (pd\mu)d + T^\bullet \quad (\text{A.125})$$

$$(pd\mu)t + H_2(\uparrow\uparrow) \xrightarrow{\lambda_{125}} (pd\mu)p + HT \quad (\text{A.126})$$

$$(pd\mu)t + H_2(\uparrow\downarrow) \xrightarrow{\lambda_{126}} (pd\mu)p + HT \quad (\text{A.127})$$

$$(pd\mu)t + HD \xrightarrow{\lambda_{127}} (pd\mu)p + DT \quad (\text{A.128})$$

$$(pd\mu)t + HD \xrightarrow{\lambda_{128}} (pd\mu)d + HT \quad (\text{A.129})$$

$$(pd\mu)t + D_2(\uparrow\uparrow) \xrightarrow{\lambda_{129}} (pd\mu)d + DT \quad (\text{A.130})$$

$$(pd\mu)t + D_2(\uparrow\downarrow) \xrightarrow{\lambda_{130}} (pd\mu)d + DT \quad (\text{A.131})$$

$$(pd\mu)t + HT \xrightarrow{\lambda_{131}} (pd\mu)p + T_2 \quad (\text{A.132})$$

$$(pd\mu)t + DT \xrightarrow{\lambda_{132}} (pd\mu)d + T_2 \quad (\text{A.133})$$

$$(pt\mu)p + D^\bullet \xrightarrow{\lambda_{133}} (pt\mu)d + H^\bullet \quad (\text{A.134})$$

$$(pt\mu)p + T^\bullet \xrightarrow{\lambda_{134}} (pt\mu)t + H^\bullet \quad (\text{A.135})$$

$$(pt\mu)p + HD \xrightarrow{\lambda_{135}} (pt\mu)d + H_2 \quad (\text{A.136})$$

$$(pt\mu)p + HT \xrightarrow{\lambda_{136}} (pt\mu)t + H_2 \quad (\text{A.137})$$

$$(pt\mu)p + D_2(\uparrow\uparrow) \xrightarrow{\lambda_{137}} (pt\mu)d + HD \quad (\text{A.138})$$

$$(pt\mu)p + D_2(\uparrow\downarrow) \xrightarrow{\lambda_{138}} (pt\mu)d + HD \quad (\text{A.139})$$

$$(pt\mu)p + DT \xrightarrow{\lambda_{139}} (pt\mu)d + HT \quad (\text{A.140})$$

$$(pt\mu)p + DT \xrightarrow{\lambda_{140}} (pt\mu)t + HD \quad (\text{A.141})$$

$$(pt\mu)p + T_2(\uparrow\uparrow) \xrightarrow{\lambda_{141}} (pt\mu)t + HT \quad (\text{A.142})$$

$$(pt\mu)p + T_2(\uparrow\downarrow) \xrightarrow{\lambda_{142}} (pt\mu)t + HT \quad (\text{A.143})$$

$$(pt\mu)d + H^\bullet \xrightarrow{\lambda_{143}} (pt\mu)p + D^\bullet \quad (\text{A.144})$$

$$(pt\mu)d + T^\bullet \xrightarrow{\lambda_{144}} (pt\mu)t + D^\bullet \quad (\text{A.145})$$

$$(pt\mu)d + H_2(\uparrow\uparrow) \xrightarrow{\lambda_{145}} (pt\mu)p + HD \quad (\text{A.146})$$

$$(pt\mu)d + H_2(\uparrow\downarrow) \xrightarrow{\lambda_{146}} (pt\mu)p + HD \quad (\text{A.147})$$

$$(pt\mu)d + HD \xrightarrow{\lambda_{147}} (pt\mu)p + D_2 \quad (\text{A.148})$$

$$(pt\mu)d + HT \xrightarrow{\lambda_{148}} (pt\mu)p + DT \quad (\text{A.149})$$

$$(pt\mu)d + HT \xrightarrow{\lambda_{149}} (pt\mu)t + HD \quad (\text{A.150})$$

$$(pt\mu)d + DT \xrightarrow{\lambda_{150}} (pt\mu)t + D_2 \quad (\text{A.151})$$

$$(pt\mu)d + T_2(\uparrow\uparrow) \xrightarrow{\lambda_{151}} (pt\mu)t + DT \quad (\text{A.152})$$

$$(pt\mu)d + T_2(\uparrow\downarrow) \xrightarrow{\lambda_{152}} (pt\mu)t + DT \quad (\text{A.153})$$

$$(pt\mu)t + H^\bullet \xrightarrow{\lambda_{153}} (pt\mu)p + T^\bullet \quad (\text{A.154})$$

$$(pt\mu)t + D^\bullet \xrightarrow{\lambda_{154}} (pt\mu)d + T^\bullet \quad (\text{A.155})$$

$$(pt\mu)t + H_2(\uparrow\uparrow) \xrightarrow{\lambda_{155}} (pt\mu)p + HT \quad (\text{A.156})$$

$$(pt\mu)t + H_2(\uparrow\downarrow) \xrightarrow{\lambda_{156}} (pt\mu)p + HT \quad (\text{A.157})$$

$$(pt\mu)t + HD \xrightarrow{\lambda_{157}} (pt\mu)p + DT \quad (\text{A.158})$$

$$(pt\mu)t + HD \xrightarrow{\lambda_{158}} (pt\mu)d + HT \quad (\text{A.159})$$

$$(pt\mu)t + D_2(\uparrow\uparrow) \xrightarrow{\lambda_{159}} (pt\mu)d + DT \quad (\text{A.160})$$

$$(pt\mu)t + D_2(\uparrow\downarrow) \xrightarrow{\lambda_{160}} (pt\mu)d + DT \quad (\text{A.161})$$

$$(pt\mu)t + HT \xrightarrow{\lambda_{161}} (pt\mu)p + T_2 \quad (\text{A.162})$$

$$(pt\mu)t + DT \xrightarrow{\lambda_{162}} (pt\mu)d + T_2 \quad (\text{A.163})$$

$$(dd\mu)p + D^\bullet \xrightarrow{\lambda_{163}} (dd\mu)d + H^\bullet \quad (\text{A.164})$$

$$(dd\mu)p + T^\bullet \xrightarrow{\lambda_{164}} (dd\mu)t + H^\bullet \quad (\text{A.165})$$

$$(dd\mu)p + HD \xrightarrow{\lambda_{165}} (dd\mu)d + H_2 \quad (\text{A.166})$$

$$(dd\mu)p + HT \xrightarrow{\lambda_{166}} (dd\mu)t + H_2 \quad (\text{A.167})$$

$$(dd\mu)p + D_2(\uparrow\uparrow) \xrightarrow{\lambda_{167}} (dd\mu)d + HD \quad (\text{A.168})$$

$$(dd\mu)p + D_2(\uparrow\downarrow) \xrightarrow{\lambda_{168}} (dd\mu)d + HD \quad (\text{A.169})$$

$$(dd\mu)p + DT \xrightarrow{\lambda_{169}} (dd\mu)d + HT \quad (\text{A.170})$$

$$(dd\mu)p + DT \xrightarrow{\lambda_{170}} (dd\mu)t + HD \quad (\text{A.171})$$

$$(dd\mu)p + T_2(\uparrow\uparrow) \xrightarrow{\lambda_{171}} (dd\mu)t + HT \quad (\text{A.172})$$

$$(dd\mu)p + T_2(\uparrow\downarrow) \xrightarrow{\lambda_{172}} (dd\mu)t + HT \quad (\text{A.173})$$

$$(dd\mu)d + H^\bullet \xrightarrow{\lambda_{173}} (dd\mu)p + D^\bullet \quad (\text{A.174})$$

$$(dd\mu)d + T^\bullet \xrightarrow{\lambda_{174}} (dd\mu)t + D^\bullet \quad (\text{A.175})$$

$$(dd\mu)d + H_2(\uparrow\uparrow) \xrightarrow{\lambda_{175}} (dd\mu)p + HD \quad (\text{A.176})$$

$$(dd\mu)d + H_2(\uparrow\downarrow) \xrightarrow{\lambda_{176}} (dd\mu)p + HD \quad (\text{A.177})$$

$$(dd\mu)d + HD \xrightarrow{\lambda_{177}} (dd\mu)p + D_2 \quad (\text{A.178})$$



$$(dd\mu)d + HT \xrightarrow{\lambda_{178}} (dd\mu)p + DT \quad (\text{A.179})$$

$$(dd\mu)d + HT \xrightarrow{\lambda_{179}} (dd\mu)t + HD \quad (\text{A.180})$$

$$(dd\mu)d + DT \xrightarrow{\lambda_{180}} (dd\mu)t + D_2 \quad (\text{A.181})$$

$$(dd\mu)d + T_2(\uparrow\uparrow) \xrightarrow{\lambda_{181}} (dd\mu)t + DT \quad (\text{A.182})$$

$$(dd\mu)d + T_2(\uparrow\downarrow) \xrightarrow{\lambda_{182}} (dd\mu)t + DT \quad (\text{A.183})$$

$$(dd\mu)t + H^\bullet \xrightarrow{\lambda_{183}} (dd\mu)d + T^\bullet \quad (\text{A.184})$$

$$(dd\mu)t + D^\bullet \xrightarrow{\lambda_{184}} (dd\mu)p + T^\bullet \quad (\text{A.185})$$

$$(dd\mu)t + H_2(\uparrow\uparrow) \xrightarrow{\lambda_{185}} (dd\mu)p + HT \quad (\text{A.186})$$

$$(dd\mu)t + H_2(\uparrow\downarrow) \xrightarrow{\lambda_{186}} (dd\mu)p + HT \quad (\text{A.187})$$

$$(dd\mu)t + HD \xrightarrow{\lambda_{187}} (dd\mu)p + DT \quad (\text{A.188})$$

$$(dd\mu)t + HD \xrightarrow{\lambda_{188}} (dd\mu)d + HT \quad (\text{A.189})$$

$$(dd\mu)t + D_2(\uparrow\uparrow) \xrightarrow{\lambda_{189}} (dd\mu)d + DT \quad (\text{A.190})$$

$$(dd\mu)t + D_2(\uparrow\downarrow) \xrightarrow{\lambda_{190}} (dd\mu)d + DT \quad (\text{A.191})$$

$$(dd\mu)t + HT \xrightarrow{\lambda_{191}} (dd\mu)p + T_2 \quad (\text{A.192})$$

$$(dd\mu)t + DT \xrightarrow{\lambda_{192}} (dd\mu)d + T_2 \quad (\text{A.193})$$

$$(dt\mu)p + D^\bullet \xrightarrow{\lambda_{193}} (dt\mu)d + H^\bullet \quad (\text{A.194})$$

$$(dt\mu)p + T^\bullet \xrightarrow{\lambda_{194}} (dt\mu)t + H^\bullet \quad (\text{A.195})$$

$$(dt\mu)p + HD \xrightarrow{\lambda_{195}} (dt\mu)d + H_2 \quad (\text{A.196})$$

$$(dt\mu)p + HT \xrightarrow{\lambda_{196}} (dt\mu)t + H_2 \quad (\text{A.197})$$

$$(dt\mu) p + D_2(\uparrow\uparrow) \xrightarrow{\lambda_{197}} (dt\mu) d + HD \quad (\text{A.198})$$

$$(dt\mu) p + D_2(\uparrow\downarrow) \xrightarrow{\lambda_{198}} (dt\mu) d + HD \quad (\text{A.199})$$

$$(dt\mu) p + DT \xrightarrow{\lambda_{199}} (dt\mu) d + HT \quad (\text{A.200})$$

$$(dt\mu) p + DT \xrightarrow{\lambda_{200}} (dt\mu) t + HD \quad (\text{A.201})$$

$$(dt\mu) p + T_2(\uparrow\uparrow) \xrightarrow{\lambda_{201}} (dt\mu) t + HT \quad (\text{A.202})$$

$$(dt\mu) p + T_2(\uparrow\downarrow) \xrightarrow{\lambda_{202}} (dt\mu) t + HT \quad (\text{A.203})$$

$$(dt\mu) d + H^\bullet \xrightarrow{\lambda_{203}} (dt\mu) p + D^\bullet \quad (\text{A.204})$$

$$(dt\mu) d + T^\bullet \xrightarrow{\lambda_{204}} (dt\mu) t + D^\bullet \quad (\text{A.205})$$

$$(dt\mu) d + H_2(\uparrow\uparrow) \xrightarrow{\lambda_{205}} (dt\mu) p + HD \quad (\text{A.206})$$

$$(dt\mu) d + H_2(\uparrow\downarrow) \xrightarrow{\lambda_{206}} (dt\mu) p + HD \quad (\text{A.207})$$

$$(dt\mu)d + HD \xrightarrow{\lambda_{207}} (dt\mu)p + D_2 \quad (\text{A.208})$$

$$(dt\mu)d + HT \xrightarrow{\lambda_{208}} (dt\mu)p + DT \quad (\text{A.209})$$

$$(dt\mu)d + HT \xrightarrow{\lambda_{209}} (dt\mu)t + HD \quad (\text{A.210})$$

$$(dt\mu)d + DT \xrightarrow{\lambda_{210}} (dt\mu)t + D_2 \quad (\text{A.211})$$

$$(dt\mu)d + T_2(\uparrow\uparrow) \xrightarrow{\lambda_{211}} (dt\mu)t + DT \quad (\text{A.212})$$

$$(dt\mu)d + T_2(\uparrow\downarrow) \xrightarrow{\lambda_{212}} (dt\mu)t + DT \quad (\text{A.213})$$

$$(dt\mu)t + H^\bullet \xrightarrow{\lambda_{213}} (dt\mu)d + T^\bullet \quad (\text{A.214})$$

$$(dt\mu)t + D^\bullet \xrightarrow{\lambda_{214}} (dt\mu)p + T^\bullet \quad (\text{A.215})$$

$$(dt\mu)t + H_2(\uparrow\uparrow) \xrightarrow{\lambda_{215}} (dt\mu)p + HT \quad (\text{A.216})$$

$$(dt\mu)t + H_2(\uparrow\downarrow) \xrightarrow{\lambda_{216}} (dt\mu)p + HT \quad (\text{A.217})$$

$$(dt\mu)t + HD \xrightarrow{\lambda_{217}} (dt\mu)p + DT \quad (\text{A.218})$$

$$(dt\mu)t + HD \xrightarrow{\lambda_{218}} (dt\mu)d + HT \quad (\text{A.219})$$

$$(dt\mu)t + D_2(\uparrow\uparrow) \xrightarrow{\lambda_{219}} (dt\mu)d + DT \quad (\text{A.220})$$

$$(dt\mu)t + D_2(\uparrow\downarrow) \xrightarrow{\lambda_{220}} (dt\mu)d + DT \quad (\text{A.221})$$

$$(dt\mu)t + HT \xrightarrow{\lambda_{221}} (dt\mu)p + T_2 \quad (\text{A.222})$$

$$(dt\mu)t + DT \xrightarrow{\lambda_{222}} (dt\mu)d + T_2 \quad (\text{A.223})$$

$$(tt\mu)p + D^\bullet \xrightarrow{\lambda_{223}} (tt\mu)t + H^\bullet \quad (\text{A.224})$$

$$(tt\mu)p + T^\bullet \xrightarrow{\lambda_{224}} (tt\mu)d + H^\bullet \quad (\text{A.225})$$

$$(tt\mu)p + HD \xrightarrow{\lambda_{225}} (tt\mu)d + H_2 \quad (\text{A.226})$$

$$(tt\mu)p + HT \xrightarrow{\lambda_{226}} (tt\mu)t + H_2 \quad (\text{A.227})$$

$$(tt\mu)p + D_2(\uparrow\uparrow) \xrightarrow{\lambda_{227}} (tt\mu)d + HD \quad (\text{A.228})$$

$$(tt\mu)p + D_2(\uparrow\downarrow) \xrightarrow{\lambda_{228}} (tt\mu)d + HD \quad (\text{A.229})$$

$$(tt\mu)p + DT \xrightarrow{\lambda_{229}} (tt\mu)d + HT \quad (\text{A.230})$$

$$(tt\mu)p + DT \xrightarrow{\lambda_{230}} (tt\mu)t + HD \quad (\text{A.231})$$

$$(tt\mu)p + T_2(\uparrow\uparrow) \xrightarrow{\lambda_{231}} (tt\mu)t + HT \quad (\text{A.232})$$

$$(tt\mu)p + T_2(\uparrow\downarrow) \xrightarrow{\lambda_{232}} (tt\mu)t + HT \quad (\text{A.233})$$

$$(tt\mu)d + H^\bullet \xrightarrow{\lambda_{233}} (tt\mu)p + D^\bullet \quad (\text{A.234})$$

$$(tt\mu)d + T^\bullet \xrightarrow{\lambda_{234}} (tt\mu)t + D^\bullet \quad (\text{A.235})$$

$$(tt\mu)d + H_2(\uparrow\uparrow) \xrightarrow{\lambda_{235}} (tt\mu)p + HD \quad (\text{A.236})$$

$$(tt\mu)d + H_2(\uparrow\downarrow) \xrightarrow{\lambda_{236}} (tt\mu)d + HD \quad (\text{A.237})$$

$$(tt\mu)d + HD \xrightarrow{\lambda_{237}} (tt\mu)p + D_2 \quad (\text{A.238})$$

$$(tt\mu)d + HT \xrightarrow{\lambda_{238}} (tt\mu)p + DT \quad (\text{A.239})$$

$$(tt\mu)d + HT \xrightarrow{\lambda_{239}} (tt\mu)t + HD \quad (\text{A.240})$$

$$(tt\mu)d + DT \xrightarrow{\lambda_{240}} (tt\mu)t + D_2 \quad (\text{A.241})$$

$$(tt\mu)d + T_2(\uparrow\uparrow) \xrightarrow{\lambda_{241}} (tt\mu)t + DT \quad (\text{A.242})$$

$$(tt\mu)d + T_2(\uparrow\downarrow) \xrightarrow{\lambda_{242}} (tt\mu)t + DT \quad (\text{A.243})$$

$$(tt\mu)t + H^\bullet \xrightarrow{\lambda_{243}} (tt\mu)p + T^\bullet \quad (\text{A.244})$$

$$(tt\mu)t + D^\bullet \xrightarrow{\lambda_{244}} (tt\mu)d + T^\bullet \quad (\text{A.245})$$

$$(tt\mu)t + H_2(\uparrow\uparrow) \xrightarrow{\lambda_{245}} (tt\mu)p + HT \quad (\text{A.246})$$

$$(tt\mu)t + H_2(\uparrow\downarrow) \xrightarrow{\lambda_{246}} (tt\mu)p + HT \quad (\text{A.247})$$

$$(tt\mu)t + HD \xrightarrow{\lambda_{247}} (tt\mu)p + DT \quad (\text{A.248})$$

$$(tt\mu)t + HD \xrightarrow{\lambda_{248}} (tt\mu)d + HT \quad (\text{A.249})$$

$$(tt\mu)t + D_2(\uparrow\uparrow) \xrightarrow{\lambda_{249}} (tt\mu)d + DT \quad (\text{A.250})$$

$$(tt\mu)t + D_2(\uparrow\downarrow) \xrightarrow{\lambda_{250}} (tt\mu)d + DT \quad (\text{A.251})$$

$$(tt\mu)t + HT \xrightarrow{\lambda_{251}} (tt\mu)p + T_2 \quad (\text{A.252})$$

and

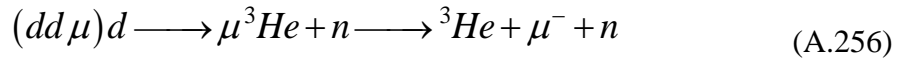
$$(tt\mu)t + DT \xrightarrow{\lambda_{252}} (tt\mu)d + T_2 \quad (\text{A.253})$$



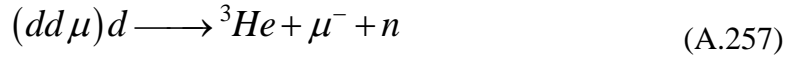
Regeneration reactions which “free” muons bound to helium nuclei will not be considered directly in the rate equations presented in this appendix



In actuality, regeneration reactions are not as simple as is shown in equations (A.254) and (A.255), rather they involve collisions with other particles and most often involve the transfer of a muon rather than actually “freeing” it. These reactions can be accounted for through the use of “effective” reactions rates. This means that reaction paths such as

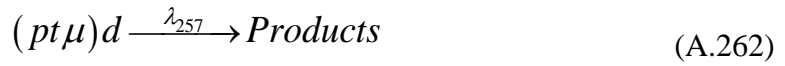


are considered to be the same as



with the rate constants being adjusted to account for both reaction paths. Rather than expressing a reaction rate constant for each reaction path leading to fusion, it is more convenient to express the individual reaction rates as the total fusion rate of a given

reactant times the probability that a specific path will be taken. The following reactions are expressed in this manner:



$$(dt\mu)p \xrightarrow{\lambda_{262}} Products \quad (A.267)$$

$$(dt\mu)d \xrightarrow{\lambda_{263}} Products \quad (A.268)$$

$$(dt\mu)t \xrightarrow{\lambda_{264}} Products \quad (A.269)$$

$$(tt\mu)p \xrightarrow{\lambda_{265}} Products \quad (A.270)$$

$$(tt\mu)d \xrightarrow{\lambda_{266}} Products \quad (A.271)$$

and

$$(tt\mu)t \xrightarrow{\lambda_{267}} Products \quad (A.272)$$

Defining effective sticking probability ( $\omega_i$ ) to be the probability that a muon is “stuck” to a nucleus during fusion and remains “stuck” until it decays,

$\omega_1$  = The effective probability of  $\mu^3He$  sticking during  $p\mu d$  fusion

$\omega_2$  = The effective probability of  $\mu^4He$  sticking during  $p\mu t$  fusion

$\omega_3$  = The effective probability of  $t\mu$  sticking during  $d\mu d$  fusion

$\omega_4$  = The effective probability of  $\mu^3He$  sticking during  $d\mu d$  fusion

$\omega_5$  = The effective probability of  $\mu^4He$  sticking during  $d\mu t$  fusion

$\omega_6$  = The effective probability of  $\mu^4He$  sticking during  $t\mu t$  fusion

From this it is possible to express the fusion rate constants in terms of their effective sticking probability. The sticking probability is not a constant; rather it is a function of the temperature and pressure in the reaction chamber. How much these values change with temperature and pressure is an ongoing area of research.[2; 3; 4]

Nuclear fusion occurs via the following reactions (note: although electrons are not always shown in the reaction equations presented in this section, gammas and electron-positron pairs which have reasonably high formation rates are).

$$(pd\mu)p \xrightarrow{\lambda_{253}(1-\omega_1)(1-\gamma_1)} \mu^- + {}^3He + H^\bullet \quad (A.273)$$

$$(pd\mu)p \xrightarrow{\lambda_{253}\omega_1} \gamma + \mu^3He + H^\bullet \quad (A.274)$$

$$(pd\mu)p \xrightarrow{\lambda_{253}(1-\omega_1)\gamma_1} \gamma + \mu + {}^3He + H^\bullet \quad (A.275)$$

$$(pd\mu)d \xrightarrow{\lambda_{254}(1-\omega_1)(1-\gamma_1)} \mu^- + {}^3He + D^\bullet \quad (A.276)$$

$$(pd\mu)d \xrightarrow{\lambda_{254}\omega_1} \gamma + \mu^3He + D^\bullet \quad (\text{A.277})$$

$$(pd\mu)d \xrightarrow{\lambda_{254}(1-\omega_1)\gamma_1} \gamma + \mu + {}^3He + D^\bullet \quad (\text{A.278})$$

$$(pd\mu)t \xrightarrow{\lambda_{255}(1-\omega_1)(1-\gamma_1)} \mu^- + {}^3He + T^\bullet \quad (\text{A.279})$$

$$(pd\mu)t \xrightarrow{\lambda_{255}\omega_1} \gamma + \mu^3He + T^\bullet \quad (\text{A.280})$$

$$(pd\mu)t \xrightarrow{\lambda_{255}(1-\omega_1)\gamma_1} \gamma + \mu + {}^3He + T^\bullet \quad (\text{A.281})$$

$$(pt\mu)p \xrightarrow{\lambda_{256}(1-\omega_2)(1-\gamma_2)(1-\rho_1)} \mu^- + {}^4He + H^\bullet \quad (\text{A.282})$$

$$(pt\mu)p \xrightarrow{\lambda_{256}\omega_2(1-\rho_1)} \gamma + \mu^4He + H^\bullet \quad (\text{A.283})$$

$$(pt\mu)p \xrightarrow{\lambda_{256}(1-\omega_2)\gamma_2(1-\rho_1)} \gamma + \mu + {}^4He + H^\bullet \quad (\text{A.284})$$

$$(pt\mu)p \xrightarrow{\lambda_{256}\omega_2\rho_1} e^+e^- + \mu^4He + H^\bullet \quad (\text{A.285})$$

$$(pt\mu)d \xrightarrow{\lambda_{257}(1-\omega_2)(1-\gamma_2)(1-\rho_1)} \mu^- + {}^4He + D^\bullet \quad (\text{A.286})$$

$$(pt\mu)d \xrightarrow{\lambda_{257}\omega_2(1-\rho_1)} \gamma + \mu^4He + D^\bullet \quad (\text{A.287})$$

$$(pt\mu)d \xrightarrow{\lambda_{257}(1-\omega_2)\gamma_2(1-\rho_1)} \gamma + \mu + {}^4He + D^\bullet \quad (\text{A.288})$$

$$(pt\mu)d \xrightarrow{\lambda_{257}\omega_2\rho_1} e^+e^- + \mu^4He + D^\bullet \quad (\text{A.289})$$

$$(pt\mu)t \xrightarrow{\lambda_{258}(1-\omega_2)(1-\gamma_2)(1-\rho_1)} \mu^- + {}^4He + T^\bullet \quad (\text{A.290})$$

$$(pt\mu)t \xrightarrow{\lambda_{258}\omega_2\gamma_2(1-\rho_1)} \gamma + \mu^4He + T^\bullet \quad (\text{A.291})$$

$$(pt\mu)t \xrightarrow{\lambda_{258}(1-\omega_2)\gamma_2(1-\rho_1)} \gamma + \mu + {}^4He + T^\bullet \quad (\text{A.292})$$

$$(pt\mu)t \xrightarrow{\lambda_{258}\rho_1} e^+e^- + \mu^4He + T^\bullet \quad (\text{A.293})$$

$$(dd\mu)p \xrightarrow{\lambda_{259}(1-\omega_3)(1-B_n)} t + p + H^\bullet + \mu^- \quad (\text{A.294})$$

$$(dd\mu)p \xrightarrow{\lambda_{259}\omega_3(1-B_n)} t\mu + p + H^\bullet \quad (\text{A.295})$$

$$(dd\mu)p \xrightarrow{\lambda_{259}(1-\omega_4)B_n} {}^3He + H^\bullet + n_1 + \mu^- \quad (\text{A.296})$$

$$(dd\mu)p \xrightarrow{\lambda_{259}\omega_4 B_n} \mu^3 He + H^\bullet + n_1 \quad (\text{A.297})$$

$$(dd\mu)d \xrightarrow{\lambda_{260}(1-\omega_3)(1-B_n)} t + p + D^\bullet + \mu^- \quad (\text{A.298})$$

$$(dd\mu)d \xrightarrow{\lambda_{260}\omega_3(1-B_n)} t\mu + p + D^\bullet \quad (\text{A.299})$$

$$(dd\mu)d \xrightarrow{\lambda_{260}(1-\omega_4)B_n} {}^3He + D^\bullet + n_1 + \mu^- \quad (\text{A.300})$$

$$(dd\mu)d \xrightarrow{\lambda_{260}\omega_4 B_n} \mu^3 He + D^\bullet + n_1 \quad (\text{A.301})$$

$$(dd\mu)t \xrightarrow{\lambda_{261}(1-\omega_3)(1-B_n)} t + p + T^\bullet + \mu^- \quad (\text{A.302})$$

$$(dd\mu)t \xrightarrow{\lambda_{261}\omega_3(1-B_n)} t\mu + p + T^\bullet \quad (\text{A.303})$$

$$(dd\mu)t \xrightarrow{\lambda_{261}(1-\omega_4)B_n} {}^3He + T^\bullet + n_1 + \mu^- \quad (\text{A.304})$$

$$(dd\mu)t \xrightarrow{\lambda_{261}\omega_4 B_n} \mu^3 He + T^\bullet + n_1 \quad (\text{A.305})$$

$$(dt\mu)p \xrightarrow{\lambda_{262}(1-\omega_5)} {}^4He + H^\bullet + n_2 + \mu^- \quad (\text{A.306})$$

$$(dt\mu)p \xrightarrow{\lambda_{262}\omega_5} \mu^4He + H^\bullet + n_2 \quad (\text{A.307})$$

$$(dt\mu)d \xrightarrow{\lambda_{263}(1-\omega_5)} {}^4He + D^\bullet + n_2 + \mu^- \quad (\text{A.308})$$

$$(dt\mu)d \xrightarrow{\lambda_{263}\omega_5} \mu^4He + D^\bullet + n_2 \quad (\text{A.309})$$

$$(dt\mu)t \xrightarrow{\lambda_{264}(1-\omega_5)} {}^4He + T^\bullet + n_2 + \mu^- \quad (\text{A.310})$$

$$(dt\mu)t \xrightarrow{\lambda_{264}\omega_5} \mu^4He + T^\bullet + n_2 \quad (\text{A.311})$$

$$(tt\mu)p \xrightarrow{\lambda_{265}(1-\omega_6)} {}^4He + H^\bullet + 2n_2 + \mu^- \quad (\text{A.312})$$

$$(tt\mu)p \xrightarrow{\lambda_{265}\omega_6} \mu^4He + H^\bullet + 2n_2 \quad (\text{A.313})$$

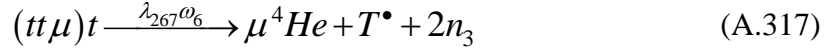
$$(tt\mu)d \xrightarrow{\lambda_{266}(1-\omega_6)} {}^4He + D^\bullet + 2n_2 + \mu^- \quad (\text{A.314})$$

$$(tt\mu)d \xrightarrow{\lambda_{266}\omega_6} \mu^4He + D^\bullet + 2n_2 \quad (\text{A.315})$$

$$(tt\mu)t \xrightarrow{\lambda_{267}(1-\omega_6)} {}^4He + T^\bullet + 2n_3 + \mu^- \quad (\text{A.316})$$



and



Reactions A.273 through A.317 can be used to determine the fusion rate of specific paths.  $\gamma_i$  represents the probability of gamma formation.  $\rho_i$  is the probability of an electron positron pair ( $e^-e^+$ ) forming.  $dud$  fusion can follow a path which produces tritium and a proton, or which produces  $^3He$  and a neutron. The branching ration for these two paths is the same as it is for conventional fusion. The probability ( $B_n$ ) of the  $^3He$  and neutron path being followed is about 58%. [5] The rate constants shown in the following equations assume the non-reacting hydrogen to have negligible impact on the sticking probability, the probability of electron positron pair ( $e^-e^+$ ) production and the probability of gamma production.

From the reaction equations presented in this appendix, it is possible to derive kinetic rate equations for the various products and intermediates:

$$\begin{aligned} \frac{\partial[p\mu]}{\partial t} = & \lambda_1[H^\bullet][\mu^-] + \lambda_2[H_2][\mu^-] + \lambda_3[HD][\mu^-] + \lambda_4[HT][\mu^-] - \lambda_0[p\mu] \\ & - \lambda_{13}[p\mu][D^\bullet] - \lambda_{14}[p\mu][T^\bullet] - \lambda_{15}[p\mu][HD] - \lambda_{16}[p\mu][HT] \\ & - \lambda_{17}[p\mu][D_2] - \lambda_{18}[p\mu][DT] - \lambda_{19}[p\mu][DT] - \lambda_{20}[p\mu][T_2] \\ & - \lambda_{37}[p\mu][H_2(\uparrow\uparrow)] - \lambda_{38}[p\mu][H_2(\uparrow\downarrow)] - \lambda_{39}[p\mu][HD] \\ & - \lambda_{40}[p\mu][HD] - \lambda_{41}[p\mu][D_2(\uparrow\uparrow)] - \lambda_{42}[p\mu][D_2(\uparrow\downarrow)] \\ & - \lambda_{43}[p\mu][HT] - \lambda_{44}[p\mu][HT] - \lambda_{45}[p\mu][DT] - \lambda_{46}[p\mu][DT] \\ & - \lambda_{47}[p\mu][T_2(\uparrow\uparrow)] - \lambda_{48}[p\mu][T_2(\uparrow\downarrow)] \end{aligned} \quad (\text{A.318})$$

$$\begin{aligned}
\frac{\partial[d\mu]}{\partial t} = & \lambda_5[D^\bullet][\mu^-] + \lambda_6[HD][\mu^-] + \lambda_7[D_2][\mu^-] + \lambda_8[DT][\mu^-] - \lambda_0[d\mu] \\
& - \lambda_{21}[d\mu][H^\bullet] - \lambda_{22}[d\mu][T^\bullet] - \lambda_{23}[d\mu][H_2] - \lambda_{24}[d\mu][HD] \\
& - \lambda_{25}[d\mu][HT] - \lambda_{26}[d\mu][HT] - \lambda_{27}[d\mu][DT] - \lambda_{28}[d\mu][T_2] \\
& - \lambda_{49}[d\mu][H_2(\uparrow\uparrow)] - \lambda_{50}[d\mu][H_2(\uparrow\downarrow)] - \lambda_{51}[d\mu][HD] \\
& - \lambda_{52}[d\mu][HD] - \lambda_{53}[d\mu][D_2(\uparrow\uparrow)] - \lambda_{54}[d\mu][D_2(\uparrow\downarrow)] \\
& - \lambda_{55}[d\mu][HT] - \lambda_{56}[d\mu][HT] - \lambda_{57}[d\mu][DT] - \lambda_{58}[d\mu][DT] \\
& - \lambda_{59}[d\mu][T_2(\uparrow\uparrow)] - \lambda_{60}[d\mu][T_2(\uparrow\downarrow)]
\end{aligned} \tag{A.319}$$

$$\begin{aligned}
\frac{\partial[t\mu]}{\partial t} = & \lambda_9[T^\bullet][\mu^-] + \lambda_{10}[HT][\mu^-] + \lambda_{11}[DT][\mu^-] + \lambda_{12}[T_2][\mu^-] - \lambda_0[d\mu] \\
& - \lambda_{29}[t\mu][H^\bullet] - \lambda_{30}[t\mu][D^\bullet] - \lambda_{31}[t\mu][H_2] - \lambda_{32}[t\mu][H_2] \\
& - \lambda_{33}[t\mu][HD] - \lambda_{34}[t\mu][D_2] - \lambda_{35}[t\mu][HT] - \lambda_{36}[t\mu][DT] \\
& - \lambda_{61}[t\mu][H_2(\uparrow\uparrow)] - \lambda_{62}[t\mu][H_2(\uparrow\downarrow)] - \lambda_{63}[t\mu][HD] - \lambda_{64}[t\mu][HD] \\
& - \lambda_{65}[t\mu][D_2(\uparrow\uparrow)] - \lambda_{66}[t\mu][D_2(\uparrow\downarrow)] - \lambda_{67}[t\mu][HT] - \lambda_{68}[t\mu][HT] \\
& - \lambda_{69}[t\mu][DT] - \lambda_{70}[t\mu][DT] - \lambda_{71}[t\mu][T_2(\uparrow\uparrow)] - \lambda_{72}[t\mu][T_2(\uparrow\downarrow)] \\
& + \lambda_{275}[(dd\mu)p] + \lambda_{279}[(dd\mu)d] + \lambda_{283}[(dd\mu)t]
\end{aligned} \tag{A.320}$$

$$\begin{aligned}
\frac{\partial[(pp\mu)p]}{dt} = & \lambda_{37}[p\mu][H_2(\uparrow\uparrow)] + \lambda_{38}[p\mu][H_2(\uparrow\downarrow)] - \lambda_0[(pp\mu)p] \\
& - \lambda_{73}[(pp\mu)p][D^\bullet] - \lambda_{74}[(pp\mu)p][T^\bullet] - \lambda_{75}[(pp\mu)p][HD] \\
& - \lambda_{76}[(pp\mu)p][HT] - \lambda_{77}[(pp\mu)p][D_2(\uparrow\uparrow)] \\
& - \lambda_{78}[(pp\mu)p][D_2(\uparrow\downarrow)] - (\lambda_{79} + \lambda_{80})[(pp\mu)p][DT] \\
& - \lambda_{81}[(pp\mu)p][T_2(\uparrow\uparrow)] - \lambda_{82}[(pp\mu)p][T_2(\uparrow\downarrow)]
\end{aligned} \tag{A.321}$$

$$\begin{aligned}
\frac{\partial[(pp\mu)d]}{dt} = & \lambda_{39}[p\mu][HD] - \lambda_0[(pp\mu)d] - \lambda_{83}[(pp\mu)d][H^\bullet] \\
& - \lambda_{84}[(pp\mu)d][T^\bullet] - \lambda_{85}[(pp\mu)d][H_2(\uparrow\uparrow)] \\
& - \lambda_{86}[(pp\mu)d][H_2(\uparrow\downarrow)] - \lambda_{87}[(pp\mu)d][HD] \\
& - (\lambda_{88} + \lambda_{89})[(pp\mu)d][HT] - \lambda_{90}[(pp\mu)d][DT] \\
& - \lambda_{91}[(pp\mu)d][T_2(\uparrow\uparrow)] - \lambda_{92}[(pp\mu)d][T_2(\uparrow\downarrow)]
\end{aligned} \tag{A.322}$$

$$\begin{aligned}
\frac{\partial[(pp\mu)t]}{dt} = & \lambda_{43}[p\mu][HT] - \lambda_0[(pp\mu)t] - \lambda_{93}[(pp\mu)t][H^\bullet] \\
& - \lambda_{94}[(pp\mu)t][D^\bullet] - \lambda_{95}[(pp\mu)t][H_2(\uparrow\uparrow)] \\
& - \lambda_{96}[(pp\mu)t][H_2(\uparrow\downarrow)] - (\lambda_{97} + \lambda_{98})[(pp\mu)t][HD] \\
& - \lambda_{99}[(pp\mu)t][D_2(\uparrow\uparrow)] - \lambda_{100}[(pp\mu)t][D_2(\uparrow\downarrow)] \\
& - \lambda_{101}[(pp\mu)t][HT] - \lambda_{102}[(pp\mu)t][DT]
\end{aligned} \tag{A.323}$$

$$\begin{aligned}
\frac{\partial[(pd\mu)p]}{dt} = & \lambda_{40}[p\mu][HD] + \lambda_{49}[d\mu][H_2(\uparrow\uparrow)] + \lambda_{50}[d\mu][H_2(\uparrow\downarrow)] \\
& - \lambda_0[(pd\mu)p] - \lambda_{103}[(pd\mu)p][D^\bullet] - \lambda_{104}[(pd\mu)p][T^\bullet] \\
& - \lambda_{105}[(pd\mu)p][HD] - \lambda_{106}[(pd\mu)p][HT] \\
& - \lambda_{107}[(pd\mu)p][D_2(\uparrow\uparrow)] - \lambda_{108}[(pd\mu)p][D_2(\uparrow\downarrow)] \\
& - (\lambda_{109} + \lambda_{110})[(pd\mu)p][DT] - \lambda_{111}[(pd\mu)p][T_2(\uparrow\uparrow)] \\
& - \lambda_{112}[(pd\mu)p][T_2(\uparrow\downarrow)] - \lambda_{253}[(pd\mu)p]
\end{aligned} \tag{A.324}$$

$$\begin{aligned}
\frac{\partial[(pd\mu)d]}{dt} = & \lambda_{41}[p\mu][D_2(\uparrow\uparrow)] + \lambda_{42}[p\mu][D_2(\uparrow\downarrow)] + \lambda_{51}[d\mu][HD] \\
& - \lambda_0[(pd\mu)d] - \lambda_{113}[(pd\mu)d][H^\bullet] - \lambda_{114}[(pd\mu)d][T^\bullet] \\
& - \lambda_{115}[(pd\mu)d][H_2(\uparrow\uparrow)] - \lambda_{116}[(pd\mu)d][H_2(\uparrow\downarrow)] \\
& - \lambda_{117}[(pd\mu)d][HD] - (\lambda_{118} + \lambda_{119})[(pd\mu)d][HT] \\
& - \lambda_{120}[(pd\mu)d][DT] - \lambda_{121}[(pd\mu)d][T_2(\uparrow\uparrow)] \\
& - \lambda_{122}[(pd\mu)d][T_2(\uparrow\downarrow)] - \lambda_{254}[(pd\mu)d]
\end{aligned} \tag{A.325}$$

$$\begin{aligned}
\frac{\partial[(pd\mu)t]}{dt} = & \lambda_{45}[p\mu][DT] + \lambda_{55}[d\mu][HT] - \lambda_0[(pd\mu)t] - \lambda_{123}[(pd\mu)t][H^\bullet] \\
& - \lambda_{124}[(pd\mu)t][D^\bullet] - \lambda_{125}[(pd\mu)t][H_2(\uparrow\uparrow)] \\
& - \lambda_{126}[(pd\mu)t][H_2(\uparrow\downarrow)] - (\lambda_{127} + \lambda_{128})[(pd\mu)t][HD] \\
& - \lambda_{129}[(pd\mu)t][D_2(\uparrow\uparrow)] - \lambda_{130}[(pd\mu)t][D_2(\uparrow\downarrow)] \\
& - \lambda_{131}[(pd\mu)t][HT] - \lambda_{132}[(pd\mu)t][DT] - \lambda_{255}[(pd\mu)t]
\end{aligned} \tag{A.326}$$

$$\begin{aligned}
\frac{\partial[(pt\mu)p]}{dt} = & \lambda_{44}[p\mu][HT] + \lambda_{61}[t\mu][H_2(\uparrow\uparrow)] + \lambda_{62}[t\mu][H_2(\uparrow\downarrow)] \\
& - \lambda_0[(pt\mu)p] - \lambda_{133}[(pt\mu)p][D^\bullet] - \lambda_{134}[(pt\mu)p][T^\bullet] \\
& - \lambda_{135}[(pt\mu)p][HD] - \lambda_{136}[(pt\mu)p][HT] \\
& - \lambda_{137}[(pt\mu)p][D_2(\uparrow\uparrow)] - \lambda_{138}[(pt\mu)p][D_2(\uparrow\downarrow)] \\
& - (\lambda_{139} + \lambda_{140})[(pt\mu)p][DT] - \lambda_{141}[(pt\mu)p][T_2(\uparrow\uparrow)] \\
& - \lambda_{142}[(pt\mu)p][T_2(\uparrow\downarrow)] - \lambda_{256}[(pt\mu)p]
\end{aligned} \tag{A.327}$$

$$\begin{aligned}
\frac{\partial[(pt\mu)d]}{dt} = & \lambda_{46}[p\mu][DT] + \lambda_{63}[t\mu][HD] - \lambda_0[(pt\mu)d] - \\
& \lambda_{143}[(pt\mu)d][H^\bullet] - \lambda_{144}[(pt\mu)d][T^\bullet] \\
& - \lambda_{145}[(pt\mu)d][H_2(\uparrow\uparrow)] - \lambda_{146}[(pt\mu)d][H_2(\uparrow\downarrow)] \\
& - \lambda_{147}[(pt\mu)d][HD] - (\lambda_{148} + \lambda_{149})[(pt\mu)d][HT] \\
& - \lambda_{150}[(pt\mu)d][DT] - \lambda_{151}[(pt\mu)d][T_2(\uparrow\uparrow)] \\
& - \lambda_{152}[(pt\mu)d][T_2(\uparrow\downarrow)] - \lambda_{257}[(pt\mu)d]
\end{aligned} \tag{A.328}$$

$$\begin{aligned}
\frac{\partial[(pt\mu)t]}{dt} = & \lambda_{47}[p\mu][T_2(\uparrow\uparrow)] + \lambda_{48}[p\mu][T_2(\uparrow\downarrow)] + \lambda_{67}[t\mu][HT] \\
& - \lambda_0[(pt\mu)t] - \lambda_{153}[(pt\mu)t][H^\bullet] - \lambda_{154}[(pt\mu)t][D^\bullet] \\
& - \lambda_{155}[(pt\mu)t][H_2(\uparrow\uparrow)] - \lambda_{156}[(pt\mu)t][H_2(\uparrow\downarrow)] \\
& - (\lambda_{157} + \lambda_{158})[(pt\mu)t][HD] - \lambda_{159}[(pt\mu)t][D_2(\uparrow\uparrow)] \\
& - \lambda_{160}[(pt\mu)t][D_2(\uparrow\downarrow)] - \lambda_{161}[(pt\mu)t][HT] \\
& - \lambda_{162}[(pt\mu)t][DT] - \lambda_{258}[(pt\mu)t]
\end{aligned} \tag{A.329}$$

$$\begin{aligned}
\frac{\partial[(dd\mu)p]}{dt} = & \lambda_{52}[d\mu][HD] + -\lambda_0[(dd\mu)p] - \lambda_{163}[(dd\mu)p][D^\bullet] \\
& - \lambda_{164}[(dd\mu)p][T^\bullet] - \lambda_{165}[(dd\mu)p][HD] \\
& - \lambda_{166}[(dd\mu)p][HT] - \lambda_{167}[(dd\mu)p][D_2(\uparrow\uparrow)] \\
& - \lambda_{168}[(dd\mu)p][D_2(\uparrow\downarrow)] - (\lambda_{169} + \lambda_{170})[(dd\mu)p][DT] \\
& - \lambda_{171}[(dd\mu)p][T_2(\uparrow\uparrow)] - \lambda_{172}[(dd\mu)p][T_2(\uparrow\downarrow)] \\
& - \lambda_{259}[(dd\mu)p]
\end{aligned} \tag{A.330}$$

$$\begin{aligned}
\frac{\partial[(dd\mu)d]}{dt} = & \lambda_{53}[d\mu][D_2(\uparrow\uparrow)] + \lambda_{54}[d\mu][D_2(\uparrow\downarrow)] - \lambda_0[(dd\mu)d] \\
& - \lambda_{173}[(dd\mu)d][H^\bullet] - \lambda_{174}[(dd\mu)d][T^\bullet] \\
& - \lambda_{175}[(dd\mu)d][H_2(\uparrow\uparrow)] - \lambda_{176}[(dd\mu)d][H_2(\uparrow\downarrow)] \\
& - \lambda_{177}[(dd\mu)d][HD] - (\lambda_{118} + \lambda_{119})[(dd\mu)d][HT] \\
& - \lambda_{120}[(dd\mu)d][DT] - \lambda_{121}[(dd\mu)d][T_2(\uparrow\uparrow)] \\
& - \lambda_{122}[(dd\mu)d][T_2(\uparrow\downarrow)] - \lambda_{260}[(dd\mu)d]
\end{aligned} \tag{A.331}$$

$$\begin{aligned}
\frac{\partial[(dd\mu)t]}{dt} = & \lambda_{57}[d\mu][DT] - \lambda_0[(dd\mu)t] - \lambda_{183}[(dd\mu)t][H^\bullet] \\
& - \lambda_{184}[(dd\mu)t][D^\bullet] - \lambda_{185}[(dd\mu)t][H_2(\uparrow\uparrow)] \\
& - \lambda_{186}[(dd\mu)t][H_2(\uparrow\downarrow)] - (\lambda_{187} + \lambda_{188})[(dd\mu)t][HD] \\
& - \lambda_{189}[(dd\mu)t][D_2(\uparrow\uparrow)] - \lambda_{190}[(dd\mu)t][D_2(\uparrow\downarrow)] \\
& - \lambda_{191}[(dd\mu)t][HT] - \lambda_{192}[(dd\mu)t][DT] - \lambda_{261}[(dd\mu)t]
\end{aligned} \tag{A.332}$$

$$\begin{aligned}
\frac{\partial[(dt\mu)p]}{dt} = & \lambda_{56}[d\mu][HT] + \lambda_{64}[t\mu][HD] - \lambda_0[(dt\mu)p] - \lambda_{193}[(dt\mu)p][D^\bullet] \\
& - \lambda_{194}[(dt\mu)p][T^\bullet] - \lambda_{195}[(dt\mu)p][HD] - \lambda_{196}[(dt\mu)p][HT] \\
& - \lambda_{197}[(dt\mu)p][D_2(\uparrow\uparrow)] - \lambda_{198}[(dt\mu)p][D_2(\uparrow\downarrow)] \\
& - (\lambda_{199} + \lambda_{200})[(dt\mu)p][DT] - \lambda_{201}[(dt\mu)p][T_2(\uparrow\uparrow)] \\
& - \lambda_{202}[(dt\mu)p][T_2(\uparrow\downarrow)] - \lambda_{262}[(dt\mu)p]
\end{aligned} \tag{A.333}$$

$$\begin{aligned}
\frac{\partial[(dt\mu)d]}{dt} = & \lambda_{58}[d\mu][DT] + \lambda_{65}[t\mu][D_2(\uparrow\uparrow)] + \lambda_{65}[t\mu][D_2(\uparrow\uparrow)] \\
& - \lambda_0[(dt\mu)d] - \lambda_{203}[(dt\mu)d][H^\bullet] - \lambda_{204}[(dt\mu)d][T^\bullet] \\
& - \lambda_{205}[(dt\mu)d][H_2(\uparrow\uparrow)] - \lambda_{206}[(dt\mu)d][H_2(\uparrow\downarrow)] \\
& - \lambda_{207}[(dt\mu)d][HD] - (\lambda_{208} + \lambda_{209})[(dt\mu)d][HT] \\
& - \lambda_{210}[(dt\mu)d][DT] - \lambda_{211}[(dt\mu)d][T_2(\uparrow\uparrow)] \\
& - \lambda_{212}[(dt\mu)d][T_2(\uparrow\downarrow)] - \lambda_{263}[(dt\mu)d]
\end{aligned} \tag{A.334}$$

$$\begin{aligned}
\frac{\partial[(dt\mu)t]}{dt} = & \lambda_{59}[d\mu][T_2(\uparrow\uparrow)] + \lambda_{60}[d\mu][T_2(\uparrow\downarrow)] + \lambda_{69}[t\mu][DT] - \lambda_0[(dt\mu)t] \\
& - \lambda_{213}[(dt\mu)t][H^\bullet] - \lambda_{214}[(dt\mu)t][D^\bullet] - \lambda_{215}[(dt\mu)t][H_2(\uparrow\uparrow)] \\
& - \lambda_{216}[(dt\mu)t][H_2(\uparrow\downarrow)] - (\lambda_{217} + \lambda_{218})[(dt\mu)t][HD] \\
& - \lambda_{219}[(dt\mu)t][D_2(\uparrow\uparrow)] - \lambda_{220}[(dt\mu)t][D_2(\uparrow\downarrow)] \\
& - \lambda_{221}[(dt\mu)t][HT] - \lambda_{222}[(dt\mu)t][DT] - \lambda_{264}[(dt\mu)t]
\end{aligned} \tag{A.335}$$

$$\begin{aligned}
\frac{\partial[(tt\mu)p]}{dt} = & \lambda_{68}[t\mu][HT] - \lambda_0[(tt\mu)p] - \lambda_{223}[(tt\mu)p][D^\bullet] \\
& - \lambda_{224}[(tt\mu)p][T^\bullet] - \lambda_{225}[(tt\mu)p][HD] \\
& - \lambda_{226}[(tt\mu)p][HT] - \lambda_{227}[(tt\mu)p][D_2(\uparrow\uparrow)] \\
& - \lambda_{228}[(tt\mu)p][D_2(\uparrow\downarrow)] - (\lambda_{229} + \lambda_{230})[(tt\mu)p][DT] \\
& - \lambda_{231}[(tt\mu)p][T_2(\uparrow\uparrow)] - \lambda_{232}[(tt\mu)p][T_2(\uparrow\downarrow)] \\
& - \lambda_{265}[(tt\mu)p]
\end{aligned} \tag{A.336}$$

$$\begin{aligned}
\frac{\partial[(tt\mu)d]}{dt} = & \lambda_{70}[t\mu][DT] - \lambda_0[(tt\mu)d] - \lambda_{233}[(tt\mu)d][H^\bullet] \\
& - \lambda_{234}[(tt\mu)d][T^\bullet] - \lambda_{235}[(tt\mu)d][H_2(\uparrow\uparrow)] \\
& - \lambda_{236}[(tt\mu)d][H_2(\uparrow\downarrow)] - \lambda_{237}[(tt\mu)d][HD] \\
& - (\lambda_{238} + \lambda_{239})[(tt\mu)d][HT] - \lambda_{240}[(tt\mu)d][DT] \\
& - \lambda_{241}[(tt\mu)d][T_2(\uparrow\uparrow)] - \lambda_{242}[(tt\mu)d][T_2(\uparrow\downarrow)] \\
& - \lambda_{266}[(tt\mu)d]
\end{aligned} \tag{A.337}$$

$$\begin{aligned}
\frac{\partial[(tt\mu)t]}{dt} = & \lambda_{71}[t\mu][T_2(\uparrow\uparrow)] + \lambda_{72}[t\mu][T_2(\uparrow\downarrow)] - \lambda_0[(tt\mu)t] \\
& - \lambda_{243}[(tt\mu)t][H^\bullet] - \lambda_{244}[(tt\mu)t][D^\bullet] \\
& - \lambda_{245}[(tt\mu)t][H_2(\uparrow\uparrow)] - \lambda_{246}[(tt\mu)t][H_2(\uparrow\downarrow)] \\
& - (\lambda_{247} + \lambda_{248})[(tt\mu)t][HD] - \lambda_{249}[(tt\mu)t][D_2(\uparrow\uparrow)] \\
& - \lambda_{250}[(tt\mu)t][D_2(\uparrow\downarrow)] - \lambda_{251}[(tt\mu)t][HT] \\
& - \lambda_{252}[(tt\mu)t][DT] - \lambda_{267}[(tt\mu)t]
\end{aligned} \tag{A.338}$$

$$\frac{d[n_1]}{dt} = \lambda_{259}B_n[(dd\mu)p] + \lambda_{260}B_n[(dd\mu)d] + \lambda_{261}B_n[(dd\mu)t] \tag{A.339}$$

$$\frac{d[n_2]}{dt} = \lambda_{262}[(dt\mu)p] + \lambda_{263}[(dt\mu)d] + \lambda_{264}[(dt\mu)t] \tag{A.340}$$

$$\frac{d[n_3]}{dt} = 2\{\lambda_{265}[(tt\mu)p] + \lambda_{266}[(tt\mu)d] + \lambda_{267}[(tt\mu)t]\} \tag{A.341}$$



and

$$\begin{aligned}
\frac{d[\mu^-]}{dt} = & -[\mu^-] \left\{ \lambda_0 + \lambda_1[H^\bullet] + \lambda_2[H_2] + \lambda_3[HD] + \lambda_4[HT] + \lambda_5[D^\bullet] \right. \\
& + \lambda_6[HD] + \lambda_7[D_2] + \lambda_8[DT] + \lambda_9[T^\bullet] + \lambda_{10}[HT] + \lambda_{11}[DT] + \lambda_{12}[T_2] \left. \right\} \\
& + \lambda_{253}(1-\omega_1)[(pd\mu)p] + \lambda_{254}(1-\omega_1)[(pd\mu)d] \\
& + \lambda_{255}(1-\omega_1)[(pd\mu)t] + \lambda_{256}(1-\omega_2)(1-\rho_1)[(pt\mu)p] \\
& + \lambda_{257}(1-\omega_2)(1-\rho_1)[(pt\mu)d] + \lambda_{258}(1-\omega_2)(1-\rho_1)[(pt\mu)p] \\
& + \left\{ \lambda_{259}(1-\omega_3)(1-B_n) + \lambda_{259}(1-\omega_4)B_n \right\} [(dd\mu)p] \\
& + \left\{ \lambda_{260}(1-\omega_3)(1-B_n) + \lambda_{260}(1-\omega_4)B_n \right\} [(dd\mu)d] \\
& + \left\{ \lambda_{261}(1-\omega_3)(1-B_n) + \lambda_{261}(1-\omega_4)B_n \right\} [(dd\mu)t] \\
& + \lambda_{262}(1-\omega_5)[(dt\mu)p] + \lambda_{263}(1-\omega_5)[(dt\mu)d] + \lambda_{264}(1-\omega_5)[(dt\mu)t] \\
& + \lambda_{265}(1-\omega_6)[(tt\mu)p] + \lambda_{266}(1-\omega_6)[(tt\mu)d] + \lambda_{267}(1-\omega_6)[(tt\mu)t]
\end{aligned} \tag{A.342}$$

The probability density of free muons  $[\mu^-]$  in the system is equal to the concentration of muons input in the chamber minus the probability the muon has decayed or is bound to a molecule in the chamber. This is written as

$$\begin{aligned}
[\mu^-] = & [\mu_{total}^-] - [p\mu] - [d\mu] - [t\mu] - [(pp\mu)p] - [(pp\mu)d] - [(pp\mu)t] \\
& - [(pd\mu)p] - [(pd\mu)d] - [(pd\mu)t] - [(pt\mu)p] - [(pt\mu)d] \\
& - [(pt\mu)t] - [(pt\mu)p] - [(pt\mu)d] - [(pt\mu)t] - [(dd\mu)p] \\
& - [(dd\mu)d] - [(dd\mu)t] - [(dt\mu)p] - [(dt\mu)d] - [(dt\mu)t] \\
& - [{}^3\text{He}\mu] - [{}^4\text{He}\mu]
\end{aligned} \tag{A.343}$$

The total amount of muons in a reaction chamber can be expressed as

$$\left[ \mu_{total}^{-} \right] = \left[ \mu_0^{-} \right] e^{-\lambda_0 t} \quad (\text{A.344})$$

where  $\mu_0^{-}$  is the initial concentration of negative muons.

Neglected from all of the equations in this appendix are the effects of “muon scavenging.” Muon scavenging, as it relates to muon-catalyzed fusion, refers to free muons binding to elements other than hydrogen, and muons bound to hydrogen being transferred to other elements. If significant quantities of helium are present in the reaction chamber, regardless if the helium is a product of fusion, or a decay product of tritium, then muon scavenging needs to be added to the rate equations. Muon scavenging also needs to be considered if there is a significant probability of muonic molecular molecules interacting with chamber walls.

Most of the reaction rate constants presented in this appendix have been looked at computationally, experimentally or both, however, the accuracy to which the values are known varies greatly. Some possible reactions which are not believed to occur in any significant amount (*e.g.*,  $dd\mu \rightarrow T^{\bullet} + p\mu$ ) have been omitted. Some of the reactions listed (*e.g.*,  $t\mu \rightarrow d\mu$ ) occur so seldom that they can be neglected. The reaction rate constants that have the greatest need for further study are those that form tri-atomic muonic molecules. It has been shown that the non-fusing hydrogen in tri-atomic muonic molecules has a significant impact on the formation rate of these molecules.[6; 7] The mass of the non-fusing atom affects the separation distance, vibrations, and stability of the fusing atoms, and as a result affects the fusion rate.

## References

- [1] H. E. Rafelski and B. Muller, "Density Dependent Stopping Power and Muon Sticking in Muon-Catalyzed D-T Fusion," in *Muon-Catalyzed Fusion*, Sanibel Island, 1989.
- [2] W. H. Breunlich, P. Kammel, J. S. Cohen and M. Leon, "Muon-Catalyzed Fusion," *Annual Review of Nuclear and Particle Science*, vol. 39, pp. 311-355, 1989.
- [3] K. Nagamine, *Introductory Muon Science*, Cambridge: Cambridge University Press, 2003.
- [4] M. Leon, "Theory of Muonic Molecule Formation: Survey of Progress and Open Questions," *Hyperfine Interactions*, vol. 82, pp. 151-160, 1993.
- [5] N. Kawamura, K. Ishida, T. Matsuzaki, H. Imao and K. Nagamine, "Muonic Molecule Formation in Muon-Catalyzed Fusion," in *Advanced Science Research Symposium 2009 Positron, Muon and other exotic particle beams for materials and atomic/molecular sciences (ASR2009)*, vol. 225 no. 1, Tokai, 2010.
- [6] S. E. Jones, A. Anderson, A. J. Caffrey, C. d. Van Sicien, K. D. Watts, J. N. Bradbury, J. S. Cohen, p. A. M. Gram, M. Leon, H. R. Maltrud and M. A. Paciotti, "Observation of Unexpected Density Effects in Muon-Catalyzed d-t Fusion," *Physical Review Letters*, vol. 56, pp. 588-591, 1986.
- [7] A. Adamczak and M. P. Faifman, "Resonant dtμ Formation In Condensed Hydrogen Isotopes," *Physical Review A*, vol. 72, pp. 052501:1-14, 2005.

## Appendix B. Equilibrium Concentration of Hydrogen Isotopes

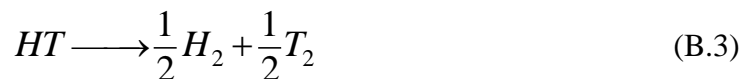
In order to determine the relative amounts of various hydrogen molecules which will be present in a reaction chamber at a given temperature and pressure, it is necessary to know the equilibrium constants ( $K_{eq}$ ) of the isotopes involved. Equilibrium constants are most often calculated from the Gibb's free energy ( $\Delta G$ ) by the equation:[1; 2]

$$\Delta G = -RT \ln K_{eq} \quad (B.1)$$

where  $R = 8.3144$  J/mole K and  $T$  is the temperature in Kelvin.

Gibb's free energy can be determined from partition functions.[3] For non-tritium containing hydrogen molecules these values have been published in the *Journal of Physical and Chemical Reference Data*. [4]

Protium ( $P$ ), deuterium ( $D$ ), and tritium ( $T$ ) combine to form a variety of hydrogen molecules. In order to determine the equilibrium concentration of these molecules it is necessary to consider the reactions:





and



Using reaction equations B.1 to B.6 it is possible to derive the following equilibrium equations:

$$K_{C,H} \equiv \frac{C_H}{\sqrt{C_{H_2}}} \quad (\text{B.8})$$

$$K_{C,D} \equiv \frac{C_D}{\sqrt{C_{D_2}}} \quad (\text{B.9})$$

$$K_{C,T} \equiv \frac{C_T}{\sqrt{C_{T_2}}} \quad (\text{B.10})$$

$$K_{C,HD} \equiv \frac{\sqrt{C_H C_D}}{C_{HD}} \quad (\text{B.11})$$

$$K_{C,HT} \equiv \frac{\sqrt{C_H C_T}}{C_{HT}} \quad (\text{B.12})$$

and

$$K_{C,DT} \equiv \frac{\sqrt{C_D C_T}}{C_{DT}} \quad (\text{B.13})$$

These equations do not include all possible molecules that form; however, they do include all of the molecules that occur in quantities that can affect normal muon-catalyzed fusion reaction conditions.[1; 5:20]

From the initial concentrations of  $H_2$ ,  $D_2$ , and  $T_2$  the following can be derived.

$$C_{H_2} = C_{i,H} - \frac{1}{2}C_H - \frac{1}{2}C_{HD} - \frac{1}{2}C_{HT} \quad (\text{B.14})$$

$$C_{D_2} = C_{i,D} - \frac{1}{2}C_D - \frac{1}{2}C_{HD} - \frac{1}{2}C_{DT} \quad (\text{B.15})$$

$$C_{T_2} = C_{i,T} - \frac{1}{2}C_T - \frac{1}{2}C_{HT} - \frac{1}{2}C_{DT} \quad (\text{B.16})$$

Where  $C_H$ ,  $C_D$ ,  $C_T$ ,  $C_{HD}$ ,  $C_{HT}$ , and  $C_{DT}$  represent equilibrium concentrations and  $C_{i,H}$ ,  $C_{i,D}$ , and  $C_{i,T}$  represent the initial molecular concentrations of  $H_2$ ,  $D_2$ , and  $T_2$  respectively.

$K_C$  is the molar ( $n$ ) equilibrium constant and can be calculated for the equilibrium pressure constant  $K_p$ . [6:169-179] Assuming ideal gas behavior,  $K_p = K_{eq}$ .

$$K_C = P^{-\Delta n} K_{eq} \quad (\text{B.17})$$

At temperatures less than 2000 K only diatomic hydrogen molecules occur in significant quantities and many of the terms in the above equations approach zero.

## References

- [1] E. V. Sheely, S. E. Jones, L. M. Rees, S. F. Shurtleff, S. F. Taylor and J. M. Thorne, "Predicted Methods of Changing the Muon Catalized Fusion Cycling Rate," *American Institute of Physics Conference Proceedings*, vol. 181, pp. 79-91, 1988.
- [2] I. N. Levine, *Physical Chemistry*, 4th ed., New York: McGraw-Hill, inc., 1995, p. 317.
- [3] D. A. McQuarrie, *Statistical Mechanics*, New York: Harper and Row Pub., 1976.
- [4] M. W. Chase Jr., J. R. Davies, D. J. Davies Jr., R. A. Fulrip, R. A. McDonald and A. N. Syverud, "JANAF Thermochemical Tables," *Journal of Physical and Chemical Reference Data*, Vols. 14, Supplement 1, pp. 991, 1211, 1985.
- [5] J. T. Gill and O. J. Coffin, "Tritium Handling in Vacuum Systems," in *Proceedings of the 19th Annual Symposium of the New Mexico Chapter of the American Vacuum Society*, Albuquerque, 1983.
- [6] G. N. Lewis and M. Randall, *Thermodynamics*, McGraw-Hill, 1961.



## Bibliography

Adamczak, A., and M. P. Faifman. "Resonant  $\text{d}\mu$  Formation In Condensed Hydrogen Isotopes." *Physicl Review A* 72 (2005): 052501:1-14.

Adamson, P. E. *A General Quantum Mechanical Method to Predict Positron Spectroscopy*. PhD dissertation, AFIT/DS/ENP/07-04. Graduate School of Management and Engineering, Air Force Institute of Technology (AU), Wright-Patterson AFB OH, June 2007 (0704-0188).

Adamson, P. E., X. F. Duan, L. W. Burggraf, M. V. Pak, C. Swalina, and S. Hammes-Schiffer. "Modeling Positrons in Molecular Electronic Structure Calculations with the Nuclear-Electronic Orbital Method." *Journal of Physical Chemistry A* 112, no. 6 (2008): 1346-1351.

Adir, R. K., and H. Kasha. *Cosmic Ray Muons*. Vol. 1, in *Muon Physics: Electromagnetic Interactions*, edited by V. W. Hughes and C. S. Wu. New York: Academic Press, (1977): 323-385.

Aguilar, J, E. Rafael, and D Greynat. "Muon Anomaly From Lepton Vacuum Polarization and the Mellin-Barnes Representation." *Physical Review D, particles, fields, gravitation and cosmology* 77 (2008): 093010:1-27.

Ahlrichs, R., and K. May. "Contracted All-Electron Gaussian Basis Sets for Atoms Rb to Xe." *Physical Chemistry, Chemical Physics* 2, no. 5 (2000): 943-945.

Aissing, G., and H. J. Monkhorst. "Relativistic Corrections to Binding Energies of Muonic Molecules." *Physical Review A: Atomic, Molecular, and Optical Physics* vol. 42, no. 7 (1990): 3789-3794.

Alekseev, I. A., I. A. Baranov, V. A. Novozhilov, G. A. Sukhorukova, and V. D. Trenin. "Separation of Hydrogen Isotopes  $\text{H}_2$ -HT and  $\text{D}_2$ -DT by Adsorption on NaA Synthetic Zeolites." *Atomnaya Energiya* 54, no. 6 (1982): 409-411.

Alexander, S. A., and H. J. Monkhorst. "High-Accuracy Calculation of Muonic Molecules Using Random-Tempered Basis Sets." *Physical Review A* 38, no. 1 (1988): 26-32.

Alexander, S. A., H. J. Monkhorst, and K. Szalewicz. "A Comparison of Muonic Molecular Calculations." 181 (1988): 246-258.

Alfaro, R. "Radiographic Images Produced by Cosmic-Ray Muons." *Particles and Fioelds, Part B: Commemorative Volume of the Division of Particles and Fields of the Mexican Physical Society*. Mexico City: AIP Conference Proceedings, (2006):. 373-381.

- Alfaro, R., E. Belmont-Moreno, A. Cervantes, V. Grabski, j. M. López-Robles, L. Manzanilla, A. Martínez-Dávalos, M. Moreno, A. Menchaca-Rocha. "A Muon Detector to be Installed at the Pyramid of the Sun." *Revista Mexicana de Física* 49, no. 4 (2003): 54-59.
- Alfaro, R., E. Belmont, V. Grabski, L. Manzanilla, A. Martinez-Davalos, A. Menchaca-Rocha, M. Moreno, and A. Sandoval. "Searching for Possible Hidden Chambers in the Pyramid of the Sun." *Proceedings of the 30th International Cosmic Ray Conference* (Universidad Nacional Autónoma de México), 2007: 1265-1268.
- Alvarez, L. W., J. A. Anderson, F. E. Bedwei, J. Burkhard, A. Fakhry, A. Girgis, A. Goneid, H. Fikhry, D. Iverson, G. Lynch, Z. Miligy, A. Hilmy, M. Sharkawi, and L. Yazolino. "Search for Hidden Chambers in the Pyramids." *Science* 167, no. 3919 (1970): 832-839.
- Armour, E. A. G., D. M. Lewis, and S. Hara. "Calculations of the Auger deexcitation rate of  $dt\mu$  within the muonic quasimolecule  $(dt\mu)dee$ ." *Physical Review A* 46, no. 11 (1992): 6888-6893.
- Auer, B., M. V. Pak, and S. Hammes-Schiffer. "Nuclear-Electronic Orbital Method within the Fragment Molecular Orbital Approach." *Journal of Physical Chemistry C* 114, no. 12 (2010): 5582-5588.
- Bakalov, D. D., and V. I. Korobov. "Relativistic Corrections to Energy Levels of Weakly Bound States of Mesic Molecules  $dd\mu$  and  $dt\mu$ ." *JINR Rapid Communications* 35, no. 2 (1989): 15-20.
- Balin, D. V., E. M. Maev, V. I. Medvedev, G. G. Semenchuk, Yu. V. Smirenin, A. A. Vorobyov, An. A. Vorobyov, Yu. K. Zalite,. "Experimental Investigation of the Muon Catalyzed dd-Fusion." *Physics Letters B* 141, no. 3-4 (1984): 173-176.
- Bardo, R. D., and K. Ruedenberg. "Even-Tempered Atomic Orbitals. III. Economic Deployment of Gaussian Primitives in Expanding Atomic SCF Orbitals." *Journal of Chemical Physics* 59, no. 11 (1973): 5956-5965.
- Bardo, R. D., and K. Ruedenberg. "Even-Tempered Atomic Orbitals. IV. Atomic Orbital Bases with Pseudoscaling Capability for Molecular Calculations." *Journal of Chemical Physics* 59, no. 11 (1973): 5966-77.
- Bardo, R. D., and K. Ruedenberg. "Even-Tempered Atomic Orbitals. VI. Optimal Orbital Exponents and Optimal Contractions of Gaussian Primitives for Hydrogen, Carbon, and Oxygen in Molecules." *Journal of Chemical Physics* 60, no. 3 (1974): 918-931.

Bardo, R. D., and K. Ruedenberg. "Even-Tempered Atomic Orbitals. VII. Theoretical Equilibrium Geometries and Reaction Energies for Carbon Suboxide and Other Molecules Containing Carbon, Oxygen, and Hydrogen." *Journal of Chemical Physics* 60, no. 3 (1974): 932-936.

Becke, A. D. "A Multicenter Numerical Integration Scheme for Polyatomic Molecules." *Journal of Chemical Physics* 88 (1988): 2547-2553.

Bedewi, F. I., A. Goned, and A. H. Girgis. "Energy Spectrum and Angular Distribution of Cosmic Ray Muons in the Range 50-70 GeV." *Journal of Physics A* 5, no. 2 (1972): 292-302.

Bettini, A. *Introduction to Elementary Particle Physics*. New York: Cambridge University Press, 2008.

Bevelacqua, J. J. *Basic Health Physics, Problems and Solutions*. New York: John Wiley & Sons, inc., 1999.

Blundell, S. A., and C. W. Palmer. "Recalculation of the Nuclear Volume Correction in Hyperfine Structure." *Journal of Physics B: Atomic, Molecular and Optical Physics* 21 (1988): 3809-3818.

Body, R. G., D. S. McClure, and E. Clementi. "SCF Wavefunctions for the NH<sub>3</sub> Molecule. Potential-Energy Surface and Vibrational Force Constants." *Journal of Chemical Physics* 49, no. 11 (1968): 4916-4924.

Born, M., and J. R. Oppenheimer. "Zur Quantentheorie der Moleküln." *Annalen der Physik* 84 (1927): 457-484.

Bossy, H., H. Daniel, F. J. Hartmann, H. S. Plendi, G. Schmidt, and T. von Egidy. "Determination of Muonic Helium X-Ray Yields after Muon-Catalyzed pd, dd, and dt Fusion." *Physical Review Letters* 59 (1987): 2864-2867.

Bouferguene, A., and D. Rinaldi. "A New Single-Center Method to Compute Molecular Integrals of Quantum Chemistry in Slater-Type Orbital Basis of Functions." *International Journal of Quantum Chemistry* 50, no. 1 (1993): 21-42.

Boukour, A., R. Hewitt, and C. Leclercq-Willain. "The Coulomb Capture of Negative Muons by Hydrogen Atoms in the Non-Adiabatic Close-Coupling Approximation." *Hyperfine Interactions* 101-102, no. 1 (1996): 263-269.

Breunlich, W. H., P. Kammel, J. S. Cohen, and M. Leon. "Muon-Catalyzed Fusion." *Annual Review of Nuclear and Particle Science* 39 (1989): 311-355.

Bubin, S., and L. Adamowicz. "Non-Born–Oppenheimer Study of Positronic Molecular Systems: e+LiH." *Journal of Chemical Physics* 120, no. 13 (2004): 6051:1-5.

Bubin, S., and L. Adamowicz. "Nonrelativistic Molecular Quantum Mechanics Without Approximations: Electron Affinities of LiH and LiD." *Journal of Chemical Physics* 121, no. 13 (2004): 6249:1-5.

Bubin, S., L. Adamowicz, and M. Molski. "An Accurate Non-Born–Oppenheimer Calculation of the First Purely Vibrational Transition in LiH Molecule." *Journal of Chemical Physics* 123, no. 13 (2005): 134310:1-5.

Burden, R. L., and J. D. Faires. *Numerical Analysis*. 5th. Boston: PWS Pub., 1993.

Burggraf, L., interview by Eugene sheely. *Muon Regeneration in Electric Fields* (2010).

Cafiero, M., S. Bubin, and L. Adamowicz. "Non-Born-Oppenheimer Calculations of Atoms and Molecules." *Physical Chemistry Chemical Physics*, no. 5 (2003): 1491-1501.

Carlson, B. C., and J. M. Keller. "Orthogonalization Procedures and the Localization of Wannier Functions." *Physical Review* 105, no. 1 (1957): 102-103.

Carney, G. D., and R. N. Porter. "The Lowest Rotation States of H<sub>3</sub><sup>+</sup> and Symmetry Considerations in Dissociative e Capture." *The Journal of Chemical Physics* vol. 66, no. 6 (1977): 2756-2758.

Chakraborty, A., and S. Hammes-Schiffer. "Density Matrix Formulation of the Nuclear-Electronic Orbital Approach with Explicit Electron-Proton Correlation." *Journal of Chemical Physics* 129 (2008): 204101:1-16.

Chakraborty, A., M. V. Pak, and S. Hammes-Schiffer. "Inclusion of Explicit Electron-Proton Correlation in the Nuclear-Electronic Orbital Approach Using Gaussian-Type Geminal Functions." *Journal of Chemical Physics*, no. 122 (2008): 014101:1-13.

Challacombe, M. "A Simplified Density Matrix Minimization for Linear Scaling Self-Consistent." *Journal of Chemical Physics* vol. 110, no. 5 (1999): 2332-2342.

Charlton, M., and J. W. Humberston. *Positron Physics*. Cambridge: Cambridge University Press, 2001.

Chase Jr., M. W., J. R. Davies, D. J. Davies Jr., R. A. Fulrip, R. A. McDonald, and A. N. Syverud. "JANAF Thermochemical Tables." *Journal of Physical and Chemical Reference Data* 14, Supplement 1 (1985): 991, 1211.

Childs, K. D., B. A. Carlson, , L. A. Vanier, J. F. Moulder, D. F. Paul, W. F. Stickle, D. G. Watson. "Handbook of Auger Electron Spectroscopy." In *Physical Electronics*, by C. L. Hedberg. Eden Prairie, MN, 1995.

Cohen, J. S. "Slowing Down and Capture of Negative Muons by Hydrogen: Classical-Trajectory Monte Carlo Calculation." *Physical Review A: Atomic, Molecular, and Optical Physics* 27, no. 1 (1983): 167-179.

- Cohen-Tannoudji, C., B. Diu, and F. Laloe. *Quantum Mechanics*. ed. 2. Vol. 2. New York: John Wiley and Sons, 1977.
- Cohen-Tannoudji, C., B. Diu, and F. Laloë. *Quantum Mechanics*. ed. 2. Vol. 1. New York: John Wiley and Sons, 1977.
- Coleman, P. G. "Experimental Techniques in Positron Spectroscopy." In *Principles and Applications of Positron and Positronium Chemistry*, edited by Y. C. Jean, P. E. Mallon and D. M. Schrader, 37-73. Singapore: World Scientific Publishing Company, 2003.
- Crabtree, K. N., B. A. Tom, and B. J. McCall. "Nuclear Spin Dependence of the Reaction of  $H_3^+$  with  $H_2$ . I. Kinetics and Modeling." *The Journal of Chemical Physics* 134, no. 19 (2011): 194311:1-13.
- Cripps, G., A. A. Harms, and B. Goel. "Muon Catalyzed Fusion of Deuterium-Tritium at Elevated Densities." *Hyperfine Interactions* 77, no. 1 (1993): 181-199.
- Danos, M., L. C. Biedenharn, and A. Stahlhofen. "Comprehensive Theory of Nuclear Effects on the Intrinsic Sticking Probability: I." *American Institute of Physics Conference Proceedings* 181 (1988): 308-319.
- Danos, M., L. C. Biedenharn, and A. Stahlhofen. "Comprehensive Theory of Nuclear Effects on the Intrinsic Sticking Probability: II." *American Institute of Physics Conference Proceedings* 181 (1988): 320-329.
- Davies, J. D., J. B. A. England, G. J. Pyle, G. T. A. Squier, F. D. Brooks, W. A. Cilliers, A. Bertin, M. Bruschi, M. Piccinini, A. Vitale, A. Zoccoli, S. E. Jones, V. R. Bom, C. W. E. van Eijk, H. de Hann, A. H. Anderson, M. A. Paciotti, G. H. Eaton, and B. Alper, "A Direct Measurement of the Alpha-Muon Sticking Coefficient in Muon-Catalysed d-t Fusion." *Journal of Physics G: Nuclear and Particle Physics* 16, no. 10 (1990): 1529-1538.
- Dinelli, B. M., L. Neale, O. L. Polyansky, and J. Tennyson. "New Assignments for the Infrared Spectrum of  $H_3^+$ ." *Journal of molecular spectroscopy* 181 (1997): 142-150.
- Ehrenreich, H., and M. H. Cohen. "Self-Consistent Field Approach to the Many-Electron Problem." *Physical Review* 115, no. 4 (1959): 786-790.
- Eliezer, S. "Muon Catalyzed Nuclear Fusion." *Laser and Particle Beams* 6 (1988): 63-81.
- Emery, L. C., and W. D. Edwards. "Intermolecular Dynamics for Weakly Bound Donor-Acceptor Complexes." *International Journal of Quantum Chemistry* 40, no. S25 (1991): 347-358.

Emery, L. C., J. E. Sheldon, W. D. Edwards, and J. L. McHale. "Intermolecular Ground and Excited State Potential Energy Surfaces and Charge-Transfer Spectrum of Benzene: TCNE Electron Donor—Acceptor Complex." *Spectrochimica Acta Part A: Molecular Spectroscopy* 48A, no. 5 (1972): 715-724.

Faifman, M. P., and L. I. Ponomarev. "Resonant Formation of  $d\bar{\mu}$  Mesic Molecules in the Triple  $H_2+D_2+T_2$  Mixture." *Physics Letters B* 265 (1991): 201-206.

Faifman, M. P., L. I. Men'shikov, and T. A. Strizh. "Studies on Muonic Dynamics of Liquid D–T–H in  $d\bar{\mu}$ ." *Muon Catalyzed Fusion* 4 (1989): 1.

Fisher, A. "Cold Fusion." *Popular Science*, 1987: 54-55,100.

Flores-Riveros, A., and J. F. Rivas-Silva. "Variational Description of the 3-body Coulomb Problem Through a Correlated Eckart-Gaussian Wavefunction." *Brazilian Journal of Physics* 29, no. 3 (1999): 529-540.

Frank, F. C. "Hypothetical Alternative Energy Sources for the 'Second Meson' Events." *Nature*, 1947: 525-527.

Frisch, M. J., M. Head-Gordon, G. W. Trucks, J. B. Foresman, H. B. Schlegel, K. Raghavachari, M. A. Robb, J. S. Binkley, C. Bonzalez, D. J. Defrees, D. J. Fox, R. A. Whiteside, R. Seeger, C. F. Melius, J. Baker, R. L. Martin, L. R. Kahn, J. J. P. Stewart, S. Topiol, and J. A. Pople. *Gaussian 90 User's Guide and Programmer's Reference*. Pittsburg: Gaussian, Inc, 1990.

Froelich, P., and G Larson. " $\alpha\mu$  Stripping by Ionization in Dense Deuterium/Tritium Mixture, and its Implication for Muon Catalyzed Fusion." *Journal of Molecular Structure: Theochem* 199 (1989): 189-200.

Gajewski, R. "The Political Economy of Muon-Catalyzed Fusion Research." *American Institute of Physics Conference Proceedings*, Vol. 181. Sanibel Island, FL, 1988. xi-xii.

Gerstein, S. S., and L. I. Ponomarev. " $\mu^-$  Meson Catalysis of Nuclear Fusion in a Mixture of Deuterium and Tritium." *Physics Letters B* 72, no. 1 (1977): 80-82.

Gill, J. T., and O. J. Coffin. "Tritium Handling in Vacuum Systems." *Proceedings of the 19th Annual Symposium of the New Mexico Chapter of the American Vacuum Society*. Albuquerque: Los Alamos National Lab, 1983.

Gordon, M. S., and M. W. Schmidt. "Advances in Electronic Structure Theory: GAMESS a Decade Later." In *Theory and Applications of Computational Chemistry, the first forty years*, edited by C. E. Dykstra, G. Frenking, K. S. Kim and G. E. Scuseria, 1167-1190. Amsterdam: Elsevier Inc., 2005.

- Grabski, V., A. Morales, R. Reche, and O. Orozco. "Feasibility for p+/p- Flow-Ratio Evaluation in the 0.5-1.5 TeV Primary Energy Range, Based on Moon-Shadow Muon Measurements, to be Carried Out in the Pyramid of the Sun, Teotihuacan, Experiment." *Proceedings of the 30th International Cosmic Ray Conference 5* (HE part 2) (2007): 1543-1546.
- Grotendorst, J., and E. O. Steinborn. "Numerical Evaluation of Molecular One- and Two-Electron Multicenter Integrals with Exponential-Type Orbitals via the Fourier-Transform Method." *Physical Review A* 38, no. 8 (1988): 3857-3876.
- Halzen, F., and A. D. Martin. *Quarks and Leptons: an Introductory Course in Modern Particle Physics*. New York: John Wiley and Sons, 1984.
- Hamahata, Y., E. Hiyama, and M. Kamimura. "Non-Adiabatic Four-Body Calculation of Double-Muonic Hydrogen Molecules." *Hyperfine Interactions*. Kluwer Academic Publishers, 2001. 187-190.
- Hamahata, Y., E. Hiyama, and M. Kamimura. "Non-Adiabatic Four-Body Calculation of Double-Muonic Hydrogen Molecules." *Hyperfine Interactions* 138 (2001): 187-190.
- Harley, D., B. Muller, and J. Rafelski. "Muon Catalysed Fusion of Nuclei with  $Z > 1$ ." *Journal of Physics G: Nuclear and Particle Physics* 16, no. 2 (1990): 281-294.
- Heb, B. A., C. M. Marian, U. Wahlgren, and O. Gropen. "A Mean-Field Spin-Orbit Method Applicable to Correlated Wavefunctions." *Chemical Physics Letters* 251, no. 5-6 (1996): 365-371.
- Hehre, W. J., R. F. Stewart, and J. A. Pople. "Self-Consistent Molecular-Orbital Methods. I. Use of Gaussian Expansions of Slater-Type Atomic Orbitals." *Journal of Chemical Physics* 51, no. 6 (1969): 2657-2664.
- Heming, R. E., I. D. Reid, P. F. W. Louwrier, J. W. Schneider, H. Deller, W. Odermatt, B. D. Patterson, H. Simmler, B. Pumpin, and I. M. Savic. "The Separation of Chemical Reactivity and Heisenberg Spin-Exchange Effects in a Radical-Radical reaction by Avoided Level Crossing  $\mu$ SR." *Chemical Physics* 129, no. 3 (1989): 335-350.
- Henis, Z., S. Eliezer, and V. B. Mandelzweig. "Can the  $\mu\alpha$  stripping probability be enhanced by strong electromagnetic fields?" *Physics Letters A* 146, no. 4 (1990): 222-225.
- Hoch, R. C. "Advances in Cosmic Ray Muon Tomography Reconstruction Algorithms." *Thesis*. Florida Institute of Technology, December 2009.
- Hopkin, M. "Archaeology: Pyramid Power." *Nature* 430, no. 7002 (2004): 828.
- Hurley, A. C. *Introduction to the Electron Theory of Small Molecules*. London: Academic Press, 1976.

Huzinaga, S., and M. Klobukowski. "The Well-Tempered GTF Basis Set and the ab initio Molecular Calculation." *Journal of Molecular Structure: THEOCHEM* 135 (1986): 403-408.

Huzinaga, S., and M. Klobukowski. "Well-Tempered Gaussian Basis Sets for the Calculation of Matrix Hartree—Fock Wavefunctions." *Chemical Physics Letters* 212, no. 3-4 (1993): 260-264 .

Huzinaga, S., and M. Miguel. "A Comparison of the Geometrical Sequence Formula and the Well-Tempered Formulas for Generating GTO Basis Orbital Exponents." *Chemical Physics Letters* 175, no. 4 (1990): 289-291.

Huzinaga, S., M. Klobukowski, and H. Tatewaki. "The Well-Tempered GTF Basis Sets and their Applications in the SCF Calculations." *Canadian Journal of Chemistry* 63 (1985): 1812-1828.

Iordanov, T., and S. Hammes-Schiffer. "Vibrational Analysis for the Nuclear-Electronic Orbital Method." *Journal of Chemical Physics*, 2003: 9489-9496.

Itou, Y., K. Mori, T. Udagawa, M. Tachikawa, T. Ishimoto, and U. Nagashima. "Quantum Treatment of Hydrogen Nuclei in Primary Kinetic Isotope Effects in a Thermal [1,5]-Sigmatropic Hydrogen (or Deuterium) Shift from (Z)-1,3-Pentadiene." *International Journal Quantum Chemistry* 111, no. 2 (2007): 261-267.

Jackson, J. D. "Catalysis of Nuclear Reactions between Hydrogen Isotopes by  $\mu$ -Mesons." *Physical Review* 106, no. 2 (1957): 330-339.

Jändel, M., P. Froelich, G. Larson, and C. D. Stodden. "Reactivation of  $\alpha\mu$  in Muon-Catalyzed Fusion under Plasma Conditions." *Physical Review A* 40, no. 5 (1989): 2799-2802.

Jändel, M., P. Froelich, G. Larson, and C. D. Stodden. "Reactivation of  $\alpha\mu$  in Muon-Catalyzed Fusion Under Plasma Conditions." *Physical Review A* 40 (1989): 2799-2802.

Jeziorski, B., K. Szalewicz, A. Scrinzi, X. Zhao, and R. Moshinsky. "Muon Sticking Fractions for S States of the  $t\bar{\mu}$  Ion Including the Effects of Nuclear Interactions." *Physical Review A* 43, no. 3 (1991): 1281-1292.

Jones, S. E. "Muon-Catalysed Fusion Revisited." *Nature* 321, no. 6066 (1986): 127-133.

—. "Survey of Experimental Results in Muon-Catalyzed Fusion." *American Institute of Physics Conference Proceedings*, vol. 181. Sanibel Island, FL, 1988. 2-16.

Jones, S. E., A. N. Anderson, A. J. Caffrey, J. B. Walter, K. D. Watts, J. N. Bradbury, P. A. M. Gram, M. Leon, H. R. Maltrud, M. A. Paciotti. "Experimental Investigation of Muon-Catalyzed d-t Fusion." *Physical Review Letters* 51 (1983): 1757-1760.



Jones, S. E., A. N. Anderson, A. J. Caffrey, C. deW. Van Sicien, K. D. Watts, J. N. Bradbury, J. S. Cohen, P. A. M. Gram, M. Leon, H. R. Maltrud, and M. A. Paciotti. "Observation of Unexpected Density Effects in Muon-Catalyzed d-t Fusion." *Physical Review Letters* 56 (1986): 588-591.

Jones, Steve E., interview by Eugene Sheely. (1988).

Kamimura, M. "Effect of Nuclear Interaction on Muon Sticking to Helium in Muon-Catalyzed d-t Fusion." *American Institute of Physics Conference Proceedings* 181 (1988): 330-343.

Kane, G. *Modern Elementary Particle Physics: The Fundamental Particles and Forces?* Boulder: Westview Press, 1993.

Kawamura, N., K. Ishida, T. Matsuzaki, H. Imao, and K. Nagamine. "Muonic Molecule Formation in Muon-Catalyzed Fusion." *Advanced Science Research Symposium 2009 Positron, Muon and other exotic particle beams for materials and atomic/molecular sciences (ASR2009)*, vol. 225 no. 1. Tokai: Journal of Physics: Conference Series, 2010. 12025:1-5.

Komornicki, A., and J. W. McIver Jr. "An Efficient ab initio Method for Computing Infrared and Raman Intensities: Application to Ethylene." *Journal of Chemical Physics* 70, no. 4 (1979): 2014-2016.

Konkel, T. "Container Security: Preventing a Nuclear Catastrophe." *The Journal of International Policy Solutions* 3 (2005): 1-23.

Krane, K.S. *Introductory Nuclear Physics*. Hoboken NJ: John Wiley and Sons, Inc., 1988.

Krzysztof, S., and J. Bogumil. "Nonadiabatic Calculations for  $\mu$  Relevant for Muon Catalyzed Fusion." *International Journal of Quantum Chemistry* 40, no. S25 (1991): 671-686.

Kuang, J., and C. D. Lin. "Molecular Integrals Over Spherical Gaussian-Type Orbitals: I." *Journal of Physics B: Atomic, Molecular and Optical Physics* 30, no. 11 (1997): 2529-2548.

Kulsrud, R. M. "A Proposed Method for Reducing the Sticking Constant in M. C. F." *American Institute of Physics Conference Proceedings* 181 (1988): 367-380.

Leon, M. "Theory of Muonic Molecule Formation: Survey of Progress and Open Questions." *Hyperfine Interactions* 82 (1993): 151-160.

Levine, I. N. *Physical Chemistry*. 4th. New York: McGraw-Hill, 1995.

Levine, I. N. *Quantum Chemistry*. Boston: Allyn and Bacon, Inc., 1983.

- Lewis, G. N., and Merle Randall. *Thermodynamics*. McGraw-Hill, 1961.
- Lindsay, C. M., and B. J. McCall. "Comprehensive Evaluation and Compilation of H<sub>3</sub><sup>+</sup> Spectroscopy." *Journal of Molecular Spectroscopy* 210, no. 1 (2001): 60-83.
- Löwdin, P. O. "Quantum Theory of Cohesive Properties of Solids." *Advances in Physics* 5, no. 17 (1956): 1-171.
- Marple, S. L. *Digital Spectral Analysis with Applications*. Upper Saddle River: Prentice-Hall, 1987.
- Matsuoka, O., and S. Huzinaga. "Relativistic Well-Tempered Gaussian Basis Sets." *Chemical Physics Letters* 140, no. 6 (1987): 567-571.
- Matsuoka, O., and S. Huzinaga. "Well-Tempered Gaussian Basis Set Expansions of Roothaan-Hartree-Fock Atomic Wavefunctions for Lithium through Mercury." *Journal of Molecular Structure: THEOCHEM* 167, no. 1-2 (1988): 1-209.
- Matsuzaki, T., K. Nagamine, K. Ishida, S. N. Nakamura, N. Kawamura, M. Tanase, M. Kato, K. Kurosawa, M. Hashimoto, H. Sugai, K. Kudo, N. Takeda, and G. Eaton. "Muon Catalyzed Fusion and Muon to <sup>3</sup>He Transfer in Solid T<sub>2</sub> Studied by X-ray and Neutron Detection." *RIKEN Review* 20 (1999): 18-20.
- Matsuzaki, T., K. Nagamine, K. Ishida, S. N. Nakamura, N. Kawamura, M. Tanase, M. Kato, K. Kurosawa, M. Hashimoto, H. Sugai, K. Kudo, N. Takeda, and G. Eaton. "Muon-Catalyzed Fusion and Muon to <sup>3</sup>He Transfer in Solid T<sub>2</sub> Studied by X-ray and Neutron Detection." *Hyperfine Interactions* 118, no. 1-4 (1999): 229-234.
- McQuarrie, D. A. *Statistical Mechanics*. New York: Harper and Row Pub., 1976.
- Meyer, W., and P Pulay. "Near Hartree—Fock Calculations of the Force Constants and Dipole Moment Derivatives in Methane." *Journal of Chemical Physics* 56, no. 5 (1972): 2109-2116.
- Mohr, P. J., B. N. Taylor, and D. B. Newell. "CODATA Recommended Values of the Fundamental Physical Constants: 2006." *Reviews of Modern Physics* 80, no. 2 (2008): 633-730.
- Mohr, P. J., B. N. Taylor, and D. B. Newell. "CODATA Recommended Values of the Fundamental Physical Constants: 2006." *Journal of Physical Chemistry Reference Data* 37, no. 3 (2008): 1187-1284.
- Moncada, F., S. A. Gonzalez, and A. Reyes. "First Principles Investigation of Hydrogen Isotope Effects in [XSO<sub>4</sub>-H-SO<sub>4</sub>X]- (X = H, K) Complexes." *Molecular Physics* 198, no. 11 (2010): 1545-1552.

Morris, C. L., C. C. Alexander, J. D. Bacon, K. N. Borozdin, D. J. Clark, R. Chartrand, C. J. Espinoza, A. M. Fraser, M. C. Galassi, J. A. Green, J. S. Gonzales, J. J. Gomez, N. W. Hengartner, A. V. imenko, M. Makela, J. J. Medina, F. E. Pazuchanics, W. C. Priedhorsky, J. C. Ramsey, A. Saunders, R. C. Schirato, L. J. Schultz, M., J. Sossong, and G. S. Blanpied. "Tomographic Imaging with Cosmic Ray Muons." *Science & Global Security* 16, no. 1 & 2 (2008): 37-53.

Nagamine, K. *Introductory Muon Science*. Cambridge: Cambridge University Press, 2003.

Nagamine, K., and M. Kamimura. "Muon Catalyzed Fusion: Interplay Between Nuclear and Atomic Physics." *Advances in Nuclear Physics* 24 (1998): 151-205.

Nagamine, K., T. Matsuzaki, K. Ishida, Y. Hirata, Y. Watanabe, R. Kadono, Y. Miyake, K. Nishiyama, S. E. Jones, and H. R. Maltrud. "Muonic x-ray measurement on the.  $\mu$ . /sup -/ sticking probability for muon catalyzed fusion in liquid d-t mixture." *Muon Catalyzed Fusion* 1 (1987): 137-138.

Nagamine, K., K. Ishida, S. Sakamoto, Y. Watanabe, and T. Matsuzaki. "X-Ray Measurement on Muon to Alpha Sticking in Muon Catalyzed d-t Fusion; Present and Future." *Hyperfine Interactions* 82, no. 1-4 (1993): 343-353.

Nagamine, K., T. Matsuzaki, K. Ishida, S. N. Nakamura, N. Kawamura, and Y. Matsuda. "Contribution of Muon Catalyzed Fusion to Fusion Energy Development." *18th International Conference on Fusion Energy 2000*. International Atomic Energy Agency, 2000. 1-5.

Nakai, H., H. Minoru, K. Miyamoto, and S. Hyodo. "Elimination of Translational and Rotational Motions in Nuclear Orbital plus Molecular Orbital Theory." *Journal of Chemical Physics* 122 (2005): 164101:1-10.

Nakai, H., K. Sodeyama, and M. Hoshino. "Non-Born-Oppenheimer Theory for Simultaneous Determination of Vibrational and Electronic Excited States: ab initio NO+MO/CIS theory." *Chemical Physics Letters* 345 (2001): 118-124.

National Research Council (U.S.), Elementary-Particle Physics Panal. *Elementary-Particle Physics*. Washington DC: National Academy Press, 1990.

Ohta, Y., A. V. Soudackof, and S. Hammes-Schiffer. "Extended Spin-Boson Model for Nonadiabatic Hydrogen Tunneling in the Condensed Phase." *Journal of Chemical Physics* 125, no. 14 (2006): 144522:1-16.

Oka, T. "Spectroscopy and astronomy: H<sub>3</sub><sup>+</sup> from the laboratory to the Galactic center." *Faraday Discussions* 150, no. 0 (2011): 9-22.

Oka, T., and E. Epp. "The Nonthermal Rotational Distribution of H<sub>3</sub><sup>+</sup>." *The Astrophysical Journal* 613, no. 1 (2004): 349-354.

Paciotti, M. A., A. N. Anderson, A. J. Caffrey, and S. E. Jones, interview by Eugene Sheely. Los Alamos, NM, (1988).

Paciotti, M. A., O. K. Baker, J. N. Bradbury, J. S. Cohen, M. Leon, H. R. Maltrud, L. L. Sturgess, S. E. Jones, P. Li, L. M. Rees, E. V. Sheely, J. K. Shurtleff, S. F. Taylor, A. N. Anderson, A. J. Caffrey, J. M. Zabriskie, F. D. Brooks, W. A. Cilliers, J. D. Davis, J. B. A. England, G. J. Pyle, G. T. A. Squier, A. Bertin, M. Bruschi, M. Piccinini, A. Vitale, A. Zoccoli, V. R. Bom, C. W. E. van Eijk, H. de Haan, and G. H. Eaton. "First Direct Measurement of  $\alpha$ - $\mu$  Sticking in dt- $\mu$ CF." *American Institute of Physics Conference Proceedings* 181 (1988): 38-51.

Pahlavani, M. R., and S. M. Motevalli. "Study of Muon Catalyzed Fusion in Deuterium-Tritium Fuel under Compressive Conditions." *ACTA Physica Polonica B* 40, no. 2 (2009): 319-329.

Pahlavani, M. R., and S. M. Motevalli. "The Probability of Muon Sticking and X-Ray Yields in the Muon Catalyzed Fusion Cycle in a Deuterium and Tritium Mixture." *ACTA Physica Polonica B* 39, no. 3 (2008): 683-694.

Pak, M. V., A. Chakraborty, and S. Hammes-Schiffer. "Analysis of Nuclear Quantum Effects on Hydrogen Bonding." *Journal of Physical Chemistry, A* 111, no. 11 (2007): 2206-2212.

Pak, M. V., A. Chakraborty, and S. Hammes-Schiffer. "Calculation of the Positron Annihilation Rate in PsH with the Positronic Extension of the Explicitly Correlated Nuclear-Electronic Orbital Method." *Journal of Physical Chemistry A* 113, no. 16 (2009): 4004-4008.

Pak, M. V., and S. Hammes-Schiffer. "Electron-Proton Correlation for Hydrogen Tunneling Systems." *Physical Review Letters* 92, no. 10 (2004): 103002:1-4.

Pak, M. V., S. P. Swalina, S. P. Webb, and S. Hammes-Schiffer. "Application of the Nuclear-Electronic Orbital Method to Hydrogen Transfer Systems: Multiple Centers and Multiconfigurational Wavefunctions." *Chemical Physics* 304 (2004): 227-236.

Pak, Mike, interview by Eugene v. Sheely. (June 2010).

Pallante, E. "The Hadronic Vacuum Polarization Contribution to the Muon  $g-2$  in the Quark-Resonance Model." *Physics Letters B* 341 (1994): 221-227.

Petersson, G. A., and S. Zhong. "On the Optimization of Gaussian Basis Sets." *Journal of Chemical Physics* 118, no. 3 (2003): 1101-1109.

Petitjean, C., D. V. Balin, V. N. Baturin, P. Baumann, W. H. Breunlich, T. Case, K. M. Crowe, H. Daniel, Yu. S. Grigoriev, F. J. Hartmann, A. I. Ilyin, M. Jeitler, P. Kammel, B. Lauss, K. Lou, E. M. Maev, J. Marton, M. Muhlbauer, G. E. Petrov, W. Prymas, W. Schott, G. G. Semenchuk, Yu. V. Smirenin, A. A. Vorobyov, N. I. Voropaev, P. Wojciechowski, and J. Zmeskal. "Experimental Survey of the Sticking Problem in Muon Catalyzed de Fusion." *Hyperfine Interactions* 82, no. 1-4 (1993): 273-293.

Petrov, Yu. V. "Conceptual Scheme of a Hybrid Mesocatalytic Fusion Reactor." *Atomnaya Énergiya* (Plenum publishing corporation) 63, no. 5 (1987): 333-341.

Petrov, Yu. V. "Muon Catalysis for Energy Production by Nuclear Fusion." *Nature* 285 (1980): 466-468.

Polyansky, O. L., and J. Tennyson. "Ab initio Calculation of the Rotation-Vibration Energy Levels of H<sub>3</sub><sup>+</sup> and its Isotopomers to Spectroscopic Accuracy." *The Journal of Chemical Physics* 110, no. 11 (1999): 5056-5064.

Ponomarev, L. I. "Muon Catalysed Fusion." *Contemporary Physics* 31, no. 4 (1990): 219-245.

Ponomarev, L. I. "Muon-Catalyzed Fusion and Fundamental Physics." *Hyperfine Interactions* 103 (1996): 137-145.

Pople, J. A., R. Krishnan, H. B. Schlegel, and J. S. Binkley. "Derivative Studies in Hartree-Fock and Møller-Plesset Theories." *International Journal of Quantum Chemistry: Symposium* . 1979. 225-241.

Porezag, D., and M. R. Pederson. "Optimization of Gaussian Basis Sets for Density-Functional Calculations." *Physical Review A*, 1999: 2840-2847.

Press, W. H., B. P. Flannery, S. A. Teukolsky, and W. T. Vetterling. *Numerical Recipes in FORTRAN: The Art of Scientific Computing*. 2nd. Cambridge: Cambridge University Press, 1992.

Press, W. H., B. P. Teukolsky, W. T. Vetterling, and B. P. Flannery. *Numerical Recipes, the Art of Scientific Computing*. 5th. Cambridge: Cambridge University Press, 2007.

Priedhorsky, W. C., K. N. Borozdin, G. E. Hogan, C. Morris, A. Saunders, L. J. Schultz, and M. E. Teasdale. "Detection of High-Z Objects Using Multiple Scattering of Cosmic Ray Muons." *Review of Scientific Instruments* 74, no. 10 (2003): 4294-4297.

Pulay, P. "Improved SCF Convergence Acceleration." *Journal of Computaitonal Chemistry* 3, no. 4 (1982): 556-560.

Pulay, P., and W. Meyer. "Force Constants and Dipole Moment Derivatives of Ammonia from Hartree-Fock Calculations." *Journal of Chemical Physics* 57 (1972): 3337-3340.

Rafelski, H. E., and B. Müller. "Density Dependent Stopping Power and Muon Sticking in Muon-Catalyzed D-T Fusion." *American Institute of Physics Conference Proceedings* 181 (1988): 355-366.

Rafelski, J. "The Challenges of Muon Catalyzed Fusion." *American Institute of Physics Conference Proceedings*, vol. 181. Sanibel Island, FL, 1988. 451-464.

Rafelski, J., and S. E. Jones. "Cold Nuclear Fusion." *Scientific American* 255, no. 7 (1987): 84-89.

Raffenetti, R. C. "Even-Tempered Atomic Orbitals II. Atomic Self-Consistent-Field Wave Functions in Terms of Even-Tempered Exponential Bases." *Journal of Chemical Physics* 59 (1973): 5936-5950.

Raffenetti, R. C., and K. Ruedenberg. "Even-Tempered Atomic Orbitals V. SCF Calculations of Trialkali Ions with Pseudo-scaled Non-Orthogonal Bases." *Journal of Chemical Physics* 59 (1973): 5978-5991 .

Raghavachari, K., and J. A. Pople. "Calculation of One-Electron Properties Using Limited Configuration Interaction Techniques." *International Journal of Quantum Chemistry* 20, no. 5 (1981): 1067-1071.

Refaelski, H. E., D. Harley, G. R. Shin, and J. Rafelski. "Cold Fusion: Muon-Catalysed Fusion." *Journal of Physics B: Atomic, Molecular and Optical Physics* 24 (1991): 1469-1516.

Reyes, A., M. V. Pak, and S. Hammes-Schiffer. "Investigation of isotope Effects with the Nuclear-Electronic Orbital Approach." *Journal of Chemical Physics* 123 (2005): 064104:1-8.

Roothaan, C. C. J. "Self-Consistent Field Theory for Open Shells of Electronic Systems." *Reviews of Modern Physics* 32 (1960): 179-185.

Saini, S., and K. C. Kulander. "Muon Catalyzed Fusion: Muon Capture by Proton From K- and L-Shells of  $\alpha\mu^*$ ." *Chines Journal of Physics* 29, no. 2 (1991): 115-129.

Sakharov, A. D. "Passivnye Mezony." FIAN, Moscow, 1948.

Salvador, P., and I Mayer. "Energy Artitioning For "Fuzzy" Atoms." *Jounal of Chemical Physics*, 2004: 1646354 (pages 1-7).

Schmidt, M. W., K. K. Baldridge, J. A. Boatz, S. T. Elbert, M. S. Gordon, J. H. Jensen, S. Koseki, N. Matsunaga, K. A. Nguyen, S. J. Su, T. L. Windus, M. Dupuis, and J. A. Montgomery. "General Atomic and Molecular Electronic Structure System." *Journal of Computational Chemistry* 14 (1993): 1347-1363.

Sheely, E. V. *Quasi-Classical Molecular Dynamics of Weakly Bound Donor-Acceptor Complexes*. Ann Arbor: UMI, Bell & Howell, 1997.

Sheely, E. V., L. W. Burggraf, P. E. Adamson, F. D. Xiaofeng, and M. W. Schmidt. "Application of GAMESS/NEO to Quantum Calculations of Muonic Molecules." *Advanced Science Research Symposium 2009 Positron, Muon and other exotic particle beams for materials and atomic/molecular sciences (ASR2009)*, vol. 225 no. 1. Tokai: Journal of Physics: Conference Series, (2010) 012049:1-8.

Sheely, E. V., S. E. Jones, L. M. Rees, S. F. Shurtleff, S. F. Taylor, and J. M. Thorne. "Predicted Methods of Changing the Muon Catalyzed Fusion Cycling Rate." *American Institute of Physics Conference Proceedings* 181 (1988): 79-91.

Skone, J. H., M. V. Pak, and S. Hammes-Schiffer. "Nuclear-Electronic Orbital Nonorthogonal Configuration Interaction Approach." *Journal of Chemical Physics* 123 (2005): 134108:1-8.

Slater, J. C. "Atomic Shielding Constants." *Physical Review* 36 (1930): 57-64.

Srivastava, V. "A Unified View of the Orthogonalization Methods." *Journal of Physics A: Mathematical and General* 33 (2000): 6219–6222.

Stodden, C. D., H. J. Monkhorst, K. Szalewicz, and T. G. Winter. "Muon Reactivation in Muon-Catalyzed d-t Fusion from Accurate p-He<sup>+</sup> Stripping and Excitation Cross Sections." *Physical Review A* 41, no. 3 (1990): 1281-1292.

Swalina, C., and S. Hammes-Schiffer. "Impact of Nuclear Quantum Effects on the Molecular Structure of Bihalides and the Hydrogen Fluoride Dimer." *Journal of Physical Chemistry A* 109, no. 45 (2005): 10410-10417.

Swalina, C., M. V. Pak, A. Chakraborty, and S. Hammes-Schiffer. "Explicit Dynamical Electron--Proton Correlation in the Nuclear--Electronic Orbital Framework." *Journal of Physical Chemistry A* 110, no. 33 (2006): 9983-9987.

Swalina, C., M. V. Pak, and S. Hammes-Schiffer. "Alternative Formulation of Many-Body Perturbation Theory for Electron-Proton Correlation." *Chemical Physics Letters* 404 (2005): 394-399.

Swalina, C., M. V. Pak, and S. Hammes-Schiffer. "Analysis of the Nuclear-Electronic Orbital Method for Model Hydrogen Transfer Systems." *Journal of Chemical Physics* 123, no. 1 (2005): 014303:1-6.

Szabo, A., and N. S. Ostlund. *Modern Quantum Chemistry, Introduction to Advanced Electronic Structure Theory*. Mineola: Dover Publications, inc., 1989.

Szalewicz, K., B. Jeziorski, A. Scrinzi, X. Zhao, R. Moszynski, W. Kolos, P. Froelich, H. Monkhorst, and A. Velenik. "Effects of Nuclear Forces in Muon-Catalyzed Fusion: Nonadiabatic Treatment of Energy Shifts and Fusion Rates for S States of  $\text{td}\mu$ ." *Physical Review A, atomic, molecular, and optical physics* (APS) 42, no. 7 (1990): 3768-3778.

Tachikawa, M. "Simultaneous Optimization of Gaussian Type Function Exponents for Electron and Positron with Full-CI Wavefunction – Application to Ground and Excited States of Positronic Compounds with Multi-Component Molecular Orbital Approach." *Chemical Physics Letters* 350 (2001): 269-276.

Takahashi, H. "Muon Sticking in Muon-Catalysed d-t Fusion." *Journal of Physics G: Nuclear Physics* 12, no. 12 (1986): L271.

Takashi, T., M. Abe, T. Nakajima, and K. Hirao. "Accurate Relativistic Gaussian Basis Sets for H Through Lr Determined by Atomic Self-Consistent Field Calculations With the Third-Order Douglas–Kroll Approximation." *Journal of Chemical Physics* 115, no. 10 (2001): 4463:1-10.

Tulub, A. V., V. F. Brattsev, and M. V. Pack. "Electron Density in the Interior of Nuclei with Allowance for QED Effects in the Many-Electron Theory of Atoms." *Physics of Atomic Nuclei* 61, no. 4 (1998): 520-524.

van Gunsteren, W. F., and H. J. C. Berendsen. "Computer Simulation of Molecular Dynamics: Methodology, Applications and Perspectives in Chemistry." *Angewandte Chemie, International Edition in English* 29 (1990): 992-1023.

Watson, J. K. G. "The Vibration-Rotation Spectrum and Anharmonic Potential of  $\text{H}_3^+$ ." *Chemical Physics* 190 (1995): 291-300.

Webb, S. P., T. Iordanov, and S. Hammes-Schiffer. "Multiconfigurational Nuclear-Electronic Orbital Approach: Incorporation of Nuclear Quantum Effects in Electronic Structure Calculations." *Journal of Chemical Physics* 117 (2002): 4160-4118.

Weeks, D. E. "Molecular Orbital Theory." *Unpublished*. Air Force Institute of Technology, 2009.



REPORT DOCUMENTATION PAGE				Form Approved OMB No. 074-0188	
<p>The public reporting burden for this collection of information is estimated to average 1 hour per response, including the time for reviewing instructions, searching existing data sources, gathering and maintaining the data needed, and completing and reviewing the collection of information. Send comments regarding this burden estimate or any other aspect of the collection of information, including suggestions for reducing this burden to Department of Defense, Washington Headquarters Services, Directorate for Information Operations and Reports (0704-0188), 1215 Jefferson Davis Highway, Suite 1204, Arlington, VA 22202-4302. Respondents should be aware that notwithstanding any other provision of law, no person shall be subject to a penalty for failing to comply with a collection of information if it does not display a currently valid OMB control number.</p> <p><b>PLEASE DO NOT RETURN YOUR FORM TO THE ABOVE ADDRESS.</b></p>					
1. REPORT DATE (DD-MM-YYYY) 22-03-2012		2. REPORT TYPE Doctoral Dissertation		3. DATES COVERED (From – To) October 2008-March 2012	
4. TITLE AND SUBTITLE  Theoretical Study of the Effects of Di-Muonic Molecules on Muon-Catalyzed Fusion				5a. CONTRACT NUMBER	
				5b. GRANT NUMBER	
				5c. PROGRAM ELEMENT NUMBER	
6. AUTHOR(S)  Sheely, Eugene V., LTC, USA				5d. PROJECT NUMBER	
				5e. TASK NUMBER	
				5f. WORK UNIT NUMBER	
7. PERFORMING ORGANIZATION NAMES(S) AND ADDRESS(S) Air Force Institute of Technology Graduate School of Engineering and Management (AFIT/EN) 2950 Hobson Way WPAFB, OH 45433-7765				8. PERFORMING ORGANIZATION REPORT NUMBER  AFIT/DS/ENP/12-M02	
9. SPONSORING/MONITORING AGENCY NAME(S) AND ADDRESS(ES)  Intentionally left blank.				10. SPONSOR/MONITOR'S ACRONYM(S)	
				11. SPONSOR/MONITOR'S REPORT NUMBER(S)	
12. DISTRIBUTION/AVAILABILITY STATEMENT DISTRIBUTION STATEMENT A; APPROVED FOR PUBLIC RELEASE; DISTRIBUTION UNLIMITED					
13. SUPPLEMENTARY NOTES This material is declared a work of the US Government and is not subject to copyright protection in the United States.					
14. ABSTRACT <p>This document presents a theoretical study di-muonic hydrogen and helium molecules that have the potential of enhancing the muon-catalyzed fusion reaction rate. In order to study these di-muonic molecules a method of non-adiabatic quantum mechanics referred to as a General Particle Orbital (GPO) method was developed. Three mechanisms that have the possibility of enhancing the muon-catalyzed fusion rate were discovered. Two involve the formation of di-muonic hydrogen molecules, and the other uses di-muonic molecules to liberate muons stuck to <math>^3\text{He}</math> nuclei. The effects of muon spin on di-muonic hydrogen molecules was studied. The nuclear separation in di-muonic hydrogen molecules with parallel muon spin is too great for the molecules to have a fusion rate which can enhance the fusion yield. The possibility of these molecules transitioning to single muon molecules or triatomic oblate symmetric top molecules which may fuse faster is examined. Using two muons to catalyze <math>^3\text{He}-^3\text{He}</math> fusion is shown to be impractical; however, using two muons to catalyze <math>^3\text{He}-d</math> fusion is possible. While studying the physical properties of di-muonic hydrogen and helium molecules some unique properties were discovered. Correlation interactions in these molecules result in an increase in the calculated nuclear bond length.</p>					
15. SUBJECT TERMS Muon, Di-Muonic, Fusion, Muon-Catalyzed Fusion, Non-Adiabatic, Quantum Mechanics, General Particle Orbital, Exotic Particle					
16. SECURITY CLASSIFICATION OF:		17. LIMITATION OF ABSTRACT  UU	18. NUMBER OF PAGES 250	19a. NAME OF RESPONSIBLE PERSON Larry W. Burggraf, AFIT/ENP	
REPORT U	ABSTRACT U			c. THIS PAGE U	19b. TELEPHONE NUMBER (Include area code) (937) 255-3636 x4503